

**GLUTAMATERGIC SYNAPSE FUNCTION IN A VPS35 D620N KNOCK-IN MODEL  
OF PARKINSONISM**

by

**Chelsie Ayn Kadgien**

**B.Sc., The University of Victoria, 2008**

**A THESIS SUBMITTED IN PARTIAL FULFILLMENT OF  
THE REQUIREMENTS FOR THE DEGREE OF**

**DOCTOR OF PHILOSOPHY**

in

**THE FACULTY OF GRADUATE AND POSTDOCTORAL STUDIES  
(Neuroscience)**

**THE UNIVERSITY OF BRITISH COLUMBIA  
(Vancouver)**

**August 2020**

**© Chelsie Ayn Kadgien, 2020**

The following individuals certify that they have read, and recommend to the Faculty of Graduate and Postdoctoral Studies for acceptance, the dissertation entitled:

Glutamatergic synapse function in a VPS35 D620N knock-in model of familial parkinsonism

submitted by Chelsie Ayn Kadgien in partial fulfillment of the requirements for

the degree of Doctor of Philosophy

in The Faculty of Graduate and Postdoctoral Studies, Neuroscience

**Examining Committee:**

Dr. Austen J. Milnerwood, Neurology

Co-supervisor

Dr. Matthew J. Farrer, Medical Genetics

Co-supervisor

Dr. Elizabeth Conibear, Medical Genetics

University Examiner

Dr. Yu Tian Wang, Neurology

University Examiner

**Additional Supervisory Committee Members:**

Dr. Ann Marie Craig, Psychiatry

Supervisory Committee Member

Dr. Lynn Raymond, Psychiatry

Supervisory Committee Member

## Abstract

Vacuolar protein sorting 35 (VPS35) is a core component of the retromer complex that regulates protein recycling from maturing endosomes to the *trans*-Golgi network or plasma membrane. A pathogenic substitution in VPS35 (D620N) leads to autosomal-dominant, clinically-typical, late-onset Parkinson's disease (PD). Initial studies on the effects of the D620N on neuronal functions of retromer have been prone to overexpression effects. Here, we modeled VPS35 D620N parkinsonism in a knock-in mouse that expresses mutant protein at endogenous levels and used it to examine mutant effects on protein trafficking and glutamate synapse function.

In cultured neurons and brain tissue from VKI mice, we show that the levels, interaction, and localization of retromer core subunits (VPS35 and VPS26) are maintained; however, VPS35 binding to the WASH complex subunit FAM21 is decreased by the D620N mutation in brain lysate. In cultured neurons, the mutation results in an accumulation of VPS35-FAM21-positive clusters and recycling endosomes in dendrites, increased glutamate release and increased post-synaptic AMPA-receptor surface expression, without alterations to dendritic morphology or synapse numbers. Glutamate transmission phenotypes were less severe in homozygous mutant cells, possibly due to compensatory or aberrant downregulation of presynaptic VGluT1.

LRRK2 kinase is another protein implicated in late-onset PD that interacts physically and functionally with VPS35. PD-causing mutations of LRRK2 increase its kinase activity. We hypothesized D620N expression would increase LRRK2 kinase activity, representing a convergence of pathogenic mechanisms between PD proteins. D620N expression increased LRRK2 kinase activity, which was robustly inhibited by the selective LRRK2 inhibitor MLI-2. LRRK2 kinase inhibition exerted genotype-specific effects on post-synaptic receptor expression, mimicking PD-like phenotypes in WT cells, and having opposing effects in mutant cells. The

interpretation of mutant effects was obscured by mutant-specific effects of the solubilization vehicle, Captisol, on electrophysiological readouts.

This novel knock-in mouse improves our understanding of the early neurochemical and cellular effects of the D620N mutation in neurons. These observations provide candidate pathophysiological pathways that may drive eventual transition to late-stage parkinsonism in VPS35 families, and support the emerging synaptopathy model of neurodegeneration. These findings suggest caution should be employed regarding widespread use of LRRK2 kinase inhibition in non-LRRK2 PD.

## **Lay summary**

The causes of neurodegeneration in Parkinson's disease are poorly understood, making the development of neuroprotective treatments challenging. We can model genetic predisposition to PD in experimental animals, providing a unique opportunity to study early changes in the brain that may lead to disease. Here we put the human PD mutation in a protein that has a role in neuron-neuron communication into the mouse genome. The mutation causes increases in communication between brain cells. Science shows that the wrong kind of communication between brain cells is detrimental, eventually causing neurodegeneration. The effects of the mutation were similar to other known causes of PD. We tested a promising experimental drug, but found that it increases communication in healthy cells in a manner similar to the PD-causing mutation. The study provides useful information about the early changes that could lead to PD, and suggests that neuroprotective treatments may need to be personalized.

## **Preface**

The work contained in this dissertation was conceptualized by myself with initial guidance from my post-doctoral mentor Dr. Lise Munsie, and my co-supervisors Dr. Austen J. Milnerwood and Dr. Matthew J. Farrer. Husbandry and experiments received ethical approvals from UBC (breeding A16-0088; experimentation A15-0105) and McGill University (2017-7888B), in accordance with Canadian Council on Animal Care regulations. Animal husbandry was carried out by the excellent teams at Animal Care Services at UBC and the Centre for Neurological Disease Modeling at McGill.

The experiments herein were conducted at the Centre for Applied Neurogenetics in the Djavad Mowafaghian Centre for Brain Health at the University of British Columbia (Chapter 2) and at the Brain Tumour Research Centre in the Montreal Neurological Institute and Hospital at McGill University (Chapter 2 & 3). I conducted the majority of the experimental work, performed the data & statistical analyses, wrote this dissertation, and created all of the figures with the exclusion of those in the introduction (detailed below). At UBC, animal colony management, genotyping, and neuronal cultures were performed by Dr. Liping Cao and Dr. Stefano Cataldi; at McGill I prepared all of my own neuronal cultures, and managed the animal colony.

Chapter 1: Portions of section 1.3 “Leucine-rich repeat kinase 2” were adapted from a manuscript that I contributed to writing, along with Dr. Naila Kulhmann and Dr. Austen Milnerwood, which will be submitted for publication soon. All figures in the introduction, with the exclusion of Fig 1-2, were reproduced from published reviews with the permission of the copyright holder. Section 1.2 “Vacuolar protein sorting 35” will be adapted into a review article in the coming months.

Chapter 2: Most of the neuronal cultures were prepared by Dr. Liping Cao at UBC. Later cultures I prepared myself at McGill. Co-immunoprecipitations and WES capillary-based western blots in Figure 2-1 were performed by Jaskaran Khinda. Cell counts in Figure 2-2 were performed by Jesse Fox. The remaining experimental work, analysis, and presentation were performed by me. This work in this Chapter was prepared as a publication with assistance from Dr. Milnerwood in 2017, but rejected pending additional experiments. It will be revised and resubmitted for publication in the coming months.

Chapter 3: I conducted all sample preparations myself. Anusha Kamesh performed the whole-cell patch clamp experiments and analysis of mEPSC amplitude, frequency, and decay. The remainder of the experimental work, analysis, and presentation was prepared by me. Small portions of this chapter will be included in the publication being prepared from the work in Chapter 2.

# Table of contents

<b>Abstract .....</b>	<b>iii</b>
<b>Lay summary .....</b>	<b>v</b>
<b>Preface.....</b>	<b>vi</b>
<b>Table of contents.....</b>	<b>viii</b>
<b>List of tables.....</b>	<b>xiii</b>
<b>List of figures.....</b>	<b>xiv</b>
<b>List of abbreviations .....</b>	<b>xvi</b>
<b>Acknowledgements .....</b>	<b>xix</b>
<b>Dedication .....</b>	<b>xxi</b>
<b>Chapter 1: Introduction .....</b>	<b>1</b>
1.1 Parkinson's disease .....	1
1.1.1 Clinical presentation and diagnosis.....	3
1.1.2 Pathology .....	5
1.1.3 Etiology .....	8
1.1.3.1 Late onset, autosomal dominant Parkinson's disease .....	9
1.1.3.2 Early-onset autosomal recessive Parkinson's disease .....	11
1.1.3.3 Genetic risk factors.....	12
1.1.3.4 Environmental risk factors.....	14
1.1.3.5 Gene x environment interaction .....	16
1.1.4 Treatment .....	17
1.1.5 Modeling PD in mice.....	20
1.1.5.1 Chemical lesion models .....	21
1.1.5.2 Chronic exposure models .....	22



1.1.5.3	<i>Genetic models.....</i>	23
1.2	Vacuolar protein sorting 35 .....	24
1.2.1	The canonical retromer complex in mammalian cells.....	25
1.2.2	Non-canonical retromer complexes .....	32
1.2.3	Functions .....	35
1.2.3.1	<i>Lysosomal maturation.....</i>	35
1.2.3.2	<i>Metabolic homeostasis.....</i>	35
1.2.3.3	<i>Transcytosis and maintenance of cell polarity .....</i>	36
1.2.3.4	<i>Wnt signalling.....</i>	36
1.2.3.5	<i>Mitochondrial vesicle trafficking and quality control .....</i>	37
1.2.4	Neuron-specific functions.....	38
1.2.4.1	<i>Nervous system development .....</i>	39
1.2.4.2	<i>Postsynaptic receptor trafficking .....</i>	40
1.2.4.3	<i>Putative presynaptic roles .....</i>	44
1.2.4.4	<i>Retromer in Alzheimer's disease.....</i>	46
1.2.5	The retromer complex in Parkinson's disease.....	46
1.2.5.1	<i>Findings from exogenous mutant expression in cell-lines .....</i>	47
1.2.5.2	<i>Findings from exogenous expression in neurons .....</i>	50
1.2.5.3	<i>Findings from a novel knock-in D620N knock-in model .....</i>	53
1.3	Leucine-rich repeat kinase 2.....	56
1.3.1	A brief primer on neuronal dysfunction in LRRK2 models of PD.....	57
1.3.2	LRRK2 kinase substrates.....	59
1.4	Hypothesis & rationale .....	60
<b>Chapter 2: Exploring the neuronal role of VPS35 and the effect of the D620N mutation on glutamatergic synapses.....</b>		<b>63</b>

2.1	Introduction.....	63
2.2	Materials and methods .....	65
2.2.1	VPS35 D620N knock-in mice and genotyping .....	65
2.2.2	Western blots and co-immunoprecipitations .....	66
2.2.3	Primary cortical cultures .....	69
2.2.4	Immunocytochemistry and imaging analysis.....	70
2.2.5	Electrophysiology.....	72
2.2.6	Fluorescence recovery after photo-bleaching.....	74
2.2.7	Statistics.....	75
2.3	Results.....	75
2.3.1	Altered protein-protein binding relationships in VKI brain .....	75
2.3.2	No mutation effect on survival or morphology of primary cortical neurons .....	78
2.3.3	Increased colocalization and density of endosomal recycling proteins .....	80
2.3.4	VPS35 association with GluA1 not altered by D620N mutation .....	84
2.3.5	Altered surface stability and kinetics of GluA1 turnover.....	85
2.3.6	Increased glutamatergic transmission and surface AMPAR expression.....	88
2.4	Discussion .....	92
2.4.1	D620N increases the capacity for GluA1 trafficking.....	92
2.4.2	Identification of two putative novel retromer cargoes .....	100
2.4.3	Functional consequences are pre- and postsynaptic .....	100
2.4.4	Divergent functional outcomes in heterozygous and homozygous contexts.....	104
2.5	Conclusion .....	108
<b>Chapter 3: Investigating the interplay of VPS35 and LRRK2 in glutamatergic synapse function. ....</b>		<b>109</b>
3.1	Introduction.....	109

3.2	Materials and methods .....	112
3.2.1	VPS35 D620N knock-in mice and genotyping .....	112
3.2.2	LRRK2 kinase inhibition with MLi2 treatment.....	112
3.2.3	Western blots .....	113
3.2.4	Primary cortical cultures .....	114
3.2.5	Immunocytochemistry.....	114
3.2.6	Electrophysiology.....	114
3.2.7	Statistics.....	114
3.3	Results.....	115
3.3.1	LRRK2 kinase activity is increased in VKI brain.....	115
3.3.2	Captisol has little effect on protein expression, phosphorylation, or surface GluA1 expression in WT neurons .....	119
3.3.3	LRRK2 kinase inhibition in VKI affects postsynaptic AMPAR trafficking .....	120
3.3.4	Rab10 does not localize with retromer or GluA1 in dendrites.....	126
3.4	Discussion.....	129
3.4.1	MLi-2 abolishes phosphorylation of LRRK2 S935 and normalizes phosphorylation of Rab10 T73 to wild-type levels .....	130
3.4.2	Consideration of the effect of Captisol on basal phenotypes.....	131
3.4.3	LRRK2 kinase inhibition effect in cultures is primarily postsynaptic.....	133
3.4.4	Implications for treatment of PD with MLi-2.....	138
3.5	Conclusion .....	141
<b>Chapter 4: Conclusion.....</b>		<b>142</b>
4.1	Caveats and Limitations .....	142
4.1.1	Reductionist modeling.....	142
4.1.2	Developmental time point .....	143

4.1.3	Subjectivity of immunostaining cluster analysis .....	143
4.1.4	Incomplete control experiments for drug vehicle effects .....	144
4.1.5	Lack of mechanistic insight .....	145
4.2	Future research directions.....	146
4.2.1	Mutant effects on mature & intact systems .....	146
4.2.2	Mechanistic inquiry .....	146
4.2.3	Retromer trafficking of D2R and GluN1.....	148
4.2.4	VPS35, LRRK2, and Rab10 at the presynapse.....	148
4.3	Contributions to the field.....	149
<b>Bibliography .....</b>		<b>151</b>
<b>Appendices .....</b>		<b>192</b>
Appendix A - Supplements to Chapter 2 .....		192
Appendix B - Supplements to Chapter 3 .....		195

## List of tables

<b>Table 1-1</b> List of known SNX-BAR-retromer and SNX3-retromer pathways at the outset of my dissertation work .....	37
--	----

## List of figures

<b>Figure 1-1</b> Proposed mechanism of canonical SNX-BAR-Rab7-retromer cargo retrieval.. .....	30
<b>Figure 1-2</b> Diagram of the endolysosomal maturation pathway and the pathways of cargo recycling through tubular endosomal extensions. ....	34
<b>Figure 1-3</b> Hierarchy of AMPAR insertion during LTP or removal during LTD based on subunit composition .....	41
<b>Figure 2-1</b> Expression levels and co-immunoprecipitation of retromer and associated endolysosomal proteins reveals altered FAM21 binding in VKI mouse brain .....	77
<b>Figure 2-2</b> Cell density and dendritic morphology are not altered in mature cortical cultures from VKI mice .....	79
<b>Figure 2-3</b> Visualization of retromer and associated endosomal proteins reveals accumulation of VPS35- FAM21 co-clusters and recycling endosomes in mouse cortical neuron dendrites ....	83
<b>Figure 2-4</b> Dendritic localization and surface delivery kinetics of GluA1 altered in the absence of changes to protein expression or association with VPS35 in the cortex. ....	87
<b>Figure 2-5</b> Excitatory synapse function, but not number, is altered in cortical cultures from VKI mice.....	91
<b>Figure 2-6</b> Working model of increased surface AMPAR expression in D620N mutants.....	107
<b>Figure 3-1</b> LRRK2 kinase activity is increased in VKI brain tissue with no effect on protein expression .....	118
<b>Figure 3-2</b> The cyclodextrin solubilizing agent Captisol has no effect on protein expression, phosphorylation, or surface expression of GluA1 .....	120
<b>Figure 3-3</b> MLI-2 treatment inhibits LRRK2 kinase activity and has genotype-dependent effects on glutamate transmission.....	124

<b>Figure 3-4</b> MLi-2 treatment alters localization of synaptic proteins in a genotype-dependent manner .....	125
<b>Figure 3-5</b> Rab10 does not colocalize with VPS35 or GluA1 in cortical neurites .....	128
<b>Appendix A-1</b> Co-immunoprecipitation in cortical and striatal lysates reveals novel neuronal VPS35 cargoes and no mutant effects on neurotransmitter cargo binding.....	192
<b>Appendix A-2</b> Co-immunoprecipitation of whole brain lysate from 3-month-old mice shows that immunoprecipitation of FAM21 can pull down VPS35.....	194
<b>Appendix B-1</b> Western blot of whole brain lysate from 3-month-old mice reveals a statistically significant genotype effect on Rab10 phosphorylation.....	195
<b>Appendix B-2</b> Knock-out testing of specificity of Rab10 antibody for immunocytochemistry.....	196
<b>Appendix B-3</b> Visualization of VGluT1 and Rab10 in cultured cortical neuron dendrites reveals that mutant-specific increases in Rab10 cluster density are not associated with VGluT1-positive terminals.....	197

## List of abbreviations

6-OHDA	6-hydroxydopamine
ACh	Acetylcholine
ACSF	Artificial cerebrospinal fluid
AMPA	$\alpha$ -amino-3-hydroxy-5-methyl-4-isoxazolepropionic acid
AMPAR	$\alpha$ -amino-3-hydroxy-5-methyl-4-isoxazolepropionic acid receptor
AP	Adaptor protein
BACE1	$\beta$ -secretase 1
CI-MPR	Cation-independent mannose-6-phosphate receptor
CO <sub>2</sub>	Carbon dioxide
CoIP	Co-immunoprecipitation
DA	Dopamine
DAT	Dopamine transporter
ECS	Extra-cellular solution
FAM21	Family with sequence similarity 21
FSCV	Fast-scan cyclic voltammetry
FRAP	Fluorescence recovery after photobleaching
GAP	GTPase activating protein
GAPDH	Glyceraldehyde 3-phosphate dehydrogenase
GBA	Glucocerebrosidase
GDP	Guanosine diphosphate
GEF	Guanine nucleotide exchange factor
GFP	Green fluorescent protein
GPCR	G-protein coupled receptor
GTP	Guanosine triphosphate



GWAS	Genome-wide association study
HBSS	Hank's balanced salt solution
Het	Heterozygous
Homo	Homozygous
ICC	Immunocytochemistry
IHC	Immunohistochemistry
iPSC	Induced pluripotent stem cell
L-DOPA	L-3,4-dihydroxyphenylalanine
LRRK2	Leucine-rich repeat kinase 2
LTD	Long-term depression
LTP	Long-term potentiation
MAP2	Microtubule-associated protein 2
MCI	Mild cognitive impairment
mEPSC	Miniature excitatory postsynaptic current
MPTP	1-methyl-4-phenyl-1,2,3,6-tetrahydropyridine
MSN	Medium spiny neuron
NEEP21	Neuron-enriched endosomal protein of 21kDa
NMDAR	N-methyl-D-aspartate receptor
NSF	N-ethylmaleimide-sensitive factor
NSFA	Non-stationary fluctuation analysis
PBS	Phosphate-buffered saline
PCR	Polymerase chain reaction
PD	Parkinson's disease
PDL	Poly-D-lysine
Penstrep	Penicillin-streptomycin

PINK1	PTEN-induced kinase 1
PFA	Paraformaldehyde
PSD95	Postsynaptic density protein 95
Rab	Ras-related protein
RBD	REM sleep behaviour disorder
REM	Rapid eye movement
RME-8	Receptor-mediated endocytosis 8
RNA	Ribonucleic acid
RT	Room temperature
SNP	Single nucleotide polymorphism
SNpc	<i>Substantia nigra pars compacta</i>
SNX	Sorting nexin
SNX-BAR	Bar-domain-containing sorting nexin
SSRI	Selective serotonin reuptake inhibitor
TBC1D5	TBC1 domain family member 5
TBI	Traumatic brain injury
TBS	Tris-buffered saline
TH	Tyrosine hydroxylase
VGluT1	Vesicular glutamate transporter 1
VGluT2	Vesicular glutamate transporter 2
VKI	<i>Vps35</i> p.D620N knock-in
VMAT2	Vesicular monoamine transporter2
VPS	Vacuolar protein sorting
WASH	Wiskott–Aldrich syndrome protein and SCAR homologue
WT	Wild-type

## Acknowledgements

This PhD has been an enormous undertaking, which I could not have done without the support of many people. I must first thank my primary supervisor and Science Dad, Dr. Austen Milnerwood, for taking a chance on a sociologist and for his unwavering support of my growth as a scientist over the last 7 years. His clear passion for research, willingness to volley ideas at all hours, and encouragement have kept me inspired through all the ups and downs. Thanks are also due to my co-supervisor Dr. Matthew Farrer, for his encouragement, support, and alternate perspective on my studies, and to my supervisory committee, Dr's. Ann Marie Craig, Hurt Haas, and Lynn Raymond, for their guidance, constructive feedback, and flexibility.

I was fortunate to receive the Porridge for Parkinson's Dr. Lorne Alexander Graduate Student Award through the Parkinson Society Canada. Thank you to the Parkinson Society Canada, and especially to Mrs. Alexander, and the Parr and McLeod families, for the financial support and for bringing me to Toronto. Our conversations left a profound impression on me, and have undoubtedly shaped the way I view my role and responsibilities as a biomedical researcher.

Many thanks are also in order to my brilliant lab mates over the years. Dr. Lise Munsie, my postdoctoral mentor, taught me to be fastidious, helped turn me into a molecular biologist, and gave me a sweet bicycle. Dr. Dayne Beccano-Kelly was always ready with excellent advice on navigating the life of a scientist, and made me feel immediately welcome into the lab family. Dr. Naila, my lab sister, has made the journey with me from start to finish. She has been a well of support, treats, crying-shoulders, and joyous celebratory dancing. Dr. Thaiany Quevedo-Melo's late-night pep talks have gotten me through these last stressful phases of my doctorate. Anusha Kamesh contributed excellent electrophysiology experiments and fun musical outings. And thank you, too, to all of the other lab members who have helped both scientifically and socially:

Daisy Cao, Jaskaran Khinda, Igor Tatarnikov, Mattia Volta, Emil Gustavsson, Joanne Trihn, Danielle Masellis-Smith, Yuting Zhang, Bruno Vieira, and many others.

In the wider research community, I thank the Bamji lab at UBC – Dr. G. Stefano Brigidi, Dr. Fergil Mills, and Dr. Andrea Globa for the memorable neuroscience socials and sense of camaraderie. At McGill, I could not have gotten things up and running without the tireless support of Nadine Lauinger, who still wanted to be a climbing partner and a kind friend after all my annoying questions, and the wider support of the Fon and McPherson labs.

In my life outside, my friends near and far have been overwhelmingly supportive. Special thanks are due to my friend Gwenn who helped me get on my feet when my PhD brought me to Vancouver. My roommate soulmate Randi tolerated my strange work hours and habits, and was always there with a blanket fort, cookies, and giggles when I needed them. My idiots in Montreal tried, but never succeeded, to bring me to meet my end in the mountains. Our brief temporal intersection in Montreal was one of the happiest times of my life.

I would never have ended up here without the support of my family. I owe my desire to find answers to my mother, who always said “if you want to know something, look it up” and provided a full set of encyclopedia in which to do so. Her endless faith in me has been invaluable. My big sister Jen has been my life-long friend and accomplice, and always my biggest cheerleader. My dad has never treated me like I could not or should not do anything just because I was a girl. Lastly my grandparents Gert and Ron, who were always huge supporters of my education and would have been so proud to have a doctor in the family. Together they have made me feel (perhaps foolishly) like I can accomplish anything I put my mind to, and have provided me the safety net to try.

## **Dedication**

*“I don’t really understand what it is you do, exactly, but I sure wish I had had those kinds of opportunities when I was your age.”*

–Gertrude Bunn, beloved grandmother, 1917-2018

# Chapter 1: Introduction

*“The disease, respecting which the present inquiry is made, is of a nature highly afflictive...; some have regarded its characteristic symptoms as distinct and different diseases, and others have given its name to diseases differing essentially from it; whilst the unhappy sufferer has considered it as an evil, from the domination of which he had no prospect of escape.”*

- “An essay on the shaking palsy” James Parkinson, 1817

## 1.1 Parkinson’s disease

Parkinson’s disease (PD) is a neurodegenerative disease of aging, typically characterized by slowly worsening motor function, manifest as resting tremor and a reduced ability to initiate movement (bradykinesia) (Parkinson, 1817; reviewed in: Samii, Nutt and Ransom, 2004; Goetz, 2011; Beitz, 2014; Kalia and Lang, 2015). Despite the diagnostic focus on the motor aspects caused by a loss of dopamine-producing cells in the *substantia nigra*, this disease broadly impairs nervous system functioning, and comes with a host of pernicious non-motor symptoms (reviewed in: Samii, Nutt and Ransom, 2004; Langston, 2006; Dickson, Fujishiro, *et al.*, 2009; Beitz, 2014; Goldman and Postuma, 2014; Kalia and Lang, 2015). These both precede motor onset, and have a more negative impact on the quality of life of individuals with PD (reviewed in: Langston, 2006; Goldman and Postuma, 2014; Kalia and Lang, 2015).

Ancient Chinese and Indian texts dating as early as 1000 B.C. contain descriptions of individuals suffering from the classic motor symptoms of Parkinson’s disease (reviewed in: Manyam, 1990); and, in Western tradition, the characteristic resting tremor that is a primary feature of PD has been discussed as far back as Galen, de la Boe, and Sauvages (Parkinson, 1817). Although historical evidence shows that PD has impacted humans since long before the industrial

revolution, the description by James Parkinson, in his '*An essay on the shaking palsy*' (1817), detailed not only the cardinal motor symptoms (still recognized as diagnostic today), but also non-motor impairments. More than 50 years later, the renowned neurologist Jean-Martin Charcot described Parkinson's report as so complete as to propose an eponymous disease be accredited to James Parkinson.

In his essay, Parkinson describes individuals who present with a motor disorder that progresses so slowly that most do not recall when it started. It begins with unilateral weakness, followed by a slight tremor in one limb at rest, then eventually spreads to the contralateral side, and worsens slowly both in the severity of the tremor, and the number of body regions affected. He describes a lack of responsiveness of the limbs to 'the dictates of the will' (Parkinson, 1817; which we would now term bradykinesia), rigidity, and a stooped posture that develops later on in the progression of the disease. These symptoms escalate to the point that an individual is so afflicted that they cannot sleep for shaking, cannot walk, nor eat, nor find a moment's peace.

James Parkinson's essay was a plea to medical researchers to focus their energies on this disease so that we could bring relief to individuals living with it. The medical community responded. In the mid-nineteenth century, Jean-Martin Charcot contributed immensely to defining the features of typical Parkinson's disease versus atypical PD and other degenerative motor disorders, and to the dissemination of this information to the wider medical community (reviewed in: Goetz, 2011). These days, we know that Parkinson's disease is the second most common neurodegenerative disease of aging, affecting ~1% of the general population (Dorsey *et al.*, 2018) and up to 4% of the population over 65 (reviewed in: Beitz, 2014). Age is the single greatest risk factor in developing PD. A person's risk increases nearly exponentially over time, until it plateaus at around 80 years of age (reviewed in: Kalia and Lang, 2015). Race and sex also

affect one's risk: men are more likely than women to get PD, at a ratio of up to 3:2 in some populations, and the prevalence is higher in people of European and Latin American descent (reviewed in: Kalia and Lang, 2015).

In spite of two centuries of research since James Parkinson's plea, there are still many unanswered questions as to the cause of PD. While those years have seen the development (or perhaps Western rediscovery) of medications that can alleviate some of the motor symptoms, we have yet to discover a disease-modifying treatment that can slow or halt the progression of this devastating disease.

### **1.1.1 Clinical presentation and diagnosis**

The three cardinal features described by Parkinson and refined by Charcot remain the basis for clinical diagnosis of PD. The exact diagnostic criteria vary slightly depending on the framework followed, but, generally, a person must present with two of: asymmetric resting tremor, asymmetric rigidity, or asymmetric bradykinesia, and their symptoms must be responsive to dopaminergic therapy (reviewed in: Stoessl and Rivest, 1999; Samii, Nutt and Ransom, 2004; Dickson, Braak, *et al.*, 2009). There are a number of exclusion criteria that rule out atypical parkinsonian disorders such as essential tremor or drug-induced parkinsonism. Additional motor characteristics are many and can include: postural instability, gait abnormalities, freezing, stooped posture, masked facial expressions, decreased blink rate, blurred vision, impaired upward gaze, dystonia, difficulty turning in bed, kyphosis, scoliosis, and speech impairments (reviewed in: Dickson, Braak, *et al.*, 2009; Beitz, 2014).

Whilst diagnostic, such symptoms may not be the worst of the disease's manifestations. Non-motor symptoms are reported to be the biggest contributors to reduced quality of life for



affected individuals, and they do not respond well to dopaminergic therapies (reviewed in: Beitz, 2014). To name but a few: autonomic dysfunction, hyposmia, constipation, sleep disturbances, REM sleep behaviour disorder, excessive daytime sleepiness, fatigue, apathy, depression, anxiety, cognitive impairment, and restless leg syndrome (reviewed in: Samii, Nutt and Ransom, 2004; Chaudhuri, Healy and Schapira, 2006; Langston, 2006; Dickson, Fujishiro, *et al.*, 2009; Beitz, 2014; Goldman and Postuma, 2014). The onset of non-motor symptoms can precede motor onset by up to 15 years, and in 20% of cases they are the motivating complaint behind the physician visit leading to clinical diagnosis (reviewed in: Goldman and Postuma, 2014).

Clinical researchers have long recognized the importance of these prodromal, non-motor symptoms, and have searched for biomarkers that can diagnose the disease before motor onset. Unfortunately, the identification of a robust PD 'prodrome' has thus far remained elusive. REM sleep behaviour disorder (RBD) is the strongest predictor, with up to 81% of people with RBD having developed a neurodegenerative disease after longitudinal follow-up (reviewed in: Goldman and Postuma, 2014), though it should be noted this is not specific to PD. Hyposmia is a common feature, and up to 85% of people with PD have a reduced sense of smell; however, in a large longitudinal cohort only 2% of individuals with hyposmia went on to develop PD (*ibid*). Mild cognitive impairment (MCI) and dementia are also common with PD, with over 40% of newly diagnosed cases comorbid for MCI, and MCI a strong predictor of later dementia (*ibid*).

No single prodromal symptom is a perfect predictor of PD; thus research into the detection of biomarkers is a major focus of clinical research. Imaging of striatal and cardiac dopamine levels, and quantification of concentrations of  $\alpha$ -synuclein (and other PD-related proteins) in cerebrospinal fluid and peripheral tissues, are among the potential biomarkers being investigated (Ibanez *et al.*, 2017; reviewed in: Kalia and Lang, 2015; Borghammer and Van Den

Berge, 2019). While an early diagnosis is of limited usefulness without the availability of disease modifying treatment, the ongoing effort to find reliable early diagnostic criteria represents an important parallel avenue of study with regards to PD etiology and pathogenesis. Disease modification, when it arrives, will be of most benefit when applied early.

While once considered a single disease with a defining set of clinical features, it is becoming clear that clinical presentation exists on a heterogeneous spectrum. Typical PD can be split into two subtypes that have differing etiology and prognoses (reviewed in: Kalia and Lang, 2015). A contributing factor to the heterogeneity is the wide-spread dysfunction of multiple brain regions, that progress at different rates from individual to individual (reviewed in: Stoker and Greenland, 2018). Also, because of the broad spectrum of parkinsonian disorders that closely resemble PD, and heterogeneity even within 'typical' Parkinson's disease, a true diagnosis can only occur by post-mortem autopsy to confirm the presence of neuropathological hallmarks.

### **1.1.2 Pathology**

Parkinson's disease is classically defined as a hypodopaminergic movement disorder. The hallmark neuropathology that leads to a confirmed diagnosis of PD is the loss of the dark neuromelanin pigmented dopaminergic neurons of the *substantia nigra pars compacta* (SNpc), and the presence of characteristic protein aggregates, termed Lewy bodies and Lewy neurites.

The cells of the ventrolateral SNpc provide dopaminergic innervation to the putamen / dorsolateral striatum. Dopamine is essential for the function of the striatum in action selection and execution, thus, the loss of nigro-striatal innervation is largely believed to be responsible for the characteristic motor symptoms (reviewed in: Gerfen and Surmeier, 2011). Early research focused on the striking loss of dopamine and nigral cells in late-stage PD. For a long time it was

believed that cells of the SNpc were selectively vulnerable in the disease. This view has become antiquated, as the field now considers extra-nigral pathology and related early non-motor features as integral to disease onset and progression. Recent studies have implicated widespread neuronal dysfunction in both motor and non-motor aspects of PD (reviewed in: Dickson, Fujishiro, *et al.*, 2009; Goldman and Postuma, 2014; Kalia and Lang, 2015), and non-motor symptoms can precede dopaminergic terminal and cell loss by many years (Kordower *et al.*, 2013). Widespread cortical cell loss, and changes to cortical plasticity, have been documented in the brains of people with PD, and are evident before severe motor symptom onset, or significant loss of SN neurons (MacDonald and Halliday, 2002; reviewed in: Foffani and Obeso, 2018), indicating that the SNpc is not the only region affected.

Typical sporadic PD is defined neuropathologically by the presence of intraneuronal protein aggregates in neuronal soma (Lewy bodies) and/or neurites (Lewy neurites). These aggregates are enriched in:  $\alpha$ -synuclein, ubiquitin, tau, parkin, LRRK2, huntingtin, heat shock proteins, and other cytoskeletal and lysosomal proteins (reviewed in: Dickson, Braak, *et al.*, 2009; Olanow and Mcnaught, 2011; Stoker and Greenland, 2018). The proteins therein are highly ubiquitinated, oxidated, and nitrated (Good *et al.*, 1998; reviewed in Samii, Nutt and Ransom, 2004). Lewy aggregates are the most common inclusion type in the brains of people with PD, but they are not always present. For instance, people with late-onset autosomal-dominant PD arising from mutations in LRRK2 can present with either Lewy or tau pathology; many brains of people with PD have been found *post mortem* to exhibit amyloid plaques and neurofibrillary tangles that are most oft associated with Alzheimer's disease (Braak *et al.*, 2003; reviewed in: Kalia and Lang, 2015). Thus, while the presence of Lewy pathology is still considered a diagnostic criterion, there exists a heterogeneous array of neuropathology, even within people with typical clinical features.

Braak and colleagues (2003) have famously proposed a correlation between disease severity and the progression of Lewy body deposition in human *post-mortem* brain. They found that Lewy body deposition tended to start in the periphery and move up through the brainstem, reaching the SNpc and cortical regions at later stages of disease progression. This 'Braak staging' is touted as evidence that Lewy pathology is causal to PD, and begins outside the nigra; however, it is contentious (reviewed in: Volta, Milnerwood and Farrer, 2015); e.g., the Braak study (2003) did not include non-PD controls. Extensive incidental Lewy bodies have been found in a large number of asymptomatic individuals (reviewed in: Samii, Nutt and Ransom, 2004; Kalia and Lang, 2015), people with PD do not always have Lewy bodies *post-mortem* (reviewed in: Stoker and Greenland, 2018), and non-motor symptom severity generally does not correlate well with the progression of Lewy deposition throughout the brain (reviewed in: Dickson, Fujishiro, *et al.*, 2009). More recent studies of  $\alpha$ -synuclein have found that synuclein is not prone to aggregate in healthy cells (Bartels, Choi and Selkoe, 2011). In PD, misfolded oligomers and protofibrils are toxic species that can impair synaptic transmission (reviewed in: Bridi and Hirth, 2018; Burré, Sharma and Südhof, 2018) and can pass trans-synaptically to seed toxic misfolding in unaffected cells in a prion-like manner (Volpicelli-Daley *et al.*, 2016; reviewed in: Volpicelli-Daley and Brundin, 2018).

It has recently been posited that PD can either begin in the periphery, where progression tracks nicely with the Braak hypothesis, or in the brain (gut first vs. brain first; reviewed in: Borghammer and Van Den Berge, 2019). This could be reflective of the varied etiologies of this multifactorial disease, with gut-first PD being associated with a higher degree of exposure to environmental toxins, and brain-first PD with genetic, or systemic, factors.

PD is also associated with changes in brain physiology outside the SNpc. Studies of human post-mortem striata show reductions in dendritic complexity and spine number (McNeill *et al.*, 1988; Stephens *et al.*, 2005; Zaja-Milatovic *et al.*, 2005), with larger VGluT1-positive cortical terminals (glutamatergic synapses) (Kashani *et al.*, 2007). There is also evidence for atrophy of glutamatergic systems. Cortical plasticity is impaired in brains from prodromal individuals (reviewed in: Foffani and Obeso, 2018), and there is evidence for early cortical cell loss increasing up to 40% loss at later stages (MacDonald and Halliday, 2002).

Detailed analyses of pathological features reveal that PD is much more heterogeneous than originally believed. Pathology, like clinical presentation, can vary from individual to individual. This pathological and clinical heterogeneity hints at a spectrum of underlying etiological factors, outside of the traditional bias toward pathological changes which are specific to the SNpc.

### **1.1.3 Etiology**

Until the late 1990s, the etiology of Parkinson's disease was believed to be purely environmental. Following several familial linkage studies that honed in on genetic risk loci, this supposition was severely challenged in 1997 with the discovery of a single point mutation in  $\alpha$ -synuclein that causes late-onset, autosomal-dominant PD (Polymeropoulos *et al.*, 1997). This observation eventually lead to the discovery that  $\alpha$ -synuclein is a major component of Lewy bodies. Studies have since found that up to 10% of PD follows a classical Mendelian inheritance pattern, which is currently much higher than the contribution of all known monogenic causes (reviewed in: Lesage and Brice, 2009). The remaining cases of idiopathic PD are likely brought about through a combination of environmental and genetic risk factors (reviewed in: Ritz, Paul and Bronstein, 2016; Bandres-Ciga *et al.*, 2020).

### **1.1.3.1 Late onset, autosomal dominant Parkinson's disease**

Most familial forms of late-onset, autosomal-dominant PD are clinically indistinguishable from idiopathic cases (reviewed in: Healy *et al.*, 2008; Appel-Cresswell *et al.*, 2014; Struhal *et al.*, 2014; Volta, Milnerwood and Farrer, 2015), making them an encouraging means by which to understand the pathogenesis of both genetic and potentially idiopathic PD. All of the validated late-onset gene mutations linked to PD are within proteins implicated in protein/membrane trafficking, and synapse maintenance, either through involvement in synaptic vesicle cycling, or through endosomal recycling of post-synaptic neurotransmitter receptors (reviewed in: Picconi, Piccoli and Calabresi, 2012; Volta, Milnerwood and Farrer, 2015). Several studies have identified other putative Mendelian late-onset gene mutation candidates, that either have yet to be replicated (possibly due to the rarity of some mutations), or that are currently still contested within the literature (reviewed in: Bandres-Ciga *et al.*, 2020) e.g., DNAJC13 (Vilariño-Güell *et al.*, 2013), VPS26A (Gustavsson *et al.*, 2015). These will not be discussed further here; however, it is clear that our current understanding of the heritability of PD is still far from comprehensive.

Firstly, the most common known causes of autosomal-dominant PD are mutations in LRRK2, which account for up to 5% of all familial cases (reviewed in: Healy *et al.*, 2008). LRRK2 is a large multi-domain protein that contains both kinase and GTPase domains. Most, if not all, PD-causing mutations in LRRK2 increase its kinase activity toward its substrates, many of which have important roles in protein trafficking and synaptic function (reviewed in: Nguyen *et al.*, 2019; Taylor and Alessi, 2020; Kuhlmann and Milnerwood, *in press*). This makes LRRK2 kinase inhibition an attractive candidate for therapeutic intervention in PD. In neurons, it is involved in glutamate release (Beccano-Kelly, Kuhlmann, *et al.*, 2014; Cirnaru *et al.*, 2014), presynaptic plasticity, dopamine tone, and dopamine release (Melrose *et al.*, 2010; Beccano-Kelly, Kuhlmann, *et al.*, 2014; Beccano-Kelly, Volta, *et al.*, 2014; Yue *et al.*, 2015), and acts

postsynaptically in spine maintenance (Parisiadou *et al.*, 2014; Matikainen-Ankney *et al.*, 2016), AMPAR expression (Parisiadou *et al.*, 2014), and regulation of synaptic strength (Sweet *et al.*, 2015; Matikainen-Ankney *et al.*, 2016, 2018).

Secondly, the *SNCA* gene codes for  $\alpha$ -synuclein, a major protein component of Lewy inclusions, and is the central player in the prion hypothesis of PD pathogenesis (reviewed in: Bridi and Hirth, 2018; Burré, Sharma and Südhof, 2018; Volpicelli-Daley and Brundin, 2018). *SNCA* mutations (Polymeropoulos *et al.*, 1997; Kruger *et al.*, 1998; Zarranz *et al.*, 2004; Kiely *et al.*, 2013; Lesage *et al.*, 2013; Pasanen *et al.*, 2014) and multiplications (Singleton *et al.*, 2003; Chartier-Harlin *et al.*, 2004; Ibanez *et al.*, 2004) cause autosomal-dominant PD, and the copy number of multiplications is associated with earlier age of onset, and more severe disease (reviewed in: Trinh and Farrer, 2013; Kalia and Lang, 2015).  $\alpha$ -synuclein associates with a reserve pool of synaptic vesicles, where it is proposed to have a negative regulatory role on vesicle trafficking/SV release (Westphal and Chandra, 2013; Vargas *et al.*, 2014; reviewed in: Volta, Milnerwood and Farrer, 2015; Venda *et al.*, 2010; Picconi, Piccoli and Calabresi, 2012), although its physiology is still highly contentious (reviewed in: Sulzer and Edwards, 2019).

Last, but not least (in my highly biased opinion), a single point mutation in VPS35 has also been shown to be causal to autosomal-dominant, clinically-typical, late-onset PD (Vilariño-Güell *et al.*, 2011; Zimprich *et al.*, 2011; Struhal *et al.*, 2014). VPS35 is involved in the endosomal trafficking of a wide array of transmembrane proteins. At the outset of this project (2013) the neuron-specific functions of VPS35 were just beginning to be discovered. We then knew that it trafficked  $\beta$ 2-adrenergic receptors (Temkin *et al.*, 2011; Choy *et al.*, 2014) and AMPA-type glutamate receptors (Zhang *et al.*, 2012; Tsika *et al.*, 2014; Munsie *et al.*, 2015; Tian *et al.*, 2015). In the intervening years it has also been shown to associate with: GluN2-containing

NMDA-type glutamate receptors (Ma *et al.*, 2017); D1-type dopamine receptors (C. Wang *et al.*, 2016); dopamine transporter (Wu *et al.*, 2017); vesicular monoamine transporter 2 (Wu *et al.*, 2016), and neuroligins 1 & 3 (Kang *et al.*, 2014; Binda *et al.*, 2019). It also localizes to presynaptic compartments, where it may act in synaptic vesicle cycling or other protein trafficking pathways (Munsie *et al.*, 2015; Inoshita *et al.*, 2017; Vazquez-Sanchez *et al.*, 2018). Given that it is the central focus of my doctoral work, I will discuss the many functions of VPS35 in detail later in this introduction.

The genetic etiology of late-onset PD clearly converges on protein trafficking and synaptic transmission, and has spurred the theory that prolonged synaptic dysfunction is a common pathogenic mechanism in PD. Indeed, a growing body of evidence from humans with PD (Good *et al.*, 1998; Kordower *et al.*, 2013; Fazio *et al.*, 2018) and from animal models (Morales *et al.*, 2015; Phan *et al.*, 2017) supports the notion that dysfunctional striatal circuitry leads to dopaminergic terminal degeneration and axonal dying back, causing eventual cell death (reviewed in: Foffani and Obeso, 2018). Research on other neurodegenerative disorders further supports the notion that early synaptic dysregulation is a common pathogenic mechanism across many neurological diseases (reviewed in: Selkoe, 2002; Wishart, Parson and Gillingwater, 2006; Milnerwood and Raymond, 2010; Picconi, Piccoli and Calabresi, 2012).

### **1.1.3.2 Early-onset autosomal recessive Parkinson's disease**

Recessive gene mutations can be causal to PD; however, these mutations result in atypical parkinsonism with an earlier age of onset. I will discuss them only briefly. All three genes (PINK1, Parkin, and DJ-1) have known functions in mitochondrial quality control. PINK1 is a mitochondrial kinase, whereas Parkin and DJ-1 are both ubiquitin ligases. PINK1 phosphorylates Parkin in response to mitochondrial stress to induce mitophagy. DJ-1 promotes



PINK1 expression and interacts with PINK1 and parkin in mitophagy pathways, interlinking all three early onset genes (reviewed in: Cookson, 2010; Requejo-Aguilar *et al.*, 2015). These findings have resulted in much attention being paid to mitochondrial function and oxidative stress in the pathogenesis of PD; however, manipulations of all three proteins can also result in changes to dopamine release (reviewed in: Picconi, Piccoli and Calabresi, 2012).

It has yet to be determined in the literature whether prolonged mitochondrial dysfunction causes synaptic dysregulation in PD, or vice versa. Mitochondria reside in a subset of synapses where they regulate energy metabolism and buffer calcium, contributing to synaptic regulation (reviewed in: Lee *et al.*, 2018). On the other hand, alterations of synaptic activity can lead to oxidative stress and mitochondrial dysfunction (Good *et al.*, 1998; reviewed in: Picconi, Piccoli and Calabresi, 2012; Perfeito, Cunha-Oliveira and Rego, 2013). It is fascinating that mutations directly affecting mitochondrial quality control result in an early age of onset, whereas mutations that disrupt protein trafficking and synaptic function cause late onset disease. Nigral neurons have been suggested to be particularly vulnerable to mitochondrial dysfunction due to their highly branched morphology, tonic activity, and the reactive oxygen species produced by dopamine metabolism (reviewed in: Kalia and Lang, 2015). One is compelled to speculate on how synaptic dysfunction that we observe in late-onset autosomal dominant PD could trigger eventual mitochondrial-dysfunction-induced cell death, through a less direct route than the early-onset mutations.

### **1.1.3.3 Genetic risk factors**

Multiple genome-wide association studies (GWAS) have uncovered allelic variations in genes that either modify the disease progression of monogenic PD, or modify the risk of developing idiopathic PD. A large meta-analysis of GWAS has uncovered over 90 risk signals associated

with PD (Nalls *et al.*, 2019). Within these studies, a high burden of genetic risk has been primarily associated with endolysosomal trafficking and immune response (reviewed in: Bandres-Ciga *et al.*, 2020).

The most relevant (and replicated) findings to date have been variations in *SNCA*, *LRRK2*, *MAPT*, *GBA*, and *PARK16* (Satake *et al.*, 2009; Simón-Sánchez *et al.*, 2009; Trotta *et al.*, 2012; Nalls *et al.*, 2014, 2019; Chang *et al.*, 2017). *SNCA* and *LRRK2* are associated with late-onset familial PD and were discussed above. Briefly, they both have roles in intracellular trafficking and synaptic transmission. *MAPT* codes for tau, another protein component of Lewy bodies that associates with microtubules and thus is linked to intracellular trafficking (reviewed in: Pellegrini *et al.*, 2017). *GBA* variation is the strongest known modifier of the age of onset in *LRRK2* monogenic PD, and certain variants, when expressed homozygously, cause Gaucher's disease (Simón-Sánchez *et al.*, 2009; Murphy and Halliday, 2014; Nalls *et al.*, 2014; Chang *et al.*, 2017). *GBA* codes for glucocerebrosidase, a lysosomal enzyme necessary for lipid metabolism (reviewed in: Riboldi and Di Fonzo, 2019). Variants in *PARK16* sit upstream of the coding region for Rab7L1 (elsewhere Rab29), a Rab-GTPase that recruits *LRRK2* to intracellular compartments and activates its kinase domain (MacLeod *et al.*, 2013; Beilina *et al.*, 2014; Liu *et al.*, 2018; Purlyte *et al.*, 2018).

It is important to remember that genetic variation can also confer protection. GWAS studies have uncovered several protective genetic polymorphisms. Among those identified are variants in *SNCA* and *MAPT* (Trotta *et al.*, 2012; reviewed in: Kalia and Lang, 2015), further highlighting the importance of  $\alpha$ -synuclein and tau in the etiology of PD.

#### **1.1.3.4 Environmental risk factors**

One of the first clear demonstrations that exposure to toxins is associated with parkinsonism was the discovery that extracts of the plant *Rauwolfia serpentina*, used initially by pharmacologists in India as an anti-hypertensive, caused eventual parkinsonian symptoms in people using it (reviewed in: Fahn, 2015). Among other factors correlated with increased risk are: pesticide exposure, herbicide exposure, well water consumption, rural living, agricultural occupation, head injury, and beta-blocker use (reviewed in: Kalia and Lang, 2015; Ritz, Paul and Bronstein, 2016; Stoker and Greenland, 2018). As with genetic variability, risk works both ways, and some factors have been linked to reduced PD risk, such as tobacco use, coffee consumption, and anti-inflammatory drug use (NSAIDs) (reviewed in: Kalia and Lang, 2015; Breckenridge *et al.*, 2016; Stoker and Greenland, 2018).

Studies of environmental risk and protection are by nature correlative, and thus plagued by a lack of clear causation. Take for example the finding that smoking is associated with a lower risk of developing PD. Activation of nicotinic ACh receptors on DA neurons by nicotine is neuroprotective in animal models, but humans with PD are less prone to addictive behaviour and quit smoking more easily. In this light, it may be that a genetic predisposition to PD is protective against tobacco addiction (reviewed in: Stoker and Greenland, 2018).

Environmental toxins are one of the most well-studied and convincing cases of environmental etiology. Rotenone and paraquat are herbi/pesticides used on industrial farms. Rural lifestyle factors, such as being a farmer or just living in a rural area, have been correlated with a higher risk of PD (reviewed in: Lai *et al.*, 2002; Breckenridge *et al.*, 2016; Ritz, Paul and Bronstein, 2016). These toxins are mitochondrial complex I inhibitors, which induce mitochondrial dysfunction (reviewed in: Martinez and Greenamyre, 2012). Chronic exposure models in

rodents recapitulate many of the pathological features of PD, including selective nigral degeneration and motor phenotypes (reviewed in: Martinez and Greenamyre, 2012; Pan-Montojo *et al.*, 2012; Stoker and Greenland, 2018). While these studies do not prove causation in humans, the volume of evidence is compelling. Alternatively, it has been suggested that rotenone itself may not increase risk, as it is not very persistent in the environment or in ground-water; however, farms tend to use cocktails of chemically related compounds that are more persistent (reviewed in: Bové *et al.*, 2005).

Recently, attention has fallen on the impact of diet and the gut microbiome on PD pathogenesis. The complement of bacteria in a person's gut microbiome are correlated with increased risk or protection from PD (reviewed in: Parashar and Udayabanu, 2017; Fitzgerald, Murphy and Martinson, 2019), and gastrointestinal symptoms are amongst the earliest prodromal features of the disease (reviewed in: Beitz, 2014; Goldman and Postuma, 2014; Kalia and Lang, 2015). There is evidence that  $\alpha$ -synuclein deposition in the intestinal lining can be detected long before motor onset (reviewed in: Fitzgerald, Murphy and Martinson, 2019), consistent with the hypothesis that some PD begins in the periphery (Braak *et al.*, 2003; reviewed in: Borghammer and Van Den Berge, 2019). These studies are still in their infancy, but the early work provides intriguing evidence for a role of the microbiome in PD risk.

Inflammation is also a pathological feature of PD, and the protective nature of anti-inflammatory drug (NSAID) use suggests that inflammation could be a causal factor, rather than a protective response (reviewed in: Kalia and Lang, 2015). Bacterial and viral infections, even ones as common as gum disease, have been correlated to increased risk of PD (Bu *et al.*, 2015; Chen, Wu and Chang, 2017). Major histocompatibility complexes are reported to present specifically on dopaminergic neurons, which can then be attacked by T-cells in the brain,

providing yet another mechanism for nigral vulnerability, this time through inflammatory responses (reviewed in: Cebrián, Loike and Sulzer, 2014; Garretti *et al.*, 2019). Our understanding of inflammation in neurodegenerative disease is also still at its beginning; however, it is becoming clear that inflammatory processes have a role to play.

#### **1.1.3.5 Gene x environment interaction**

In spite of recent advances in understanding genetic and environmental risk for PD, most cases are idiopathic, arising with no family history. These likely represent an interaction between multiple environmental exposures and/or allelic risk factors (reviewed in: Sulzer, 2007; Kalia and Lang, 2015; Ritz, Paul and Bronstein, 2016; Bandres-Ciga *et al.*, 2020).

Studies of the interplay between genetics and environment provide further evidence in support of the environmental risk factors put forward. They also lend credence to the idea that most PD arises from the convergence of multiple factors. Allelic variants in the dopamine transporter (DAT) interact with pesticide exposures to increase risk (Kelada *et al.*, 2006; reviewed in: Ritz, Paul and Bronstein, 2016), and DAT inhibition can prevent paraquat toxicity in a cell culture model of PD (Shimizu *et al.*, 2003). The length of a polymorphic mixed dinucleotide repeat in the *SNCA* promoter region can modify the risk of PD occurring after traumatic brain injury (TBI) (reviewed in: Kalia and Lang, 2015), and a history of TBI is a modifier to age of onset in monogenic familial PD (reviewed in: Yahalom *et al.*, 2020). Coffee consumption likewise modifies age of onset in monogenic PD (*ibid*) and these protective effects are moderated by SNPs in the genes coding for caffeine-metabolizing enzymes and the NMDA-receptor subunit GRIN2A (reviewed in: Kalia and Lang, 2015). It is becoming evident from these studies that the interplay between risk factors is complex; recent extensions of this work hope to be able to trace individual histories of exposure, creating ‘exposome’ maps that can help understand the

complex interplay of factors contributing to the development of PD (reviewed in: Chen and Ritz, 2018).

The large volume of work on the etiology of PD makes it clear that this is a complex, multifactorial disorder. A parkinsonian syndrome with different complex etiologies for each individual would explain the array of symptomatic and pathological heterogeneity observed in the clinic, and suggests that personalized treatments may be the way forward for treating PD.

#### **1.1.4 Treatment**

The clear heterogeneity in the etiology and pathology between individuals combined with an incomplete understanding of the pathogenesis of the disease has kept disease modification elusive; despite over 200 years of research, treatment remains purely symptomatic.

The neurochemical underpinnings of motor dysfunction were unknown until the late 1950s, when the discovery was made that dopamine is a neurotransmitter, suggested first by Kathleen Montagu and confirmed by Arvid Carlsson, and then found by Oleh Hornykiewicz to be depleted in the brains of people with PD (reviewed in: Fahn, 2015). Inspired by others' previous success treating dopamine-depletion-induced motor phenotypes in reserpine-treated rabbits, Hornykiewicz was immediately compelled to try L-DOPA to treat PD. He mailed his entire experimental stash to a neurologist in Vienna, and applied pressure for it to be administered to people with PD. The first trial was very successful in treating the advanced motor symptoms of parkinsonism (for a first-hand retrospective, see Hornykiewicz, 2002). We now know that some traditional plant medicines used as early as 1000 B.C. (cowage beans and ergot) contain levodopa, or otherwise agonize dopamine (reviewed in: Manyam, 1990; Goetz, 2011).

Contemporary treatment still focuses on dopamine, either through replacement with L-DOPA (a dopamine precursor), or dopamine receptor agonism. These provide stark symptomatic benefit for motor symptoms, but often come with a host of undesirable side effects, including: impulse control disorders, psychosis, and, after long-term use, dyskinesia. Dyskinesia is arguably as debilitating as the symptoms the drugs are meant to treat (reviewed in: Beitz, 2014), though more modern preparations of L-DOPA, such as slow-release capsules or a direct-to-gut delivery pump, can help temper them (*ibid*). Unfortunately, these treatments do nothing to help the non-motor symptoms considered by many to be the most afflictive part of the disease, nor do they prevent progression (reviewed in: Beitz, 2014; Goldman and Postuma, 2014).

Dopamine therapy is central to treatment but is by no means the only intervention. Anti-cholinergic drugs can help with tremor (reviewed in: Perfeito, Cunha-Oliveira and Rego, 2013; Beitz, 2014; Kalia and Lang, 2015). Non-motor symptoms are also often addressed with other drugs (tricyclics and SSRIs for depression, methylphenidate for fatigue, laxatives for constipation)(reviewed in: Kalia and Lang, 2015). There are also a host of additional drugs used to treat the side effects of dopaminergic treatments themselves. For example, amantadine and clozapine can treat dyskinesia, and antipsychotics such as quetiapine (and again clozapine) are used for treatment-induced psychosis.

A cocktail of drugs comes with complications, thus some people with PD choose to manage as many symptoms as possible through non-pharmacological interventions. Exercise and physical therapy have proven beneficial to help with rigidity, postural changes, and balance problems (reviewed in: Beitz, 2014) . Similarly, speech therapy can help with hypophonia and difficulty swallowing. A high-fibre, well-curated diet can act in place of laxatives to manage constipation

and weight loss (*ibid*). Bright light therapy is being explored to improve sleep disturbances (reviewed in: Kalia and Lang, 2015).

A handful of surgical interventions have been developed thus far. Deep-brain stimulation is an option for L-DOPA responsive individuals, whereby electrical stimulation from implanted electrodes combined with low-dose L-DOPA can eliminate motor dysfunction. DBS also reduces dyskinesias, but is obviously a very invasive procedure that is only effective in about 5% of people – although it is remarkably effective for these individuals (reviewed in: Kalia and Lang, 2015; Stoker and Greenland, 2018). Early studies on stem cell transplantation showed promise, but led to the discovery that misfolded proteins can spread from the diseased brain into transplanted cells in a prionogenic manner (Kordower *et al.*, 2008). Whether prion-like propagation of misfolded  $\alpha$ -synuclein represents a pathogenic mechanism, or an epiphenomenon, is still a hotly contested issue (reviewed in: Volpicelli-Daley and Brundin, 2018; Killinger and Kordower, 2019), thus it is still unclear if stem cell transplantation will have enough long-term benefit to outweigh its invasiveness.

Fortunately, the study of the genetic etiology and pathophysiology of PD are beginning to converge on the same subcellular pathways. Promising new treatments are in development that target LRRK2 kinase activity, inflammation, mitochondrial stress, and alpha-synuclein deposition. Gene therapy is also on the table as an option for monogenic PD. While we hope for a perfect intersection onto one target molecule, the reality is that disease modification may require treatment strategies as heterogeneous as the underlying causes.



### 1.1.5 Modeling PD in mice

There are many ways to model Parkinson's disease, each with distinct advantages and caveats. Yeast, flies, and worms have helped us understand some of the basic molecular functions of the proteins implicated in PD in well-defined systems, but they represent anatomically and molecularly simplistic models. Each model lacks homologs of some of the important players in the pathways thought to be disrupted in human PD – for instance, LRRK2 and  $\alpha$ -synuclein (reviewed in: Kin *et al.*, 2019). To complement these studies, immortalized cell lines and induced-pluripotent stem-cell (iPSC)-derived models allow us to confirm molecular function and dysfunction experimentally in human cells. Cell lines are easy to grow and manipulate, but lack the high specialization/polarity of neurons. They have produced conflicting results, likely due to the wide array of lines available, and lack of consistency in those employed in the literature. iPSC-derived neuron-like cells can be produced from tissues donated by human PD mutation carriers, and can circumvent some of the issues with cell lines. Unfortunately, iPSCs still represent an emerging technology and are plagued with issues of heterogeneity within cultures grown from the same sample, and vastly different differentiation protocols employed between labs. They are also expensive, labour intensive, and slow to grow (cell cultures models of PD are reviewed in: Ferrari *et al.*, 2020). Primates are of course the most closely related animals in which to model human disease, but they are expensive to house, age slowly, and come with many ethical considerations.

Mouse models are the most widely used to study neurological disorders (reviewed in: Kin *et al.*, 2019), as they sit at the fulcrum between the advantages and caveats of disease modelling. They share a high degree of gene homology with humans, while being easy to house, and relatively fast to breed. The technology exists to create knock-out, knock-in, and conditional knock-in animals with relative ease. Their neurons tolerate being grown dissociated in culture fairly well,

and brain slices for *ex vivo* electrophysiology experiments can be maintained for many hours, under the right conditions. While their nervous systems are less developed than a human's, mice possess all of the same brain regions of interest to PD research. A main criticism, which is true of all models, is that they are behaviourally quite different from humans, making study of behaviour and 'mood' difficult to interpret.

There are several considerations to make when choosing a model. How closely does it mirror the etiology of the disease you're studying (construct validity)? How well are the pathological and behavioural aspects of the disease reproduced (face validity)? And how well are the treatments developed in the model translated into humans (predictive validity) (reviewed in: Chesselet and Richter, 2011)? Construct validity is the easiest to achieve in a mouse, now that we know of monogenic causes (modeled by mutation knock-ins), and we have some clues as to environmental factors that we can easily model in the laboratory (low-dose toxin exposure). Face validity, on the other hand, is usually achieved through harsh manipulations at the sacrifice of etiological resemblance to human PD. The predictive validity of any model is impossible to ascertain without an actual clinical trial, and may vary from treatment to treatment, in translation from mouse to human.

#### **1.1.5.1 Chemical lesion models**

Chemical lesion models take advantage of the selective vulnerability of dopaminergic neurons to toxins such as 6-OHDA and MPTP, using toxin administration to selectively lesion the SN (and other cells). Acute treatment with 6-OHDA and MPTP both cause rapid, non-progressive dopaminergic cell death, albeit through different mechanisms, which cause slightly different lesions (reviewed in: Bové *et al.*, 2005; Melrose *et al.*, 2006; Kin *et al.*, 2019). The primary drawback of chemical lesion models is that they do not recreate the slow and progressive

etiology of idiopathic PD, and perhaps more accurately model the effects of dopaminergic denervation in the later stages of the disease. Changes in corticostriatal glutamatergic pathways have been widely studied in these models, where medium spiny neurons (MSNs) of the striatum show a reduced dendritic arbor and spine density (Smith, Villalba and Raju, 2009), very similar to what is observed in human *post-mortem* brain samples. While chemical lesions do not provide many clues as to the pathogenesis of PD, they have been extremely useful for studying the effects of dopaminergic denervation, and the dyskinesias associated with long-term L-DOPA treatment (reviewed in: Melrose *et al.*, 2006; Chesselet and Richter, 2011).

#### **1.1.5.2 Chronic exposure models**

A response to the construct validity issues of acute chemical lesions was the development of chronic low-dose toxin models. These models are based on toxins that are correlated with increased risk of PD (such as the complex I inhibitors rotenone or paraquat), and use multiple low-dose exposures to induce pathology. Rotenone models have been particularly successful; chronic exposure, including via intranasal administration, can cause upregulation in  $\alpha$ -synuclein, progressive Lewy-like pathology, nigral cell death, and motor impairments (Betarbet *et al.*, 2000; reviewed in: Melrose *et al.*, 2006; Chesselet and Richter, 2011; Pan-Montojo *et al.*, 2012; Vingill, Connor-Robson and Wade-Martins, 2018). Other success has been achieved using paraquat, which is a complex I inhibitor like rotenone (reviewed in: Bové *et al.*, 2005; Vingill, Connor-Robson and Wade-Martins, 2018), but is more persistent in the environment and has been linked to neurotoxicity in humans following acute poisoning events (reviewed in: Bové *et al.*, 2005). These models also recapitulate some of the pathological inflammation seen in the brains of people with idiopathic PD, further adding to their face validity (reviewed in: Vingill, Connor-Robson and Wade-Martins, 2018)

### **1.1.5.3 Genetic models**

The discovery of monogenic causes of PD have allowed for etiological modeling over the last 20 years. Knock-out and overexpression mice have given us clues as to the basic functions of PD-related proteins in mammalian neurons, whereas knock-in models have given us the exceptional construct validity of studying a known causative mutation at endogenous levels of protein expression. A primary criticism of true knock-in models is that they tend to have lower face validity, often having subtle (or no detectable) motor phenotypes, whereas the models that do achieve high face validity often do so by sacrificing construct validity. For example, *SNCA* modeling has recapitulated a number of pathological and behavioural characteristics of PD, but has done so by overexpressing the A53T human mutant protein to a high degree within nigral cells, which may not express much endogenously (reviewed in: Melrose *et al.*, 2007; Chesselet and Richter, 2011; Foffani and Obeso, 2018).

Knock-in models of LRRK2 G2019S have produced promising results. The mice have early increases in dopamine release followed by a loss in dopamine tone as they age, alongside subtle motor and behavioural phenotypes (Beccano-Kelly, Kuhlmann, *et al.*, 2014; Adeosun *et al.*, 2017; Lim *et al.*, 2018), although there is little cellular pathology observed even in aged animals (Volta *et al.*, 2017). In cells cultured from these mice, endogenous levels of G2019S make cells more vulnerable to seeding of insoluble alpha-synuclein fibrils (Volpicelli-Daley *et al.*, 2016; MacIsaac *et al.*, 2020), and environmental toxin exposure (Cannon and Greenamyre, 2013).

I have been using a novel VPS35 D620N model of late-onset autosomal-dominant PD for my doctoral research. Initial characterization of the mice showed that they also have altered dopamine release in the striatum, specifically increases at young ages (Ishizu *et al.*, 2016; Cataldi *et al.*, 2018), subtle gait impairment at older ages (Chen *et al.*, 2019), and tau pathology

(Chen *et al.*, 2019) reminiscent of that seen in many brains of human LRRK2 carriers at autopsy.

Modeling of PD should take into consideration the subtle and prolonged nature of disease in a human being, where motor symptoms arise only after 50+ years. One must ask oneself if it is reasonable to expect a motor phenotype in a mouse that lives ~2 years, if the model faithfully reflects the etiology of PD. I would argue that it is just as, if not more, valuable to study the very early changes to cellular processes that occur prior to onset of overt phenotypes in models of familial PD, in the hope that earlier detection and intervention would prevent the onset of many of the later symptoms in humans. It is upon this opinion that my doctoral work was conducted in the knock-in mouse model of VPS35 parkinsonism.

## **1.2 Vacuolar protein sorting 35**

Biologists studying protein trafficking in *S. Cerevisiae* were the first to discover Vacuolar Protein Sorting 35, hereafter VPS35. They found that mutations in VPS35 (then vpt7) resulted in surface expression of cargo that typically resides in the vacuole (Bankaitis, Johnson and Emr, 1986). In yeast, it was found to be part of a pentameric protein complex that was dubbed the ‘retromer’ complex, due to its role in the retrograde trafficking of the carboxypeptidase receptor Vps10 back to the trans-Golgi network for recycling after delivering its bound enzymes to the vacuole (Seaman *et al.*, 1997; Seaman, McCaffery and Emr, 1998). Several independent groups cloned murine and human retromer homologs in the year 2000 (Edgar and Polak, 2000; Haft *et al.*, 2000; Zhang *et al.*, 2000). Several years later it was confirmed to have a similar role in mammalian cells as in yeast, trafficking cation-independent mannose-6-phosphate receptor (CI-MPR) out of endosomes and back to the *trans*-Golgi network after the delivery of acid hydrolase enzymes (Arighi *et al.*, 2004; Seaman, 2004).

In the years since, scientists have found that the retromer complex is a ubiquitous and highly conserved eukaryotic protein complex whose mammalian homologs have a versatile array of interacting partners and thus functions. Mammalian retromer forms a cytoplasmic coat on membranous organelles and participates in the intracellular trafficking of myriad transmembrane receptors, channels, and transporters. Its functions support lysosomal maturation, metabolic homeostasis, maintenance of cell polarity, and mitochondrial quality control, to name a few. With such a broad range of functions, it is perhaps of little surprise that a full knock-out of VPS35 or VPS26 (another retromer complex member) in mice is embryonic lethal (Muhammad *et al.*, 2008; Wen *et al.*, 2011) and perturbations to retromer have been linked to multiple neurodegenerative diseases in humans. Understanding retromer's many interconnected jobs is both fascinating from a cell biological standpoint and important for unraveling the etiology of human disease.

### **1.2.1 The canonical retromer complex in mammalian cells**

There is an expansive literature on retromer function in *S. Cerevisiae*, *D. melanogaster*, and *C. elegans*. The contribution of these studies to our understanding of endosomal protein trafficking should not be understated; however, due to the observed divergence in the interactions between homologous proteins between species, and the existence of additional binding partners in mammalian cells, I will focus primarily on the structure and functions of the mammalian retromer complex here.

The full mammalian retromer complex comprises two sub-complexes: the so-called cargo recognition complex (CRC; elsewhere the cargo selective complex/CSC), a trimer comprised of VPS26, VPS29, and VPS35 (Edgar and Polak, 2000; Haft *et al.*, 2000), and a dimer of two BAR-domain-containing sorting nexin (SNX) proteins (SNX-BAR dimer). The SNX-BAR dimer is

comprised of either SNX1 and 6, or SNX 2 and 5 (Haft *et al.*, 2000; Griffin, Trejo and Magnuson, 2005; Wassmer *et al.*, 2007).

VPS35 is the 92kDa central protein of the CRC, bookended by VPS29 bound on its C-terminus, and VPS26 bound on its N-terminus (Arighi *et al.*, 2004; Hierro *et al.*, 2007). The trimer appears to be a flexible bar-like structure that can arch with the curvature of membrane tubules extending from endosomes (Kovtun *et al.*, 2018; Kendall *et al.*, 2020). VPS35 itself has a helical solenoid structure, similar to the cargo-binding subunits of AP adaptor proteins and COPII coats, responsible for endocytosis of cargo at the plasma membrane (Hierro *et al.*, 2007). The curvature of VPS35 exposes hydrophobic grooves between helices, which are putative cargo binding sites (*ibid*), and VPS35 is able to bind the cytoplasmic tail of some cargos directly (Arighi *et al.*, 2004). VPS29 has a mellatophosphoesterase fold that was originally believed to act as a cargo, or coat protein, phosphatase (Wang *et al.*, 2005), but has since been shown to be a catalytically inactive structural scaffold for VPS35 binding (Collins *et al.*, 2005; Hierro *et al.*, 2007). VPS26 is structurally related to the arrestin proteins that bind the cytoplasmic tail regions of activated G-protein coupled receptors (GPCRs; Shi *et al.*, 2006). It is proposed to play a role in cargo recognition, either by binding cargo directly (McGarvey *et al.*, 2016) or through cargo-specific adaptors (Steinberg *et al.*, 2013; Gallon *et al.*, 2014; Lucas *et al.*, 2016). An additional role has been proposed in terminating GPCR signaling, by displacing  $\beta$ -arrestin from the receptor (Feinstein *et al.*, 2011, 2013). There are two known paralogs of VPS26 in mammalian cells, VPS26A and VPS26B, which confer some redundancy in the case of knock-down studies (Gallon *et al.*, 2014), but are believed to form functionally distinct retromer complexes (Bugarcic *et al.*, 2011, 2015).

Retromer is involved in the trafficking of numerous transmembrane proteins that have divergent cellular destinations, leading to the question of how it identifies cargoes bound for different locations. The existence of two VPS26 paralogs with different functions is one way of conferring some flexibility. Another is the binding of various adaptor proteins that enhance binding of specific cargoes and thus code for destination.

SNX27 (a non-BAR SNX) has been shown to be necessary for the surface trafficking of several retromer cargoes (Temkin *et al.*, 2011; Steinberg *et al.*, 2013; Gallon *et al.*, 2014; Clairfeuille *et al.*, 2016; Lee, Chang and Blackstone, 2016; Binda *et al.*, 2019). It contains a PDZ-domain binding motif that confers cargo specificity for cargoes with a PDZ domain in their cytoplasmic tail. SNX27 can bind both VPS26 and PDZ domains simultaneously (Steinberg *et al.*, 2013), an interaction that increases its avidity for cargo proteins (Gallon *et al.*, 2014). SNX27 also binds transmembrane proteins without PDZ domains, provided they are phosphorylated at an appropriate residue, allowing for extra control over the recycling of these cargoes (Clairfeuille *et al.*, 2016). Similarly, SNX3 is another non-BAR SNX that can bind VPS26 and cargo cooperatively, forming a cargo binding pocket at the interface between them (Lucas *et al.*, 2016). Some studies have even found that retromer cargoes themselves can act as adaptors for further cargo binding. Sortilin is an acid hydrolase receptor that is rescued from maturing endosomes by classical retromer retrograde trafficking (Canuel *et al.*, 2008), and has been shown to bind other transmembrane proteins prior to its recycling, acting as a cargo adaptor itself (X. Pan *et al.*, 2017).

The CRC is capable of binding cargos, either directly or through adaptors, but possesses no domain by which it can intrinsically bind membranes. The SNX proteins contain a phox-homology (px) domain that can bind phosphoinositides directly and are required for their



endosomal localization (Carlton *et al.*, 2004). VPS35 binds SNX1 (Haft *et al.*, 2000), and knock-down of SNX1 reduces the endosomal localization of the CRC considerably (Rojas *et al.*, 2007), suggesting the SNX-BAR dimer binds the membrane first, and CRC is recruited after. BAR domains can both sense curvature and, at high concentrations, generate it (Carlton *et al.*, 2004). Retromer complexes can form dimers, tetramers, or chains through VPS35-VPS35 and VPS26-VPS26 interactions (Kovtun *et al.*, 2018; Kendall *et al.*, 2020). This could be the mechanism by which the SNX-BAR dimer becomes condensed enough to generate tubules once associated with cargo-bound CRC, and indeed, most SNX-BAR tubulation is observed around the time of the Rab5-7 switch (van Weering, Verkade and Cullen, 2012) when the CRC is recruited to the endosome. Whilst SNX1 & 2 bind membranes, their requisite partners SNX5 & 6 bind to p150<sup>glued</sup>, linking cargo-filled tubules to dynein motor proteins on microtubules to generate the tension necessary for membrane fission and/or transport (Wassmer *et al.*, 2007).

The retromer complex is itself a Rab7 effector; it also interacts and colocalizes with GTP-bound (active) Rab7 on late endosomes, which is required for normal levels of CRC membrane recruitment (Rojas *et al.*, 2008; Seaman *et al.*, 2009). TBC1D5 is a GTPase-activating protein (GAP) that interacts with retromer and deactivates Rab7, acting as a negative regulatory signal for Rab7-retromer-mediated trafficking (Seaman *et al.*, 2009; Jia *et al.*, 2016; Jimenez-Orgaz *et al.*, 2018; Seaman, Mukadam and Breusegem, 2018). In the absence of TBC1D5, active Rab7 becomes sequestered at lysosomal membranes, and inactive Rab7 is reduced on originating membranes (Jimenez-Orgaz *et al.*, 2018), thus interfering with some of its non-endosomal cellular functions. It is interesting that knock-down of TBC1D5 does not impair endosome-to-Golgi or surface recycling of some cargoes, but results in the accumulation of others, such as CI-MPR, in vesicular structures outside early endosomes (Harbour *et al.*, 2010; Jia *et al.*, 2016;

Jimenez-Orgaz *et al.*, 2018). This suggests that some, but not all, retromer trafficking is mediated by Rab7.

The generation of cargo-filled tubules tethered to dynein and activation of Rab7 alone are not sufficient for the sorting and trafficking of retromer cargoes. Retromer also associates with the WASH complex, an Arp2/3 actin nucleation complex that has no homolog in yeast (Linardopoulou *et al.*, 2007). Manipulations of WASH1 (the subunit responsible for f-actin nucleation), or the prevention of f-actin polymerization, results in elongated SNX1 extensions from endosomes that run parallel to microtubules (Derivery *et al.*, 2009; Gomez and Billadeau, 2009; Duleh and Welch, 2010; Harbour *et al.*, 2010). These manipulations also impair the retrograde trafficking of a canonical retromer cargo, CI-MPR (Gomez and Billadeau, 2009; Harbour *et al.*, 2010). WASH interacts with dynamin II, and inhibition of dynamin with dynasore results in a similar elongated SNX-tubule phenotype (Derivery *et al.*, 2009). It is thus believed that WASH-mediated polymerization of f-actin generates a pushing force counter to the pulling by SNX5/6 along microtubules, and recruits dynamin II to promote scission of cargo-loaded tubules for transport.

WASH complex localizes most strongly with SNX1 in early endosomes (Derivery *et al.*, 2009; Gomez and Billadeau, 2009; Duleh and Welch, 2010), overlapping only partially with Rab7- (Derivery *et al.*, 2009) and Rab11-positive endosomal domains (*Ibid*; Duleh and Welch, 2010). The WASH complex can colocalize with SNX1 or 2 (Gomez and Billadeau, 2009; Harbour *et al.*, 2010); however, the SNX-BAR dimer is not required for WASH recruitment to the membrane (Gomez and Billadeau, 2009). Knock-down of the WASH complex member FAM21 prevents WASH1 recruitment to the endosomal membrane (Gomez and Billadeau, 2009; Jia *et al.*, 2012), and multiple groups have replicated the finding that FAM21 binds to VPS35 directly (Harbour,

Breusegem and Seaman, 2012; Jia *et al.*, 2012; Helfer *et al.*, 2013). It is intriguing that if you knock-down the CRC, WASH1 can still be recruited to SNX1-positive structures but FAM21 signal is lost (Harbour *et al.*, 2010), suggesting that continued WASH1 membrane association is independent of FAM21 inclusion in the complex and does not rely on FAM21 binding to retromer. FAM21 can also bind directly to the surface-adaptor SNX27 (Temkin *et al.*, 2011; Freeman, Hesketh and Seaman, 2014), which may provide a mechanism for its ability to recruit WASH1 to the endosome in the absence of the CRC.

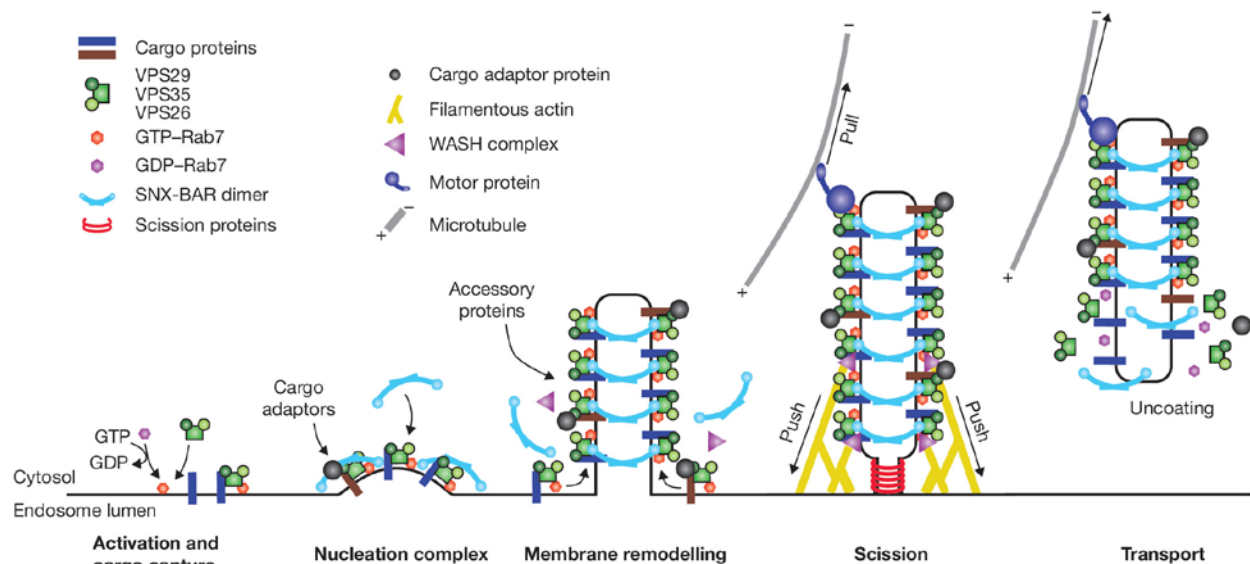


**Figure 1-1 Proposed mechanism of canonical SNX-BAR-Rab7-retromer cargo retrieval.** Activated membrane-bound Rab7 and target cargo recruit the CRC to the membrane, followed by the inclusion of SNX-BAR dimers to generate membrane tubulation. Further binding of WASH generates f-actin patches at the base of the tubule with scission proteins (dynaminII) and SNX-BAR association to motor proteins creates a dynamic force necessary for tubule scission. The membrane coat is proposed to disassemble following scission (possibly mediated by TBC1D5 - not shown). *Reprinted by permission from Springer Nature, Nature Cell Biology, Sorting nexins provide diversity for retromer-dependent trafficking events, Cullen & Korswagen © 2011.*

FAM21 has a globular head group with a long unstructured tail. Overexpressing truncated tail-only FAM21 reduces WASH1 localization to the membrane (Harbour, Breusegem and Seaman, 2012; Helfer *et al.*, 2013). Once on the membrane, WASH1 activity is negatively regulated by the amount of actin polymerization, which dissociates WASH1 from the membrane (Derivery *et al.*, 2012). One study (albeit in *Dictostylium*) found that knock-down of FAM21 resulted in extended patches of f-actin localized with WASH1 (Park *et al.*, 2013). A mammalian knock-down study found that FAM21 was not required to rescue surface recycled cargoes out of the degradative pathway, but was necessary for the eventual delivery of cargo-filled vesicles to the surface (Lee, Chang and Blackstone, 2016), calling into question whether FAM21 is actually necessary for WASH1 actin nucleation. The implication of this is that FAM21 is not required for cargo rescue from the degradative pathway, but may be necessary to get them to their destination (perhaps by signaling the removal of WASH and allowing the assembly of new coat proteins required for surface delivery).

The FAM21 tail contains multiple repeating binding motifs that can bind more than one retromer CRC, and has been proposed to act as a coincidence detector when it binds across several units of retromer condensed in a tubular membrane (Jia *et al.*, 2012). This has largely been interpreted as a way for the WASH complex to be recruited to areas of dense cargo binding to assist with tubule dynamics, but again it is possible that this multivalent binding acts to detect when enough cargo has been loaded into the tubule and signals for the release of the WASH complex.

Many other proteins have been implicated in the process of cargo capture, membrane tubulation, and trafficking. EHD1 binds retromer, and its knock-down destabilizes SNX1-positive tubules (Gokool, Tattersall and Seaman, 2007). RME8 binds both SNX1 and FAM21

and is thought to coordinate WASH complex activation. RME8 knock-down results in tubulation phenotypes similar to WASH knock-downs, and prevents SNX1 turnover on endosomes (Freeman, Hesketh and Seaman, 2014). VARP is a Rab32/38 effector that is recruited to membranes via binding to VPS29 and further binds and traffics the R-SNARE VAMP7, which mediates vesicle fusion events (Hesketh *et al.*, 2014)

It is evident from the literature that retromer-mediated trafficking involves the coordination of many proteins at different steps, many of which have likely not yet been discovered. One study assayed the effects of manipulating various retromer interactors on surface-bound cargoes, and found that these manipulations had different (or no) effects dependent on the cargo being used as a readout (Ian J. McGough *et al.*, 2014). It appears that there is a great deal of flexibility in the way these proteins interact to form multiple pathways for different cargoes.

### **1.2.2 Non-canonical retromer complexes**

The above description is the ‘classical’ or ‘canonical’ retromer story, but unlike in yeast, the association between the CRC and the SNX-BAR dimer in mammalian cells is weak (Rojas *et al.*, 2008), allowing the CRC and SNX-BAR dimer to exist independently and associate with other proteins. CRC components can be found localized to early endosomes apart from Rab7 (Rojas *et al.*, 2008; Temkin *et al.*, 2011). There it does not interact with Rab5, nor reside in the same subdomains on early endosomes, making it unlikely that VPS35 also acts as a Rab5 effector (Rojas *et al.*, 2008; Seaman *et al.*, 2009). While SNX1 tubules can form on early endosomes if the Rab5-7 switch is blocked, retromer does not decorate those tubules (van Weering, Verkade and Cullen, 2012), implying that early endosomal retromer trafficking pathways exist independently of the SNX-BAR dimer.

The CRC coIPs with and colocalizes on early endosomes with the non-BAR SNX3 (Harterink *et al.*, 2011; Harrison *et al.*, 2014; McGough *et al.*, 2018). Some retromer cargoes sorted from early endosomes colocalize with SNX3 and clathrin, and form small vesicles rather than extended tubulo-vesicular structures, leading Harterink and colleagues (*ibid*) to propose that SNX3-CRC is a distinct complex that traffics cargo out of early endosomes through clathrin-mediated vesicular budding. Since Rab7 does not reside on early endosomes and VPS35 is a Rab effector, it seems likely that another Rab-GTPase mediates this process, though which one has yet to be identified.

Similarly, some SNX27-retromer cargoes traffic from early endosomes in a Rab7-independent manner and associate with Rab4 (Temkin *et al.*, 2011), whereas others require SNX-BAR dimer not for their rescue out of endosomes, but for their efficient surface trafficking (Steinberg *et al.*, 2013). SNX27 itself is not always required for retromer surface delivery; one team has proposed a retromer-NSF surface recycling complex (McGarvey *et al.*, 2016). It is worth noting that a retromer-independent SNX27 surface trafficking pathway has also been discovered (Binda *et al.*, 2019) indicating that, like the CRC itself, these adaptor proteins can participate in multiple trafficking pathways.

It has already been mentioned that two VPS26 paralogs exist that result in distinct retromer complexes. Further investigation into CRC assembly has found that VPS35 and VPS29 can form a stable dimer when overexpressed together (Haft *et al.*, 2000) or after VPS26A and B double knock-down (Fuse *et al.*, 2015). The possible functions of a VPS29-VPS35 only retromer are unknown. In light of this finding, it is interesting to revisit some of the original studies of retromer depletion (which were conducted by knocking down VPS26), where endosome-to-Golgi cargo surface labeling was increased by this manipulation (Seaman, 2004). This could

have been due to knock-down of only VPS26A (as this was prior to the discovery of VPS26B), resulting in a shift toward one pathway, or it could have resulted from a VPS26-less retromer complex redirecting traffic to the cell surface, though it is unknown to me if the siRNAs used in this study could deplete both proteins.

A recent study has also found that VPS29 is part of another mammalian protein complex, the retriever complex, that is very similar to retromer in structure, resides in the same endosomal subdomains, and can bind WASH (McNally *et al.*, 2017). Haft and colleagues (2000) predicted this discovery when they first studied the tissue expression of retromer components and discovered that VPS29 expression was enriched in some tissues that were not enriched for VPS35 and VPS26.

Given the incredible flexibility of retromer to bind different arrangements of accessory proteins, is it of little surprise that it has been associated with the trafficking of numerous cargoes, in support of a broad spectrum of cellular functions.

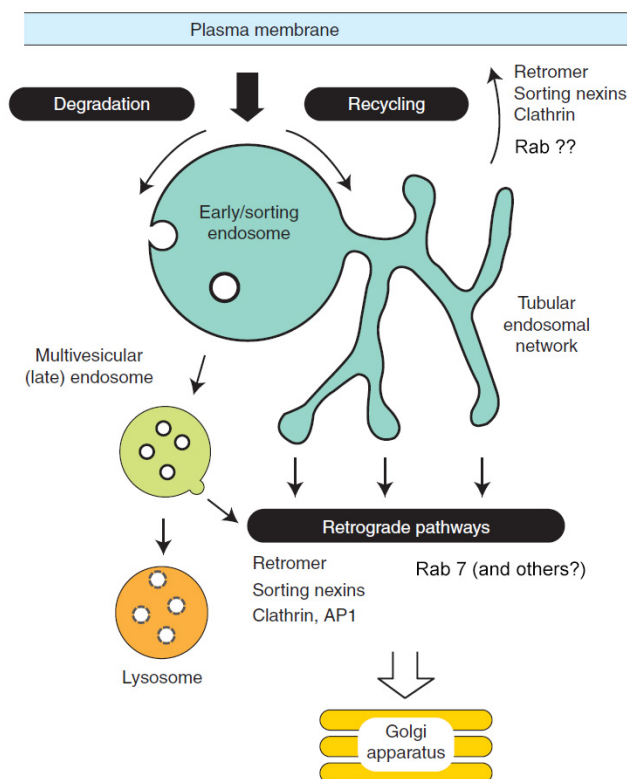


**Figure 1-2** Diagram of the endolysosomal maturation pathway and the pathways of cargo recycling through tubular endosomal extensions. Endocytosed cargo can remain in endosomes as they mature from early-late endosomes and are fused with lysosomes for degradation, or, they can enter into retromer-mediated surface or Golgi trafficking routes for reuse. *Reproduced with permission from Burd & Cullen, 2014 © Cold Spring Harbor Laboratory Press.*

### **1.2.3 Functions**

#### **1.2.3.1 Lysosomal maturation**

After the initial discovery that yeast retromer traffics acid hydrolase receptor Vps10 out of the vacuole, the first function of the mammalian retromer complex to be tested and described in the literature was the retrograde trafficking of the similar cation-independent mannose-6-phosphate receptor from maturing endosomes back to the trans-Golgi network (Arighi *et al.*, 2004; Seaman, 2004). Other Vps10-family sorting receptors in mammalian cells are trafficked by retromer including sortilin and SorLA (Canuel *et al.*, 2008; Muhammad *et al.*, 2008). These receptors deliver acid hydrolases to maturing endosomes and, accordingly, impairments in retromer function have been shown to impair lysosomal degradation, likely due to the inability of these receptor proteins to return to the TGN to be reloaded with their enzymatic cargoes (Arighi *et al.*, 2004; Seaman, 2004; Rojas *et al.*, 2007; Canuel *et al.*, 2008; Cui *et al.*, 2019). Recently, a retromer-independent trafficking pathway for CI-MPR through SNX-BAR dimers has been discovered (Kvainickas *et al.*, 2017; Simonetti *et al.*, 2017), calling into question whether retromer is truly involved. For a review of the arguments for and against this, I suggest a short piece by one of key stake-holders in this discussion, Dr. Matthew Seaman (Seaman, 2018).

#### **1.2.3.2 Metabolic homeostasis**

The retromer has been implicated in the trafficking of a host of nutrient and ion transporters including, but not limited to, glucose transporter 1 (Steinberg *et al.*, 2013), glucose transporter 4 (X. Pan *et al.*, 2017), copper transporter ATP7A (Steinberg *et al.*, 2013), and divalent metal transporter I (Hirayama *et al.*, 2019). In adipocytes, for example, Glut4 is internalized following glucose uptake and, rather than being degraded, it is trafficked via retromer back to the TGN where it is stored in insulin-responsive vesicles to await signalling by insulin for its return to the



plasma membrane (X. Pan *et al.*, 2017). Retromer is also involved in the homeostatic surface regulation of hormone and protease receptors such as the  $\beta$ 2-adrenergic receptor ( $\beta$ 2-AR) (Puthenveedu *et al.*, 2010; Temkin *et al.*, 2011), parathyroid hormone receptor (Feinstein *et al.*, 2011; Chan *et al.*, 2016), protease activated receptor-2 (Bugarcic *et al.*, 2015), and vasopressin receptor type II (Feinstein *et al.*, 2013).

#### **1.2.3.3 Transcytosis and maintenance of cell polarity**

Retromer mediated recycling specificity appears to be necessary for the maintenance of cell polarity by ensuring polarized sorting of receptors. For instance, TGF $\beta$  is required for epithelial cell polarity; it is internalized after activation and recycled via a retromer and Rab11-dependent pathway back to the basolateral membrane (Yin *et al.*, 2013). When retromer is knocked down the receptor can still recycle, but is dispersed between apical and basolateral membranes (*ibid*). Similarly, retromer is involved in the transcytotic trafficking of the polymeric immunoglobulin receptor, a process that is necessary for the maintenance of cell polarity (Vergés *et al.*, 2004).

#### **1.2.3.4 Wnt signalling**

Wnt proteins are secreted glycoproteins that are central regulators of tissue morphogenesis and repair (Budnik and Salinas, 2011; Spang, 2011; Salinas, 2012). They are delivered to the cell surface for secretion on wntless receptors, which are then endocytosed, and undergo SNX3-retromer mediated recycling back to the TGN for reloading (Belenkaya 2008; Yang 2008). This important role in development is likely the reason that VPS35 or VPS26 full knock-out in mice is embryonic lethal (Muhammad *et al.*, 2008; Wen *et al.*, 2011).

#### **1.2.3.5 Mitochondrial vesicle trafficking and quality control**

Retromer has also been shown to localize to mitochondria, where it is involved in the formation of mitochondrial-derived vesicles and transport of mitochondrial-anchored protein ligase (MAPL) to peroxisomes (Braschi *et al.*, 2010). MAPL is a ubiquitin ligase, and, as such, retromer depletion causes increased ubiquitination and degradation of mitochondrial proteins (F. L. Tang *et al.*, 2015). Retromer, in association with EHD1, has also been shown to be necessary for the turnover of inactive dynamin-like protein 1 (Dlp1) on mitochondria, which is important for mitochondrial fission and complex I assembly (W. Wang *et al.*, 2016; Farmer *et al.*, 2017; Wang *et al.*, 2017; Zhou *et al.*, 2017). Furthermore, Rab7 is activated in response to mitochondrial stress and Rab7-retromer appears to be necessary for PINK1-parkin-mediated mitophagy (Heo *et al.*, 2018; Jimenez-Orgaz *et al.*, 2018).

**Table 1-1 List of known SNX-BAR-retromer and SNX3-retromer pathways at the outset of my dissertation work.** Reprinted by permission from Springer Nature, *Nature Cell Biology*, *Sorting nexins provide diversity for retromer-dependent trafficking events*, Cullen & Korswagen © 2011.

Table 1 Identified retromer cargo proteins	
Process	Mechanism
Cargo sorting of intracellular receptors including Vps10, MPRs, DMT1-II, sortilin, SorLA, AtVSR1/AtELP, in various organisms	Retrieval of the receptors from endosomes-to-TGN. Described tripeptide sorting motifs through which VPS35 associates with cargo being: WLM (CI-MPR); FLV (sortilin); YLL (DMT1-II)
Transcytosis of polymeric immunoglobulin receptor (pIgR) and its ligand, polymeric IgA	Retrieval of internalized pIgR-pIgA, thus allowing for its transport to the opposite plasma membrane
Maintenance at the plasma membrane of the reductive iron transporter, Fet3-Ftr1, under low iron conditions in <i>Saccharomyces cerevisiae</i>	Retrieval of internalised transporter to the TGN mediated in conjunction with the adaptor Grd19 (also known as Snx3)
Termination of cyclic AMP by internalized parathyroid hormone receptor (PTHr)	Retrieval of PTHR from endosomes-to-TGN
Recycling of $\beta$ 2-adrenoreceptor	Retrieval of internalized receptor directly to the plasma membrane in conjunction with the adaptor SNX27
Cell polarity and organ initiation mediated by the phytohormone auxin, and plant growth and senescence in vegetative organs in <i>Arabidopsis thaliana</i>	Retrieval and polarized delivery of the auxin efflux carrier, PIN. Transport of proteins to protein storage vacuoles (PSVs)
Secretion of Wnt morphogens and generation of Wnt gradients during development	SNX3-retromer regulated retrieval of the Wnt receptor/chaperone, Wntless, from endosomes-to-TGN to allow for further rounds of Wnt secretion
Endocytic trafficking, signalling and tumour suppression in <i>Drosophila melanogaster</i>	Inhibition of Rac1-dependent actin polymerization
Apoptotic cell clearance in <i>C. elegans</i>	Retrieval of internalized phagocytic receptor, CED-1, back to cell surface
Maintaining apico-basal polarity and integrity of epithelial tissues in <i>D. melanogaster</i>	Retrieval of the apical determinant Crumbs from endosomes
Neurodegenerative disease	Retrieval of the amyloid precursor protein (APP), its sorting receptor (SorLA) or its processing peptidase ( $\beta$ - and $\gamma$ -secretase). Link with late onset Alzheimer's disease. VPS35 mutation, Asp620Asn, associated with late onset Parkinson's disease
Trafficking of pathogens ( <i>Salmonella</i> , Herpesvirus saimiri), and toxins (for example, <i>Shiga</i> toxin).	Retrieval of membrane and cargo from <i>Salmonella</i> -containing vacuole. Endosomes-to-TGN transport of internalized toxins. VPS35 target of HVS Tip protein, which by inhibiting retromer contributes to efficient T cell transformation.
Type 2 Diabetes	Genome-wide association study identified variants in VPS26A in South Asians.
Mitochondria to peroxisome transport	Association with mitochondrial-anchored protein ligase, MAPL.

#### 1.2.4 Neuron-specific functions

VPS35 is highly expressed in the brain (Haft *et al.*, 2000), yet had only been studied in peripheral cells and cell lines in mammalian systems until the 2005 discovery that retromer protein levels are reduced in the brain regions most prone to degeneration in people with late-onset Alzheimer's disease (Small *et al.*, 2005). In 2011, our wider research group, and another,

simultaneously discovered a missense mutation in VPS35 that causes late-onset autosomal-dominant Parkinson's disease. The involvement of retromer in neurodegeneration begged the question of whether it has neuron-specific functions, or if perturbations to its more universal cellular functions were the root cause of neuronal vulnerability in brain disease. This question has motivated a flurry of research by neuroscientists interested in retromer.

Retromer is expressed throughout the brain in both neurons and glia, and seems particularly enriched in pyramidal cells in the hippocampus and cortex (Muhammad *et al.*, 2008; Wen *et al.*, 2011; Tsika *et al.*, 2014), ventral midbrain, brainstem, and cerebellum (Tsika *et al.*, 2014). Within neurons, retromer clusters are dynamically active in soma, axons, presynaptic terminals, dendrites, and dendritic spines of primary cultured neurons (Bhalla *et al.*, 2012; Choy *et al.*, 2014; Munsie *et al.*, 2015; Vazquez-Sanchez *et al.*, 2018). It has been implicated in a number of neuronal functions from neurite development to pre- and postsynaptic maintenance.

#### **1.2.4.1 Nervous system development**

Retromer is ubiquitously expressed and is critically required for mammalian development, given the embryonic lethality of VPS35 or VPS26 knock-outs (Muhammad *et al.*, 2008; Wen *et al.*, 2011). In mice, expression of VPS35 peaks at P10-15, then lowers and remains stable in adulthood (Wang *et al.*, 2012), timing that coincides with neurite development and glutamate synapse formation (Sharpe and Tepper, 1998; Tepper *et al.*, 1998; Sohur *et al.*, 2014). Indeed, VPS35 haploinsufficiency or *in utero* knock-down results in reduced neurite outgrowth, reduced spine density, and axonal swelling in glutamatergic pyramidal cells of the hippocampus and cortex (Wen *et al.*, 2011; Wang *et al.*, 2012; Tian *et al.*, 2015; Tang *et al.*, 2020). Overexpression of VPS35 in cultured cortical neurons also results in neurite outgrowth impairments (Tsika *et al.*, 2014) and reductions in synapse number (Munsie *et al.*, 2015). Even in adult hippocampi,

haploinsufficiency results in a reduction in the number of spines, with no resultant change in electrophysiological readouts, suggesting that, in the adult brain, VPS35 plays a role in the stabilization or maturation of immature spines lacking AMPA receptors (Tian *et al.*, 2015; Temkin *et al.*, 2017). Together, these studies highlight the importance of VPS35 for the development, maturation, and maintenance of neurites and synapses.

Recall that retromer-mediated trafficking of the wntless receptor is a regulator of wnt signaling. Wnts have an established role in neuronal development, axon outgrowth, recovery, and spine plasticity (Inestrosa and Arenas, 2010; Budnik and Salinas, 2011; Salinas, 2012). Antagonism of wnt signalling in cultured hippocampal cells results in the degeneration of glutamatergic synapses (Galli *et al.*, 2014). While these studies have yet to implicate retromer directly, it will be interesting to follow the research to see if wntless trafficking lies at the heart of the neurodevelopmental roles of retromer.

#### **1.2.4.2 Postsynaptic receptor trafficking**

Reports released by our group and others just prior to, and throughout, the course of my doctorate work have implicated VPS35 in the surface trafficking of multiple neurotransmitter receptors and excitatory neuroligins. To date, it has been shown to associate with:  $\beta$ 2-adrenergic receptors (Temkin *et al.*, 2011; Choy *et al.*, 2014); glycine receptors (del Pino *et al.*, 2011); GluA1-containing AMPA-type glutamate receptors (Zhang *et al.*, 2012; Tsika *et al.*, 2014; Munsie *et al.*, 2015; Tian *et al.*, 2015); D1-type dopamine receptors (C. Wang *et al.*, 2016); GluN2-containing NMDA-type glutamate receptors (Clairfeuille *et al.*, 2016; Ma *et al.*, 2017); and neuroligins 1 and 3 (Kang *et al.*, 2014; Binda *et al.*, 2019).

Given the ubiquity of glutamatergic transmission throughout the brain, and the well-characterized nature of synaptic maturation and plasticity in the hippocampus and, to a lesser extent the cortex, retromer-mediated trafficking of AMPARs in these brain regions is the primary focus of most brain-specific retromer research. VPS35 co-immunoprecipitation preferentially pulls GluA1-containing AMPARs (though it does also pull GluA2 to a lesser extent) (Munsie *et al.*, 2015). GluA1 has a long cytoplasmic tail containing a PDZ domain and its surface expression depends upon a SNX27-dependent trafficking route (Hussain *et al.*, 2014). GluA1-containing AMPARs are vital to both the establishment of new synapses in the developing brain and the signal-mediated initiation of LTP in the adult brain, whereas GluA2/3 heteromers cycle constitutively in and out of mature glutamatergic synapses and are more important for LTD (reviewed in: Diering and Huganir, 2018).

In immature glutamatergic cells in culture, VPS35 knock-down reduces AMPAR-mediated currents (Choy *et al.*, 2014), and haploinsufficiency impairs spine maturation, reduces dendritic clustering, and impairs surface expression of GluA1, but not GluA2 (Tian *et al.*, 2015). Overexpression of GluA2, but not GluA1, can rescue the spine maturation phenotype (*ibid*). The authors interpret this finding to mean that GluA2 is preferentially trafficked by retromer, but I

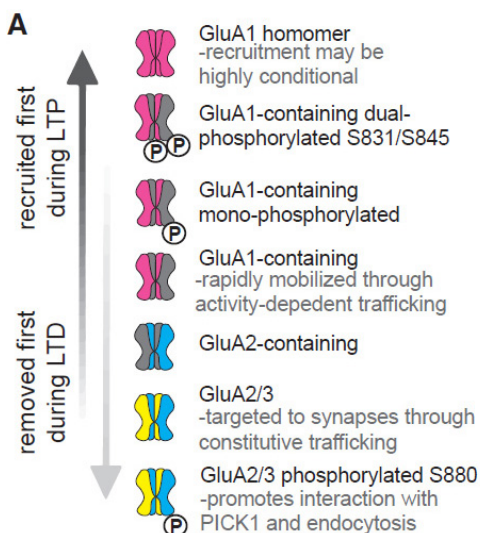


**Figure 1-3 Hierarchy of AMPAR insertion during LTP or removal during LTD based on subunit composition.**

GluA1 homomers are recruited to potentiated sites first, and GluA1 containing AMPARs are preferentially associated with the earlier stages of LTP induction. Similar hierarchies are believed to be in play during development. *Reprinted from Neuron, 100(2), Diering & Huganir, The AMPA Receptor Code of Synaptic Plasticity, pg 320, © 2018, with permission from Elsevier.*

would argue for the opposite – that overexpressed GluA2 is trafficked through a retromer-independent route. In mouse cortical neurons, we showed that overexpression of wild-type VPS35 also reduces synapse density, the frequency of excitatory synaptic currents, and AMPAR trafficking (Munsie *et al.*, 2015). The similar effects of knock-down and overexpression suggest that proper retromer functioning depends upon having appropriate ratios of VPS35 and its accessory binding partners.

In 2-month-old mice, Tian and colleagues (2015) found that haploinsufficiency reduces the amplitude and frequency of mEPSCs alongside reduced mature spines and synapse density in the hippocampus. They also measured synaptosomal proteins and discovered reductions in GluA1, GluA2, PSD95, and (possibly compensatory) increases in presynaptic protein synapsin I. Conversely, Temkin *et al.* (2017) used *in vivo* lentiviral knock-down of VPS35 in mature neurons in 5-7 week-old mice, and found that basal transmission in the hippocampus was unaltered, whereas LTP was impaired. These differences suggest that 1) early developmental deficits created by haploinsufficiency persist into adulthood; and 2) retromer-mediated trafficking of GluA1 supports synapse development, and activity-dependent synaptic plasticity in adult brains. These findings are perhaps unsurprising given the previously described roles of GluA1 itself in development and plasticity. Complicating things slightly, Muhammad *et al.* (2008) found that VPS26 haploinsufficient mice were impaired in LTP but not basal transmission; however, given that we now know VPS26 has several paralogs with different trafficking functions, and that VPS29 and VPS35 can form a stable dimer, it is possible that VPS26A supports LTP, but not development.

Based on overexpression and knock-out studies, retromer is clearly important in synapse development, maintenance, and functional connectivity (Wen *et al.*, 2011; Wang *et al.*, 2012;

Choy *et al.*, 2014; Tsika *et al.*, 2014; Munsie *et al.*, 2015; Tian *et al.*, 2015; Temkin *et al.*, 2017).

It is important to keep in mind that none of these studies has assayed whether retromer-dependent trafficking in neurons represents the recycling of internalized receptors or the delivery of newly synthesized AMPARs, though the canonical literature would suggest the latter. New work has shown that AMPARs can be locally synthesized in dendrites where they bypass the regular Golgi-routed secretory route and are trafficked via retromer-adjacent organelles into recycling endosomes prior to surface delivery (Mikhaylova *et al.*, 2016; Bowen *et al.*, 2017).

Of course, AMPARs are not the only neuron-specific retromer cargo. A recent bioinformatics study listed over 400 putative cargoes for retromer in the brain (Clairfeuille *et al.*, 2016).

Though less well-characterized, retromer also traffics G-protein-coupled neurotransmitter receptors (GPCR) such as  $\beta$ 2-adrenergic receptors and D1-type dopamine receptors (C. Wang *et al.*, 2016). In striatal MSNs, live-cell TIRF imaging has shown that retromer delivers  $\beta$ 2-ARs to the cell surface close to post-synaptic densities (Choy *et al.*, 2014). It likely plays a role in GPCR signal regulation in the brain, as VPS26 has been shown to displace  $\beta$ -arrestins and end GPCR signaling of hormone receptors (Feinstein *et al.*, 2011, 2013), though this regulation has yet to be studied in the context of GPCRs in neurons specifically.

Considering the vast number of putative neuron-specific retromer cargoes, it is evident that our understanding of retromer function in the brain is in its infancy; however, it is already clear that retromer is involved in the development, maturation, and plasticity of synapses by delivering neurotransmitter receptors to the post-synaptic membrane.



#### **1.2.4.3 Putative presynaptic roles**

Emerging reports provide tantalizing evidence that, in addition to its now-well-established role in post-synaptic receptor trafficking, VPS35 is also involved in synapse maintenance in the presynapse via an as-yet uncharacterized role. In primary neuronal cultures, retromer clusters are dynamically active not only in dendrites and soma, but in axons as well (Choy *et al.*, 2014; Munsie *et al.*, 2015). VPS35 haploinsufficiency leads to stunted, vesicular axons (Wen *et al.*, 2011; Wang *et al.*, 2012; Tian *et al.*, 2015; Tang *et al.*, 2020), and VPS35 has been localized to a subset of presynaptic terminals in cultured hippocampal cells and brain slices (Vazquez-Sanchez *et al.*, 2018).

A recent study of presynaptic VPS35 looked at the effect of haploinsufficiency at neuromuscular terminals in larval *Drosophila melanogaster*. VPS35 haploinsufficiency resulted in larger synaptic vesicles, with larger mEPSC amplitudes, and delayed synaptic vesicle regeneration during tetanic stimulation (Inoshita *et al.*, 2017). These effects were rescued by overexpression of Rab5 or Rab11, two proteins involved in membrane trafficking with known roles in synaptic vesicle cycling. The localization of VPS35 to enlarged SVs led the authors to hypothesize that retromer is involved in the regeneration of SVs from bulk endocytosed membrane.

However, studies of mammalian retromer at the presynapse to date do not support the involvement of retromer in synaptic vesicle regeneration. Multiple studies of retromer insufficiency or knock-down have reported no change to the basal glutamate transmission, evoked release, or paired-pulse ratio, suggesting that retromer does not directly affect the presynaptic probability of transmitter release (Muhammad *et al.*, 2008; Tian *et al.*, 2015; Temkin *et al.*, 2017; Vazquez-Sanchez *et al.*, 2018). Acute knock-down of VPS35 in cultured hippocampal cells had no effect on SVs size, density, or release in the presynaptic terminal

(Vazquez-Sanchez *et al.*, 2018), indicative of differential presynaptic roles of retromer between vertebrates and invertebrates, between synapse types, or at different developmental time points.

VPS35 only localizes to a subset of presynaptic compartments in murine hippocampal cells (Vazquez-Sanchez *et al.*, 2018) and is transported dynamically in axons (Munsie *et al.*, 2015), suggesting that its function in the presynapse is either not as ubiquitous as local SV regeneration, or that it traffics transiently in and out of synapses. It is possible that retromer is involved in the axonal trafficking of degradative organelles full of old SV proteins out of synaptic terminals. In support of this, VPS35 haploinsufficiency results in axonal varicosities that are LAMP1 positive (Wang *et al.*, 2012) and an accumulation of synaptic vesicles in the reserve pool outside the active zone (Tian *et al.*, 2015). It has been shown that older SV proteins that are no longer fully functional tend to reside on these reserve pool SVs, which may represent a pool of vesicles awaiting retrograde transport and degradation (Truckenbrodt *et al.*, 2018).

An alternative possibility is that presynaptic VPS35 is associated with mitochondria. Mitochondria are also present in only a subset of presynaptic terminals, where they have important roles in metabolism and calcium homeostasis (reviewed in: Lee *et al.*, 2018) that could have secondary impacts on synaptic function. To my knowledge, there has been no study yet of the colocalization of VPS35 and mitochondria in mammalian presynaptic terminals.

VPS35 also has a role in presynaptic transporter recycling in non-glutamatergic cells. It has been shown to recycle the dopamine transporter, which resides on the plasma membrane at dopaminergic release sites, and is involved in the reuptake of dopamine after release (Wu *et al.*, 2017). It similarly associates with the vesicular monoamine transporter 2 (Wu *et al.*, 2016),

though studies of both transporters were conducted in cell lines, and retromer-dependent trafficking of these transporters has yet to be replicated in neurons.

In summary, there is still much to be discovered about the many roles of retromer trafficking in neurons.

#### **1.2.4.4 Retromer in Alzheimer's disease**

The discovery that VPS35 is depleted in the brains of individuals with Alzheimer's disease (AD) (Small *et al.*, 2005) led to many of the studies of retromer function in neurons discussed above. These studies also found that VPS35 coIPs with the transmembrane enzyme  $\beta$ -secretase 1 (BACE1) (Wen *et al.*, 2011) that is responsible for cleaving amyloid precursor protein and producing amyloid- $\beta$  (A $\beta$ ) – a major component of the amyloid plaques and tangles that are the neuropathological hallmark of AD. Multiple studies have now linked retromer depletion to impaired BACE1 trafficking, abnormal A $\beta$  production, and AD-like pathology and memory phenotypes in mice (Muhammad *et al.*, 2008; Wen *et al.*, 2011; Bhalla *et al.*, 2012; Wang *et al.*, 2012). A full review of retromer in AD is outside the scope of this project (for a nice review see Small and Petsko, 2017). However, I would like to direct the reader's attention to the facts that A $\beta$  pathology is frequently found in the brains of people with PD alongside Lewy bodies (Braak *et al.*, 2003), and that mild cognitive impairment and dementia are common non-motor symptoms or comorbidities of PD (Goldman and Postuma, 2014).

#### **1.2.5 The retromer complex in Parkinson's disease**

In 2011, our group and others discovered a missense mutation (Asp620Asn; D620N) in VPS35 that is responsible for an autosomal-dominant, highly penetrant form of familial parkinsonism (Vilariño-Güell *et al.*, 2011; Zimprich *et al.*, 2011). Mutations in other retromer components and

associated proteins have also been linked with late-onset PD, atypical PD, and related motor disorders (Vilariño-Güell *et al.*, 2013; Gustavsson *et al.*, 2015; Rajput *et al.*, 2015; Lin *et al.*, 2018; Follett *et al.*, 2019).

VPS35 D620N mutations have since been identified in >70 multi-incident families, all presenting with a syndrome that is clinically indistinguishable from idiopathic PD (Struhal *et al.*, 2014). The D620N mutation is an acidic to neutral change. Modeling predicts it would disrupt hydrogen bonding between helices in the same groove believed to bind the canonical cargo CI-MPR, and perhaps others (Arighi *et al.*, 2004; Zimprich *et al.*, 2011), though evidence thus far suggests there is no impact on cargo binding (Follett *et al.*, 2013; C. Wang *et al.*, 2016). A recent study on higher order oligomerization of retromer into tetramers and chains noted that the D620N mutation lies within a cluster of acidic residues that are essential for these interactions, and could interfere with higher-order assembly on membranes, though that has yet to be tested (Kendall *et al.*, 2020).

In the last decade, VPS35 in PD models has been studied in a number of systems, starting with simple studies in cell lines, then in cultured neurons, and is now being studied in a novel D620N knock-in mouse.

#### **1.2.5.1 Findings from exogenous mutant expression in cell-lines**

Mutant VPS35, when exogenously expressed in cell lines, does not impact assembly of the CRC (Follett *et al.*, 2013; Ian J. McGough *et al.*, 2014; Miura *et al.*, 2014; Zavodszky *et al.*, 2014). It does reliably reduce the association of WASH-complex components, including FAM21, by co-immunoprecipitation (Ian J. McGough *et al.*, 2014; Zavodszky *et al.*, 2014; Kvainickas *et al.*, 2017; Chen *et al.*, 2019), an association believed to be vital for the trafficking functions of

retromer as discussed above. While this was originally believed to represent a defect in the innate ability of mutant retromer to bind FAM21, a more recent study showing that TBC1D5 knock-down can rescue D620N-mediated loss of FAM21 binding suggests the mutation's effects on WASH coIPs may not be mediated by a loss of innate ability to bind (Seaman, 2018).

Multiple studies of CI-MPR trafficking/function in cells expressing VPS35 D620N have turned up conflicting results. Two found impairments in CI-MPR localization (Ian J. McGough *et al.*, 2014) with concomitant lysosomal defects (Follett *et al.*, 2013), whereas another three found CI-MPR localization (Zavodszky *et al.*, 2014; F.-L. Tang *et al.*, 2015), cathepsin-D processing, and lysosomal function (Miura *et al.*, 2014) to be unaffected by mutant expression. It should be noted that these studies used three different exogenous expression strategies in four different cell lines: knock-down and siRNA-resistant replacement in RPE1 cells (Ian J. McGough *et al.*, 2014), overexpression in A431 cells (Follett *et al.*, 2013) or HEK293 cells (Miura *et al.*, 2014; F.-L. Tang *et al.*, 2015), and stable expression in modified HeLa cells (Zavodszky *et al.*, 2014). An emerging theme in the literature is that changing ratios of VPS35 to its multiple binding partners can shift its function, thus these differing strategies may be responsible for the different outcomes. Alternatively, other trafficking pathways exist for CI-MPR that could be favoured in different cell types and obscure mutant effects (Kvainickas *et al.*, 2017; Simonetti *et al.*, 2017).

Two studies have surveyed mutant expression effects on the trafficking of surface cargoes in cell lines. McGough and colleagues (2014) found D620N to have no effect on surface trafficking of Glut1 in RPE1 cells. Conversely, Wang *et al.* (2016) studied surface trafficking of D1DR in N2A cells. They found that WT VPS35 expression, but not D620N, can rescue retromer-depletion induced impairments to D1DR surface expression and signalling. Given the known heterogeneity in the retromer-mediated pathways for different surface cargoes (discussed above;

Ian J. McGough *et al.*, 2014), it is perhaps unsurprising that the mutation impacts the trafficking of some cargoes, but not others.

Cell line studies have also shown the D620N mutation to have deleterious effects on its mitochondrial functions. Retromer depletion results in mitochondrial fragmentation and abnormal protein ubiquitination that can be rescued by WT, but not mutant, VPS35 expression (F. L. Tang *et al.*, 2015). This may be mediated by mutant-enhanced association of retromer with dynamin-like protein 1 (a mitochondrial fission protein) and its subsequent turnover on mitochondrial membranes, increasing mitochondrial fission and fragmentation (W. Wang *et al.*, 2016; Wang *et al.*, 2017). It is interesting to note here that retromer depletion causes the same phenotype (mitochondrial fragmentation) as an increase in function (Dlp1 turnover). Mitochondrial complex I and II assembly is impaired in D620N carrier fibroblasts, which can be rescued by inhibition of mitochondrial fission, suggesting that fragmentation could lead to downstream bioenergetic impairments (Zhou *et al.*, 2017). Lastly, trafficking of ATG9A, a Rab7-retromer cargo involved in signaling for mitophagy, is impaired by the D620N mutation (Zavodszky *et al.*, 2014), suggesting the mutation may also prevent the proper degradation of malfunctioning mitochondria under conditions of stress.

The PD-associated protein parkin has recently been implicated in retromer-mediated endolysosomal trafficking, by ubiquitinating both VPS35 and Rab7 (Song *et al.*, 2016; Martinez *et al.*, 2017; Williams *et al.*, 2018). Parkin depletion impairs VPS35 and SNX1 membrane association, tubule formation, and CI-MPR rescue (Song *et al.*, 2016). Parkin-dependent ubiquitination of Rab7 regulates its membrane association, which could act as an upstream regulator of retromer-mediated trafficking (*ibid*). Expression of PD-causing mutant parkin in cell lines impairs ubiquitination of VPS35 itself without affecting VPS35 levels, suggesting that

this may act as a functional modifier of retromer trafficking rather than a flag for degradation (Williams *et al.*, 2018). These studies provide an interesting point of intersection between early-onset PD mutations and retromer.

#### **1.2.5.2 Findings from exogenous expression in neurons**

Given the canonical function of retromer in maturation of endosomes into lysosomes, several of the first studies of VPS35 D620N expression in neurons queried the localization of canonical cargoes and protein degradation. Our group and another found that overexpression of mutant VPS35 in mouse or rat cortical neurons does not affect its colocalization with VPS26, endolysosomal markers, or the cargo sortilin compared to WT overexpression (Tsika *et al.*, 2014; Munsie *et al.*, 2015). We did find that mutant expression conferred a subtle perinuclear deficit in CI-MPR (Munsie *et al.*, 2015) in agreement with others (MacLeod *et al.*, 2013).

Studies of the degradative pathways have uncovered an interaction between VPS35 and other PD-associated proteins. MacLeod and colleagues (2014) found that expression of G2019S mutant LRRK2 (another mutation causal to late-onset autosomal dominant PD), results in a similar CI-MPR mislocalization as D620N overexpression in rat primary cortical cultures. It is particularly noteworthy that co-expressing WT-VPS35 with LRRK2 G2019S in these cultures can rescue the LRRK2-mutant phenotype, suggestive of some interaction between them. They also found that LRRK2 and VPS35 interact by coIP in rodent brains (MacLeod *et al.*, 2013), a finding that our group has replicated (Vilariño-Güell *et al.*, 2013).

Further evidence has shown that VPS35 interacts functionally with  $\alpha$ -synuclein, perhaps by influencing its degradation. Manipulations of VPS35 can affect  $\alpha$ -synuclein-mediated hippocampal cell death in a transgenic  $\alpha$ -synuclein overexpression model of PD, with

overexpression of VPS35 preventing cell death, and knock-down or D620N expression exacerbating it (Dhungel *et al.*, 2015). Tang *et al.* (2015) found that the neurons in the SNpc and striatum of retromer-deficient mice accumulated  $\alpha$ -synuclein and, while having a slight swelling of Lamp1-positive endosomes, showed a much more striking decrease in the levels of autophagy-associated Lamp2a which is a proposed degradative pathway for  $\alpha$ -synuclein.

More evidence exists, albeit purely correlative at this point, for a functional intersection of PD-related proteins and retromer function, in a study by Williams and colleagues (2018) of VPS35 in parkin knock-out mice. VPS35 levels were not affected by parkin knock-out, however they measured significant reductions in VPS35 ubiquitination and levels of WASH complex members. Knocking down parkin in cortical cultures altered the localization of ATG9A, a putative retromer cargo, though the retromer-dependence of this defect was not assayed. Lastly, they found that D620N expression in the brain can induce DA cell degeneration independent of the presence of parkin. While the study authors interpret this as evidence that VPS35 acts downstream of parkin to induce cell death, it could also be that catastrophic impairments are occurring in other VPS35 functions.

Some evidence exists for mitochondrial dysfunction in neurons expressing mutant VPS35, though it has not yet been comprehensively explored. Conditional knock-out of VPS35 from dopaminergic neurons in DAT-cre mice induces dopaminergic cell loss and PD-like pathology (F. L. Tang *et al.*, 2015). While not necessarily a surprising finding, given the essential role of retromer in cell functioning, it is interesting that these authors could replicate mitochondrial fragmentation phenotypes by lentiviral expression of VPS35 D620N in the nigra. Unfortunately, this experiment suffers from a major methodological flaw wherein the control animals were



uninjected WT mice. This makes it unclear whether the fragmentation results from VPS35 overexpression, or represents a unique mutant effect.

In terms of more whole-neuron effects, Tsika and colleagues (2014) found that overexpression of both WT and D620N VPS35 in rat cortical cultures impaired neurite outgrowth, caused cell death, and increased cell vulnerability to environmental toxins; they did not observe any differences in these measures between WT or mutant overexpression. They also found that viral overexpression of WT or D620N in rat SN resulted in dopaminergic cell death and axonal spheroid formation. In this case, the effect was exacerbated by the mutation. The authors concluded that the mutation most likely confers a gain-of-function, at least with regards to their chosen measures, as WT and D620N expression had similar effects.

Our group, in work led by my post-doctoral mentor Lise Munsie, performed the first study of mutant VPS35 expression on neuronal cargo trafficking, by examining GluA1 trafficking in murine cortical neurons. Exogenous expression of D620N mutant protein produced similar effects as wild-type upon excitatory synapse density and mEPSC frequency, but the mutant form additionally impaired VPS35 motility, and reduced the percentage of dendritic spines containing VPS35 clusters (Munsie *et al.*, 2015). Furthermore, the D620N mutation in mouse neurons resulted in increased excitatory current amplitudes compared to wild-type, and increases in AMPA receptor cluster intensities in both mouse neurons and dopaminergic neuron-like cells from human mutation carrier-derived iPSCs (Munsie *et al.*, 2015); findings we interpreted at the time as a loss-of-function in the context of AMPAR surface trafficking. The only other study to date to investigate the effect of the D620N mutation on AMPAR trafficking, found that D620N expression in cultured hippocampal neurons was insufficient to rescue impairments in LTP

caused by retromer depletion (Temkin *et al.*, 2017), also supportive of D620N being a loss-of-function with regards to AMPAR trafficking.

Early work in *Drosophila* hinted that VPS35 mutant expression leads to dopaminergic cell dysfunction, sensitivity to rotenone, and can interact with loss-of-function of parkin (Wang *et al.*, 2014; Malik, Godena and Whitworth, 2015). Unfortunately, this work is muddled by the use of human VPS35 constructs, which have since been shown not to be fully functional in *Drosophila* (Malik, Godena and Whitworth, 2015; Inoshita *et al.*, 2017).

More recently, Inoshita and colleagues (2017) explored VPS35 mutant effects in synapses, and found a functional link between dVPS35 and dLRRK (the nearest fly equivalent to LRRK2; although it should be noted that this is more similar to LRRK1, a protein not implicated in PD). They found that dVPS35 localizes downstream of dLRRK on SVs at the neuromuscular junction, and that the two proteins interact functionally in the synaptic vesicle cycle; dVPS35 haploinsufficiency creates larger synaptic vesicles, stalled endocytic invaginations, increases in the number of synaptic boutons, and delayed synaptic vesicle regeneration, that can be attenuated by dLRRK overexpression and, curiously, also by dLRRK haploinsufficiency. These effects were also rescued by overexpression of Rab5 or Rab11, two proteins involved in membrane trafficking with known roles in both synaptic vesicle cycling and post-synaptic receptor recycling. While they did not study PD-mutant effects specifically, it provides evidence for two PD-associated proteins interacting functionally at synapses, albeit in flies.

### **1.2.5.3 Findings from a novel knock-in D620N knock-in model**

The inconsistent results that come from overexpression and re-expression studies (for instance the discord in the CI-MPR trafficking findings), highlights the importance of model consistency

when assaying mutant effects. In order to circumvent these issues, my co-supervisor Dr. Matthew Farrer created a D620N knock-in mouse model of VPS35 parkinsonism that expresses mutant protein in the endogenous mouse gene, at endogenous levels.

Independent characterizations of D620N knock-in mice have been carried out by three research groups, including ours, and each represent different age points. The first finding to note, consistent across all three studies, is that homozygous mutant expression has no effect on birth ratios or survival (Ishizu *et al.*, 2016; Cataldi *et al.*, 2018; Chen *et al.*, 2019), in contrast with the embryonic lethality of full VPS35 or VPS26 knock-out (Muhammad *et al.*, 2008; Wen *et al.*, 2011). This is a clue as to the nature of the D620N mutation – it necessarily does not confer a full loss-of-function.

In our initial characterization of young (3-month-old) animals, we found that VPS35 is expressed at normal levels, and up to this age there are no mutation effects on birth ratios, animal weight, or survival (Cataldi *et al.*, 2018). We observed no impairments in behaviour or motor functioning (open-field, cylinder, rotarod), and no loss of TH-positive cell bodies in the SNpc or TH-positive terminals in the striatum. Extracellular dopamine levels assayed by *in vivo* microdialysis in freely moving animals revealed no changes in dopamine levels, however the ratio of metabolites provided evidence for increased dopamine turnover, and fast-scan cyclic voltammetry (FSCV) in *ex vivo* brain slices revealed increases in evoked dopamine currents with a slower decay. Changes in FSCV were correlated with decreases in dopamine transporter by western blot and immunohistochemistry (IHC; which could impair dopamine reuptake, leading to the slower decay), and increased responsiveness to the D2R-agonist quinpirole (suggesting that these terminals have increased D2 inhibitory auto-receptor expression). IHC staining did not reveal any  $\alpha$ -synuclein pathology at 3 months.

Ishizu and colleagues characterized similar knock-in animals at 20 weeks (5 months) (Ishizu *et al.*, 2016). They similarly observed no alterations in expression of retromer proteins, assembly between VPS35 and VPS26 by coIP, nor in levels of cathepsin D, CI-MPR,  $\alpha$ -synuclein, or LC3-II. They also observed no loss of TH-positive cells, or  $\alpha$ -synuclein pathology up to 70 weeks of age. At 5 months, they observed no change in dopamine levels, or turnover, by *in vivo* microdialysis; but potassium-induced DA release in *ex vivo* slices was significantly impaired in the homozygous animals after 20-50 minutes. These findings are not inconsistent with ours for several reasons. First, other knock-in models of PD genes can cause early increases in dopamine measures that are attenuated over time (Volta *et al.*, 2017), and these mice are two months older than those in our study. Secondly, their measure of evoked dopamine release used high extracellular potassium rather than electrical stimulation, and was measured 20-50 minutes later rather than instantaneously as in FSCV. Their results are more likely reflective of either impaired ability to regenerate dopamine vesicles after exhaustive stimulation, or an increased (perhaps D2R-mediated) attenuation of sustained release over time.

Most recently, Chen *et al.* have released a study of aged VPS35 D620N knock-in mice (2019). They observed that the mutants were viable, fertile, normal in appearance, born at normal ratios, and showed no survival impairments up to 24 months of age. They similarly found no mutant effects on VPS35 expression, nor association with CRC components by coIP. They did observe subtle loss of TH-positive cells in the SN by IHC at 3-months in homozygous mice, and in both genotypes by 12 months, accompanied by a mild gait phenotype in the homozygotes. It is interesting that this loss of TH cells was not accompanied by a loss of TH staining in the striatum, nor in a loss of DA or serotonin levels in the striatum by HPLC up to 12 months. Differences between this and our study might reflect differences in the sensitivity of the antibodies/techniques to detect subtle changes to TH cell density, or, as environmental factors

can exacerbate dopaminergic cell loss, this could reflect differences in animal husbandry between the two sites. An assay of the neuropathology found evidence of neurite degeneration and axonal spheroid formation. Tau pathology was uncovered at 12 months that was most severe in the cortex, hippocampus, and ventral midbrain, but nearly absent from the striatum (recall that these are the cell types with the highest level of VPS35 expression). Of interest, this group was unable to coIP FAM21 in brain tissue (using the same protocol that produced reproducible coIP in cell lines); leading the authors to hypothesize that WASH-mediated retromer trafficking is not important in the brain.

A very recent report using young D620N knock-in mice has found that the mutant brains have higher levels of phosphorylated LRRK2 kinase substrate Rab10. This phosphorylation can be reversed by LRRK2 inhibition with the selective inhibitor MLI-2 (Mir *et al.*, 2018), corroborating the mounting evidence that VPS35 and LRRK2 interact functionally in Parkinson's disease.

### **1.3 Leucine-rich repeat kinase 2**

LRRK2 is a large protein with two structural scaffolding domains on its terminal ends and a central catalytic domain (reviewed in: Greggio and Cookson, 2009; P. Gómez-Suaga *et al.*, 2014). The catalytic region contains a kinase domain and a ROC-COR (Ras of complex – C-terminal of ROC) domain conferring it with both kinase and GTPase activity (Webber *et al.*, 2011). LRRK2 is broadly expressed in human and murine tissues, and is enriched in the brain (Paisan-Ruiz *et al.*, 2004; Zimprich *et al.*, 2004). It localizes to early endosomes (Schreij *et al.*, 2015) and the *trans*-Golgi-network (Beilina *et al.*, 2014, 2020; Liu *et al.*, 2018; Purlyte *et al.*, 2018), and has been implicated in multiple cellular functions including autophagy (reviewed in P. Gómez-Suaga *et al.*, 2014), endolysosomal sorting (MacLeod *et al.*, 2013; Gómez-Suaga, Rivero-Ríos, *et al.*, 2014), and cytoskeletal dynamics (Parisiadou *et al.*, 2009; Pellegrini *et al.*,

2017). Like VPS35, LRRK2 has been linked to late-onset autosomal dominant PD that is nearly indistinguishable from idiopathic PD (Paisan-Ruiz *et al.*, 2004; Zimprich *et al.*, 2004), leading to a large volume of research on its neuronal functions in a disease context.

### **1.3.1 A brief primer on neuronal dysfunction in LRRK2 models of PD**

LRRK2 mutations represent the most frequent known cause of familial PD with the most common pathogenic mutation (G2019S) accounting for up to 2% of cases globally (reviewed in: Ozelius *et al.*, 2006; Healy *et al.*, 2008; Hulihan *et al.*, 2008).

Studies of LRRK2 in neuronal systems have implicated it in the functioning of dopaminergic and glutamatergic synapses. As with VPS35, its expression is increased during the first few post-natal weeks, coinciding with glutamatergic synaptogenesis (Piccoli *et al.*, 2011; Beccano-Kelly, Kuhlmann, *et al.*, 2014). LRRK2 is enriched in both the cortex and the striatum, though it does not appear to be highly expressed in dopaminergic cells themselves (Biskup *et al.*, 2006; Galter *et al.*, 2006; Simón-Sánchez *et al.*, 2006; Melrose *et al.*, 2007).

Many LRRK2 models have reported alterations in synaptic transmission (reviewed in Benson *et al.* 2018). In G2019S knock-in mice, the mutation leads to elevated glutamate transmission in cortical cell cultures (Beccano-Kelly, Kuhlmann, *et al.*, 2014) and brain slices (Matikainen-Ankney *et al.*, 2016; Volta *et al.*, 2017) at early age points, followed by gradual impairments in synaptic transmission (Volta *et al.*, 2017). Dopamine release in these mice is similarly higher at early ages and relatively impaired in aged animals (Yue *et al.*, 2015; Volta *et al.*, 2017).

Expression of G2019S inhibits endocytosis in neurons (Shin *et al.*, 2008; Belluzzi *et al.*, 2016; P. Y. Pan *et al.*, 2017; Nguyen and Krainc, 2018) and decreases the number of SVs in the readily releasable pool (Yun *et al.*, 2013), which would account for the older aged phenotypes, but not

the young. However, LRRK2 mutant expression can also increase calcium current through interaction with the  $\beta 3$  subunit of CaV2.1 channels (Bedford *et al.*, 2016; Carrion *et al.*, 2017), possibly accounting for an increased presynaptic probability of release at earlier time points.

In support of a presynaptic function of LRRK2 in neurons, LRRK2 modulation affects synaptic vesicle mobilization (Piccoli *et al.*, 2011; Cirnaru *et al.*, 2014) and it co-purifies with synaptic vesicles (Piccoli *et al.*, 2014). Many proteins involved in the synaptic vesicle cycle have been found to associate with LRRK2 including: clathrin heavy chain, AP-2, AP180, syntaxin1A, dynamin 1, VAMP2, SNAP25, NEM sensitive factor (NSF), synapsin-1 and endophilin-A (Piccoli *et al.*, 2011, 2014; Matta *et al.*, 2012; Yun *et al.*, 2013; Gómez-Suaga, Rivero-Ríos, *et al.*, 2014; Belluzzi *et al.*, 2016).

In addition to its presynaptic effects, a handful of studies have uncovered effects of LRRK2 depletion or mutant expression on spine morphology (Parisiadou *et al.*, 2014; Matikainen-Ankney *et al.*, 2016), AMPAR expression (Parisiadou *et al.*, 2014), D1DR expression (Migheli *et al.*, 2013), and regulation of synaptic strength (Sweet *et al.*, 2015; Matikainen-Ankney *et al.*, 2016, 2018). It has been proposed that these post-synaptic effects could be mediated through LRRK2 modulation of PKA. LRRK2 binds to PKA regulatory subunits, and negatively regulates PKA activity in response to D1DR activation (Parisiadou *et al.*, 2014). PKA regulates post-synaptic AMPAR trafficking and recycling (Ehlers, 2000; reviewed in: Diering and Huganir, 2018); however, Rab8 and Rab10 are newly discovered LRRK2 kinase substrates (Steger *et al.*, 2017; Jeong *et al.*, 2018) that have been shown to traffic AMPARs as well (Gerges, Backos and Esteban, 2004; Brown *et al.*, 2007; Glodowski *et al.*, 2007; Bowen *et al.*, 2017).

### 1.3.2 LRRK2 kinase substrates

Pathogenic PD-causing mutations in LRRK2 have all been shown to increase its kinase activity (West *et al.*, 2005; Steger *et al.*, 2016; reviewed in: Taylor and Alessi, 2020), making the identification of its substrates an important task for PD researchers.

LRRK2 itself is phosphorylated at numerous sites in response to its own kinase activity. Some sites (such as S1292) represent true autophosphorylation sites (Sheng *et al.*, 2012), whereas others are contested to be true sites of autophosphorylation, yet still provide a reliable readout of LRRK2 kinase activity or inhibition (such as S935; Fell *et al.*, 2015). Active LRRK2 kinase is dimeric (Greggio *et al.*, 2008; Berger, Smith and Lavoie, 2010), with the dimerization potentially mediated through protein-protein interactions and resulting in the autophosphorylation (Greggio *et al.*, 2008; Sheng *et al.*, 2012).

Multiple neuron-relevant substrates for LRRK2 have been proposed, but have yet to be replicated. These include, but are not limited to, endophilin-A1 (Arranz *et al.*, 2015), NSF (Belluzzi *et al.*, 2016), synaptojanin (Islam *et al.*, 2016), and auxilin (Nguyen and Krainc, 2018). Several recent proteomics studies have shown that LRRK2 directly phosphorylates a subset of Rab-GTPases at a conserved threonine in the switch II domain (T72 or T73) (Steger *et al.*, 2016, 2017; Jeong *et al.*, 2018). Rab GTPases are master regulators of endosomal and vesicular trafficking, and are critical to synaptic transmission (reviewed in Pavlos and Jahn, 2011).

Phosphorylation of Rab10 at the T73 residue is 0.5 to 3-fold higher in embryonic fibroblast cells from G2019S knock-in mice, and is reversed by LRRK2 kinase inhibition (Ito *et al.*, 2016; Steger *et al.*, 2016; Lis *et al.*, 2018); however, the G2019S-mediated increase is not universally observed (Liu *et al.* 2017; Fan *et al.* 2018; Atashrazm *et al.* 2019). The effects of kinase inhibition are also



variable. They can either take exceptionally long timeframes to exert an effect (Thirstrup *et al.*, 2017), or appear ineffective in certain tissue types (Kelly *et al.*, 2018).

In spite of the somewhat contradictory findings on LRRK2 kinase inhibition in various tissues, studies in neurons have found that LRRK2 kinase inhibition can affect synaptic vesicle release (Cirnar *et al.*, 2014) and rescue glutamatergic transmission phenotypes in a G2019S knock-in model (Sweet *et al.*, 2015; Matikainen-Ankney *et al.*, 2016; Kuhlmann *et al.*, *in submission*). Recent reports have also shown that LRRK2-mediated Rab phosphorylation is elevated in *substantia nigra* of people with idiopathic PD, as well as in alpha-synuclein overexpressing, rotenone-treated (Di Maio *et al.*, 2018), and VPS35 D620N knock-in rodent models (Mir *et al.*, 2018). These studies provide evidence for the convergence of multiple etiological factors in PD onto LRRK2 kinase activity, providing hope that kinase inhibition may represent a good therapeutic target for several, if not all, forms of late-onset PD.

#### **1.4 Hypothesis & rationale**

At the outset of my doctorate in 2013, we knew little about the neuron-specific functions of retromer. The literature on the cell biological effects of D620N expression consisted of two overexpression studies in cell lines (Follett *et al.*, 2013; MacLeod *et al.*, 2013). Much of the information discussed above was published throughout the course of my work. At the outset, we knew that the D620N mutation caused late-onset autosomal dominant PD (Vilariño-Güell *et al.*, 2011; Zimprich *et al.*, 2011), that retromer was involved in AMPAR trafficking in *C.elegans* (Zhang *et al.*, 2012), and that LRRK2 and VPS35 mutant overexpression caused similar CI-MPR trafficking defects in cell lines (MacLeod *et al.*, 2013). We also knew, through ongoing work in the lab at the time, that G2019S mutations in LRRK2 caused increases in glutamatergic transmission in cultured cortical neurons from young knock-in mice (Beccano-Kelly, Kuhlmann,

*et al.*, 2014) and that D620N overexpression in cultured cortical neurons altered AMPAR localization and glutamate transmission (Munsie *et al.*, 2015). Widespread cortical cell loss is common in PD, suggesting that dopaminergic cells are not selectively affected (MacDonald and Halliday, 2002), and justifying the study of glutamatergic regulation in PD models.

I set out to study the effects of endogenously expressed mutant VPS35 D620N in our novel knock-in mouse, and to investigate the link between D620N parkinsonism and LRRK2 in this model. The underlying hypotheses for this body of work were:

- 1) That the pathogenic D620N mutation would impair GluA1-containing AMPAR surface expression and glutamate transmission when expressed at endogenous levels in mouse brain; and,
- 2) That VPS35 and LRRK2 interact in glutamatergic synapse maintenance, representing a potential target for therapeutic development.

In order to achieve these goals, I employed a number of biochemical and cell biological techniques in brain tissue and cultured cortical cells from these mice. I used western blotting and co-immunoprecipitation to assay protein expression levels, protein-protein interactions, and substrate phosphorylation in brain tissue. I learned to culture cortical neurons to 21-days-*in-vitro*, in order to observe protein localization in mature, spiny glutamatergic cells by immunocytochemistry. I also employed live-cell studies to observe the real-time effects of mutant expression on GluA1 trafficking by fluorescence recovery after photobleaching, and on glutamatergic transmission by whole-cell patch clamp electrophysiology. The results of my experiments were sometimes predictable, but often surprising. I will begin with the discovery of

changes in AMPAR trafficking and glutamatergic transmission in Chapter 2, then discuss some interesting but incomplete findings on the intersection of VPS35 and LRRK2 in Chapter 3.

## **Chapter 2: Exploring the neuronal role of VPS35 and the effect of the D620N mutation on glutamatergic synapses**

### **2.1 Introduction**

VPS35 protein is an integral component of the retromer complex, which binds and traffics transmembrane proteins between membranous organelles. It can bind with various accessory proteins and complexes, including sorting nexin (SNX) family proteins and the WASH complex, to recycle cargoes from endosomal structures to the *trans*-Golgi network or surface membranes, thus circumventing lysosomal degradation (reviewed in: Bonifacino and Rojas 2006; Burd and Cullen 2014; Cullen and Korswagen 2012; Seaman et al. 2013). Retromer dysfunction has been implicated in a number of neurodegenerative disorders including Alzheimer's disease (Small *et al.*, 2005), Parkinson's disease (Vilariño-Güell *et al.*, 2011, 2013; Zimprich *et al.*, 2011), and a number of atypical parkinsonian disorders (Vilariño-Güell *et al.*, 2013; Gustavsson *et al.*, 2015; Rajput *et al.*, 2015; Lin *et al.*, 2018).

Our group, and another, discovered a missense mutation in VPS35 (D620N) that causes late-onset autosomal disease clinically similar to idiopathic PD (Vilariño-Güell *et al.*, 2011; Zimprich *et al.*, 2011; Struhal *et al.*, 2014). While PD is classically thought of as a hypodopaminergic motor disorder caused by degeneration of cells in the *substantia nigra*, recent attention has been brought to its many non-motor, non-dopaminergic symptoms that often precede motor onset by years (reviewed in: Beitz, 2014; Goldman and Postuma, 2014). Impaired glutamatergic plasticity in the cortex and cortical cell loss have both been observed in the brains of people with pre-motor PD (MacDonald and Halliday, 2002; reviewed in: Foffani and Obeso, 2018) calling attention to the importance of glutamatergic systems in PD.

In primary neuronal cultures, retromer clusters are dynamically active in soma, axons, dendrites, and dendritic spines (Choy *et al.*, 2014; Munsie *et al.*, 2015). Emerging reports have implicated VPS35 in the surface delivery of GluA1-containing AMPA-type glutamate receptors (Munsie *et al.* 2015; Tian *et al.* 2015; Tsika *et al.* 2014; Zhang *et al.* 2012), functionally supporting synapse development and maturation in developing neurons (Wang *et al.*, 2012; Choy *et al.*, 2014; Munsie *et al.*, 2015; Tian *et al.*, 2015; Tang *et al.*, 2020), and LTP in mature cells (Temkin *et al.*, 2017). GluA1-containing AMPARs are transiently inserted during development when new synapses are unsilenced, and similarly in adult brains in the initial phases of LTP induction, generally being replaced with constitutively cycling GluA2/GluA3 heteromeric receptors as the newly established, or strengthened, synapse matures (reviewed in: Diering and Huganir, 2018; Park *et al.*, 2018; Benke and Traynelis, 2019; Purkey and Dell'Acqua, 2020).

Exogenous expression of WT and D620N mutant protein in cultured murine cortical neurons produced similar effects upon excitatory synapse density and mEPSC frequency, but mutant protein motility and trafficking into spines was impaired (Munsie *et al.*, 2015). Furthermore, the D620N mutation resulted in increased excitatory current amplitudes in mouse neurons and increases in AMPA receptor cluster intensities compared to controls, in both mouse neurons and dopaminergic neuron-like cells from human mutation carrier-derived iPSCs (Munsie *et al.*, 2015).

Based on overexpression and knock-out studies, retromer is clearly important in synapse development, maintenance, and functional connectivity (Wen *et al.*, 2011; Wang *et al.*, 2012; Choy *et al.*, 2014; Tsika *et al.*, 2014; Munsie *et al.*, 2015; Tian *et al.*, 2015; Temkin *et al.*, 2017). However, it is not yet clear how overexpression artefacts might impinge on normal (and/or

mutant) retromer functions, nor how endogenous levels of mutant VPS35 lead to late-onset parkinsonism.

To examine the neurobiological effects of VPS35 D620N, we examined synapse development, structure and function, protein levels, and binding relationships in brain tissue and cultured cortical neurons from D620N knock-in mice. The D620N mutation reduces retromer complex association with regulatory proteins, increases the dendritic density of proteins involved in surface recycling, and results in augmentation of glutamatergic transmission. As such, the VPS35 knock-in mouse provides insights into the molecular and cellular etiology of VPS35 PD, and is a useful model system for investigation of pre-motor parkinsonism.

## **2.2 Materials and methods**

### **2.2.1 VPS35 D620N knock-in mice and genotyping**

Constitutive VPS35 D620N knock-in mice (VKI) were generated by Ozgene (Australia) under guidance of my co-supervisor, Dr. Matthew Farrer, using gene targeting in C57Bl/6 embryo stem cells (Bruce4) as previously described (Cataldi *et al.*, 2018). The VKI strain has been deposited in Jackson Labs with open distribution supported by the Michael J Fox Foundation (VPS35 knock-in: B6(Cg)-Vps35tm1.1Mjff/J). All mice were bred, housed, and handled according to Canadian Council on Animal Care regulations. All procedures were conducted in accordance with ethical approval certificates from the UBC ACC (A16-0088; A15-0105) and the Neuro CNDM (2017-7888B). Animals were group-housed in single-sex cages with littermates after weaning. Single-housed animals were selected as breeding animals or timed pregnancies if possible, and were never used as experimental animals.

Mice were genotyped to allow ongoing colony management, planning, and for *post-mortem* confirmation of the genotype of all experimental animals. The procedure for creating the VKI resulted in 51 base-pair insertion in the non-coding regions of *VPS35*, such that PCR amplification of the WT gene using appropriate primers creates a product of 303 base pairs and the knock-in gene a product of 354 base pairs. The animals were genotyped by PCR amplification of *VPS35*, followed by confirmation of the presence of a 303bp product (WT), a 354bp product (Ho) or both (Het). Small tissue samples (tail tips collected at weaning for colony management, ear tissue collected at euthanasia for *post-mortem* confirmation, or forepaws for primary culture) were digested in 100uL 10% Chelex (Bio-Rad 142-1253) at 95°C for 20 minutes and spun down to result in DNA-containing supernatant. 2uL DNA was mixed with 18uL of master mix containing taq polymerase, buffer (DNase- and RNase-free water, 10x buffer, MgCl 25mM, dNTPs 10mM), and primers (ThermoFisher Custom DNA oligos: forward-TGGTAGTCACATTGCCTCTG; reverse-ATGAACCAACCATCAATAGGAACAC) according to the instructions for the taq polymerase kit (Qiagen 201203), and the PCR was performed in a programmable machine (program available upon request). Agarose gel electrophoresis was used to separate the products on a 3% gel with fluorescent DNA dye (ZmTech LB-001G) and visualized on a Bio-Rad ultraviolet gel imager.

### **2.2.2 Western blots and co-immunoprecipitations**

Three-month-old male mice were decapitated, and brains removed and chilled for 1 minute in ice-cold carbogen-bubbled artificial cerebrospinal fluid (ACSF; 125mM NaCl, 2.5mM KCl, 25mM NaHCO<sub>3</sub>, 1.25mM NaH<sub>2</sub>PO<sub>4</sub>, 2mM MgCl<sub>2</sub>, 2mM CaCl<sub>2</sub>, 10mM glucose, pH 7.3–7.4, 300–310 mOsm). For region-specific analysis, this was followed by rapid (<6min) microdissection of cortex, striatum, hippocampus, dorsal midbrain, olfactory bulbs, and cerebellum, with all remaining tissue pooled as ‘rest’. Tissues were flash frozen in liquid

nitrogen and either lysed for immediate use or stored at -80 °C. For *WES* and chemiluminescent western blots, tissues were mechanically homogenized in HEPES buffer (20mM HEPES, 50mM KAc, 200mM Sorbitol, 2mM EDTA, 0.1% Triton X-100, pH 7.2; Sigma Aldrich) containing protease inhibitor cocktail (Roche 11697498001), then incubated on ice for 45 minutes with occasional gentle agitation. For fluorescent western blots, tissue was homogenized by probe sonication at 20kHz for 10s in ice-cold TBS buffer (tris-buffered saline, 1% Triton X-100; pH 7.4) containing protease inhibitor (Roche 11697498001) and phosphatase inhibitor (Sigma 4906845001) cocktails. This buffer was selected to optimize detection of LRRK2 and phosphorylated proteins. Lysate concentrations were quantified by Pierce BCA assay (ThermoFisher 23255) and samples were adjusted to equal concentrations in lysis buffer prior to denaturing.

For traditional chemiluminescence detection, 10-15µg protein was prepared in 4x NuPage LDS sample buffer (Invitrogen NP0008) with 2.5% β-mercaptoethanol or 500mM DTT to a total volume of 10-24µL, and denatured at 70°C for 10 minutes. Samples were loaded into a NuPage 4-12% Bis-Tris gel (Invitrogen NP0322BOX) in an XCell II Blot module (Invitrogen) and run at 70V for 30 min, followed by 110V for 1h. Separated proteins were transferred to methanol-activated Immobilon-P PVDF membrane (Millipore IPVH00010) for 90 minutes at 25V at room temperature, then blocked with 5% milk in PBS for 1 hour at room temperature. Membranes were probed by shaking with primary antibodies in primary antibody solution (PBS, 2% BSA, 0.05% Tween-20) for either 1 hour at room temperature or overnight at 4 °C, washed 4x in PBST (PBS, 0.05% Tween-20), and detected by HRP-conjugated secondary antibodies (Invitrogen; shaken in PBS, 5% milk, 0.05% Tween-20 for 30 minutes at room temperature). Chemiluminescence was detected with Pierce ECL (ThermoFisher 32209) imaged on a Chemo-Doc imaging system (Cell-Bio).



Fluorescence western blots were performed with the following modifications to the above protocol: 1) 40ug protein samples to account for the linear and therefore weaker detection capabilities of fluorescent western blotting; 2) Bolt 4-12% Bis-Tris Plus Gels (Invitrogen NW04120BOX); 3) Fluorescence detection optimized membrane, Immobilon-FL PVDF (Millipore IPFL00010); 4) TBS was substituted for PBS in all buffers to prevent possible cross-reaction of phospho-specific antibodies with phosphate groups; 5) transfer times were increased to 2.5 hours for transfer of larger proteins (LRRK2), and; 6) LiCor fluorescent secondary antibodies were used (LI-COR) and imaged on a LI-COR Odyssey Infrared imaging system (LI-COR).

When necessary, phosphorylated or low-abundance proteins were blotted first, and membranes were stripped using LI-COR NewBlot IR stripping buffer (LI-COR 928-40028; 30m at a time until no signal remained from the first blot), then reblotted for non-phosphorylated or higher abundance proteins of similar sizes.

Images for both types of blots were background-subtracted and analyzed for band intensity with ImageLab software. Signals were normalized to a housekeeping protein quantified from the same gel (GAPDH,  $\beta$ -tubulin,  $\beta$ -actin).

Wherever possible as dictated by equipment availability and antibody compatibility, lysates were blotted on a ProteinSimple *WES* automated capillary-based size sorting system as previously described (Beccano-Kelly, Kuhlmann, *et al.*, 2014). Briefly, lysates were mixed with reducing fluorescent master mix (ProteinSimple SM-001), heated (70°C for 10min) and loaded into manufacturer microplates containing primary antibodies (see below) and blocking reagent, wash buffer, HRP-conjugated secondary antibodies, and chemiluminescent substrate

(ProteinSimple DM-001/2). *WES* data was analyzed on manufacturer-provided Compass software.

We used the following primary antibodies: NEEP21/NSG1 (Genscript A01442), FAM21 (Millipore ABT79), VPS35 (Abnova H00055737-M02), VPS26 (a kind gift from J. Bonifacino, NICHD), CI-MPR (a kind gift from M. Seaman, Oxford), GluA1 (Millipore 05-855R), D2R (Millipore AB5084P), GluN1 (Millipore 05-432),  $\beta$ -tubulin (Covance MRB-435P),  $\beta$ -Actin (Abcam ab6276), and GAPDH (Cell Signaling 2118; ThermoFisher MA5-15738).

For co-immunoprecipitation, 500 $\mu$ g of protein at 1 $\mu$ g/ $\mu$ L was rotary-incubated overnight at 4°C with VPS35 antibody (Abnova H00055737-M02) or Mouse IgG2a control antibody (Abcam ab18414) coupled to M-280 Tosyl-activated Dynabeads (Invitrogen 14204). Small aliquots of each lysate were set aside before IP to verify the equivalence of starting concentrations. 24h later, loaded beads were washed with ice-cold lysis buffer (x3) prior to resuspension in reducing 1x NuPage LDS sample buffer (for traditional; Invitrogen NP0008) or ProteinSimple fluorescent master mix (for *WES*; ProteinSimple SM-001). Protein was eluted and denatured by heating at 70°C for 10 minutes prior to western blotting as described above.

### **2.2.3 Primary cortical cultures**

We mated heterozygous VKI mice to generate embryos used for primary neuronal cultures. Dams were euthanized by rapid decapitation, and embryonic day 16.5 pups were removed and microdissected in Hank's Balanced Salt Solution (HBSS; Gibco 14170161) with 1x penicillin-streptomycin (penstrep; Sigma-Aldrich P4333) in a petri dish on ice. The cortices from each pup were held in 500 $\mu$ L supplemented Hibernate-E medium (Gibco A1247601; 1x GlutaMax Gibco 35050061; and 1% NeuroCult SM1 StemCell 5711) at 4°C while the pups were genotyped as

described above. Genotype-pooled tissue was dissociated chemically for 10min in 0.05% Trypsin-EDTA (Gibco 25300054), followed by deactivation with 10% FBS, then mechanically dissociated in supplemented Neurobasal plating medium (Neurobasal Gibco 21103049; 1x GlutaMax Gibco 35050061; and 1% NeuroCult SM1 StemCell 5711).

Cells were plated onto poly-D-lysine-coated plates or coverslips (Sigma P7280) and matured to 21 days *in-vitro* (DIV21) while incubating at 37°C with 5% CO<sub>2</sub>. For biochemistry, cells were plated in 2mL medium at 1 million cells/well in 6-well plates. For ICC experiments, cells were plated in 1mL medium onto no.1.5 glass coverslips in 24-well plates. Non-nucleofected cells were plated at 115000 cells/well. For GFP-filled neurons, 1 million cells were nucleofected with 1µg pAAV-CAG-GFP plasmid DNA (Addgene 37825) in Ingenio electroporation buffer (Mirus MIR50111) using an Amaxa Nucleofector2b (Lonza), mixed 1:1 with non-nucleofected cells, and plated at 225k cells/well in 1mL medium as above. From DIV4, 10% fresh media was added to all wells every 3-4 days until use.

#### **2.2.4 Immunocytochemistry and imaging analysis**

Cultured cortical neurons were fixed at DIV21 (4% PFA, 4% sucrose in PBS, 10min), permeabilized where appropriate (ice-cold methanol, 3min), and blocked (5% goat serum in PBS) prior to incubation with primary antibodies for 1 hour at RT or overnight at 4°C. Primary antibodies were prepared in antibody solution (2% goat serum, 0.02% Tween20 in PBS). For surface labelling, the cells were not permeabilized until after primary antibody incubation and no detergent was added to the primary antibodies. Proteins were fluorescently labeled with Alexa-conjugated secondary (Invitrogen) in antibody solution for 30 minutes (RT), and coverslips were slide mounted with Prolong Gold (Invitrogen P36930).

We used the following primary antibodies: GFP (Abcam ab1218); VPS35 (Abnova H00055737); VPS26 (a kind gift from J. Bonifacino, NICHD); FAM21C (Millipore ABT79); NEEP21/NSG1 (Genscript A01442); Rab11 (Abcam ab95375); MAP2 (Abcam ab5392); GluA1 (Millipore 05-855R); PSD95 (Thermo Scientific MA1-045); VGluT1 (Millipore AB5905); and GluA1 extracellular (Millipore ABN241).

Cells having a pyramidal morphology – triangular or teardrop shaped cell bodies with spiny, clearly identifiable apical and basal dendrites (Kriegstein and Dichter, 1983) – were selected for imaging. All images were blinded and randomized prior to processing and analysis.

Cell density counts were performed manually on DAPI and MAP2 co-labeled images acquired at 10x with an Olympus Fluoview 1000 confocal microscope. Sholl analysis images were acquired at 20x with an Evos FL epifluorescence microscope. Dendritic neurites (excluding axons) were traced and analyzed using the Simple Neurite Tracer plugin for FIJI ImageJ using a radial segmentation of 5 $\mu$ m.

Images for colocalization were acquired on either an Olympus Fluoview 1000 confocal microscope, with images taken at 60x with 2x optical zoom, in 0.5 $\mu$ m stacks, or a Zeiss Axio Observer with Apotome.2 structured illumination upon which images were taken at 63x in 0.25 $\mu$ m stacks. Z-stack acquisition was set to capture all MAP2 stained dendrite for unfilled cells, or GFP-filled dendrite for filled cells. Acquisition parameters were constrained within each culture set. Z-stacks for each channel were flattened using the max projection function in FIJI. MAP2 or GFP stains were used to mask dendrites after their first branch point; primary dendrites and cell bodies were excluded from masks. Areas of the dendritic arbor with many intersecting neurites from other cells were excluded from analyses. Images were manually

thresholded to create binary masks of clusters. Briefly, the smallest/dimmest clusters perceived to be above background were reduced to a single pixel, binarized, and then cluster masks re-expanded by a 1 pixel radius in the analysis pipeline. Cluster densities, intensities, areas, colocalization densities, and Pearson's coefficients were all calculated using automated pipelines in CellProfiler ([www.cellprofiler.org](http://www.cellprofiler.org); pipelines available upon request). Briefly, the pipeline first uses the dendrite mask to restrict all further analyses to the masked area. From there, the binary masks of clusters are used for the size, density, and colocalization densities within dendrites. Dendrite-masked greyscale images are used for Pearson's coefficients, and greyscale images are overlaid with the cluster masks to measure intensity within clusters inside the dendritic region selected for analysis.

#### **2.2.5 Electrophysiology**

Whole-cell patch-clamp recordings were performed on cortical cells at DIV18-22. Neurons were perfused at room temperature with extra-cellular solution (167mM NaCl, 2.4mM KCl, 1mM MgCl<sub>2</sub>, 10mM glucose, 10mM HEPES, 1mM CaCl<sub>2</sub>, 1μM tetrodotoxin and 100μM picrotoxin pH 7.4, 290-310mOsm). Pipettes were filled with intracellular solution (130mM Cs-methanesulfonate, 5mM CsCl, 4mM NaCl, 1mM MgCl<sub>2</sub>, 5mM EGTA, 10mM HEPES, 5mM QX-314, 0.5mM GTP, 10mM Na<sub>2</sub>-phosphocreatine, 5mM MgATP, and 0.1mM spermine, at pH 7.3 and 290 mOsm). Pipette resistance was constrained to 3-7MΩ for recording. Recordings were acquired by a Multiclamp 700B amplifier in voltage clamp mode at V<sub>h</sub> -70mV, signals were filtered at 2 kHz, digitized at 10kHz. The membrane test function was used to determine intrinsic membrane properties 1 minute after obtaining whole-cell configuration, as described previously (Kaufman *et al.*, 2012; Milnerwood *et al.*, 2012; Brigidi *et al.*, 2014; Munsie *et al.*, 2015).

Tolerance for series resistance was <28 mOhm and uncompensated, and recordings discarded if Rs changed by 10% or more. mEPSC frequency and amplitudes were analyzed with Clampfit 10 (Molecular Devices) with a detection threshold of 5pA and followed by manual confirmation of all accepted peaks; non-unitary events were suppressed from amplitude analysis but retained for frequency.

Peak-scaled nonstationary fluctuation analysis was performed on unitary events from each recording in the following way: events were aligned by peak amplitude, baselines were adjusted, and all events normalized to -1 at their maximum amplitude. Event amplitudes and variance from the mean at each recording interval were calculated using the built-in NSFA plugin in Clampfit 10 (Molecular Devices), then rescaled to pre-normalization values. Mean-variance plots were made in GraphPad Prism using values from the event peak to 5pA above baseline (due to baseline noise), and fit using the least squares method and the second order polynomial function representing the following equation:

$$\delta^2 = iI - \frac{I^2}{N} + \delta_b^2$$

where  $\delta^2$  = variance,  $i$  = single channel current,  $I$  = mean current,  $\delta_b^2$  = background variance as previously described by others (Traynelis, Silver and Cull-candy, 1993; Benke *et al.*, 2001; Hartveit and Veruki, 2007; Smith-Dijak *et al.*, 2019). For conventional NSFA,  $N$  = number of open channels at peak current; however the process of peak-normalizing required to analyze mEPSCs renders this value arbitrary. Weighted single-channel conductance was calculated by the following equation:

$$\gamma = i/(V_m - E_{rev})$$

where  $\gamma$  = weighted single-channel conductance,  $i$  = single channel current,  $V_m$  = holding potential (-70mV), and  $E_{rev}$  = reversal potential for AMPAR current (0mV in our ECS) .

Recordings were rejected if the best-fit curve had an  $R^2 < 0.5$ .

### 2.2.6 Fluorescence recovery after photo-bleaching

Primary cortical neurons were transfected with 3ug/well SEP-GluA1 plasmid (Addgene 24000) at DIV8-10 using Lipofectamine 2000 (Invitrogen 11668019) as per manufacturer's directions. At DIV21, coverslips were placed in a magnetic imaging chamber (Chamlide), bathed in 400uL HBSS (Gibco 14175095 with 1.5mM CaCl<sub>2</sub> and 1.0mM MgCl<sub>2</sub>), and imaged at room temperature. Single Z-plane images were acquired on an Olympus Fluoview 1000 confocal microscope at 63x plus 2x optical zoom. In the case of tagged protein overexpression, the intensities are a reflection of both the DNA load/expression level in the cell and changes to surface expression of the tagged protein, thus constraining acquisition settings does not allow for direct comparison of fluorescence intensities between images. As such, settings were adjusted for each cell to maximize the dynamic range. Four uniform ROIs were selected that completely encompassed SEP-GluA1-containing spine heads on each cell. A single baseline image was taken prior to bleaching, then ROIs were bleached using the Fluoview tornado function, and images were acquired every 10s for 7min, which was adequate time to reach a fluorescence recovery plateau.

Analysis ROIs were drawn tight to the photobleached spine heads, and intensity over time was quantified with the intensity over time function in FIJI. Fluorescence recovery was calculated using the following equation:

$$R_t = \frac{(F_t - F_0)}{(F_i - F_0)}$$

where  $R_t$  = recovered fluorescence at time t,  $F_0$  = fluorescence immediately after bleaching,  $F_i$  = pre-bleaching fluorescence, and  $F_t$  = fluorescence intensity at time t. To account for photobleaching by image acquisition,  $F_t$  was normalized to the amount of passive bleach on a size-matched ROI on the dendrite at each time-point.

### **2.2.7 Statistics**

All statistical analyses were conducted in GraphPad Prism 8. Because biological data is prone to lognormal distribution, outliers were only removed if inspection revealed that they resulted from an error in data collection or processing. Data sets were analyzed for normality using the D'Agostino & Pearson test. If the data failed the normality test ( $\alpha < 0.05$ ), nonparametric tests were used (Kruskal-Wallis with uncorrected Dunn's post-test). If the data passed the normality test, ( $\alpha > 0.05$ ), a parametric test was chosen. When the SDs were not significantly different, a one-way analysis of variance (ANOVA) with uncorrected Fisher's LSD post-test was used. If the SDs were significantly different, Welch's ANOVA and an unpaired t-test with Welch's correction post-test was used. In the event that the n was too low for normality testing, nonparametric tests were used. FRAP curves were analyzed using non-linear regression. Briefly, the curves were fit using one-phase association, with no weighting, and Y0 constrained to 0. Testing for K and plateau were conducted separately.

## **2.3 Results**

### **2.3.1 Altered protein-protein binding relationships in VKI brain**

Mammalian VPS35 is part of the VPS29/35/26 retromer cargo recognition trimer. With the aid of specific accessory proteins and multimeric complexes, including the WASH complex, retromer cargoes are sorted and trafficked from endosomal structures to the *trans*-Golgi network or surface membranes (reviewed in: Bonifacino and Rojas 2006; Burd and Cullen 2014; Cullen and Korswagen 2012; Seaman et al. 2013). We, and others, have previously demonstrated that exogenous wild-type VPS35 or D620N protein expression in primary cortical neurons did not alter the levels of other retromer subunits (VPS26 or VPS29), nor the known retromer endosome-to-Golgi cargo sortilin (Tsika *et al.*, 2014; Munsie *et al.*, 2015). Initial characterization of the VKI mice by our lab (Cataldi *et al.*, 2018), and since replicated by others



(Chen *et al.*, 2019), revealed no alterations in VPS35, VPS26, or VPS29 protein expression in brain tissue at 3 months of age (Cataldi *et al.*, 2018; Chen *et al.*, 2019)

Here we measured genotype effects of endogenous VPS35 D620N on expression of proteins related to retromer-mediated receptor trafficking in whole brain lysates from 3-month-old mice. In agreement with previous publications, *WES* capillary-based protein quantification found no significant genotype effect on the levels of VPS35, VPS26, or WASH complex member FAM21 relative to  $\beta$ -tubulin loading control (Fig 2-1 A.i-iv). Protein levels of NEEF21 (or NSG1) and canonical retromer cargoes CI-MPR and sortilin were also unaffected by the mutation (Fig 2-1 C.i-ii; D.i-ii; sortilin not shown).

Our lab, and others, previously showed the D620N mutation in VPS35 does not impair core retromer subunit assembly by semi-quantitative co-immunoprecipitation (coIP) in mutant overexpression systems (Follett *et al.*, 2013; Ian J. McGough *et al.*, 2014; Zavodszky *et al.*, 2014; Munsie *et al.*, 2015). Here we assayed subunit assembly by coIP in whole-brain lysate from 3-month-old VKI mice blotted on the *WES* system and similarly found no genotype effect on the amount of VPS26 pulled down (Fig 2-1 Bi-ii), replicating recently published findings (Chen *et al.*, 2019). However, in cell lines, the D620N mutation impairs retromer-WASH complex association, via reduced VPS35-FAM21 binding (Ian J. McGough *et al.*, 2014; Zavodszky *et al.*, 2014). In agreement with these reports, we found the level of FAM21 pulled by VPS35 in coIPs was subject to a statistically significant genotype effect in whole-brain lysates (Fig 2-1 Bi & iii).

In summary, in our hands, expression of D620N mutant VPS35 does not detectably alter protein expression levels of core retromer components, known interactor FAM21, endolysosomal system markers, nor canonical cargoes. While retromer complex assembly appears unaltered, we do

replicate previously published work indicating that the association of VPS35 with FAM21 is reduced in VKI mutants.

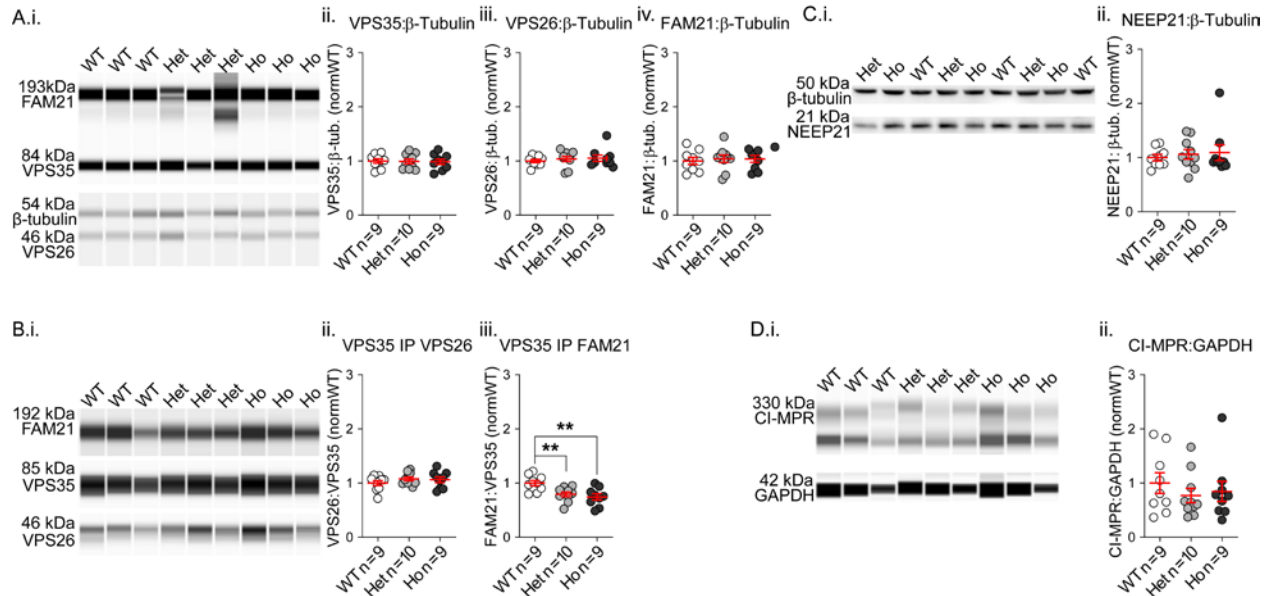


**Figure 2-1 Expression levels and co-immunoprecipitation of retromer and associated endolysosomal proteins reveals altered FAM21 binding in VKI mouse brain.** **A.i)** Proteins in brain lysates were quantified using WES capillary-based analysis that produces chemiluminescence curves displayed as a traditional western blot for visual representation. Samples were loaded with antibodies against VPS35, VPS26, FAM21 and β-tubulin (as a loading control). Band intensities were quantified relative to β-tubulin and normalized to wild-type (WT) levels. There were no significant genotype effects on protein levels of retromer components VPS35 (ii, 1-way ANOVA  $p=0.97$ ) & VPS26 (iii, Kruskal-Wallis  $p=0.73$ ), nor for the VPS35-WASH binding partner FAM21 (iv, 1-way ANOVA  $p=0.88$ ). **B.i)** Co-immunoprecipitations were performed on lysates using anti-VPS35 to pull retromer complex and associated proteins. IPs were run on the WES system, as in A, and probed for VPS35, VPS26 and FAM21. IP protein levels were normalized to the amount of VPS35 pulled and to WT. There was no genotype effect on VPS26 associated with VPS35 (ii, 1-way ANOVA  $p=0.44$ ), but a significant effect of genotype on FAM21 levels (iii, 1-way ANOVA  $p<0.003$ ), due to significantly less FAM21 being associated with VPS35 in both heterozygous (Het) and homozygous (Ho) brain lysates by *post-test (Fisher's LSD \*\* $p<0.01$ )*. **C.i)** For assessment of NEEP21, lysates were separated by gel electrophoresis and probed with antibodies against NEEP21 and β-tubulin. Quantification (relative to β-tubulin and normalized to WT levels) revealed no significant genotype effect on the levels of NEEP21 (ii, Kruskal-Wallis  $p=0.80$ ). **D.i)** Lysates were probed as in A&B for the canonical cargo CI-MPR and GAPDH (loading control). Protein levels were quantified relative to GAPDH and normalized to WT; there were no significant genotypes effects on CI-MPR (ii, Kruskal-Wallis  $p=0.66$ ). For all panels, n represents number of experimental animals.

### **2.3.2 No mutation effect on survival or morphology of primary cortical neurons**

Others have demonstrated that *in utero* (E15.5) VPS35 knock-down reduces the length of the apical dendrites of hippocampal CA1 neurons at postnatal day 7 and later (Wang *et al.*, 2012), and that transient lentiviral overexpression of either WT or D620N VPS35 impedes neurite outgrowth in rat cortical cultures to a similar extent (Tsika *et al.*, 2014). Expression of several other PD-linked mutant proteins has also been shown to alter neuronal morphology in primary cultured neurons (Dächsel *et al.*, 2010; MacLeod *et al.*, 2013), albeit only during the first 1-2 weeks *in vitro* in germ line scenarios (Sepulveda *et al.*, 2013; Beccano-Kelly, Kuhlmann, *et al.*, 2014). In light of these findings, we characterized the survival and morphology of cultured cortical neurons from VKI mice.

In primary cortical neurons at DIV21, genotype had no significant effect on cell density (Fig 2-2 B). To assess dendrite length and complexity, CAG-AAV-GFP constructs were nucleofected into a subset of cortical neurons on the day of plating and morphology was quantified at DIV21 (Fig 2-2 A). Following Sholl analysis, there were no genotype effects on the number of intersections (Fig 2-2 C), or secondary measures of neurite complexity (Fig 2-2 D-F).

We have no evidence to suggest that physiological expression of VPS35 D620N alters the survival or structural development of cultured cortical neurons at 21 days *in-vitro*.

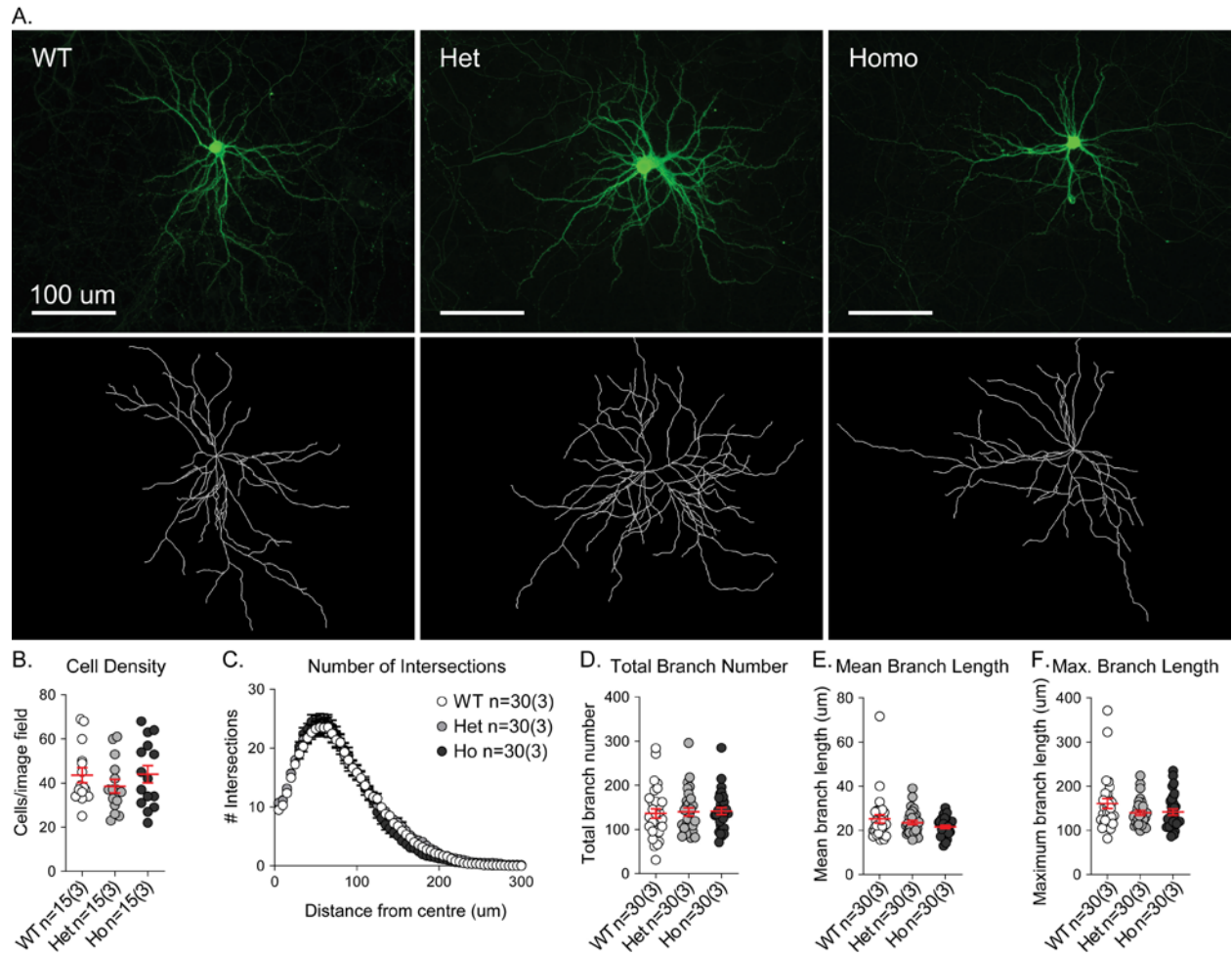


**Figure 2-2 Cell density and dendritic morphology are not altered in mature cortical cultures from VKI mice.** **A)** A subset of cortical cells were nucleofected with CAG-AAV-GFP plasmids on the day of plating and fixed at DIV21. Amplified GFP signal and imaging of individual cells (A, top panel) was conducted to produce 2D *in silico* cell reconstructions (A, bottom panel). There was no effect of genotype on the number of neurons per image field in low-magnification images of primary cortical cultures at DIV21, indicating equivalent survival (B, 1-way ANOVA  $p=0.47$ ). Sholl analysis revealed no significant effect of genotype upon neurite complexity (C, 2-way RM ANOVA radial distance x genotype interaction  $p=0.87$ ; genotype  $p=0.78$ ). There were also no significant genotype effects on total branch number, average branch length, or maximum branch length (D-F, Kruskal-Wallis  $p=0.79$ ,  $0.34$  &  $0.29$ , respectively). For all panels, n is reported as X(Y) where X=number of cells & Y=number of independent cultures.

### **2.3.3 Increased colocalization and density of endosomal recycling proteins**

Given that the D620N mutation alters the interaction of VPS35 with accessory complexes required for its trafficking functions, we looked to see if D620N affects the localization of VPS35 and its known interactors within the dendrites of cortical neurons. To achieve this, we cultured primary cortical cultures to DIV21 and stained them by immunocytochemistry for VPS35 with one of VPS26, FAM21, NEEF21, or Rab11.

Dendritic cluster densities of VPS35 itself were not affected by genotype (Fig 2-3 A.i); however, the density of retromer trimer component VPS26 was reduced in both heterozygous and homozygous cells (Fig 2-3 A.ii). As expected, we observed robust colocalization of VPS35 with VPS26 (Fig 2-3 B.i; Pearson's  $\sim 0.6$ ) and no statistically significant genotype effect on colocalized cluster density (Fig 2-3 B.ii) or Pearson's correlation coefficient (Fig 2-3 B.iii). Due to high background for the VPS26 antibody (a polyclonal antibody from serum bleed) and the necessarily subjective nature of cluster thresholding for analysis, it is possible that reduced signal intensity in heterozygous and homozygous cultures resulted in inaccuracies in cluster density measurements (e.g. an underestimation). This explanation would be consistent with previous reports from ourselves and others (Follett *et al.*, 2013; Ian J. McGough *et al.*, 2014; Zavodszky *et al.*, 2014; Munsie *et al.*, 2015), and the observations here that suggest the D620N mutation does not affect retromer trimer assembly or co-cluster density.

VPS35 binding to FAM21 was reduced by coIP (Fig 2-1 Bi & iii), thus we predicted reductions in either FAM21 dendritic cluster density, FAM21 colocalization with VPS35, or both. There was no statistically significant effect on the density of FAM21 clusters, though there were non-significant increases in the mean density in both mutant conditions (Fig 2-3 A.iii). VPS35 and FAM21 were strongly colocalized (Fig 2-3 C.i; Pearson's  $\sim 0.6$ ) and, counterintuitively, the

density of co-clusters was increased in a mutant gene dose-dependent manner, with a statistically significant increase in homozygous cells (Fig 2-3 C.ii). However, there was no statistically significant effect of genotype on the Pearson's coefficient (Fig 2-3 C.iii), which would be consistent with additional FAM21 clusters overlapping with retromer to the same degree as in WT cells.

To explore the endosomal localization of VPS35, we co-stained cultured neurons with VPS35 and NEEP21 or Rab11. Neuronal endosomal enriched protein 21 (NEEP21 or NSG1) is a transmembrane protein that is itinerant in dendritic endosomes as they mature from Rab5-positive early endosomes, through Rab7-positive late endosomes, and is rapidly degraded in lysosomes with little to no observable recycling through recycling endosomes (Yap *et al.*, 2017). We therefore used NEEP21 as a marker of the non-recycling endolysosomal pathway (Fig 2-3 D.i). We observed no genotype effect on the density of NEEP21 clusters (Fig 2-3 A.iv), nor VPS35-NEEP21 co-cluster densities (Fig 2-3 D.ii). There was, however, a statistically significant decrease in the Pearson's coefficient (Fig 2-3 D.iii). VPS35 and NEEP21 signals apposed each other with a small degree of overlap (Fig 2-3 D.i; Pearson's coefficient  $\sim 0.2$ ). A reduction in the Pearson's coefficient with no change in cluster or colocalization densities could reflect a reduction in overlap between cluster signals, or a decrease in the number of NEEP21 clusters that are associated with each cluster of VPS35 (as the colocalization density does not take into account multiplicity of NEEP21 per VPS35 parent).

Rab11 is a Rab-GTPase that resides in recycling endosomes (REs) and participates in AMPAR surface trafficking (Correia *et al.*, 2008; Jaafari, Henley and Hanley, 2012; Seeböhm *et al.*, 2012; Esteves da Silva *et al.*, 2015; Bodrikov *et al.*, 2017; Bowen *et al.*, 2017). We used it here as a marker of REs (Fig 2-3 E.i). Rab11 cluster density was increased in both heterozygous and

homozygous cells (Fig 2-3 A.v). Despite these increases, there was no genotype effect on the colocalization density of VPS35 with Rab11 (Fig 2-3 E.ii) and a decrease in Pearson's coefficient in heterozygous cells (Fig 2-3 E.iii). A reduction in Pearson's coefficient in this instance may be reflective of an accumulation of recycling endosomes that are not associated with retromer.

In DIV21 cultured cortical neurons, the D620N mutation increases dendritic expression of proteins involved in protein recycling: colocalized VPS35 with FAM21, and Rab11-positive recycling endosomes. VPS35 acts in concert with the WASH complex to drive surface recycling of receptors out of endosomes (Derivery *et al.*, 2009; Gomez and Billadeau, 2009), whereas Rab11 resides in recycling endosomes that collect surface-bound receptors for delivery to the plasma membrane (Correia *et al.*, 2008; Jaafari, Henley and Hanley, 2012; Seeböhm *et al.*, 2012; Esteves da Silva *et al.*, 2015; Bodrikov *et al.*, 2017; Bowen *et al.*, 2017). Together these observations suggest that neurons harboring the D620N mutation either have an increased capacity for surface transport of cargo, or that the surface delivery is halted resulting in an accumulation of surface-bound recycling endosomes.

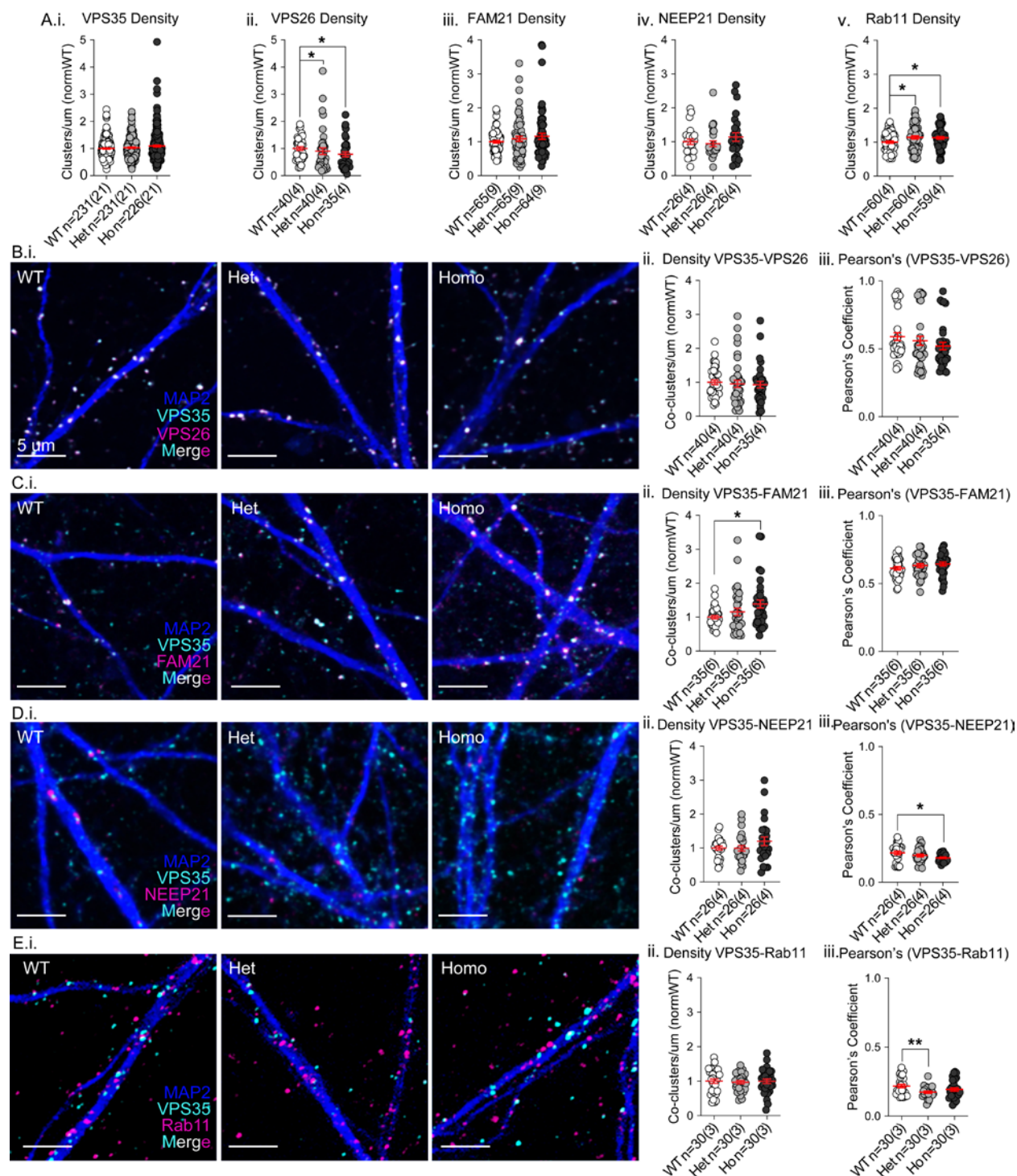


**Figure 2-3 Visualization of retromer and associated endosomal proteins reveals accumulation of VPS35- FAM21 co-clusters and recycling endosomes in mouse cortical neuron dendrites.** Primary - cortical neurons were fixed at DIV21 and immunostained for MAP2 (blue), VPS35 (cyan), and either VPS26, FAM21, NEEP21, or Rab11 (magenta). **A.i-v)** There was no significant effect of genotype on the cluster density of VPS35 (i, Kruskal-Wallis  $p=0.30$ ), FAM21 (iii,  $p=0.24$ ), or NEEP21 (iv,  $p=0.37$ ). VPS26 cluster density was significantly



**Figure 2-3 (cont.)** reduced in both genotypes (ii, Kruskal-Wallis  $p < 0.04$ ; Uncorrected Dunn's  $\text{Het } *p < 0.04$  &  $\text{Ho } *p < 0.02$ ). Rab11 densities (recycling endosomes) were significantly increased in both genotypes (v, 1-way ANOVA  $p < 0.03$ ; Uncorrected Fisher's LSD  $*p < 0.02$  &  $*p < 0.03$ ). **B.i**) Representative images of VPS35 and VPS26 staining; there was no significant effect of genotype on the colocalization of VPS35 and VPS26 by co-cluster density or Pearson's coefficient (ii & iii, Kruskal-Wallis  $p = 0.45$  &  $0.10$ , respectively). **C.i**) Representative images of VPS35 and FAM21 staining; there was a significant effect of genotype on co-cluster density (ii, Kruskal-Wallis  $p < 0.03$ ) due to significant increases in homozygous cells (uncorrected Dunn's  $*p < 0.02$ ); however there was no genotype effect on Pearson's coefficient (iv, 1-way ANOVA  $p = 0.24$ ). **D.i**) Representative images of NEEP21 and VPS35 staining; there was no genotype effect on density of co-clusters of VPS35 and NEEP21 (ii, Kruskal-Wallis  $p = 0.38$ ); however, there was a significant genotype effect on Pearson's correlation coefficient (iii, Welch's ANOVA  $p < 0.03$ ). This was due to significantly less NEEP21-VPS35 correlation in homozygous VKI dendrites (unpaired t with Welch's correction  $*p < 0.02$ ), indicating that clusters that are colocalized are less tightly overlapped. **E.i**) Representative image of VPS35 and Rab11 staining; there was no genotype effect on the co-cluster density of VPS35 and Rab11 (ii, 1-way ANOVA  $p = 0.92$ ); however, there were significant reductions in the Pearson's coefficient (iii Welch's ANOVA  $p < 0.009$ ) due to a significantly reduced correlation in heterozygous dendrites (unpaired t with Welch's correction  $**p < 0.003$ ), presumably resulting from increases in Rab11 cluster density that are not associated with VPS35. For all panels, n is reported as X(Y) where X=number of cells & Y=number of independent cultures.

### 2.3.4 VPS35 association with GluA1 not altered by D620N mutation

We, and others, previously demonstrated that VPS35 traffics AMPA-type glutamate receptors in neurons (Zhang *et al.*, 2012; Choy *et al.*, 2014; Munsie *et al.*, 2015; Tian *et al.*, 2015; Temkin *et al.*, 2017). We showed that VPS35 interacts, either directly or indirectly, with GluA1-containing AMPARs in murine brain tissue by semi-quantitative coIP, and GluA1 signals appeared increased in neurites of mutant overexpressing mouse primary neurons and human iPSC-derived dopamine neurons (Munsie *et al.*, 2015).

Here we also used western blot and coIP to investigate whether endogenous mutations in VPS35 result in changes to binding or localization with GluA1. We found no meaningful differences in GluA1 protein levels in cortical lysates from 3-month-old VKI mice as quantified by fluorescence western blot (Fig 2-4 A.i&ii). There was similarly no genotype effect upon the pull-down of GluA1 by VPS35 in our coIPs (Fig 2-4 B.i&ii). We also assayed coIP of other neurotransmitter receptors in cortical and striatal lysates and discovered that endogenous VPS35 interacts with

NMDA receptor subunit GluN1 and D2-type dopamine receptors (D2R; Appendix A-1 A.i & C.i). There was no detectable genotype effect on GluN1 or D2R protein expression levels in either cortex or striatum of VKI mice (Appendix A-1 A.iv&.vi; C.iv&.vi) and there were similarly no genotype effects on the amount of GluN1 or D2R in coIP with VPS35 in either tissue (Appendix A-1 A.v&.vii; C.v&.vii).

We then performed ICC on cultured cortical neurons at DIV21 to visualize VPS35 and GluA1 dendritic localization (Fig 2-4 C.i). We discovered statistically significant reductions in dendritic GluA1 cluster density in homozygous cortical neurons (Fig 2-4 C.ii). Colocalized cluster density was only slightly reduced (Fig 2-4 C.iii), with little effect on the Pearson's coefficient (Fig 2-4 C.iv), indicating that the reduction in GluA1 clusters is occurring outside of retromer-positive structures.

In summary, the D620N mutation had no effect on expression levels of GluA1 or association with retromer in cortical tissues. The density of dendritic GluA1 clusters was reduced in homozygous neurons, but remaining clusters localized with VPS35 to the same extent.

### **2.3.5 Altered surface stability and kinetics of GluA1 turnover**

Overexpression of WT VPS35 alters the surface recovery of GluA1 by FRAP in cultured neurons (Munsie *et al.*, 2015), and the D620N mutation has been reported to impair surface trafficking of AMPARs (Munsie *et al.*, 2015; Temkin *et al.*, 2017). To measure the kinetics of synaptic GluA1 turnover in knock-in neurons, we used fluorescence recovery after photobleaching in neurons exogenously expressing GluA1 tagged with an extracellular super-ecliptic phlorin GFP (SEP-GluA1; Fig 2-4 D.i).

SEP is a pH-sensitive GFP tag that fluoresces at much higher intensities at extracellular pH and is quenched in endosomal compartments (Kopeck *et al.*, 2006). This property allows one to visualize, and photobleach, surface-expressed SEP-GluA1. Following bleach, one can subsequently quantify the recovery of signal over time, as new receptors are surface trafficked or laterally diffused to synaptic clusters. This type of experiment gives two types of data: the rate of signal recovery over time (K), and the plateau of recovery. Changes in K reflect changes in the real-time rate of AMPAR translocation, whereas the plateau produces a measure of the 'immobile fraction' i.e., the percentage of photobleached receptors that are stable at the cell surface over the course of the experiment and that could not be replaced. Using non-linear regression modeling of best-fit curves, we found that there was a statistically significant reduction in the recovery plateau (or an increase in the immobile fraction) in heterozygous neurons (Fig 2-4 D.ii-v). There was a trend toward an increased rate of recovery in heterozygous cells (Fig 2-4 D.ii-v; WT K = 0.009205; Het K=0.009962; Ho K= 0.009058) that reached statistical significance in a WT-Het only comparison (Fig 2-4 D.ii&iv). No significant effects were observed in homozygous neurons.

In summary, we found the D620N mutation increased the rate of GluA1 recovery, and the immobile fraction of receptors in dendritic spines, but only in heterozygous mutant neurons.

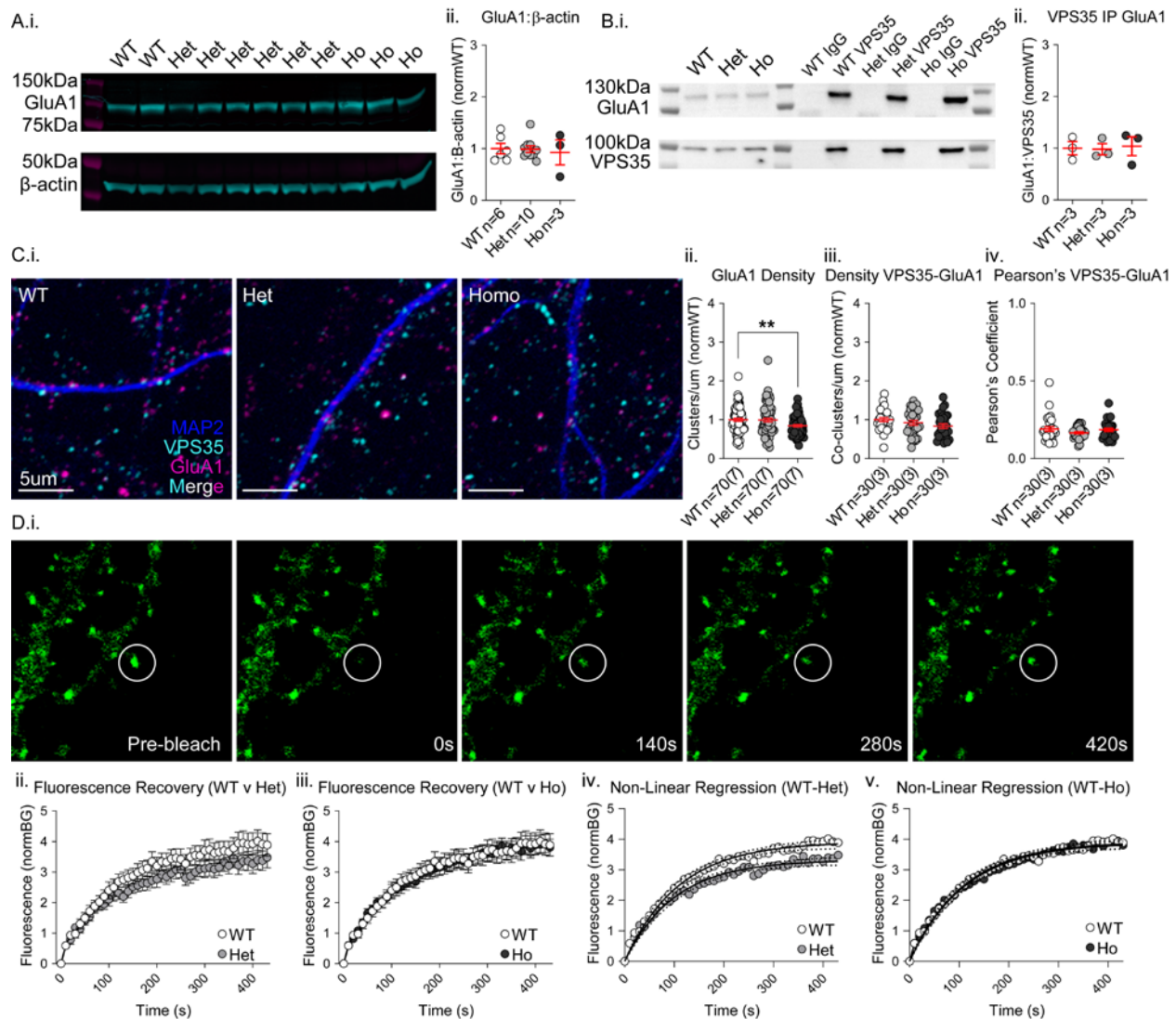


**Figure 2-4 Dendritic localization and surface delivery kinetics of GluA1 altered in the absence of changes to protein expression or association with VPS35 in the cortex** **A.i)** GluA1 expression in cortical lysates from VKI mice was quantified by running samples on an electrophoresis gel and probing for GluA1 and  $\beta$ -actin (loading control) and normalized to WT. There were no genotype effects on the expression of GluA1 (ii, Kruskal-Wallis  $p=0.99$ ). **B.i)** Co-immunoprecipitations were performed on cortical lysates using anti-VPS35 to pull GluA1, and quantified by chemi-luminescence western blot. There were no genotype effects on the association of GluA1 with VPS35 (ii, Kruskal-Wallis  $p=0.99$ ). **C.i)** Cultured cortical neurons were fixed at DIV21 and immunostained for MAP2 (blue), VPS35 (cyan), and GluA1 (magenta). Cluster analysis revealed a significant reduction in GluA1 cluster density in homozygous neurons only (ii, Kruskal-Wallis  $p<0.02$ ; Uncorrected Dunn's  $^{**}p<0.005$ ). There was no significant genotype effect on co-cluster density of VPS35 with GluA1 (iii, 1-way ANOVA  $p=0.13$ ), nor on the Pearson's coefficient (iv, Kruskal-Wallis  $p=0.57$ ). **D.i)** Cultured cortical neurons were transfected with surface-fluorescent SEP-GluA1 at DIV18, and live-cell imaged at DIV21. Individual spines were photobleached and recovery of signal imaged for 420s at room temperature. Fluorescence recovery plots were separated to facilitate visualization (ii & iii). Non-linear regression best fit curves uncovered a genotype effect on the plateau of recovery in heterozygous cells (iv. Comparison

**Figure 2-4 (cont.)** of fits  $p < 0.0001$ ). Rate of fluorescence recovery (K) was significantly altered in heterozygous cells only in a WT-Het comparison (comparison of fits WT-Het-Ho  $p = 0.70$ ; comparison of fits WT-Het  $p < 0.0001$ ). For Aii & Bii, n represents number of experimental animals. For Cii-iv & Dii-iii, n is reported as X(Y) where X=number of cells & Y=number of independent cultures.

### **2.3.6 Increased glutamatergic transmission and surface AMPAR expression**

Overexpression of WT and D620N VPS35 reduces synapse number and frequency of miniature excitatory post-synaptic currents (mEPSCs) (Munsie *et al.*, 2015). However, relative to WT, mutant overexpression results in larger mEPSC amplitudes, hinting at mutant effects on postsynaptic AMPAR trafficking (Munsie *et al.*, 2015). To confirm whether the endogenous mutation has functional effects on glutamatergic synapses, we examined the number and activity of glutamatergic synapses in primary cortical cultures from wild-type and VKI mice.

Excitatory synapse numbers were quantified by staining for presynaptic (VGluT1) and postsynaptic (PSD95) markers (Fig 2-5 A.i); cluster analysis revealed no genotype effect on synapse numbers (as reflected by colocalized cluster density) nor densities of VGluT1 or PSD95 clusters individually (Fig 2-5 A.ii-iv). In concert with the observation that neurite length and complexity were unchanged (Fig 2-2 B), this strongly supports the conclusion that there are no differences in the density of glutamatergic synapses in VKI cultures.

We also performed whole-cell patch clamp recording of mEPSCs to assess the function of glutamatergic synapses in mature (DIV21) primary cortical cultures (Fig 2-5 B.i). Event frequency was increased, particularly in heterozygous neurons (Fig 2-5 B.ii). An increase in mEPSC frequency with no change in synapse density is often regarded as indicating that the probability of release for vesicles has changed, though it could also reflect fewer silent synapses (synapses with PSD95 and VGluT1, but no surface AMPARs). The amplitude of mEPSCs was also higher in mutant neurons, again primarily in heterozygous cells (Fig 2-5 B.iii), suggestive of

elevated postsynaptic AMPAR surface expression. It is noteworthy that we observed a VGluT1 cluster intensity decrease affecting only homozygous cultures (Fig 2-5 A.v), which could contribute to the smaller magnitude of mEPSC frequency and/or amplitude effects observed in these neurons.

Another explanation for smaller amplitude differences in homozygous cells could be that the synapses have reached a more mature state more quickly. Homomeric, calcium-permeable (CP) AMPARs are transiently inserted during development when new synapses are unsilenced, and similarly in adult brains in the initial phases of LTP induction, then quickly replaced with non-calcium permeable heteromeric receptors (reviewed in: Benke and Traynelis 2019; Park et al. 2018). CP-AMPA receptors have higher conductance and faster kinetics than their heteromeric counterparts (*ibid*). In this case, differences in event amplitudes could reflect either fewer total surface AMPARs, a shift to more heteromeric AMPARs with lower channel conductance, or be mediated entirely by VGluT1 intensity reductions (if it affects quantal size) at the presynapse. In order to gain insight into the receptor profiles, we looked at the decay tau of mEPSCs as a measure of kinetics, but found no statistically significant differences between genotypes despite a trend to being reduced in homozygous neurons (Fig 2-5 B.iv). We also performed peak-scaled nonstationary fluctuation analysis (Fig 2-5 B.v), which allowed us to calculate the mean single-channel conductance of the AMPARs from each mEPSC recording. There was no statistically significant effect of genotype on the single channel conductance (Fig 2-5 B.vi).

To disambiguate the source of frequency and amplitude changes in our mEPSC recordings, we performed a surface stain for an extracellular epitope of AMPAR subunit GluA1. GluA1 was chosen as we have previously observed that VPS35 preferentially precipitates GluA1 versus GluA2 by coIP (Munsie *et al.*, 2015). Surface GluA1 cluster intensity was higher in heterozygous

cells, mirroring the mEPSC amplitude data (Fig 2-5 C.ii). The intensity of surface GluA1 signal across the entire dendritic area was not altered, reflective of the increase occurring in synaptic (clustered) GluA1 only (Fig 2-5 C.iv). Neither heterozygous nor homozygous neurons had significantly different surface GluA1 cluster densities than WT; however, the mutants were significantly different from one another, with heterozygous neurons having slightly fewer surface GluA1 clusters than WT and homozygous neurons having slightly more (Fig 2-5 C.iii). This result shows that mEPSC frequency changes, at least in heterozygous neurons, are unlikely to be the result of unsilencing of synapses through novel AMPAR insertion. They most probably reflect a change in the presynaptic probability of release of glutamate vesicles.

Together the data demonstrate that the endogenous VPS35 D620N mutation produces a gain-of-function in pre- and post-synaptic glutamate transmission. It increases postsynaptic surface AMPAR expression and mEPSC amplitude. Frequency of mEPSCs is also increased by the mutation, likely through increases to presynaptic probability of release. Homozygous neurons had an additional phenotype of reduced VGluT1 intensity and dendritic GluA1 cluster density that may contribute to more muted functional outcomes than those observed in heterozygous neurons.

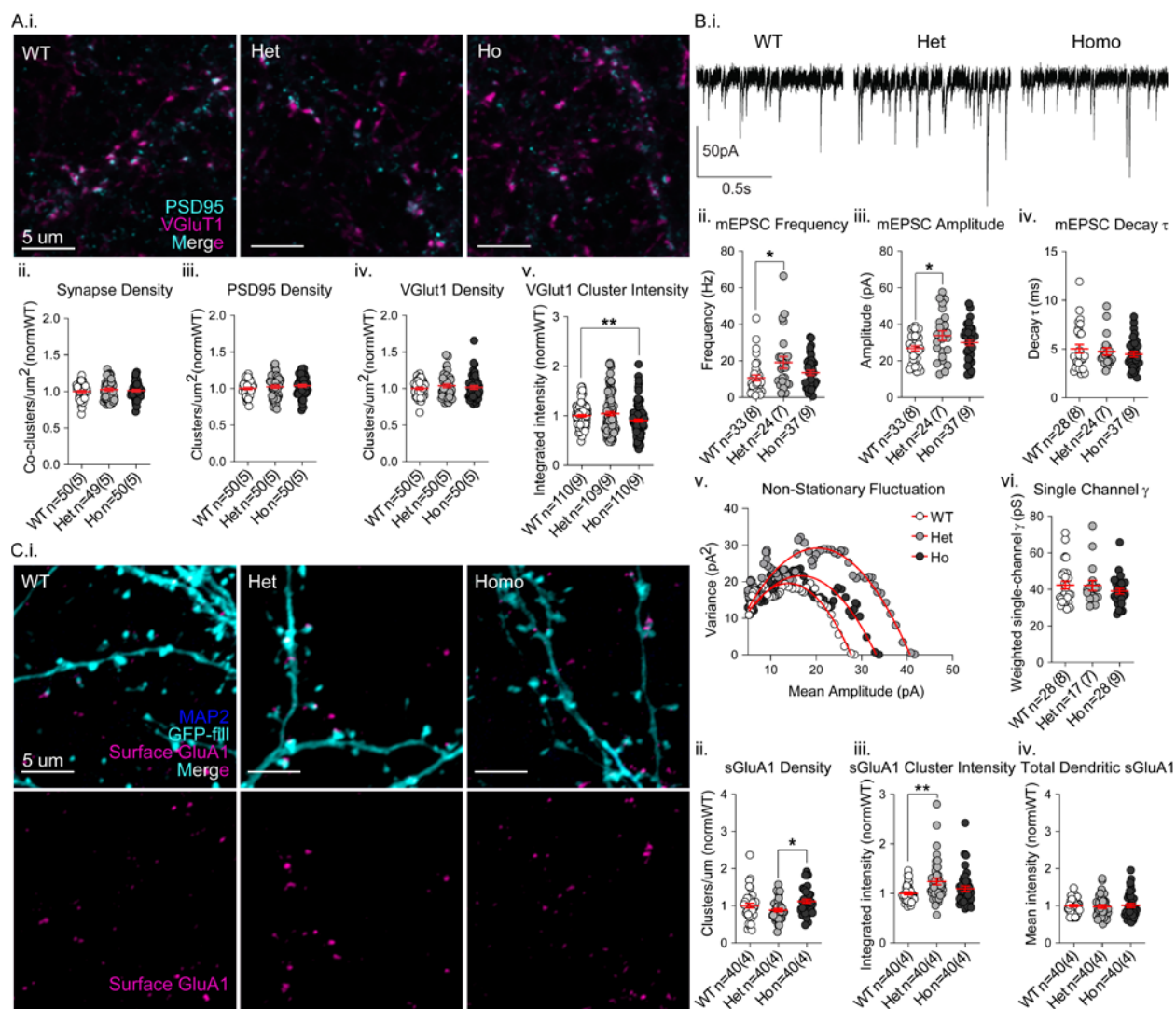


**Figure 2-5 Excitatory synapse function, but not number, is altered in cortical cultures from VKI mice.**

**A.i)** Representative images of synapse staining in cortical neurons at DIV21. Immunostaining for PSD95 (cyan) and VGLuT1 (magenta) and PSD-95 (cyan) revealed no significant effect of genotype on synapse density defined as colocalized clusters of VGLuT1 and PSD-95 (ii, 1-way ANOVA  $p=0.57$ ), PSD95 density, or VGLuT1 density (iii-iv, Welch's ANOVA  $p=0.29$  &  $0.42$ , respectively). VGLuT1 cluster intensity was significantly reduced in homozygous cells only (v, Kruskal-Wallis  $p<0.007$ ; Uncorrected Dunn's  $**p<0.003$ ). **B.i)** Representative traces from whole-cell patch clamp recording of mEPSCs in voltage clamped DIV21 cortical neurons held at  $-70$ mV. Mean mEPSC frequency (Hz) was significantly increased by large mutant effects in heterozygous neurons (ii, Kruskal-Wallis  $p<0.04$ ; Uncorrected Dunn's  $*p<0.02$ ). Mean mEPSC amplitudes were similarly increased in heterozygous cells (iii, 1-way ANOVA  $p<0.05$ ; Uncorrected Fisher's LSD  $*p<0.02$ ). Mean mEPSC decay times ( $\tau$ ) were not affected by genotype (iv, Kruskal-Wallis  $p=0.74$ ). Peak-scaled non-stationary noise analysis was performed by plotting the mean variance of traces from a recording average at each amplitude (v, representative mean-variance plots); the best fit curve allows for the calculation of weighted single channel conductance of the synapses involved in each recording. There was no significant effect of genotype on single channel conductance (vi, Kruskal-Wallis  $p=0.78$ ), indicating no change in the



**Figure 2-5 (cont.)** average AMPAR subunit composition in synapses. **C.i)** GFP-filled cortical cells were fixed at DIV21 and immunostained for MAP2 (blue; to check for areas of membrane permeabilization) and surface GluA1 (magenta)(top panel). Representative images of GluA1 surface immunostaining (bottom panel). There was a significant genotype effect on surface GluA1 cluster intensity (synaptic GluA1) due to significant increases in heterozygous cells (ii, Kruskal-Wallis  $p<0.007$ ; Uncorrected Dunn's  $**p<0.02$ ). There was also a significant difference in the GluA1 cluster density, due to opposing effects on heterozygous and homozygous cells (iii, Kruskal-Wallis  $p<0.009$ ), reflecting either a difference in AMPAR subunit composition, or alterations to the number of synapses that are active (AMPA-containing). There was no significant genotype effect on intensity of surface GluA1 signal over the entire masked dendritic area (iv, Kruskal-Wallis  $p=0.63$ ). For all panels, n is reported as X(Y) where X=number of cells & Y=number of independent cultures.

## 2.4 Discussion

We investigated the effects of the endogenous D620N mutation on protein expression, binding interactions, glutamate receptor trafficking, and glutamatergic synapse strength in brain tissue and cultured cortical neurons from VPS35 D620N knock-in mice. We found alterations in accessory protein binding in brain lysates, similar to overexpression reports of the D620N mutation. The mutation did not appear to affect binding of cargoes, nor their steady-state expression levels. Other studies have largely labeled the D620N mutation as a loss-of-function in knock-down/rescue models (Follett *et al.*, 2013; MacLeod *et al.*, 2013; Ian J. McGough *et al.*, 2014; Zavodszky *et al.*, 2014; Temkin *et al.*, 2017). Our initial characterization of VKI mice revealed early increases in dopamine release in *ex vivo* striatal slices (Cataldi *et al.*, 2018) and the present work shows that physiological expression of VPS35 D620N increases the capacity for surface recycling of GluA1-containing AMPARs, surface trafficking kinetics, presynaptic glutamate release, and postsynaptic receptor expression.

### 2.4.1 D620N increases the capacity for GluA1 trafficking

Consistent with published cell-line work by other groups (Follett *et al.*, 2013; Ian J. McGough *et al.*, 2014; Zavodszky *et al.*, 2014), we confirm a mutation-dependent reduction in the interaction of VPS35 and FAM21 by coIP in brain tissue from VKI mice. This occurred in the absence of

changes to retromer assembly or protein levels (Follett *et al.*, 2013; Ian J. McGough *et al.*, 2014; Tsika *et al.*, 2014; Zavodszky *et al.*, 2014; Munsie *et al.*, 2015; Chen *et al.*, 2019). Successful surface delivery of retromer cargo requires the WASH complex to regulate endosomal actin dynamics, and the auxiliary protein SNX27 for correct targeting (Derivery *et al.*, 2009, 2012; Gomez and Billadeau, 2009; Temkin *et al.*, 2011; Lee, Chang and Blackstone, 2016). In the complete absence of WASH-complex member FAM21, retromer surface cargo is neither degraded, nor trafficked to the surface, but rather remains in SNX27-retromer-positive vesicular structures that accumulate in the cytosol (Lee, Chang and Blackstone, 2016).

Despite previous reports suggesting that D620N results in a loss of lysosomal enzyme receptor retrieval (Follett *et al.*, 2013; MacLeod *et al.*, 2013; Ian J. McGough *et al.*, 2014; Munsie *et al.*, 2015), we found no significant differences in the expression levels of retrograde cargoes CI-MPR or sortilin. We also observed no effect on the levels of NEEP21 – a surface protein that is degraded in lysosomes after internalization with little to no recycling (Yap *et al.*, 2017). In agreement with other reports in murine brains (Tsika *et al.*, 2014), we have no evidence that the D620N mutation impairs lysosomal receptor expression or protein degradation, though we cannot rule it out.

In our immunocytochemical assays, VPS35 cluster densities in the dendrites of mature (DIV21) cultured cortical neurons were unaffected. There was no change in the colocalization of VPS35 with VPS26 by co-cluster density or Pearson's coefficient, consistent with unaltered retromer assembly. It is worthwhile to note, however, that cluster densities of VPS26 were significantly lower in mutant neurons. This occurs alongside a significant reduction in the mean VPS26 cluster intensity (data not shown). We manually threshold cluster masks to accept only clusters that are a certain threshold above background, therefore a reduction in intensity may result in

dim clusters from heterozygous and homozygous cells falling below threshold. We derive Pearson's coefficients, on the other hand, from raw images and thus subjective thresholding effects do not mar them. The data suggests that VPS26 is associating with VPS35 at normal levels (as evidenced by similar coIP, co-cluster densities, and Pearson's), but that there is perhaps additional VPS35 recruited to, or retained on, late endosomal membranes and not associated with VPS26. In support of this possibility, several groups have found that VPS35 and VPS29 are capable of forming a stable dimer without VPS26 (Haft *et al.*, 2000; Fuse *et al.*, 2015). The functions or consequences of a VPS35-VPS29-only complex are currently unknown, but it is thought provoking to revisit one of the first studies of mammalian retromer trafficking, which found that depletion of VPS26 caused either lysosomal degradation of CI-MPR or its displacement to the plasma membrane (Seaman, 2004).

NEEP21 is a neuron-enriched protein that traverses the degradative endocytic pathway through Rab5- and Rab7-positive endosomes (Yap *et al.*, 2017); the density of NEEP21 clusters and their colocalization with VPS35 were unaffected, suggesting that the D620N mutation does not affect retromer recruitment to early and late endosomes. Retromer creates tubules filled with recycling cargoes that extend from the endosome (reviewed in: Bonifacino and Rojas 2006; Burd and Cullen 2014; Cullen and Korswagen 2012; Seaman et al. 2013) accounting for the only slight overlap in NEEP21 and VPS35 signal. Elsewhere we have found abnormal elongation of SNX1-positive tubules on endosomes occurs in knock-in models of other PD mutations (Follett *et al.*, 2019). Here we observe a reduction in the Pearson's coefficient of VPS35 and NEEP21 without co-cluster density changes, compatible with elongated extension of VPS35-positive recycling tubules from endosomes in a mutant context.

The WASH complex is thought to be recruited to endosomes via the direct binding of the large C-terminal tail of FAM21 with VPS35 and SNX27 (Gomez and Billadeau, 2009; Harbour, Breusegem and Seaman, 2012; Jia *et al.*, 2012). One might predict that reduced FAM21 binding to VPS35 D620N would reduce colocalization between VPS35 and FAM21 in neuronal dendrites, and result in a loss of surface recycling. The initial evidence from cell-line models was conflicting: McGough and colleagues (2014) found no change in the colocalization of VPS35 D620N with FAM21 in overexpression systems by Pearson's and observed no loss of surface recycling with D620N expression. Zavodszky *et al.* (2014) did report a reduction in FAM21 cluster *intensity*, which was not measured in the McGough study. Either way, the loss of FAM21 binding is not absolute; it is clear from both previous studies and our current work that FAM21 can bind to VPS35, be recruited to endosomal membranes, and participate in surface recycling when VPS35 D620N is expressed (Ian J. McGough *et al.*, 2014).

In the dendrites of cultured cortical neurons, we observed a puzzling increase in the density of FAM21 clusters and their colocalization with mutant VPS35. This suggests that, at least in dendritic endosomes in neurons, endogenous expression of VPS35 D620N results in increased endosomal recruitment or retention of the WASH complex. Of import to interpretation of this data is the observation that the FAM21 tail possesses many putative VPS35 binding sites (Jia *et al.*, 2012), and further binds directly to SNX27 (Lee, Chang and Blackstone, 2016). In this context, it is possible that the D620N mutation reduces association with non-SNX27/surface-bound retromer (apparent as reduced coIP), but that it is still recruited (and possibly more available) for the trafficking of surface cargoes through the SNX27 interaction. Furthermore, another endosomal recycling complex has recently been identified in mammalian cells, the retriever complex, that localizes to the same endosomal subdomains as retromer and also binds the WASH complex; thus it is possible that retriever-mediated WASH binding is intact, and

perhaps can substitute for retromer binding when it is impaired (McNally *et al.*, 2017). Further experiments exploring the association ratios and localization with SNX27 and retriever components would be very illuminating.

Jia *et al* (2012) propose that the association of FAM21 with multiple retromer complexes allows WASH to detect enriched retromer patches on endosomes as they condense cargoes into tubules for transport. Due to the multivalence of the FAM21-VPS35 interaction, it is also possible that initial binding/recruitment is unaffected, but that FAM21 is unable to perform its function as a coincidence detector when concentrations of VPS35 are high. An emerging report suggests that retromer assembles into higher order structures on membrane tubules; the D620N mutation is an acidic to neutral change within a cluster of acidic residues that are essential for retromer-retromer interactions (Kendall *et al.*, 2020). This could result in more loosely packed clusters of VPS35, and prevent the ability of FAM21 to bind multivalently. It turns out that the epitope of the antibody we used for coIP lies across the residues proposed to act as interaction sites for oligomerization, thus oligomerized VPS35 may be more difficult to pull by coIP. In support of the mutation affecting higher-order oligomerization, we consistently found that the ratio of VPS35 pulled to VPS35 input was higher in the mutants (Appendix A-1).

It must be addressed that a recent publication was unable to detect interaction between VPS35 and FAM21 in 3 month old mouse brains by coIP or mass spectrometry, leading the authors to question whether this interaction was important in the brain (Chen *et al.*, 2019). The detection of protein-protein interactions can be highly sensitive to the conditions of their extraction, and can be further complicated in adult brain tissue by interfering fibrous matter (DeCaprio and Kohl, 2017). The buffer recipes used here and in Chen *et al.* (2019) were the same; however, other steps in the lysate preparation such as homogenization and clearance may have differed.

We replicated VPS35 interaction with FAM21 by coIP in murine brains in at least nine independent experiments from four different mouse lines, and by pulling FAM21 (Appendix A-2), making it the most robust replication in this study.

Rab11 localizes to recycling endosomes near the plasma membrane and has been shown to participate in both the recycling and forward trafficking of AMPARs (Correia *et al.*, 2008; Jaafari, Henley and Hanley, 2012; Seeböhm *et al.*, 2012; Esteves da Silva *et al.*, 2015; Bodrikov *et al.*, 2017; Bowen *et al.*, 2017). Inoshita and colleagues (2017) found that VPS35 and Rab11 interact by coIP in rat brain tissue. We show here that VPS35 and Rab11 co-clusters do co-localize in the dendrites of our cultured cortical neurons. Rab11/REs were more abundant in the mutant cells. However, these accumulated REs were not retromer-associated (as reflected by no change in the co-cluster density and a reduction in Pearson's coefficients), suggesting that recycling endosomes are accumulating downstream of retromer trafficking.

Taken together the ICC data suggest that the D620N mutation results in an increased capacity for surface recycling, through increased VPS35-WASH complex colocalization on endosomal membranes, and recycling endosome density. Conversely, this could represent an accumulation of surface-bound cargoes that are unable to reach their destination as is observed in FAM21 knock-down studies (Lee, Chang and Blackstone, 2016). VPS35 has previously been implicated in surface trafficking of GluA1-containing AMPARs in overexpression and knock-down/out studies (Choy *et al.*, 2014; Munsie *et al.*, 2015; Tian *et al.*, 2015; Temkin *et al.*, 2017; Vazquez-Sanchez *et al.*, 2018). Initial reports concluded that the D620N mutation confers a loss-of-function to surface AMPAR trafficking. Temkin *et al.* (2017) found that expressing D620N in VPS35-depleted hippocampal cultures was insufficient to rescue LTP deficits; we found that WT and D620N mutation overexpression had opposing effects on mEPSC amplitude (Munsie *et al.*,

2015). This present work represents the first study of GluA1 trafficking in a knock-in model of VPS35 D620N parkinsonism, in which we demonstrate that the D620N mutation acts as a gain-of-function in surface AMPAR expression and glutamatergic transmission.

Here there were no changes to GluA1 protein expression or association with VPS35 by coIP. Endosomal colocalization density of VPS35 with GluA1 was unchanged despite decreases in dendritic GluA1 cluster density in homozygous neurons. In non-manipulated cultures, any changes to recycling pathways do not appear to affect the quantity of GluA1 being recycled by retromer at a fixed time-point. Retromer has been shown to participate in LTP in other studies (Muhammad *et al.*, 2008; Temkin *et al.*, 2017), therefore it is possible that the induction of activity-driven synaptic remodeling would be necessary to observe changes in association. The reduced GluA1 cluster density in homozygous neurons could indicate fewer GluA1-containing structures available for surface delivery via retromer-independent pathways (new receptors), or downstream of retromer sorting.

The immobile fraction (interpreted as surface-stable receptors) in FRAP experiments was increased in heterozygous cultures only, and there was a trend toward an increased rate of recovery (K) in heterozygous cultures as well. AMPAR inclusion in synapses is believed to occur through exocytosis at extrasynaptic sites followed by diffusion and stabilization at the postsynaptic density (Ashby *et al.*, 2006; Opazo and Choquet, 2011). The increased kinetics of GluA1 turnover could reflect more extrasynaptic AMPARs already at the surface available for diffusion, but surface staining of GluA1 revealed no genotype effects on total dendritic GluA1 intensity. An increase in K in this case most likely results from changes to receptor trafficking or diffusion kinetics. Further experiments are required to disambiguate this result. We do observe

an increase in the immobile fraction, which is congruent with more receptors stabilized in the PSD (Ashby *et al.*, 2006).

To summarize, we found that the D620N mutation results in no changes to expression levels of retromer components, accessory proteins, or cargoes in brain tissue from VKI mice. Retromer assembly by coIP was unaffected, whereas association of FAM21 was reduced, not ablated. In the dendrites of cortical neurons, the presence of the mutation results in an increase in the density of proteins involved in retromer-mediated surface recycling, namely membrane-bound FAM21 colocalized with VPS35, and recycling endosomes. All of the above changes occur in both heterozygous and homozygous cells in a gene dose-dependent manner. The mutation did not affect association of VPS35 with GluA1 by coIP, nor colocalization in dendrites; indicating that the quantity of GluA1 being internalized and recycled in naïve cultures is not affected. FRAP experiments revealed increases in the kinetics of synaptic GluA1 turnover and surface receptor stability in heterozygous neurons only.

It is remarkable that the changes in biochemistry and cluster analyses of trafficking machinery discussed to this point were present in both heterozygous and homozygous cultures in a gene dose-dependent manner. Dendritic GluA1 density and trafficking kinetics reflect departures from this trend. This may be due to mechanistic differences between mixed WT-mutant and mutant-only retromer clusters, or compensatory changes occurring in homozygous cells more strongly in light of increased surface recycling. I urge the reader to keep these possibilities in the back of their mind reading on; I will acknowledge them in detail later in this discussion.



#### **2.4.2 Identification of two putative novel retromer cargoes**

Experiments have revealed many neuron-specific retromer cargoes in the years since it was first linked to neurodegeneration:  $\beta$ -2ARs (Temkin *et al.*, 2011; Choy *et al.*, 2014), glycine receptors (del Pino *et al.*, 2011), GluA1-containing AMPARs (Zhang *et al.*, 2012; Tsika *et al.*, 2014; Munsie *et al.*, 2015; Tian *et al.*, 2015), GluN2-containing NMDARs (Ma *et al.*, 2017), D1-type dopamine receptors (C. Wang *et al.*, 2016), DAT (Wu *et al.*, 2017), and possibly multiple neuroligins (Kang *et al.*, 2014; Binda *et al.*, 2019).

Thus, it is perhaps of little surprise that we identified two new putative retromer cargoes in our coIPs: NMDA receptor subunit GluN1, and the D2-type dopamine receptor (D2R). This finding adds to the growing list of neuron-specific retromer cargoes. NMDARs have an essential role in synaptic plasticity (reviewed in: Bliss and Collingridge, 2019). D2R is of particular interest due to its involvement in regulating postsynaptic response in medium spiny neurons in the striatum, and presynaptic transmitter release from cortical and nigral terminals (reviewed in: Gerfen and Surmeier, 2011). We have found changes in dopamine release in the VKI knock-in mice and in LRRK2 animal models of PD that are sensitive to D2R agonism, suggesting D2R trafficking pathways could be disrupted by PD-causing mutations (Volta *et al.*, 2017; Cataldi *et al.*, 2018). Both of these receptors have important roles within the nigrostriatal circuitry that is most affected by PD, making them very attractive candidates for future studies of retromer traffic.

#### **2.4.3 Functional consequences are pre- and postsynaptic**

Alterations to glutamatergic transmission in VKI primary neuronal cultures are consistent with mutant effects upon regulation of pre- and postsynaptic processes. Increased AMPAR-mediated mEPSC amplitudes suggest a greater number of surface receptors at synaptic sites. Indeed, we observed changes in surface GluA1 cluster intensity resembling the mEPSC amplitude changes.

These results are similar to the observed effects of larger mEPSC amplitudes with D620N overexpression compared to WT (Munsie *et al.*, 2015); however, the question arises of how impairment of FAM21 binding (a protein required for normal surface trafficking) results in increased VPS35-FAM21 co-cluster density and increased AMPAR surface expression.

FAM21 knock-down has been shown to result in the accumulation of surface-bound cargoes in VPS35 and SNX27 positive structures that do not reach the surface (Lee, Chang and Blackstone, 2016). This suggests that FAM21 is not required for sorting from endosomes, but rather for successful surface delivery. In a study of WASH-retromer function in *Dictyostelium*, FAM21 knock-down did not alter WASH complex recruitment to endosomal membranes, but WASH became co-localized with extended 'fountains' of F-actin, suggesting that FAM21 plays a negative regulatory role in ending WASH-mediated actin polymerization (Park *et al.*, 2013). If the same function holds true in mammalian systems, reduced FAM21 association with retromer (after WASH recruitment to endosomal complexes as discussed above) could result in increased WASH-mediated sorting and scission of surface-bound vesicles. It is possible that FAM21 binding across multiple retromer units acts to signal the release of WASH once adequate cargo has been sequestered, allowing the membrane association of downstream proteins required for surface delivery (such as Rab11). In the context of reduced, but not ablated, binding efficiency, it is possible increased delivery of cargo and membranes into the surface recycling pathway occurs, while still achieving the eventual release necessary for surface delivery. In support of this, one of the cell-line studies that concluded D620N conferred a loss-of-function reported aberrant CI-MPR surface localization with mutant expression, but did not consider it in their conclusions (MacLeod *et al.*, 2013). This hypothesis is consistent with the observed increases in VPS35 extension from NEEP21-positive structures, density of VPS35-FAM21 co-clusters, and

density of dendritic REs. Further study of SNX27 interactions and FAM21-tail mutant constructs could shed light on the exact mechanism of this phenomenon.

Endogenous levels of D620N VPS35 produced increases in the frequency of mEPSCs in heterozygous neurons, with no change in synapse number, or surface GluA1 density. This alludes to an increased probability of presynaptic release. Presynaptic transmission is similarly increased in cultures, and in slices from young animals, harbouring PD-causing mutations in LRRK2 (Beccano-Kelly, Kuhlmann, *et al.*, 2014; Matikainen-Ankney *et al.*, 2016; Volta *et al.*, 2017). Our initial characterization of the VKI mice revealed similar increases in dopamine release in young mice (Cataldi *et al.*, 2018).

The release phenotype we found is important, given that several proteins linked and/or associated with PD participate in the synaptic vesicle cycle. Alpha-synuclein, which confers the second highest genetic risk for PD (after LRRK2), is a presynaptic regulatory protein associated with endosomal and vesicular membranes (Bendor, Logan and Edwards, 2013; Boassa *et al.*, 2013; Westphal and Chandra, 2013; Logan *et al.*, 2017). LRRK2 is similarly endosomally localized (Schreij *et al.*, 2015), co-immunoprecipitates with VPS35 (MacLeod *et al.*, 2013; Vilariño-Güell *et al.*, 2013), and, like  $\alpha$ -synuclein, regulates presynaptic release of glutamate and dopamine (Piccoli *et al.*, 2011; Beccano-Kelly, Kuhlmann, *et al.*, 2014; Beccano-Kelly, Volta, *et al.*, 2014; Cirnaru *et al.*, 2014; Volta *et al.*, 2015; Matikainen-Ankney *et al.*, 2016). Thus our investigation of the VPS35 PD mutation adds further support to the theory that synaptic transmission is augmented at early time points, potentially representing early pathophysiological processes in PD (Picconi, Piccoli and Calabresi, 2012; Volta, Milnerwood and Farrer, 2015).

To date, reports on retromer function in presynaptic compartments have been scarce, and conflicting. We, and others, have shown that retromer is localized in axons and is present in glutamatergic synaptic boutons in cultured murine neurons (Munsie *et al.*, 2015; Vazquez-Sanchez *et al.*, 2018). We previously reported a reduction in the frequency of mEPSCs in cultured cortical neurons overexpressing WT or mutant VPS35 compared to GFP-expressing control cells; however, there was a concomitant reduction in synapse number which rendered the result inconclusive as to presynaptic effects on SV release (Munsie *et al.*, 2015).

Retromer deficiency or acute knock-down in hippocampal slices has no effect on synaptic glutamate release (Tian *et al.*, 2015; Temkin *et al.*, 2017), or SV exo- or endocytosis (Vazquez-Sanchez *et al.*, 2018). Conversely, knock-down of dVPS35 in *Drosophila melanogaster* produces enlarged synaptic vesicles and impairments to vesicle regeneration at larval neuromuscular junctions, leading the authors to propose that VPS35 participates in the regeneration of SVs from bulk-endocytosed membrane (Inoshita *et al.*, 2017). Given our lack of knowledge of the presynaptic roles of retromer in synapse development and maintenance, it is possible that mutant VPS35 causes aberrant protein function, perhaps by relocating it to synaptic vesicles in the presynapse or interfering with other functions that have downstream consequences for SV release.

In live cell studies of VPS35 trafficking in dendrites, we observed rapid axonal transport of VPS35 clusters through the imaging field (Munsie *et al.*, 2015), and retromer has been shown to associate with presynaptically expressed transmembrane proteins such as D2R (present study) and DAT (C. Wang *et al.*, 2016). Thus it is also possible that mammalian retromer does not participate directly in the SV cycle, but is involved in the axonal transport and / or local

presynaptic recycling of proteins that could indirectly modulate transmitter release in some circumstances.

Mitochondrial dysfunction represents a common pathophysiology in many PD models (reviewed in: Nguyen *et al.*, 2019). VPS35 localizes to mitochondria where it has been implicated in mitochondrial protein trafficking and homeostasis (Braschi *et al.*, 2010; F. L. Tang *et al.*, 2015; Farmer *et al.*, 2017, 2019; Zhang *et al.*, 2018). The D620N mutation, like many PD-causing mutations, has been shown to disrupt mitochondrial integrity (F. L. Tang *et al.*, 2015).

Mitochondria are localized at presynaptic terminals, where they contribute to synaptic plasticity and transmitter release, possibly through calcium-buffering (reviewed in: Lee *et al.*, 2018).

Mitochondria and VPS35 are both only localized to a subset of presynaptic terminals, thus it would be illuminating to co-stain for synaptic, VPS35, and mitochondrial markers, to determine whether VPS35 is associated with presynaptic mitochondria, and whether the D620N mutation impairs any association if it is present.

The mechanism of glutamate release phenotypes remains an enigma, for the time being. It is nevertheless clear that retromer has a role in presynaptic terminals, and the study of this is a ripe area for future investigations.

#### **2.4.4 Divergent functional outcomes in heterozygous and homozygous contexts**

Differences in biochemical associations and dendritic localization measures (coIP, ICC) were more pronounced in homozygous cells, whereas the functional phenotypes were more apparent in heterozygous neurons. It may be that the same functional synaptic alterations occur in homozygous neurons prior to the experimental time-point, which then progressively decline through altered rates of synaptic development, or the onset of compensatory mechanisms;

processes which may be accelerated by the presence of two copies of the mutation. In support of this, early increases in neurotransmission are attenuated over time in LRRK2 PD mutant knock-in models (Matikainen-Ankney *et al.*, 2016; Volta *et al.*, 2017).

Synapse development and maintenance are exquisitely complex. Homomeric, CP-AMPA receptors are transiently inserted during development when new synapses are unsilenced, and similarly in adult brains in the initial phases of LTP induction, then quickly replaced with non-calcium permeable heteromeric receptors (reviewed in: Diering and Huganir, 2018; Park *et al.*, 2018; Benke and Traynelis, 2019; Purkey and Dell'Acqua, 2020). CP-AMPA receptors have higher conductance and faster kinetics than their heteromeric counterparts (*ibid*). The observations that VPS35 preferentially pulls down GluA1 by coIP, and participates in LTP, provide tantalizing evidence for its role in CP-AMPA receptor trafficking. In this instance, an earlier increase in CP-AMPA receptor expression, or continued aberrant recycling, in mutant contexts could drive homozygous cells more quickly to a mature state where heteromeric receptors are more plentiful. These receptors generally have a lower conductance and slower kinetics, and could account for the attenuated surface GluA1 intensity and mEPSC amplitude in the homozygous cells; however, one would expect more mature synapses to be more stable (*ibid*), and we found homozygous neurons have a smaller immobile fraction in FRAP experiments. Furthermore, the mean single channel conductance was only slightly decreased by homozygous mutant expression, and there was no significant change in event decay tau, providing insufficient evidence to support accelerated maturation of synapses, thus far.

Synaptic strength is also modified in an activity-dependent manner, largely via calcium signaling, which can result in both increases and decreases in synaptic strength, via receptor forward trafficking and removal from the PSD, respectively (reviewed in: Diering and Huganir,

2018; Bliss and Collingridge, 2019). Initial increases to surface expression of GluA1 and presynaptic vesicle release could thus be attenuated over time by activity/calcium-dependent feedback mechanisms. In this scenario some aberrant GluA1 surface recycling could potentiate synapses (heterozygous cells) whereas a lot could depress them (homozygous). In support of this hypothesis, we observe a reduction in GluA1 outside of retromer clusters (indicating less available GluA1 outside of recycling pathways), and VGluT1 intensity reductions, only in homozygous cells. FRAP revealed more receptor surface stability (increased immobile fraction) in heterozygous neurons only. A normal immobile fraction in FRAP, an only-slight increase in surface GluA1 expression, and no observed effects on channel conductance or kinetics, in homozygous cultures are all consistent with this hypothesis.

Alternatively, there may be functional differences between heterozygous and homozygous mutant expression. If reduced FAM21 binding results in prolonged VPS35-FAM21 association, it may be that mutant copies increase cargo sorting to surface trafficking pathways, and WT protein confers capacity for surface delivery. With two mutant copies, forward trafficking may be further impaired to a point where surface-bound endosomes are less efficient at reaching their destination; however, if this were true, one would expect an accumulation of GluA1 clusters in the dendrites of homozygous cells. We found the opposite. Two mutant copies may reduce binding so much that the sorting of GluA1 out of maturing endosomes would be impaired, rather than promoted. Reduced GluA1 cluster density in homozygous neuron dendrites lend credence to this idea, but larger increases in co-localized VPS35-FAM21 and RE density do not.

Based on the available data, compensatory regulation in homozygous neurons seems most likely. Future investigation of receptor composition, post-translational modifications, and calcium dynamics, at earlier and later time points, would help to unravel whether such

phenomena are a result of compensatory mechanisms, accelerated maturation, or mechanistic differences.

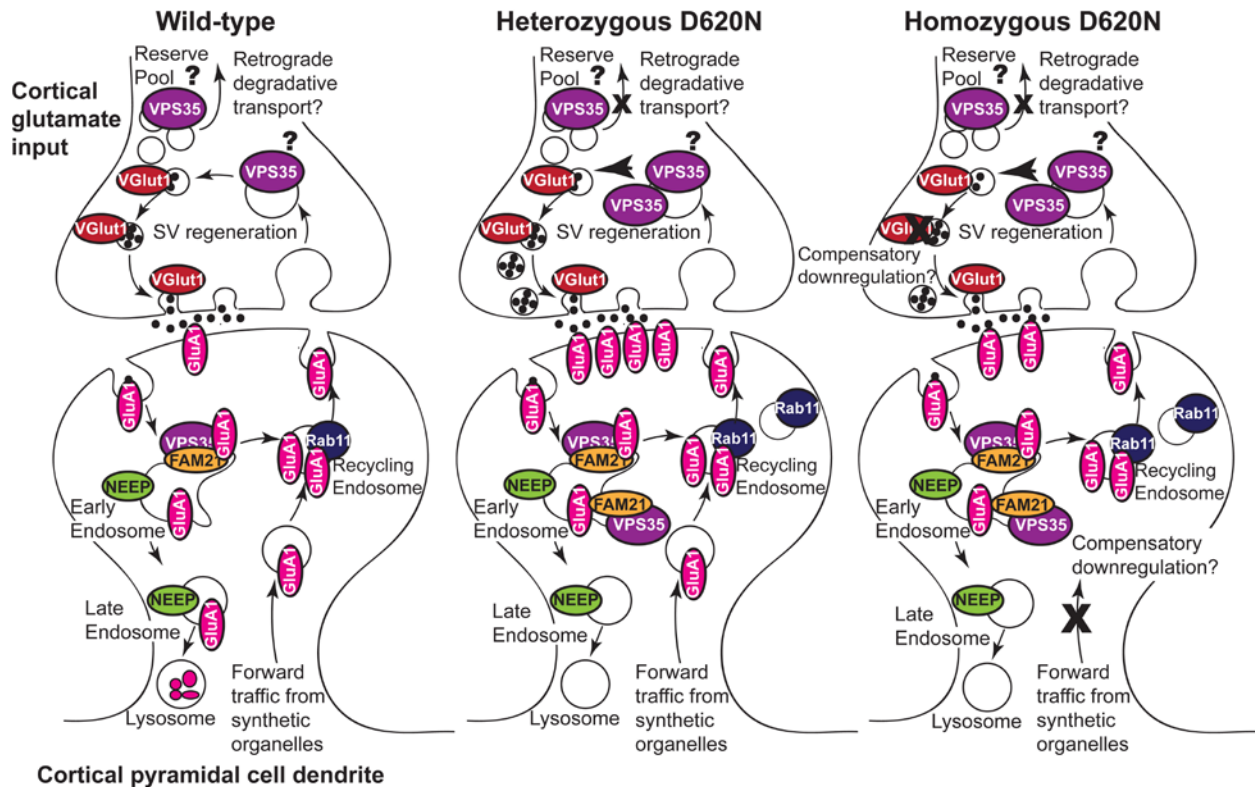


**Figure 2-6 Working model of increased surface AMPAR expression in D620N mutants.** In wild-type cells, postsynaptic VPS35 recycles GluA1-containing AMPARs. At the presynaptic terminal it may be participating in synaptic vesicle regeneration or recycling of synaptic vesicle cargoes. In heterozygous neurons, reduced FAM21 binding results in persistence of retromer on the endosomal membrane, accumulation of recycling endosomes, and increased forward trafficking/surface expression of AMPARs. Proposed mechanisms of presynaptic release increases are increased SV regeneration or reduced reserve pool retrograde traffic for degradation. Homozygous neurons have similar upregulations in retromer with FAM21 and recycling endosomes, but attenuated glutamate phenotypes and surface AMPAR expression. Attenuated phenotypes are likely due to downregulation of presynaptic VGLUT1 and downregulation of postsynaptic receptor trafficking into distal dendrites from synthesis organelles/somatic Golgi.



## 2.5 Conclusion

The results here highlight the importance of studying mutant effects on proteins when expressed at endogenous levels. We concluded in our original overexpression study that the mutation led to a loss-of-function in AMPAR recycling, and had no effect on transmitter release (Munsie et al). At endogenous levels of protein expression, the mutation confers a gain-of-function to surface trafficking and increases the probability of glutamate release. VPS35 is a promiscuous protein with multiple roles coded by different subsets of interacting partners; it is clear from the greater body of literature on retromer function that expression levels of retromer, and availability of interacting partners, matters. In this context, it may be more accurate to classify the D620N mutation as a *change-of-function*.

We also identified two novel candidate neuronal cargoes, GluN1 and D2R. We add further support to the hypothesis that PD-linked mutations converge on synaptic protein trafficking pathways, producing a common pathophysiological disturbance, that eventually manifests as parkinsonism.

While molecular and network compensation may delay catastrophic pathophysiology, compensation may fail with age. Here we have shown that a single point mutation in endogenous mouse VPS35 produces functional alterations, manifest as early cellular, biochemical, and synaptic phenotypes. This is a valuable platform on which to study the underlying etiology and pathophysiology of familial parkinsonism and design disease-modifying interventions.

## **Chapter 3: Investigating the interplay of VPS35 and LRRK2 in glutamatergic synapse function.**

### **3.1 Introduction**

In Chapter 2 I demonstrated that mutations in VPS35 increase forward trafficking of GluA1. While reduced binding of FAM21 to retromer is a possible mechanism, it does not represent a particularly great target for pharmaceutical development. Small molecule drugs can increase the stability of core retromer components and are of potential therapeutic benefit in Alzheimer's disease, where retromer depletion impairs APP processing (Mecozzi *et al.*, 2014). As the D620N mutation causes a gain-of-function in AMPAR trafficking, and VPS35 is so promiscuous, such a strategy for PD could cause unpredictable changes in function or even an exacerbation of disease processes. A better strategy for treatment may be to identify proteins and processes downstream of VPS35 that are better candidates for drug development.

LRRK2 is a large multi-domain protein that is implicated in ~5% of all familial Parkinson's disease through autosomal-dominant and risk-factor mutations (Healy *et al.*, 2008), the most common of which is the G2019S mutation. LRRK2 is involved in a number of cellular processes such as autophagy (reviewed in: P. Gómez-Suaga *et al.*, 2014), endolysosomal sorting (MacLeod *et al.*, 2013; Gómez-Suaga, Rivero-Ríos, *et al.*, 2014; Schreij *et al.*, 2015), and cytoskeletal dynamics (Parisiadou *et al.*, 2009; Pellegrini *et al.*, 2017). In neurons, it participates in synaptic vesicle recycling and release (Piccoli *et al.*, 2011; Beccano-Kelly, Kuhlmann, *et al.*, 2014; Beccano-Kelly, Volta, *et al.*, 2014; Cirnaru *et al.*, 2014; Volta *et al.*, 2015), and in post-synaptic receptor trafficking and spine development, possibly through regulation of PKA (Parisiadou *et al.*, 2014; Sweet *et al.*, 2015; Matikainen-Ankney *et al.*, 2016, 2018).

Emerging reports provide evidence that LRRK2 interacts with VPS35 both physically (MacLeod *et al.*, 2013; Vilariño-Güell *et al.*, 2013) and functionally (MacLeod *et al.*, 2013; Linhart *et al.*, 2014; Inoshita *et al.*, 2017; Mir *et al.*, 2018; Zhao *et al.*, 2018). LRRK2 is recruited to the TGN, resulting in activation of its kinase and phosphorylation of known substrates Rab8 and Rab10 (MacLeod *et al.*, 2013; Beilina *et al.*, 2014; Liu *et al.*, 2018; Purlyte *et al.*, 2018). There it interacts with syntaxin-6 (Beilina *et al.*, 2020), which has been indirectly associated with retromer function by participating in the TGN delivery and homeostatic sequestration of known retromer cargoes (Pérez-Victoria, Mardones and Bonifacino, 2007; Alshafie *et al.*, 2020). Overexpression of LRRK2 G2019S or VPS35 D620N in cell lines results in the same CI-MPR localization impairments, and the G2019S effects can be rescued by co-expression of WT-VPS35 (MacLeod *et al.*, 2013), suggesting they may interact at least indirectly in the cycling of endosome-TGN proteins.

LRRK2 has also been implicated, to a lesser extent, in protein trafficking at endosomes. It localizes with EEA1 (Schreij *et al.*, 2015) and Rab10 (Liu *et al.*, 2018) in the cell periphery, and phosphorylates Rab5 (Steger *et al.*, 2016; Jeong *et al.*, 2018) which localizes to early-endosomes. G2019S expression has been shown to interfere with the degradation of surface receptor EGFR through impaired cargo entry into Rab7-positive late endosomes and reduced Rab7 activity (Gómez-Suaga, Rivero-Ríos, *et al.*, 2014). Reduced Rab7 activity and resultant EGFR trafficking impairments can also be induced by knock-down or dominant-negative expression of LRRK2 substrates Rab8A or Rab10, and rescued by expression of constitutively active Rab7 or Rab7L1, suggesting that LRRK2 may act upstream of Rab7 in endosomal receptor recycling pathways (Rivero-Ríos *et al.*, 2019, 2020). While interaction of LRRK2 with retromer on endosomes has not yet been assayed directly, some retromer pathways are dependent on

Rab7 activation (Rojas *et al.*, 2008; Seaman *et al.*, 2009), suggesting the two may interact functionally if not also physically at endosomes.

In an exciting recent publication, Inoshita *et al.* (2017) reported that LRRK2 localizes upstream of VPS35 on synaptic vesicles at the larval *Drosophila* neuromuscular junction and that they interact functionally along with Rab5 and Rab11 to regulate synaptic vesicle cycling. It unknown at this time if this holds true at mammalian central synapses, but provides some preliminary evidence that these proteins can act together to regulate presynaptic transmission.

Most PD-associated mutations in LRRK2 increase the activity of its kinase domain (reviewed in: Taylor and Alessi, 2020). Two recent phospho-proteomics studies have revealed that a subset of Rab-GTPases are substrates of LRRK2 kinase (Steger *et al.*, 2016; Jeong *et al.*, 2018).

Noteworthy amongst these are Rab3 and Rab5 that have proposed roles in the SV cycle (reviewed in: Pavlos and Jahn, 2011; Binotti, Jahn and En Chua, 2016), and Rab8 and Rab10 which are both implicated in AMPAR surface trafficking (Gerges, Backos and Esteban, 2004; Brown *et al.*, 2007; Glodowski *et al.*, 2007; Bowen *et al.*, 2017). Increased autophosphorylation of LRRK2 and downstream phosphorylation of Rab10 have both been observed in *post-mortem* SN tissue from individuals with idiopathic PD (Di Maio *et al.*, 2018). This lead us to hypothesize that VPS35 and LRRK2 mutations, as well as other etiological factors, may converge on LRRK2 kinase activity, and that aberrant phosphorylation of Rab proteins involved in the SV cycle and in postsynaptic AMPAR trafficking may be responsible for the pre- and postsynaptic glutamate transmission phenotypes observed in Chapter 2.

Indeed, while working on this part of my dissertation project, a publication was released showing that LRRK2 kinase activity is increased in a variety of murine tissues (including brain)

from D620N knock-in mice and in monocytes from human individuals with the D620N mutation (Mir *et al.*, 2018), providing excellent evidence in support of this hypothesis.

Here we assayed LRRK2 kinase activity by phospho-specific western blot of LRRK2 and its substrate Rab10 in brain tissue and cultured cortical neurons from the D620N knock-in mice, and assayed the effects of LRRK2 kinase inhibition on the glutamatergic transmission phenotypes we had discovered in Chapter 2. Surprisingly, LRRK2 inhibition had no marked effect on presynaptic probability of glutamate release in the D620N knock-in mice. We observed effects on post-synaptic AMPAR trafficking in WT cells consistent with LRRK2 kinase activity acting as a negative regulatory brake on surface trafficking of AMPARs to developing/silent synapses. Differential mutant effects were observed in heterozygous and homozygous neurons, interpretation of which was clouded by unfortunate genotype-dependent effects of the solubilization vehicle Captisol on glutamate transmission.

## **3.2 Materials and methods**

### **3.2.1 VPS35 D620N knock-in mice and genotyping**

We used the same strain of VKI mice as in Chapter 2, bred from the same colony. They were housed, bred, handled, and genotyped following the same procedures. All procedures were conducted in the Montreal Neurological Institute's Centre for Neurological Disease Modeling, in accordance with the McGill ACC ethical approval certificate 2017-7888B.

### **3.2.2 LRRK2 kinase inhibition with MLi2 treatment**

We inhibited LRRK2 kinase activity with the selective LRRK2 inhibitor MLi-2 (Tocris 5756). MLi-2 has low solubility in water, necessitating the use of a vehicle for solubilization. We chose to use the cyclodextrin Captisol (Ligand RC-0C7-100) as a vehicle, due to its worldwide safety

approval and use in human drug formulations ([www.captisol.com/about](http://www.captisol.com/about)). We bath sonicated 1mg MLi-2 in 2mL 45% Captisol-PBS for ~2 hours at room temperature (until complete solubilization of MLi-2). Solutions were filter sterilized prior to use. Primary cortical cultures were treated with 500nM MLi-2 or Captisol-only control (each 1mL well treated with 0.4uL stock in 100mL fresh media; final Captisol concentration 0.00016%) for 2 hours prior to fixation for ICC, lysis for western blot, or transferred to the microscope chamber for electrophysiology experiments. Treatment concentrations and times were selected based on the pharmacokinetic data collected by Fell and colleagues (2015). For western blot experiments in brain tissue, animals were injected intraperitoneally with MLi-2 or Captisol-only control at a dose of 5mg/kg, 2 hours prior to rapid decapitation without anaesthesia. All tissues were collected, frozen, and stored as described in Chapter 2.

### **3.2.3 Western blots**

All western blots were performed following the fluorescence western blot protocol for LI-COR Odyssey imaging and analyzed as described in Chapter 2. Antibody specificity was tested using lysate from LRRK2 knock-out mouse brain or Rab10 knock-out AtT20 cell lysates prepared following the protocols in Chapter 2. The LRRK2 knock-out mice have been previously described by Hinkle and colleagues (2012). Rab10 knock-out AtT30 cells were a kind gift from Dr. Peter McPherson, and have been previously described (Alshafie *et al.*, 2020).

We used the following primary antibodies: LRRK2 (Abcam ab133474), LRRK2 phosphoS935 (Abcam ab133450), Rab10 phosphoT73 (Abcam ab230261), Rab10 (Abcam ab104859), VPS35 (Abnova H00055737-M02), GluA1 (Millipore 05-855R), VGluT1 (Millipore AB5905),  $\beta$ -Actin (Abcam ab6276), and GAPDH (ThermoFisher MA5-15738).

### **3.2.4 Primary cortical cultures**

Primary cultures were prepared following the protocol in Chapter 2.

### **3.2.5 Immunocytochemistry**

ICC experiments were performed, imaged, processed, and analyzed as described in Chapter 2.

All images in this Chapter were acquired using a Zeiss Axio Observer with Apotome.2 structured illumination with a 63x objective.

We used the following primary antibodies: GFP (Abcam ab1218), VPS35 (Abnova H00055737), MAP2 (Abcam ab5392), PSD95 (Thermo Scientific MA1-045), VGluT1 (Millipore AB5905), GluA1 extracellular (Millipore ABN241), Rab10 (Abcam 237703), and GluA1 (Alomone AGP-009).

### **3.2.6 Electrophysiology**

Electrophysiology experiments were conducted using the protocol described in Chapter 2, with the exception that ECS for perfusion was supplemented with 500nM MLi-2 in 45% Captisol PBS or an equal volume of 45% Captisol PBS.

### **3.2.7 Statistics**

All data analyses were performed in GraphPad Prism 8. In untreated experiments and drug effect comparisons (3 groups), statistics were conducted as described in Chapter 2. For Captisol testing, normality testing and selection of statistical tests were conducted as in Chapter 2; however, the tests chosen were appropriate for two groups (Mann-Whitney for nonparametric and unpaired two-tailed t-test for parametric). MLi-2 treatment data was analyzed using 2-way ANOVA (2-way ANOVA) with uncorrected Fisher's LSD post-tests.

### 3.3 Results

#### 3.3.1 LRRK2 kinase activity is increased in VKI brain

LRRK2 kinase activity can be readily quantified by measuring the phosphorylation of its substrates by western blot, provided there are validated phospho-specific antibodies available. Though it is unclear whether it represents a true autophosphorylation site, phosphorylation of serine 935 (S935) has been established as an effective read-out that is widely used in the field as a proxy for LRRK2 activity (Fell *et al.*, 2015). Rab10 is robustly phosphorylated by LRRK2 *in vitro*, with multiple PD mutations in LRRK2 causing increases in Rab10 phosphorylation above baseline (Steger *et al.*, 2016). There are excellent commercially available phospho-specific antibodies for both murine proteins that were knock-out tested in house (Fig 3-1 A.i). We therefore used fluorescence western blot detection of LRRK2 phospho-serine935 (pLRRK2) and Rab10 phospho-threonine73 (pRab10) in cortical lysates from 3-month-old mice as a read-out of LRRK2 kinase activity.

In agreement with others (Mir *et al.*, 2018), we found a statistically significant increase in pLRRK2 in mutant cortex (Fig 3-1 A.iii), and a gene-dose dependent increase in pRab10 that did not reach statistical significance (Fig 3-1 A.v). There was no effect of genotype on the levels of LRRK2 or Rab10 total protein in cortical lysates (Fig 3-1 A.ii&iv). It is worth noting that Rab10 phosphorylation assayed in whole-brain lysates showed the same pattern and did reach statistical significance (Appendix B-1 A&C). These results suggest that while the D620N mutation does not affect LRRK2 stability, it does result in an upregulation of its kinase activity. Several of the kinase substrates of LRRK2 have known roles in synaptic protein trafficking and the SV cycle, making this a putative mechanism for altered pre- and/or postsynaptic phenotypes.



We acutely inhibited LRRK2 kinase activity in 3-month-old mice prior to western blot of phospho-substrates to confirm the LRRK2 kinase activity-dependence of these phenotypes. We chose MLi-2, a potent and selective LRRK2 kinase inhibitor that has been developed as a potential treatment for LRRK2-associated familial PD (Fell *et al.*, 2015). We treated mice by intraperitoneal injection with 5mg/kg MLi-2, or vehicle, for 2 hours prior to tissue collection, performed western blotting on whole-brain lysates, and assayed pLRRK2 and pRab10 as above. The treatment robustly reduced pLRRK2 in all three genotypes (Fig 3-1 B.iii). MLi-2 also reduced pRab10 levels; however, they did not decrease below WT control levels. Therefore, we observed no treatment effect on pRab10 in WT, a trend in the heterozygotes, and a statistically significant reduction in homozygous brains (Fig 3-1 B.v). Acute treatment did not affect the stability of LRRK2 (Fig 3-1 B.ii) or Rab10 expression by total protein levels (Fig 3-1 B.iv). This is in agreement with work published by others during the course of our study, showing pLRRK2 and pRab10 increases in VKI brain tissue, which were reversed by MLi-2 treatment (Mir *et al.*, 2018).

Prior to assessing whether LRRK2 kinase inhibition can rescue glutamate transmission phenotypes in VKI cortical cultures, it was necessary for us to check if MLi-2 treatment has an effect on the stability of proteins directly involved in these phenotypes. We performed fluorescence western blots for VPS35, GluA1, and VGluT1 levels in control and treated brain lysates. There was no treatment effect on the level of VPS35 (Fig 3-1 B.vi), GluA1 (Fig 3-1 B.vii), or VGluT1 (Fig 3-1 B.viii).

As LRRK2 has been shown by our group, and others, to interact with VPS35 in brain tissue by coIP (MacLeod *et al.*, 2013; Vilariño-Güell *et al.*, 2013), we blotted the receptor coIPs in the previous Chapter for LRRK2 and found no statistically significant differences in the amount of

LRRK2 pulled by VPS35 in cortex or striatum (Appendix A-1 B.i-iii & C.x-xi). While we did observe a reduction in mean LRRK2 in the cortical coIPs from knock-in brains, the blots were not very clear. Only several lanes for each genotype were quantifiable. It is inconclusive as to whether there was a reduction in binding, and we observed no genotype effect in striatal tissues with a higher number of samples.

The D620N mutation in VPS35 enhanced LRRK2 substrate phosphorylation. LRRK2 kinase inhibition by MLI-2 reversed the effect, supporting increased LRRK2 kinase activity as a downstream effect of D620N mutant expression. We replicated the finding that VPS35 and LRRK2 coIP in murine brain tissue seen elsewhere (MacLeod *et al.*, 2013; Vilariño-Güell *et al.*, 2013). Thus, LRRK2 kinase activity appears to be a point of convergence of PD mutations, which is conveniently druggable.

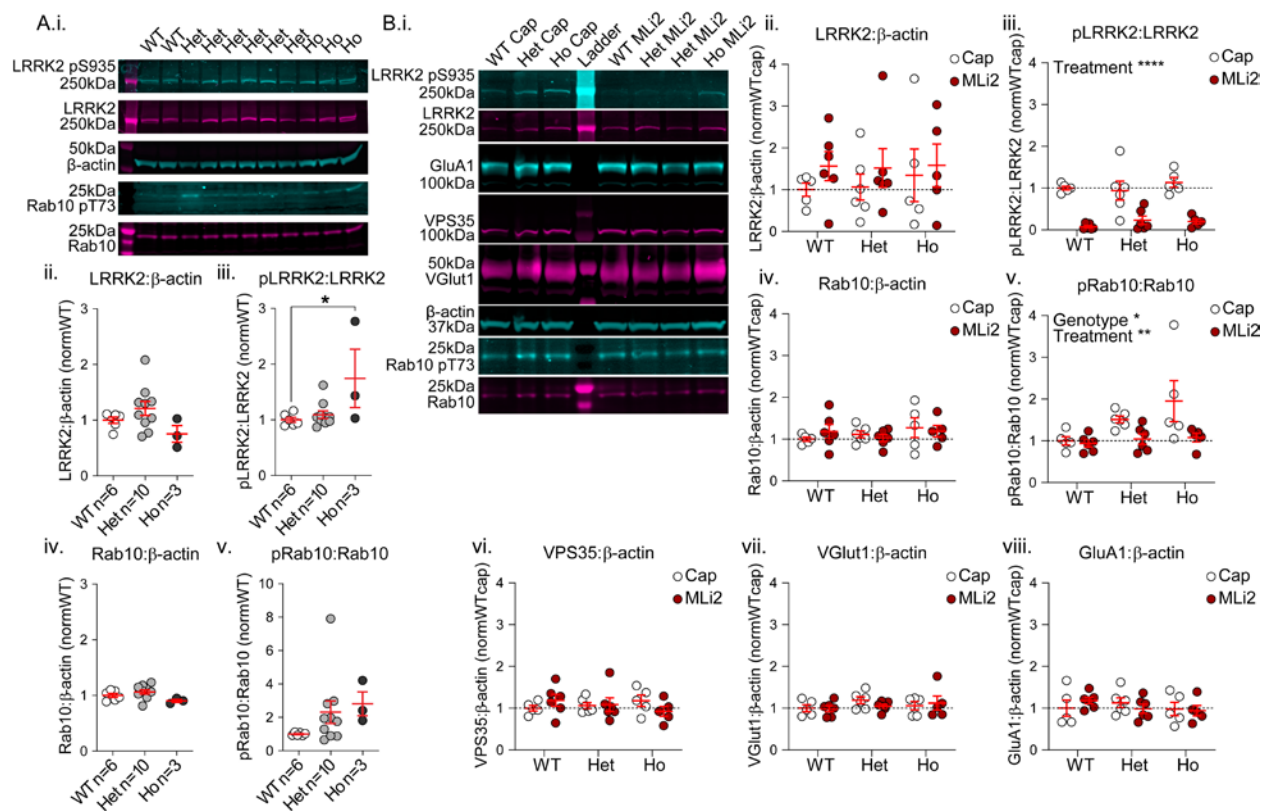


**Figure 3-1 LRRK2 kinase activity is increased in VKI brain tissue with no effect on protein expression**

**A.i)** Proteins from cortical lysates were separated in an electrophoresis gel and blotted for fluorescence detection with LRRK2, LRRK2 phospho-S935 (pLRRK2), Rab10, Rab10 phospho-T73 (pRab10), and β-actin (loading control).

Proteins levels were quantified normalized to loading control and phospho proteins normalized to their own protein levels, and all normalized to WT. There was no significant genotype effect on LRRK2 protein levels (ii, Kruskal-Wallis  $p=0.09$ ); pLRRK2 levels were significantly altered, due to an increase in phosphorylation in homozygous tissue (iii, 1-way ANOVA  $p<0.03$ ; Uncorrected Fisher's LSD  $*p<0.02$ ). Neither Rab10 levels nor phosphorylation were altered by genotype, though there were strong trends toward an increase in pRab10 (iv-v, Kruskal-Wallis  $p<0.08$ ;  $p<0.09$ , respectively).

**B.i)** Protein levels and phosphorylation in whole brain lysates from VKI animals 2 hours post-intraperitoneal injection with MLI-2 or Captisol-only control solution (Cap) were quantified as in A, probing for LRRK2, LRRK2 phospho-S935, GluA1, VPS35, VGlut1, Rab10, Rab10 phospho-T73, and β-actin (loading control).

There were no significant effects of genotype or treatment on LRRK2 levels (ii, 2-way ANOVA genotype x treatment  $p=0.93$ ; genotype  $p=0.90$ ; treatment  $p=0.24$ ). MLI2 treatment significantly reduced pLRRK2 in all genotypes (iii, 2-way ANOVA treatment  $p<0.0001$ ; Uncorrected Fisher's LSD WT-WTMLi2 \*\*\*\*  $p<0.0001$ ; Het-HetMLi2 \*\*\*  $p<0.0002$ ; Ho-HoMLi2 \*\*\*\*  $p<0.0001$ ).

There was similarly no effect of genotype or treatment on Rab10 protein levels (iv, 2-way ANOVA genotype x treatment  $p=0.5258$ ; genotype  $p=0.4683$ ; treatment  $p=0.9659$ ), but significant genotype and treatment effects on pRab10 due to significant reductions in homozygous cells (v, 2-way ANOVA genotype  $p=0.04$ ; treatment  $p<0.009$ ; Uncorrected Fisher's LSD WT-WTMLi2  $p=0.82$ ; Het-HetMLi2  $p=0.10$ ; Ho-HoMLi2 \*\*  $p=0.007$ ). Neither genotype nor treatment revealed any significant effects on protein levels of VPS35

**Figure 3-1 (cont.)** (vi, 2-way ANOVA interaction  $p=0.23$ ; genotype  $p=0.94$ ; treatment  $p=0.89$ ), VGluT1 (vii, 2-way ANOVA interaction  $p=0.55$ ; genotype  $p=0.39$ ; treatment  $p=0.69$ ), or GluA1 (viii, 2-way ANOVA interaction  $p=0.45$ ; genotype  $p=0.61$ ; treatment  $p>0.99$ ). For Aii-v, n represents number of experimental animals. For Bii-viii, n represents number of experimental animals and are as follows: WTCap n=5, WTMLi2 n=6, HetCap n=6, HetMLi2 n=6, HoCap n=5, HoMLi2 n=5.

### **3.3.2 Captisol has little effect on protein expression, phosphorylation, or surface GluA1 expression in WT neurons**

Captisol is regarded as a relatively inert vehicle for drug solubilization; however, it can deplete cholesterol from the plasma membrane and induce membrane permeability in a dose-dependent manner (Hui *et al.*, 2011). We injected WT mice intraperitoneally with either PBS or Captisol and assayed protein stability and phosphorylation by fluorescence western blot. We were unable to detect statistically significant changes in the proteins we assayed: VPS35, GluA1, VGluT1, LRRK2, Rab10, pLRRK2, and pRab10 (Fig3-2 A.i-v & B.i-iv); however, there was slightly more VGluT1 signal, which is worthy of follow-up given the relatively low sample sizes. These blots were also used to test LRRK2 / pLRRK2 / Rab10 / p Rab10 antibody specificity in lysates from LRRK2 knock-out brains and a Rab10 knock-out pituitary cell line (Fig 3-2 A). We confirmed specificity of the antibodies and, interestingly, observed some (albeit much reduced) pRab10 in the LRRK2 knock-out brain lysate, suggesting that LRRK2 may not be the only kinase that phosphorylates Rab10 in the brain. We also treated WT cultured cortical neurons with either PBS or Captisol to ascertain the effect on surface GluA1 expression, but found no significant effect on cluster density or intensity (Fig 3-2 C.i-iv).

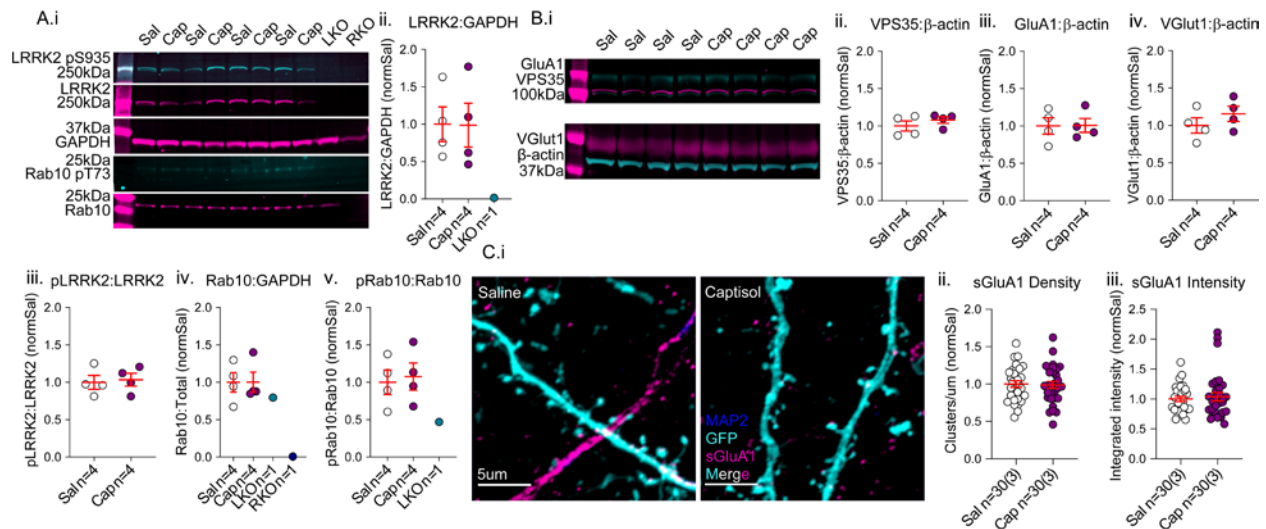


**Figure 3-2 The cyclodextrin solubilizing agent Captisol has no effect on protein expression, phosphorylation, or surface expression of GluA1.** **A.i)** WT mice were injected with Saline or 45% Captisol in solution 2 hours prior to whole brain lysate preparation. Proteins from whole brain lysates were separated in an electrophoresis gel and blotted for fluorescence detection with LRRK2, LRRK2 phospho-S935 (pLRRK2), Rab10, Rab10 phospho-T73 (pRab10), and GAPDH (loading control). Proteins levels were quantified normalized to loading control and phospho proteins normalized to their own protein levels, and all normalized to WT. There was no effect of Captisol treatment on LRRK2, pLRRK2, Rab10, or pRab10 (ii-v Mann-Whitney  $p>0.99$ ;  $p=0.89$ ;  $p=0.89$ ;  $p=0.69$ , respectively). **B.i)** Proteins were collected and quantified as in A, blotting for GluA1, VPS35, VGlut1, and β-actin (loading control). There were no significant effects of Captisol treatment on protein levels of VPS35, GluA1, or VGlut1 (ii-iv Mann-Whitney  $p=0.49$ ;  $p>0.99$ ;  $p=0.49$ , respectively). **C.i)** GFP-filled cultured cortical neurons from WT mice were treated with saline or Captisol at DIV21 and immunostained for MAP2 (blue), GFP (cyan), and extracellular GluA1 (magenta) without permeabilization. For Cii-iii, n is reported as X(Y) where X=number of cells & Y=number of independent cultures. There were no effects of Captisol treatment on surface GluA1 cluster density (active synapses) or cluster density (synaptic receptors) (ii-iii Unpaired t-test  $p=0.87$ ; Mann-Whitney  $p=0.73$ , respectively). For Aii-v & Bii-iv, n represents number of experimental animals. For Cii-iii, n is reported as X(Y) where X=number of cells & Y=number of independent cultures.

### 3.3.3 LRRK2 kinase inhibition in VKI affects postsynaptic AMPAR trafficking

LRRK2 kinase substrates are more phosphorylated in VKI brains. Therefore, we hypothesized that inhibition of LRRK2 kinase activity with a drug (MLi-2) similar to those already in clinical trial for LRRK2 parkinsonism (Zhao and Dzamko, 2019) would rescue the increased glutamatergic transmission in primary cortical cultures from VKI animals.

We inhibited LRRK2 kinase in primary cortical cultures for 2 hours by bath application of 500nM MLi-2. Due to the relative low abundance of pLRRK2, its very large size (286kDa), and the low strength of phospho-specific antibodies, it was difficult to detect pLRRK2 in cortical culture lysates in a quantifiable manner. An example image shows that LRRK2 is present in cortical cultures at DIV21, and that pLRRK2 signal is both present, and appears reduced in MLi2 treatment of all genotypes (Fig 3-3 A.i). As a secondary confirmation, we also measured pRab10 by fluorescent western blot. We observed genotype-dependent increases in pRab10 in control conditions, and a significant treatment effect, specific to mutant cells (Fig 3-3 A.ii), resembling our observations in brain lysates of adult mice. Thus, the D620N mutation increases the phosphorylation of LRRK2 substrates in cultured cortical neurons at DIV21, and acute treatment with 500nM MLi-2 for two hours is sufficient to reduce this phosphorylation.

We investigated the effect of acute MLi-2 treatment on functional outcomes with recordings of mEPSCs, by whole-cell patch clamp on DIV21 primary cortical cultures, following 2 hours of MLi-2 treatment. To ensure continued inhibition throughout the experiment, we added 500nM MLi-2 to the perfused ECS throughout recording. We found no statistically significant differences in the frequency of mEPSCs (Fig 3-3 B.ii), but did note a trend toward higher frequencies in both heterozygous and homozygous control cells, compared to WT, that are not rescued by MLi-2. We did observe a nearly 2-fold increase in the frequency of mEPSCs in WT cells treated with MLi-2, compared to control. Thus, the genotype-normalized drug effects show that MLi-2 treatment caused a large increase in mEPSC frequency in WT cells whereas there was no effect in heterozygous or homozygous neurons (Fig 3-3 B.iii).

The amplitude of mEPSCs was larger in homozygous control cells compared to heterozygous controls, although the two-way ANOVA for all groups failed to reach statistical significance (Fig

3-3 B.iv). MLi-2 rescued the mutant effects on mEPSC amplitude in homozygous cells, but increased them slightly in WT and heterozygous cells (Fig 3-3 B.v). We observed no significant differences in the decay constant (Tau,  $\tau$ ) of mEPSC (Fig 3-3 B.vi) suggesting that there were no alterations in AMPAR gating kinetics.

To disambiguate the source of changes in frequency and amplitude, we also performed ICC on MLi-2 treated cultures to stain for synapses (PSD95 & VGluT1) and for surface GluA1. There were no statistically significant effects of treatment on synapse density as measured by colocalization of PSD95 and VGluT1 clusters (Fig 3-4 A.iv), though there was a trend toward slightly increased synapse density in mutant controls compared to WT controls. These trends are mirrored in the individual protein cluster densities, with significant interaction effects on both PSD95 (Fig 3-4 A.ii) and VGluT1 cluster densities (Fig 3-3 A.iii). While the observed differences in synapse density are in the same pattern as frequency changes, it is important to note that the magnitude of the frequency change in WT cells is much higher, suggesting that changes in synapse density are not the primary factor driving changes in frequency.

Turning then to surface GluA1 cluster density, we observed statistically significant interaction effects (Fig 3-4 B.ii). This was mainly due to a substantial increase in cluster density in WT cells following treatment, with little effect observed on density in heterozygous or homozygous cells compared to their own controls (Fig 3-4 B.iv). The effect of MLi-2 treatment on surface GluA1 cluster density and mEPSC frequency, with only a minor change in synapse density, in WT cells suggests that LRRK2 kinase inhibition results in delivery of AMPARs to new sites (silent synapses).

Surface GluA1 cluster intensities were consistent with amplitude changes in untreated cells in Chapter 2, and here again we noted that surface GluA1 intensity closely resembled the mEPSC amplitude data. There were statistically significant interaction effects (Fig 3-4 B.iii), stemming from GluA1 cluster intensity increases in homozygous control cells that were rescued by MLI2 treatment. Similar to the effect of MLI-2 on mEPSC amplitudes, treatment resulted in increased surface GluA1 cluster intensity in heterozygous cells, and decreases in homozygous cells (Fig 3-4 B.v).

These experiments suggest that MLI-2 treatment in WT neurons increases mEPSC frequency to mutant levels through postsynaptic mechanisms allowing delivery of GluA1-containing AMPARs to silent synapses. MLI-2 did not rescue elevated frequency in the mutant context. There was no effect of MLI-2 on WT event amplitudes or surface GluA1 cluster intensity. It had opposite effects in the two mutant conditions: increasing mEPSC amplitudes and surface GluA1 in heterozygous cells and rescuing elevated mEPSC amplitudes and surface GluA1 expression in homozygous cells. Together the data suggests that LRRK2 kinase inhibition affects glutamatergic transmission in our model by altering postsynaptic AMPAR trafficking.



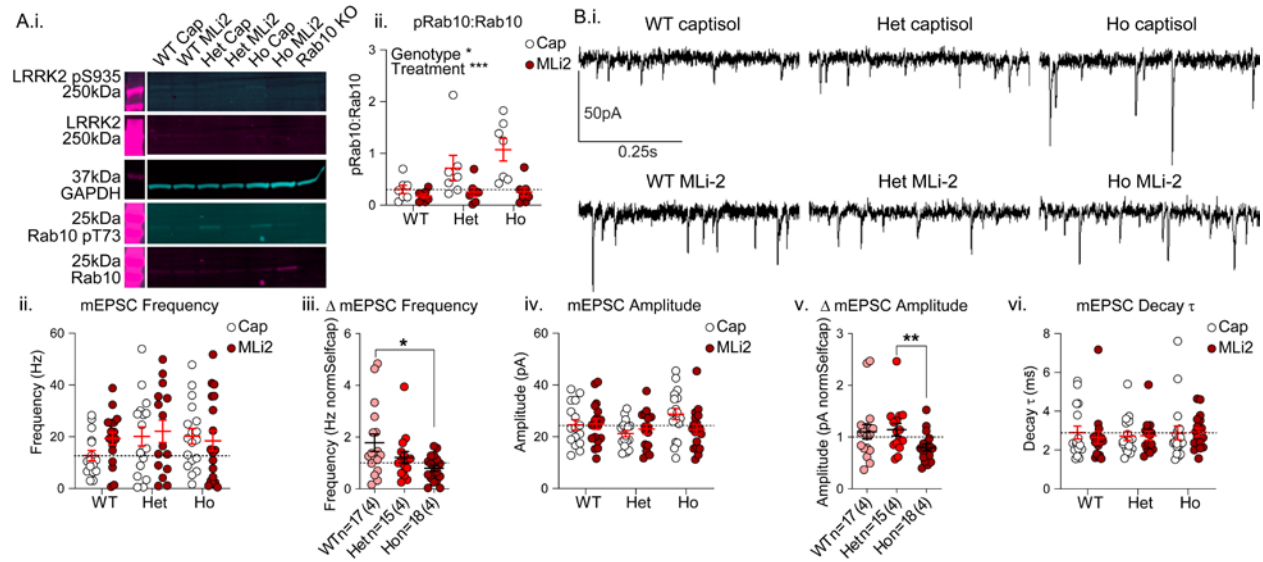


**Figure 3-3 MLI-2 treatment inhibits LRRK2 kinase activity and has genotype-dependent effects on glutamate transmission. A.i)** Cultured cortical neurons at DIV21 were treated for 2 hours with MLI-2 or Captisol (Cap), prior to lysis for western blot. Proteins were in an electrophoresis gel and blotted for fluorescence detection with LRRK2, LRRK2 phospho-S935 (pLRRK2), Rab10, Rab10 phospho-T73 (pRab10), and GAPDH (loading control). LRRK2 and pLRRK2 were present in cultured neurons but did not produce a high-quality blot sufficient for quantification. Rab10 phosphorylation (a proxy for LRRK2 kinase activity) was significantly increased by genotype and decreased by treatment (ii, 2-way ANOVA genotype x treatment  $p < 0.08$ ; genotype  $p < 0.03$ ; treatment  $p < 0.0004$ ; Uncorrected Fisher's LSD WT-WTMLi2  $p = 0.9898$ ; Het-HetMLi2  $p = 0.2554$ ; Ho-HoMLi2  $**p = 0.0047$ ). **B.i)** Representative traces from whole-cell patch clamp recording of mEPSCs in voltage clamped DIV21 cortical neurons held at  $-70\text{mV}$  following 2 hours of treatment with MLI-2 or Captisol. Treatments were added to perfusion solution throughout recording. For Biii&v, n is reported as X(Y) where X=number of cells & Y=number of independent cultures. Mean mEPSC frequency (Hz) did not reveal any significant genotype or treatment effects (ii, 2-way ANOVA interaction  $p = 0.44$ ; genotype  $p = 0.31$ ; treatment  $p = 0.40$ ); however, normalization of the treatment effect in each genotype to its own control revealed significant differences in treatment between genotypes, due to a nearly two-fold increase in mEPSC frequency in only WT cells following treatment (iii, Kruskal-Wallis  $p < 0.04$ ; Uncorrected Dunn's WT-Ho  $**p = 0.01$ ). Amplitude of mEPSCs revealed no statistically significant genotype or treatment effects by two-way ANOVA (iv, 2-way ANOVA interaction  $p = 0.10$ ; genotype  $p = 0.14$ ; treatment  $p = 0.41$ ), but similarly revealed that treatment effects in heterozygous and homozygous neurons were statistically different due to mild opposite effects of drug treatment on mEPSC amplitude (v, Kruskal-Wallis  $p < 0.03$ ; Uncorrected Dunn's Het-Ho  $**p < 0.01$ ). The mEPSC decay time ( $\tau$ ) were not significantly different (vi, 2-way ANOVA genotype x treatment  $p = 0.83$ ; genotype  $p = 0.81$ ; treatment  $p = 0.77$ ), indicating that channel gating properties are not affected. For Aii,  $n = 7$  independent cultures for all groups. For B ii-vi, n is reported as X(Y) where X=number of cells & Y=number of independent cultures. For Bii, iv, vi n are as follows: WTCap  $n = 16(4)$ , WTMLi2  $n = 17(4)$ , HetCap  $n = 17(4)$ , HetMLi2  $n = 15(4)$ , HoCap  $n = 18(4)$ , HoMLi2  $n = 18(4)$ .

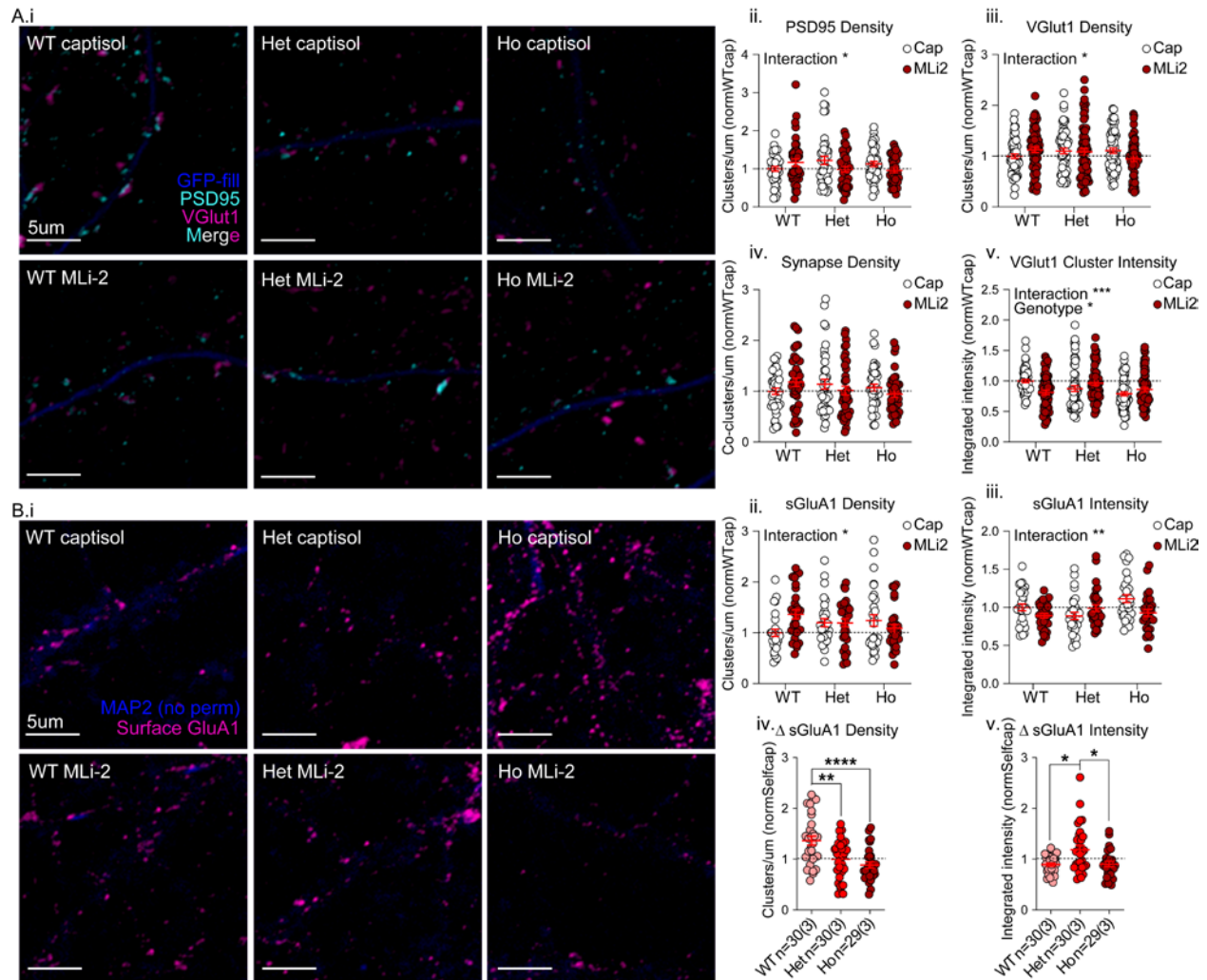


**Figure 3-4 MLI-2 treatment alters localization of synaptic proteins in a genotype-dependent manner.**

**A.i)** Cultured cortical neurons were fixed at DIV21 and immunostained for MAP2 (blue), PSD95 (cyan), and VGLUT1 (magenta) following 2 hours of treatment with MLI-2 or Captisol. There were interaction effects of treatment on both PSD95 density (ii, 2-way ANOVA genotype x treatment  $p < 0.03$ ; genotype  $p = 0.72$ ; treatment  $p = 0.22$ ; Uncorrected Fisher's LSD WT-Het  $*p < 0.05$ ; Het-HetMLi2  $*p < 0.04$ ) and VGLUT1 density (iii, 2-way ANOVA genotype x treatment  $p = 0.03$ ; genotype  $p = 0.47$ ; treatment  $p = 0.67$ ; Uncorrected Fisher's LSD Ho-HoMLi2  $*p = 0.03$ ); however, the synapse density (colocalized PSD95 and VGLUT1) was not significantly altered by either genotype or treatment (iv, 2-way ANOVA genotype x treatment  $p = 0.08$ ; genotype  $p = 0.52$ ; treatment  $p = 0.68$ ). There were significant interaction effects of genotype and treatment on VGLUT1 intensity (v, genotype x treatment  $p < 0.0002$ ; genotype  $p < 0.03$ ; treatment  $p = 0.77$ ) because of genotype effects in control conditions (Uncorrected Fisher's LSD WT-Het  $*p < 0.02$ ; WT-Ho  $****p < 0.0001$ ) and a significant treatment effect on WT cells (Uncorrected Fisher's LSD WT-WTMLi2  $***p < 0.0005$ ). **B.i)** Cultured cortical cells were treated as in A, fixed, and immunostained without permeabilization for MAP2 (blue), and surface GluA1 (magenta). For Biv & v, n is reported as X(Y) where X=number of cells & Y=number of independent cultures. Surface GluA1 cluster densities were subject to a significant interaction effect due to increased densities following treatment (ii, 2-way ANOVA genotype x treatment  $p < 0.02$ ; genotype  $p = 0.93$ ;

**Figure 3-4 (cont.)** Treatment  $p=0.34$ ; Uncorrected Fisher's LSD WT-WTMLi2  $**p<0.004$ ; Surface GluA1 intensity was similarly subject to a significant interaction effect (iii, 2-way ANOVA genotype x treatment  $p<0.005$ ; genotype  $p=0.13$ ; treatment  $p=0.08$ ) though in this case it was due to underlying differences in control heterozygous and homozygous cells and a treatment effect in homozygous cells (Uncorrected Fisher's LSD Het-Ho  $***p<0.0004$ ; Ho-HoMLi2  $**p<0.004$ ). Treatment effects normalized to within-genotype control revealed that treatment effect on GluA1 surface density was significantly larger in WT cells than mutant (iv, Welch's ANOVA  $p<0.0002$ ; Unpaired t with Welch's correction WT-Het  $**p<0.003$ ; WT-Ho  $****p<0.0001$ ), and that treatment had opposite effects in heterozygous cells than in WT and homozygous cells (v, Kruskal-Wallis  $p=0.02$ ; WT-Het  $*p<0.02$ ; Het-Ho  $*p<0.02$ ). For Aii-v,  $n=40(4)$  for all groups and for Bii-iii,  $n=30(3)$ . For all panels,  $n=X(Y)$  where X= number of cells and Y= number of independent cultures.

### 3.3.4 Rab10 does not localize with retromer or GluA1 in dendrites

We used Rab10 phosphorylation as a read-out of LRRK2 kinase activity; however, there is also evidence in the literature supporting a possible role of Rab10 in retromer-mediated recycling of GluA1. Rab10 is involved in actin dynamics at recycling endosomes (P. Wang *et al.*, 2016), in the transport of known retromer cargoes GLUT4 in adipocytes (Chen *et al.*, 2005; Bruno *et al.*, 2016; X. Pan *et al.*, 2017) and SSTR2 in pituitary cells (Alshafie *et al.*, 2020), and even in GLR1 trafficking in *C. elegans* (Glodowski *et al.*, 2007). Rab10 phosphorylation has been shown here, and by others, to be robustly increased by the VPS35 D620N mutation in knock-in mouse embryonic fibroblasts; adult knock-in murine lung, kidney, spleen, and brain tissue; and peripheral monocytes donated by human D620N mutation carriers (Mir *et al.*, 2018). Given that treatment of cultures with MLI-2 affected postsynaptic AMPAR trafficking, we wondered if the LRRK2 substrate Rab10 was involved in retromer-mediated dendritic recycling of AMPARs.

There are over 70 Rab family proteins in humans, which are small (~25kDa) proteins with a high degree of sequence homology between them (Wandinger-Ness and Zerial, 2014), making them particularly challenging targets for the development of specific antibodies for immunocytochemistry applications. We thus confirmed the specificity of the antibodies used

here in a Rab10 knock-out pituitary cell line prior to use (Appendix B-1 A&B), and found that the Rab10 antibody was specific for ICC, but the pRab10 was highly non-specific.

We analyzed clustered Rab10 along the dendritic arbor of cultured cortical neurons from VKI mice at DIV21 by ICC. Phosphorylation of Rab10 results in its accumulation on membranes (Liu *et al.*, 2018; Purlyte *et al.*, 2018), thus we measured the intensity of Rab10 clusters. We found no significant genotype effects on Rab10 cluster intensity by ICC (Fig 3-5 A.i). There was a modest increase in the cluster density of Rab10 in heterozygous and homozygous cultures, that nearly reached statistical significance (Fig 3-5 A.ii;  $p=0.0577$ ). It is notable that Rab10 appeared at the end of spines, or adjacent to their base, which left us with the as-yet-unconfirmed suspicion that at least some Rab10 is in presynaptic compartments (Fig 3-5 B.i&C.i).

Alongside Rab10, we co-stained cortical cultures for either VPS35 or GluA1 to check if Rab10 localized with recycling carriers, and if so, if there were any genotype effects on their association. Co-cluster density of VPS35 and GluA1 with Rab10 were both quite low, along with correspondingly low Pearson's coefficients (Fig 3-5 B.i&C.i; Pearson's  $\sim 0.18$  &  $0.17$ , respectively); while there was a trend toward increased co-cluster density in heterozygous cells in both cases, neither reached statistical significance (Fig 3-5 B.ii&C.ii). There did not appear to be any meaningful genotype effects on the Pearson's coefficients for VPS35, nor GluA1 co-stained for Rab10 (Fig 3-5 B.iii&C.iii).

In summary, the data do not provide any evidence that Rab10 is involved in surface delivery or local recycling of AMPARs in dendrites, but do not rule it out of participation in GluA1 trafficking from the soma. It may be involved in forward trafficking of newly synthesized AMPARs from the TGN, or, internalized AMPARs may be transported back to perinuclear

structures to await signal-mediated surface recycling, as occurs with other retromer cargoes in non-neuronal cells (X. Pan *et al.*, 2017; Alshafie *et al.*, 2020). The localization of Rab10 at the tips of spines and under spine heads suggests that it may localize to presynaptic compartments; it does occasionally colocalize with VGlut1 but the additional clusters observed in mutant cells do not appear to localize at glutamatergic synapses (Appendix B-3 A-C). This leaves open the possibility that Rab10 resides in presynaptic terminals in other cell types, such as inhibitory interneurons. Future work will be needed to confirm the pre- or postsynaptic (or both) localization of Rab10 in cortical cells, and to identify the type of synapses that Rab10 is localized to.

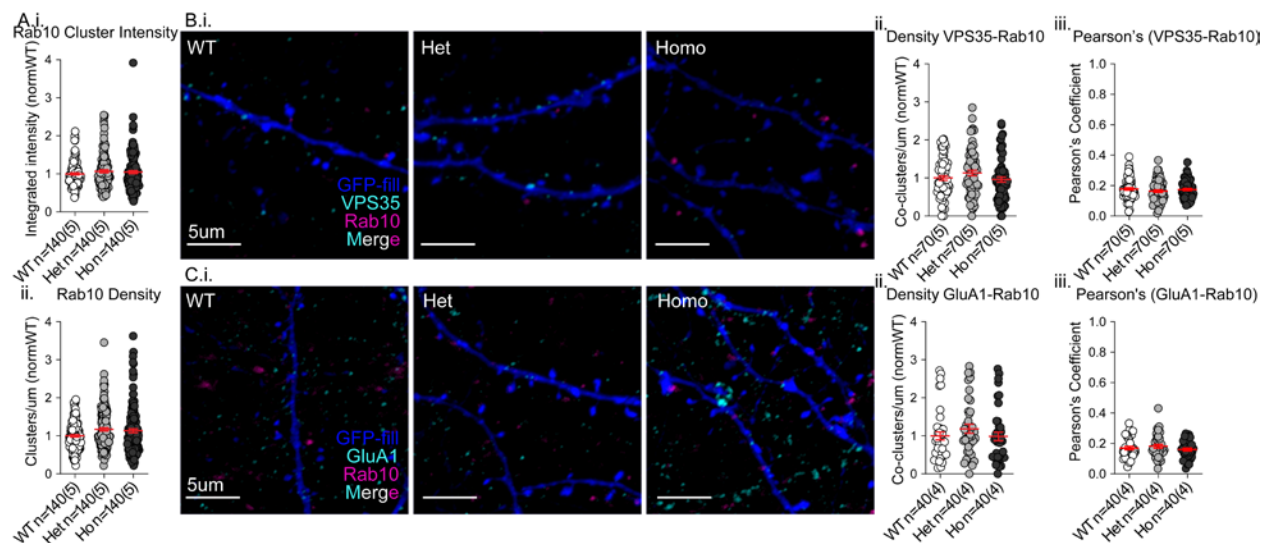


**Figure 3-5 Rab10 does not colocalize with VPS35 or GluA1 in cortical neurites.** GFP-filled cortical neurons were fixed at DIV21 and immunostained for GFP (blue), Rab10 (magenta), and either VPS35 or GluA1 (cyan). **A.i**) Rab10 cluster intensity was not significantly affected by genotype (Kruskal-Wallis  $p=0.66$ ); however, Rab10 cluster density was increased in both mutant genotypes, falling just shy of statistical significance (ii, Kruskal-Wallis  $p<0.06$ ). **B.i**) Representative images of VPS35 and Rab10 co-stained neuronal cultures. VPS35 and Rab10 co-cluster density and colocalization by Pearson's coefficient were both unaffected by genotype (ii-, 1-way ANOVA  $p=0.18$ ; Kruskal-Wallis  $p=0.38$ , respectively). **C.i**) Representative images of GluA1 and Rab10 co-stained neurites. The co-cluster densities and Pearson's coefficients of GluA1 with Rab10 were both unaffected by the mutation (ii-iii, 1-way ANOVA  $p=0.24$ ; Kruskal-Wallis  $p=0.56$ ). For all panels, n is reported as X(Y) where X=number of cells & Y=number of independent cultures.

### 3.4 Discussion

We already published that LRRK2 interacts with VPS35 by coIP (Vilariño-Güell *et al.*, 2013), and were exploring whether protein association differs with mutant expression in multiple PD knock-in mouse lines, when the first in a string of publications was released identifying Rab GTPases as substrates of LRRK2 kinase (Steger *et al.*, 2016). Rab proteins are essential for most membrane and protein trafficking pathways (reviewed in: Wandinger-Ness and Zerial, 2014) and VPS35 is a Rab effector, making Rabs an attractive candidate for the intersection point of VPS35 and LRRK2 function.

We found that phosphorylation of LRRK2 at S935 (pLRRK2) is increased in brain tissue from VKI mice, and phosphorylation of LRRK2 substrate Rab10 at T73 (pRab10) is increased in both cortical cultures and brain tissue from VKI mice, a finding that was published by another group while we were conducting these experiments (Mir *et al.*, 2018). We replicated published findings that LRRK2 and VPS35 interact in brain tissue by coIP (Vilariño-Güell *et al.*, 2011; MacLeod *et al.*, 2013), but found no mutation effects on LRRK2 association in striatal tissue. Inhibition of LRRK2 kinase activity with the selective LRRK2 inhibitor MLI-2 successfully reduced pLRRK2 levels in all genotypes, and reduced pRab10 to WT levels after 2 hours of treatment; inhibition had no effect on protein expression of LRRK2, Rab10, VPS35, GluA1, or VGluT1. MLI-2 treatment of cultured cortical cells had significant, yet different, effects on postsynaptic AMPAR trafficking in all three genotypes. We observed no clear effect of MLI-2 treatment on presynaptic glutamate release. The present study adds to our understanding of the role of LRRK2 in healthy neurons and its functional interaction with VPS35 in synaptic maintenance and disease.

### **3.4.1 MLi-2 abolishes phosphorylation of LRRK2 S935 and normalizes phosphorylation of Rab10 T73 to wild-type levels**

We were able to replicate the interaction of LRRK2 with VPS35 by coIP (MacLeod *et al.*, 2013; Vilariño-Güell *et al.*, 2013) and found no alteration in the association of the two proteins in striatal lysates. Accumulating evidence exists for a functional interaction between VPS35 and LRRK2 in neurons (MacLeod *et al.*, 2013; Linhart *et al.*, 2014; Inoshita *et al.*, 2017; Zhao *et al.*, 2018), and retromer is depleted in the brains of LRRK2 mutation carriers (Zhao *et al.*, 2018). LRRK2 substrate phosphorylation is increased in D260N knock-in mice and human mutation carriers (Mir *et al.*, 2018), inviting speculation that pathogenic mutations in LRRK2 and VPS35 converge on LRRK2 kinase activity. Furthermore, there is evidence for increases in LRRK2 kinase activity in the brains of individuals with idiopathic PD (Di Maio *et al.*, 2018), suggesting this may be a common pathological feature of all PD.

We were able to replicate the finding that the D620N mutation increases pLRRK2 and pRab10 in brains from VKI mice. It is interesting that MLi-2 was able reduce phosphorylation of pLRRK2 to almost nil, but that it only brought pRab10 levels down to WT baseline in brains. In cultured neurons we observed a nearly 50% decrease in pRab10 even in the WT cells. This could reflect a timing issue with acute treatment. Two hours via IP injection may not be equivalent to 2 hours of bath application to cultured cells, given the extra time needed to enter the brain and diffuse into tissues, resulting in slightly improved efficacy in the cultured cells.

That said, during antibody testing, we did observe some pRab10 in brains from LRRK2 knock-out animals, suggesting that LRRK2 is not the only kinase that phosphorylates Rab10 in the brain. We use a culture protocol optimized to impede glial survival and division. It could be that

LRRK2 phosphorylates Rab10 in neuronal cells but that another kinase could be active in one or more glial types, producing differences between brain homogenate and culture homogenate.

### **3.4.2 Consideration of the effect of Captisol on basal phenotypes**

Unfortunately, Captisol may affect glutamatergic synapse activity and/or protein trafficking in a genotype-dependent manner, complicating the interpretation of the MLi-2 treatment results in the mutant context. We observed different phenotypic patterns in Captisol-treated control cells than we had in untreated cells in Chapter 2. Captisol is a cyclodextrin (sultobutylether- $\beta$ -cyclodextrin) chemically engineered to circumvent the adverse cellular effects of other solubilizing compounds (Stella and He, 2008). While Captisol produces few systemic effects in animals and is well-tolerated in humans (Luke *et al.*, 2012; *Ibid*), a literature review revealed no published work on its effects on neuronal cell membranes or neurotransmission. A single study has shown that Captisol can cause membrane disruption and cholesterol depletion in HEK293 cells (Hui *et al.*, 2011), indicating that it could have implications for transmission and trafficking at the synapse. Studies of other (albeit more potently membrane-disrupting) cyclodextrins have shown they can disrupt calcium homeostasis (Fortalezas, Marques-da-Silva and Gutierrez-Merino, 2018) and neurotransmission in neurons (Wasser *et al.*, 2007; Borisova *et al.*, 2010; Tarasenko *et al.*, 2010; Sibarov, Poguzhelskaya and Antonov, 2018).

A brief study of the effects of Captisol versus PBS-injected animals revealed a slight, but not statistically significant, increase in VGluT1 expression that warrants further investigation. Further analysis by my lab colleague found that perfusion of *ex vivo* WT slices with Captisol led to slight increases in sEPSC frequencies, amplitudes, and decay tau, versus saline perfusion (personal communication, Naila Kuhlmann). The data hints at an effect on glutamatergic transmission, perhaps through increases to presynaptic glutamate release (as evidenced by



increased sEPSC frequencies and increased VGluT1 levels after treatment), though we have insufficient evidence to make any solid conclusions.

Altered transmission due to Captisol on the background of mutant effects could put additional pressure on compensatory mechanisms. If untreated homozygous cells truly display attenuated mutant effects due to advanced compensatory changes (as put forward in Chapter 2), it is possible that increasing presynaptic glutamate release with Captisol application in heterozygous cells would engage similar feedback mechanisms. Comparing the VGluT1 intensities between untreated heterozygous cells (Fig 2-5 A.v) to those treated with Captisol (Fig 3-4 A.v) reveals that Captisol-treated heterozygous neurons have less presynaptic VGluT1 (inferred from lower cluster intensity) than WT cells, an effect that was absent in untreated experiments.

Furthermore, there was no longer a difference between heterozygous and homozygous mEPSC event frequencies, indicating either a decrease in heterozygous, or an increase in homozygous neurons.

We found it interesting that Captisol seems to exacerbate the postsynaptic mutant phenotype of increased mEPSC amplitude and surface GluA1 intensity in homozygous cells. It is possible that compensatory mechanisms fail to keep up with further Captisol-induced transmission in these cells, or again, that this reflects a mechanistic difference between heterozygous and homozygous D620N expression. Further study will be required to reveal the extent and mechanism of Captisol effects. Or perhaps, more simply, the experiments bear repeating using a more inert solubilization technique.

With these caveats in mind, we must interpret the MLI-2 effects with caution. Therefore, I consider each genotype somewhat independently in the remainder of this discussion.

### **3.4.3 LRRK2 kinase inhibition effect in cultures is primarily postsynaptic**

A large body of work has shown that increased LRRK2 kinase activity has effects on presynaptic transmitter release (Beccano-Kelly, Kuhlmann, *et al.*, 2014; Matikainen-Ankney *et al.*, 2016; Volta *et al.*, 2017; reviewed in Kuhlmann and Milnerwood, *in press*) and Inoshita *et al.* (2017) placed dVPS35 downstream of dLRRK on SVs in the *Drosophila* neuromuscular junction by EM. A handful of studies have discovered effects of LRRK2 depletion or mutant expression on spine morphology (Parisiadou *et al.*, 2014; Matikainen-Ankney *et al.*, 2016), AMPAR expression (Parisiadou *et al.*, 2014), and regulation of synaptic strength (Sweet *et al.*, 2015; Matikainen-Ankney *et al.*, 2016, 2018), indicating that, like VPS35, LRRK2 may participate in both pre- and postsynaptic processes. This lead us to hope that we could globally rescue glutamate transmission in VKI neurons by inhibiting LRRK2 kinase with MLi-2.

In WT neurons, MLi-2 treatment increased the frequency of mEPSCs nearly two-fold, likely related to the increased density of surface AMPAR clusters. GluA1-containing AMPARs are delivered to quiescent synapses during development and synaptic plasticity (reviewed in: Diering and Huganir, 2018; Park *et al.*, 2018; Benke and Traynelis, 2019). In other reports, LRRK2 kinase inhibition in WT animals, or LRRK2 kinase-dead mutant expression had no effect on presynaptic neurotransmitter release (Sweet *et al.*, 2015; Matikainen-Ankney *et al.*, 2016; Kuhlmann *et al.*, *in submission*), consistent with the frequency change occurring through postsynaptic changes. These findings imply that inhibition of LRRK2 kinase activity results in AMPAR delivery to inactive sites.

Similarly, we observed no effect of MLi-2 on spontaneous presynaptic glutamate release in either heterozygous or homozygous neurons, as evidenced by no change in the frequency of mEPSCs, synapse density, or surface GluA1 density following treatment. This provides further

evidence of postsynaptic action of MLI-2. However, we cannot completely rule out the possibility that Captisol effects on glutamate release obscure any presynaptic changes, or that differences might be found under higher levels of synaptic activity, beyond that seen by assay of miniature EPSCs, such as evoked synchronous release and / or trains of activity.

The effects of MLI-2 on postsynaptic receptor expression in mutant cells are enigmatic. In heterozygous neurons, MLI-2 increased GluA1 trafficking to active synapses, as evidenced by increased mEPSC amplitude and surface GluA1 intensity, with no change in surface GluA1 cluster density. The departure from the WT effects could be the result of aberrant LRRK2 activity in the mutant context, or reflect that cells with more baseline activity are likely to have fewer silent synapses remaining prior to treatment. Conversely, in homozygous cells that had large mEPSC amplitudes and bright GluA1 clusters, LRRK2 kinase inhibition reduced these to below WT control levels.

What is clear from these experiments is that MLI-2 treatment is having a marked effect on postsynaptic AMPAR expression. Rab8 and Rab10 are LRRK2 kinase substrates (Steger *et al.*, 2016; Jeong *et al.*, 2018; Liu *et al.*, 2018; Mir *et al.*, 2018), and it is of note that both have been implicated in GluA1-containing AMPAR surface trafficking (Gerges, Backos and Esteban, 2004; Brown *et al.*, 2007; Glodowski *et al.*, 2007; Bowen *et al.*, 2017).

We do not yet know if LRRK2 participates in the recycling of internalized receptors or the forward trafficking of newly synthesized receptors, nor the organelle loci of regulation (e.g., endosomes, TGN). LRRK2 localizes to the *trans*-Golgi network with Rab7L1 (MacLeod *et al.*, 2013; Beilina *et al.*, 2014; Liu *et al.*, 2018; Purlyte *et al.*, 2018), where recruitment activates its kinase activity (Liu *et al.*, 2018; Purlyte *et al.*, 2018) resulting in downstream phosphorylation of

Rab10 and Rab8 (Liu *et al.*, 2018; Purlyte *et al.*, 2018). This causes an accumulation of membrane-bound and inactive Rabs (Liu *et al.*, 2018). There, LRRK2 further associates with the GARP complex and syntaxin-6 (Beilina *et al.*, 2020); which play a role in the tethering and TGN fusion of vesicles containing retromer-recycled CI-MPR (Pérez-Victoria, Mardones and Bonifacino, 2007; Pérez-Victoria and Bonifacino, 2009). Our colleagues at McGill University have recently discovered that internalized somatostatin receptor 2 (another retromer cargo) is translocated to a juxtanuclear syntaxin-6-positive compartment in pituitary cells, where it is held until corticotropin releasing factor signals for its (Rab10-dependent) surface delivery (Alshafie *et al.*, 2020). These studies place active LRRK2 on the TGN with an accumulation of membrane-bound but inactive Rabs that have a role in AMPAR trafficking (Rab8, Rab10), and in association with proteins that participate in retrograde trafficking (GARP) and homeostatic sequestration (syntaxin6) of retromer cargoes. This is a compelling putative point of contact between retromer trafficking and LRRK2 kinase activity.

Even so, LRRK2 is not married to the TGN: it also localizes to early endosomes (Schreij *et al.*, 2015) and Rab10-positive structures in the cell periphery (Liu *et al.*, 2018) in cell lines. It has also been shown to phosphorylate Rab5 (Steger *et al.*, 2016; Jeong *et al.*, 2018), which resides on early-endosomes. Overexpression of LRRK2 G2019S or R1441C (both of which exhibit increased LRRK2 kinase activity), decreases membrane recruitment and activation of Rab7, and prevents degradation of endocytosed EGF-receptors (Gómez-Suaga, Rivero-Ríos, *et al.*, 2014). Furthermore, knock-down of LRRK2 substrates Rab8A and Rab10 can mimic mutant LRRK2 effects on Rab7 activation and EGFR trafficking, suggesting that these proteins may act together in a cascade important for receptor recycling (Rivero-Ríos *et al.*, 2019, 2020). Rab7 recruits VPS35 to endosomal membranes (Rojas *et al.*, 2008; Seaman *et al.*, 2009; Harrison *et al.*, 2014), and is phylogenetically related to Rab7L1/Rab29 (Klöpper *et al.*, 2012). It is possible that

Rab7 acts on endosomes in a similar manner to Rab7L1 at the TGN, where it could recruit LRRK2 kinase alongside VPS35 to act as a regulator of surface delivery of recycling cargoes.

Here we did not observe dendritic colocalization of Rab10 with either VPS35 or GluA1, suggesting that if Rab10 is involved in LRRK2-mediated AMPAR trafficking, it is not directly participating in *local* recycling or delivery of AMPARs in distal dendrites. This does not rule out its involvement in sequestering or trafficking GluA1 in the soma or proximal dendrites. For example, locally synthesized GluA1 in dendrites is trafficked to Rab11 recycling endosomes prior to surface delivery (Bowen *et al.*, 2017); it is possible here that Rab10 delivers receptors synthesized or stored in the soma to new compartments for their long-distance trafficking to distal dendrites.

It is equally possible that LRRK2 is involved in AMPAR trafficking in the dendrite via a different substrate than Rab10 (e.g., through Rab8, NSF, or a currently undiscovered substrate), or indirectly through modulation of PKA (Parisiadou *et al.*, 2014). It is striking that LRRK2 and VPS35 do not colocalize in immortalized cells (Beilina *et al.*, 2014, 2020), but do coIP together in brain lysates (MacLeod *et al.*, 2013; Vilarino-Güell *et al.*, 2013). This suggests that the two proteins may interact in neuron-specific trafficking pathways. GluA1 can be locally synthesized in dendritic ER, and is processed through non-Golgi (Bowen *et al.*, 2017) or retromer-mediated Golgi-satellite (Mikhaylova *et al.*, 2016) dendritic secretory pathways, which deliver new receptors into recycling endosomes for surface trafficking. The entire complement of proteins involved in these recently described pathways have yet to be discovered.

Finally, we must address the fundamental difference between LRRK2 and VPS35 mutant phenotypes in neuronal cultures. PD-associated mutations in LRRK2 cause presynaptic changes to neurotransmitter release (Beccano-Kelly, Kuhlmann, *et al.*, 2014; Sweet *et al.*, 2015; Yue *et*

*al.*, 2015; Matikainen-Ankney *et al.*, 2016; Volta *et al.*, 2017), which can be rescued by inhibition of LRRK2 kinase (Sweet *et al.*, 2015; Matikainen-Ankney *et al.*, 2016; Kuhlmann *et al.*, *in submission*). If mutant VPS35 has a similar effect on LRRK2 kinase activity, why do we observe distinct postsynaptic mutant and treatment effects in VKI neurons? We have not yet studied the cell-autonomous pre- and postsynaptic effects of D620N expression (for instance, by growing chimeric cultures separated in microfluidic chambers). We cannot completely rule out the possibility that presynaptic increases in glutamate release drive postsynaptic increases in receptor expression; however, chronic increases in glutamate transmission typically result in homeostatic downscaling of AMPAR surface expression (reviewed in: Diering and Huganir, 2018). Furthermore, if this were the case one would expect to see similar phenotypes in the LRRK2 mutant studies. In DIV21 cortical cultures from G2019S knock-in mice, presynaptic probability of release was higher in mutants, with no effect on postsynaptic amplitudes (Beccano-Kelly, Kuhlmann, *et al.*, 2014); whereas here we observe large effects of MLI-2 treatment on postsynaptic receptor expression, in the absence of presynaptic effects.

It is relevant that multiple reports, including our own recent work, have shown that the G2019S mutation does not increase basal Rab8 or Rab10 phosphorylation (Fan *et al.*, 2018; Liu *et al.*, 2018; Atashrazm *et al.*, 2019; Kuhlmann *et al.*, *in submission*). The implication being that whatever effect the G2019S mutation is having on LRRK2 function in neurons is occurring through other substrates – perhaps Rab3, Rab5, or endophilin-A, all of which have been linked to presynaptic vesicle recycling (reviewed in: Binotti, Jahn and En Chua, 2016; Li and Kavalali, 2017). Here we observed robust increases in pRab10 in our D620N mutant cultures, which were rescued by MLI-2, an effect also seen by others (Mir *et al.*, 2018). This suggests that, unlike G2019S, the VPS35 D620N mutation leads to increased pRab10 in the brain, which could be acting in post-synaptic AMPAR delivery.

A number of other studies have shown that G2019S does increase Rab10 phosphorylation. These studies all assayed mouse embryonic fibroblast cells (Ito *et al.*, 2016; Steger *et al.*, 2016; Lis *et al.*, 2018), whereas those that did not find any differences used peripheral neutrophils and monocytes (Fan *et al.*, 2018; Atashrazm *et al.*, 2019), HEK293 cells (Liu *et al.*, 2018), or adult murine brain (Kuhlmann *et al.*, *in submission*). These findings suggest there is tissue and developmental specificity for upregulated Rab10 phosphorylation by LRRK2 G2019S, and that it may not be important in the adult brain. In our study, increases in pRab10 were observed in both cultured neurons and in adult mouse brains, suggesting that, unlike G2019S, the increases in Rab10 phosphorylation in the brain persist into adulthood.

While the site of interaction (endosomes; TGN) and underlying mechanism are still unclear, we provide evidence for a postsynaptic function of LRRK2 in the regulation of AMPAR surface expression, and propose that LRRK2 kinase activity acts as a tuning mechanism for synaptic strength. The functional and physical intersection of LRRK2, VPS35, and related proteins (GARP; syntaxin-6) is fertile ground for future investigations into the mechanisms of homeostatic, and activity-dependent, synaptic plasticity.

#### **3.4.4 Implications for treatment of PD with MLi-2**

Of course, the impetus for these experiments was to assay whether MLi-2 is a good candidate for therapeutic intervention in individuals with VPS35 D620N parkinsonism. Unfortunately, in our hands MLi-2 had no effect on presynaptic transmission in any genotype, leading us to conclude that presynaptic changes in transmitter release in D620N mutant neurons are not likely to be mediated by LRRK2 kinase activity, though it remains a possibility that presynaptic effects were occluded by the presence of Captisol. LRRK2 is a large multi-domain protein with two large

scaffolding domains (Greggio and Cookson, 2009; Gómez-Suaga, Fdez, *et al.*, 2014) and interacts with many SV cycle proteins such as: clathrin heavy chain, AP-2, AP180, syntaxin1A, dynamin 1, VAMP2, SNAP25, NEM sensitive factor (NSF), synapsin-1, and endophilin-A (Piccoli *et al.*, 2011, 2014; Matta *et al.*, 2012; Yun *et al.*, 2013; Gómez-Suaga, Rivero-Ríos, *et al.*, 2014; Belluzzi *et al.*, 2016). It is not out of the question that LRRK2 protein (but not kinase activity) is required for the deleterious effects of D620N at the presynapse, perhaps acting as a scaffolding molecule for protein-protein interactions.

In WT and heterozygous neurons, the increased surface expression of GluA1 following MLI-2 treatment is consistent with a role of LRRK2 in the homeostatic, or activity-dependent, sequestration and release of AMPARs. This has alarming implications for the use of LRRK2 kinase inhibitors in the treatment of idiopathic and non-LRRK2-mutant PD. In this case, increases in phosphorylated LRRK2 in our model, and in the brains of individuals with idiopathic PD (Di Maio *et al.*, 2018), could be compensatory, not causative. The phenotypes we had observed in homozygous mutant cells were consistent with compensatory homeostatic regulation: decreased VGluT1 intensity, and fewer GluA1 clusters in dendrites (Chapter 2). If LRRK2 kinase activity is responsible for inhibiting forward trafficking of AMPARs, the reduction in GluA1 clusters observed in dendrites may be the result of increased LRRK2 phosphorylation. GluA1 phosphorylation and targeting to synapses is scaled down in response to abnormally elevated glutamate activity, due to movement of PKA away from synapses (Diering, Gustina and Huganir, 2014; Diering and Huganir, 2018). LRRK2 has been shown to interact with the PKA regulatory subunit II $\beta$  to prevent its localization in synapses (MSNs from LRRK2 knock-out mice show higher levels of synaptic PKA and resultant phosphorylation and insertion of GluA1), making this a possible point of cross-talk between elevated glutamatergic transmission and LRRK2 regulation in the VKI model.



However, MLi-2 treatment resulted in a rescue of elevated postsynaptic AMPAR expression and mEPSC amplitude in homozygous neurons. At the Golgi, aberrantly elevated LRRK2 activity acts as a negative regulatory signal by phosphorylating Rab7L1/Rab29, and dissociating the complex from the membrane (Purlyte *et al.*, 2018). Golgi fragmentation is observed with expression of LRRK2 G2019S (Beilina *et al.*, 2014; Purlyte *et al.*, 2018) and has been identified as a cellular feature in PD (Fujita *et al.*, 2006). It is unclear whether this is due to increased trafficking out of the Golgi, or other mechanisms. Furthermore, Inoshita and colleagues (2017) observed that both knock-down and overexpression of dLRRK in *Drosophila* resulted in the same aberrant synaptic phenotype, highlighting that LRRK2 activity hangs in a delicate balance, and that manipulation in either direction may have similar consequences. In the case of homozygous D620N neurons, if Captisol is driving further increases in glutamate transmission in an already stressed system, this could push LRRK2 phosphorylation over a tipping point, where it dissociates from the membrane, resulting in release of sequestered AMPARs for forward trafficking (observed as larger mEPSCs and brighter surface GluA1 clusters in control cells). LRRK2 kinase inhibition has also been shown to reverse G2019S-induced Golgi fragmentation (Purlyte *et al.*, 2018). In this case, MLi-2 treatment may allow LRRK2 to re-associate with membranes and thus regulate AMPAR traffic.

At this point, the interpretation of the MLi-2 effects in mutant neurons is conjecture. It will be essential going forward to either study the mutant-specific effects of Captisol treatment on AMPAR trafficking, or (more simply) to repeat these experiments using a different solubilization technique which avoids confounding effects. In this light, LRRK2 kinase inhibitor treatment of individuals who have been misdiagnosed might result in a PD-like pathology of elevated synaptic activity; whereas the therapeutic usefulness for people with D620N parkinsonism is still unclear.

### **3.5 Conclusion**

This work provides further evidence that LRRK2 participates in synaptic maintenance at the postsynapse via regulation of surface AMPAR expression. It opens up a wide variety of future directions studying the site of action, the mechanisms of cargo sequestration and release, and the interplay between LRRK2 and retromer. Furthermore, we provide evidence that presynaptic release phenotypes in D620N neurons are likely independent of LRRK2 kinase activity, which has potentially profound implications for the use of LRRK2 inhibition as a therapeutic for VPS35, and potentially idiopathic PD. Future work is certainly required to discern if increased phosphorylation of LRRK2 substrates observed in D620N brain tissue represents a causative, or compensatory, mechanism in response to increased glutamatergic activity at the synapse.

## **Chapter 4: Conclusion**

### **4.1 Caveats and Limitations**

This dissertation represents an important first investigation into the cell biological effects of the VPS35 D620N mutation on neuron-specific function. As with all science, it is subject to limitations and caveats.

#### **4.1.1 Reductionist modeling**

The strength of 2D primary neuronal culture is that it allows for clear visualization of protein trafficking and localization in single neurites from live and fixed cells; however, it is a reductionist method that lacks a degree of physiological relevance. Corticostriatal degeneration is a pathological feature of PD, and thus the study of cortical/glutamatergic cells is of import to understanding degeneration; however, in the intact brain, pyramidal cells of the motor cortex project onto GABAergic medium spiny neurons (MSNs) in the striatum (Kreitzer, 2009; Gerfen and Surmeier, 2011). MSNs have different synaptic physiology than cortical cells, and plasticity of glutamatergic inputs into the striatum are highly modulated by dopamine (Kreitzer and Malenka, 2008; Shen *et al.*, 2008; Kreitzer, 2009; Tritsch and Sabatini, 2012). Thus, the synapses being studied in our culture model represent non-physiological synaptic networks. It is yet unknown what effects the mutation may have on AMPAR trafficking and post-synaptic synapse maturation in cells of the striatum, which are a focal point of PD research.

Furthermore, this culture system does not allow for certainty that presynaptic and postsynaptic phenotypes were cell-autonomous. An increase in presynaptic glutamate release could cause post-synaptic AMPAR insertion if it were high enough to drive LTP; however, chronic increases in activity would be more likely to result in homeostatic scaling down and resultant removal of AMPARs from the synapse (reviewed in: Diering and Huganir, 2018). The evidence from LRRK2

models where presynaptic release is altered, with no change in postsynaptic measures, provides some evidence that postsynaptic receptor expression increases occur via a postsynaptic mechanism (Beccano-Kelly, Kuhlmann, *et al.*, 2014), but based on my studies alone, we cannot rule out a presynaptic contribution.

#### **4.1.2 Developmental time point**

Our neuronal cell cultures were performed at E16.5 and the cells were grown to 21 days-*in-vitro*, corresponding to about post-natal day 19. The first few post-natal weeks in mice is a period of development, where proteins involved in synaptogenesis are upregulated (Sharpe and Tepper, 1998; Tepper *et al.*, 1998; Sohur *et al.*, 2014). Retromer depletion has been shown elsewhere to cause developmental effects on morphology and synapse development when depleted constitutively, whereas acute knock-down after development appears not to affect cell morphology but impairs LTP (Temkin *et al.*, 2017). GluA1, the primary retromer cargo studied here, undergoes similar developmental shifts in expression and trafficking (Pellegrini-Giampietro, Bennett and Zukin, 1992; Benke and Traynelis, 2019). My work, then, is reflective of D620N effects on developmental processes. While it does provide some clues as to the molecular effects of D620N expression on AMPAR trafficking, it is as yet unknown if activity-dependent AMPAR trafficking in adult brains utilizes the same retromer pathway, nor do we know how the mutation affects spontaneous (or evoked) synaptic transmission in adult brains. Another graduate student in our lab is now asking these important questions.

#### **4.1.3 Subjectivity of immunostaining cluster analysis**

There are many ways to define a cluster in an immunocytochemistry experiment. Programs such as ImageJ and CellProfiler have built in functions that can automatically define signal from noise based on a number of mathematical models that extract signal based on its distinction

from the background (Tsai, 1985; Demi, 2005). These functions are quick and provide consistency between images in what is determined to be a 'real' cluster, based solely on fluorescence signal to background. When using an automated threshold, you risk losing dim clusters in conditions where your clusters are less bright as a consequence of biological processes (for example if a protein is less membrane-bound and more cytosolic in one experimental condition). To circumvent these issues, we chose to use manual thresholding, whereby the clusters were defined on an image by image basis using experimenter judgement. To prevent bias and aim for consistency, all image sets that were imaged together were 'cluster thresholded' in the same session, and all images were blinded prior to thresholding. While this method prevents loss of low-end clusters, it is subject to the natural subjectivity of the human visual system, whereby dim clusters in brighter images may have been lost due to them being less well-perceived next to a bright signal. To try to account for the inherent issues in cluster analysis, all colocalization studies also employed Pearson's coefficients which are performed on unthresholded greyscale images.

#### **4.1.4 Incomplete control experiments for drug vehicle effects**

The interpretation of the effects of LRRK2 kinase inhibition on synaptic phenotypes was impaired by a poor experimental design / lack of foresight. Captisol was chosen as a solubilizing agent due to its milder effects on membranes than other cyclodextrins; however, a pilot study on the effects of Captisol was only performed in WT cells under the assumption that any effects on synaptic transmission would be genotype-independent. In retrospect, one should never make assumptions in science, and it appears from our results that it affects glutamate transmission in a genotype-dependent manner. Better study design would have included both saline-only and Captisol controls in all experiments, although this would lead to an impractical number of groups, and almost impossible statistical significance adjustments by analysis of variance.

#### **4.1.5 Lack of mechanistic insight**

The primary theory underlying this work is that prolonged synaptopathy results in neurodegeneration in PD. While my work provides interesting insight into early mutant effects on glutamatergic synapses, it does not necessarily provide evidence that this synaptic dysregulation leads to later degeneration. VPS35 is involved in many other non-neuron-specific functions that have implications for neuronal health and functioning. For example, D620N expression has been shown to impact upon mitochondrial health, and while it has been proposed that excitotoxicity from too much glutamate release can cause mitochondrial dysfunction (Good *et al.*, 1998), we have not studied this directly here. Mitochondrial dysfunction similarly impacts synaptic transmission through impairments to calcium buffering (Lee *et al.*, 2018).

A major drawback to this body of work is that it provides only correlative evidence for the links between FAM21 binding alterations, LRRK2 kinase activity, and the glutamatergic phenotypes caused by mutant expression. Reduced FAM21 binding has been replicated in multiple studies (Ian J. McGough *et al.*, 2014; Zavodszky *et al.*, 2014); however, recent work has shown that D620N-induced reductions in FAM21 association can be rescued by knocking down TBC1D5 (Seaman, Mukadam and Breusegem, 2018), suggesting that the reduced binding is not the result of direct interference in the VPS35-FAM21 association. An equally likely explanation arises from the recent discovery that the D620N mutation lies in a cluster of residues necessary for the formation of higher-order retromer oligomers on endosomal tubules (Kendall *et al.*, 2020), perhaps resulting in interference with downstream complex association.

Similarly, the study of LRRK2 kinase effects on post-synaptic AMPAR trafficking is mechanistically incomplete. We have not yet identified the localization of LRRK2, where and if it

colocalizes with VPS35 in neurons, nor the LRRK2 substrate responsible for the changes observed. Without mechanistic studies using the expression of binding mutants for FAM21, or constitutively phosphorylated or inactive LRRK2 substrates, these mechanistic questions remain open.

## **4.2 Future research directions**

Many of the limitations of this work can be turned into future, complementary studies. This work revealed many interesting avenues for new scientific explorations, which have been touched on in the text but will be reiterated here.

### **4.2.1 Mutant effects on mature & intact systems**

Knock-in models of other PD gene mutations have shown that early increases in glutamate release are eventually attenuated in the adult brain (Beccano-Kelly, Kuhlmann, *et al.*, 2014; Volta *et al.*, 2017). A logical next step for work in the D620N mice will be to track glutamate transmission phenotypes in *ex vivo* brain slices from adult mice. This will provide an opportunity to determine if D620N affects glutamate transmission in adult brains (and if, as expected, this shifts from basal transmission differences to plasticity impairments), in the context of physiological corticostriatal synapses.

### **4.2.2 Mechanistic inquiry**

Future work could also pursue the pre- and postsynaptic contributions to glutamate transmission phenotypes by growing heterologous WT/mutant cultures separated in microfluidic chambers to determine if these phenotypes truly represent distinct pre- or postsynaptic effects. As we were unable to determine conclusively whether differences in heterozygous and homozygous phenotypes represent compensatory regulation or mechanistic

differences, it would be worthwhile to track the time-course of these changes through slightly earlier and slightly later time points. Such studies could probe synaptic receptor composition, post-translational modifications, and calcium dynamics. This would allow us to know if homozygous culture phenotype attenuation is the result of compensatory changes, altered maturation, or a sustained mechanistic difference.

An important direction for future investigations will be to determine the mechanistic link between observed binding reductions in FAM21 and glutamate phenotypes, if any. For instance, the generation of FAM21 mutants that have only a subtle binding deficit with VPS35 could help uncover whether changes in FAM21 binding are causal to increased forward trafficking. Likewise, the exploration of LRRK2 site of action, mechanisms of cargo sequestration and release, and interaction with retromer function, are all worthwhile avenues for future study. Expression of constitutively active or kinase dead LRRK2 or LRRK2 substrates, alongside investigation of LRRK2 localization within neurons would provide further information on the cell biology of LRRK2, its neuronal substrates, and whether or not upregulated LRRK2 kinase activity in the D620N cells is compensatory, causative, or an epiphenomenon. It would be interesting to investigate whether neuronal LRRK2 acts through regulation of cargo release at the TGN as is observed in cell line studies (Beilina *et al.*, 2020), or if it participates in the local Golgi-independent secretory trafficking specialized to neuronal dendrites (Mikhaylova *et al.*, 2016; Bowen *et al.*, 2017), or both. Such studies will advance our understanding of protein trafficking in neurons. It is furthermore vital to understanding whether LRRK2 kinase inhibition can provide benefit, or even harm, for people with D620N parkinsonism; information which will inform future therapeutic developments.



### **4.2.3 Retromer trafficking of D2R and GluN1**

We discovered that retromer binds both D2R and GluN1 in cortical and striatal tissue from knock-in mice. As new cargoes, there is no information on the regulation of these proteins by retromer in the literature. NMDAR signalling at extrasynaptic sites has been shown to induce degeneration (Kaufman *et al.*, 2012; reviewed in: Hardingham and Bading, 2010; Bading, 2013) and is increased in other models of late-onset neurodegenerative disease (Milnerwood *et al.*, 2010; reviewed in: Milnerwood and Raymond, 2010). If mutant retromer were to result in increased forward trafficking of NMDARs, particularly at extrasynaptic sites, this may contribute to cell death in PD. D2Rs are expressed on a large population of striatal MSNs as post-synaptic receptors, and also on presynaptic cortical and nigral terminals in the striatum, where they modulate glutamate release in response to dopamine (Kreitzer, 2009; Gerfen and Surmeier, 2011; Tritsch and Sabatini, 2012). Given the importance of both receptors to corticostriatal and nigrostriatal signalling, future work investigating mutant effects on these receptors may provide further insight into nigral and more general neurodegeneration in PD.

### **4.2.4 VPS35, LRRK2, and Rab10 at the presynapse**

An interesting avenue for future work will be studies of presynaptic VPS35. In mammalian neurons it had largely been concluded that VPS35 does not affect presynaptic morphology or SV release (Munsie *et al.*, 2015; Temkin *et al.*, 2017; Vazquez-Sanchez *et al.*, 2018); however, retromer is present in a large subset of adult presynaptic terminals, at least in the hippocampus (Vazquez-Sanchez *et al.*, 2018). It is yet unknown what role it plays in the presynapse, but as discussed previously, the fact that it is only observed in a subset of synapses suggests that it likely does not play an essential role in synaptic vesicle regeneration in mammalian central synapses. It would be illuminating to study the colocalization of synaptic VPS35 with mitochondria, and investigate whether it has a role in the retrograde trafficking of old SVs/SV

proteins back to the cell body for degradation. Information is also scarce on its presynaptic role in trafficking DAT and VMAT2, though cell-line studies have shown that these two transporters can be trafficked by retromer (Wu *et al.*, 2016, 2017), making these trafficking pathways interesting areas for future research.

It would also be interesting to probe the intersection of LRRK2, Rab10, and VPS35 in the presynapse. The immunocytochemistry experiments performed on Rab10 provide rationale for investigating a possible presynaptic localization of Rab10 in glutamatergic and non-glutamatergic cells, and we have observed some colocalization of Rab10 with VGluT1. It was interesting to observe that MLi-2 treatment had no effect on the presynapse. This suggests that LRRK2 may modulate VPS35 activity presynaptically through a role as a scaffolding protein. Further investigation is warranted to help explain how VPS35 and LRRK2 parkinsonism appear to affect glutamate transmission in different ways.

### **4.3 Contributions to the field**

This dissertation is, to my knowledge, the first study of the cell biological underpinnings of synaptic dysregulation in a knock-in mouse model of D620N parkinsonism. Initial characterizations of the D620N knock-in mice presented some evidence for dysregulation of dopamine signalling (Ishizu *et al.*, 2016; Cataldi *et al.*, 2018), but it was still unknown if glutamate transmission would be equally affected. Our original study of exogenous D620N expression in cultured cortical neurons had led us to the conclusion that D620N causes a loss-of-function in AMPAR trafficking and revealed no presynaptic effects (Munsie *et al.*, 2015). Here we discovered that endogenous expression results in increased forward trafficking of AMPARs as well as having an effect on presynaptic probability of glutamate release. This work highlights

the importance of studying mutation effects at endogenous expression levels, particularly when considering proteins that have many functions and complicated interactomes.

This work identified new neuronal cargoes GluN1 and D2R, which are of particular interest in cortico-striatal-nigral circuit dysregulation.

This work also provides evidence that LRRK2 kinase acts to inhibit forward trafficking of AMPA receptors in developing cortical neurons, and excludes LRRK2 kinase activity upregulation as causal to increased presynaptic release phenotypes in the D620N mice. These findings have very important implications for the use of LRRK2 kinase inhibition in non-LRRK2 parkinsonism.

I have shown that the D620N mutation in endogenous mouse VPS35 produces functional alterations in glutamate transmission and regulation of the PD-linked kinase LRRK2. My work has added support to the hypothesis that PD-linked mutations converge on synaptic protein trafficking pathways, which could represent a common disturbance that eventually manifests as parkinsonism. The convergence of multiple etiological factors onto the same cellular pathways provides hope that the field may be close to developing neuroprotective treatment. Given the etiological heterogeneity of PD, careful diagnosis and personalized approaches may be necessary.

## Bibliography

Adeosun, S. O. *et al.* (2017) 'Human LRRK2 G2019S mutation represses post-synaptic protein PSD95 and causes cognitive impairment in transgenic mice', *Neurobiology of Learning and Memory*. Elsevier Inc., 142, pp. 182–189. doi: 10.1016/j.nlm.2017.05.001.

Alshafie, W. *et al.* (2020) 'Regulated resurfacing of a somatostatin receptor storage compartment fine-tunes pituitary secretion', *The Journal of cell biology*, 219(1). doi: 10.1083/jcb.201904054.

Appel-Cresswell, S. *et al.* (2014) 'Clinical, positron emission tomography, and pathological studies of DNAJC13 p.N855S Parkinsonism.', *Movement disorders* □: official journal of the Movement Disorder Society, 29(13), pp. 1684–7. doi: 10.1002/mds.26019.

Arighi, C. N. *et al.* (2004) 'Role of the mammalian retromer in sorting of the cation-independent mannose 6-phosphate receptor', *The Journal of Cell Biology JCB Article The Journal of Cell Biology*, 165(1), pp. 123–133. doi: 10.1083/jcb.200312055.

Arranz, A. M. *et al.* (2015) 'LRRK2 functions in synaptic vesicle endocytosis through a kinasedependent mechanism', *Journal of Cell Science*, 128(3), pp. 541–552. doi: 10.1242/jcs.158196.

Ashby, M. C. *et al.* (2006) 'Lateral diffusion drives constitutive exchange of AMPA receptors at dendritic spines and is regulated by spine morphology', *Journal of Neuroscience*, 26(26), pp. 7046–7055. doi: 10.1523/JNEUROSCI.1235-06.2006.

Atashrazm, F. *et al.* (2019) 'LRRK2-mediated Rab10 phosphorylation in immune cells from Parkinson's disease patients', *Movement Disorders*, 34(3), pp. 406–415. doi: 10.1002/mds.27601.

Bading, H. (2013) 'Nuclear calcium signalling in the regulation of brain function', *Nature Reviews Neuroscience*. Nature Publishing Group, 14(9), pp. 593–608. doi: 10.1038/nrn3531.

Bandres-Ciga, S. *et al.* (2020) 'Genetics of Parkinson's disease: An introspection of its journey

towards precision medicine', *Neurobiology of Disease*. Elsevier, 137(November 2019), p. 104782. doi: 10.1016/j.nbd.2020.104782.

Bankaitis, V. A., Johnson, L. M. and Emr, S. D. (1986) 'Isolation of yeast mutants defective in protein targeting to the vacuole', *Proceedings of the National Academy of Sciences USA*, 83(December), pp. 9075–9079.

Bartels, T., Choi, J. G. and Selkoe, D. J. (2011) 'α-Synuclein occurs physiologically as a helically folded tetramer that resists aggregation.', *Nature*. Nature Publishing Group, 477(7362), pp. 107–110. doi: 10.1038/nature10324.

Beccano-Kelly, D. A., Volta, M., *et al.* (2014) 'LRRK2 overexpression alters glutamatergic presynaptic plasticity, striatal dopamine tone, postsynaptic signal transduction, motor activity and memory.', *Human molecular genetics*, 24(October), pp. 1–14. doi: 10.1093/hmg/ddu543.

Beccano-Kelly, D. A., Kuhlmann, N., *et al.* (2014) 'Synaptic function is modulated by LRRK2 and glutamate release is increased in cortical neurons of G2019S LRRK2 knock-in mice.', *Frontiers in cellular neuroscience*, 8(September), p. 301. doi: 10.3389/fncel.2014.00301.

Bedford, C. *et al.* (2016) 'LRRK2 regulates voltage-gated calcium channel function', *Frontiers in Molecular Neuroscience*, 9(MAY), pp. 1–16. doi: 10.3389/fnmol.2016.00035.


Beilina, A. *et al.* (2014) 'Unbiased screen for interactors of leucine-rich repeat kinase 2 supports a common pathway for sporadic and familial Parkinson disease', *Proceedings of the National Academy of Sciences of the United States of America*, 111(7), pp. 2626–2631. doi: 10.1073/pnas.1318306111.

Beilina, A. *et al.* (2020) 'The Parkinson's disease protein LRRK2 interacts with the GARP complex to promote retrograde transport to the trans-Golgi network', *Cell Reports*, 31(107614).

Beitz, J. M. (2014) 'Parkinson's disease: a review', *Frontiers in Bioscience*, S6(3), pp. 65–74. doi: 10.2741/s415.

Belluzzi, E. *et al.* (2016) 'LRRK2 phosphorylates pre-synaptic N-ethylmaleimide sensitive fusion

(NSF) protein enhancing its ATPase activity and SNARE complex disassembling rate', *Molecular Neurodegeneration*. Molecular Neurodegeneration, 11(1), pp. 1–16. doi: 10.1186/s13024-015-0066-z.

Bendor, J. T., Logan, T. P. and Edwards, R. H. (2013) 'The function of  synuclein', *Neuron*. Elsevier Inc., 79(6), pp. 1044–1066. doi: 10.1016/j.neuron.2013.09.004.

Benke, T. A. *et al.* (2001) 'Mathematical modelling of non-stationary fluctuation analysis for studying channel properties of synaptic AMPA receptors', *Journal of Physiology*, 537(2), pp. 407–420.

Benke, T. and Traynelis, S. F. (2019) 'AMPA-type glutamate receptor conductance changes and plasticity: still a lot of noise', *Neurochemical Research*, 44(3), pp. 539–548. doi: 10.1016/j.physbeh.2017.03.040.

Benson, D. L. *et al.* (2018) 'Functional and behavioral consequences of Parkinson's disease-associated LRRK2- G2019S mutation', *Biochemical Society Transactions*, p. BST20180468. doi: 10.1042/BST20180468.

Berger, Z., Smith, K. A. and Lavoie, M. J. (2010) 'Membrane localization of LRRK2 is associated with increased formation of the highly active lrrk2 dimer and changes in its phosphorylation', *Biochemistry*, 49(26), pp. 5511–5523. doi: 10.1021/bi100157u.

Betarbet, R. *et al.* (2000) 'Chronic systemic pesticide exposure produces pd symptoms Betarbet', *Nature neuroscience*, 26, pp. 1301–1306.

Bhalla, A. *et al.* (2012) 'The location and trafficking routes of the neuronal retromer and its role in amyloid precursor protein transport.', *Neurobiology of disease*. Elsevier Inc., 47(1), pp. 126–34. doi: 10.1016/j.nbd.2012.03.030.

Binda, C. S. *et al.* (2019) 'Sorting nexin 27 rescues neuroligin 2 from lysosomal degradation to control inhibitory synapse number', *Biochemical Journal*, 476(2), pp. 293–306. doi: 10.1042/BCJ20180504.

- Binotti, B., Jahn, R. and En Chua, J. J. (2016) 'Functions of rab proteins at presynaptic sites', *Cells*, 5(1), pp. 1–10. doi: 10.3390/cells5010007.
- Biskup, S. *et al.* (2006) 'Localization of LRRK2 to membranous and vesicular structures in mammalian brain', *Annals of Neurology*, 60(5), pp. 557–569. doi: 10.1002/ana.21019.
- Bliss, T. and Collingridge, G. (2019) 'Persistent memories of long-term potentiation and the N - methyl-d-aspartate receptor ', *Brain and Neuroscience Advances*, 3, p. 239821281984821. doi: 10.1177/2398212819848213.
- Boassa, D. *et al.* (2013) 'Mapping the Subcellular Distribution of  $\alpha$ -Synuclein in Neurons using Genetically Encoded Probes for Correlated Light and Electron Microscopy: Implications for Parkinson's Disease Pathogenesis', *Journal of Neuroscience*, 33(6), pp. 2605–2615. doi: 10.1523/JNEUROSCI.2898-12.2013.
- Bodrikov, V. *et al.* (2017) 'Reggie-1 and reggie-2 (flotillins) participate in Rab11a-dependent cargo trafficking, spine synapse formation and LTP-related AMPA receptor (GluA1) surface exposure in mouse hippocampal neurons', *Experimental Neurology*. Elsevier Inc., 289, pp. 31–45. doi: 10.1016/j.expneurol.2016.12.007.
- Bonifacino, J. S. and Rojas, R. (2006) 'Retrograde transport from endosomes to the trans-Golgi network.', *Nature reviews. Molecular cell biology*, 7(8), pp. 568–79. doi: 10.1038/nrm1985.
- Borghammer, P. and Van Den Berge, N. (2019) 'Brain-First versus Gut-First Parkinson's Disease: A Hypothesis', *Journal of Parkinson's Disease*, 9(s2), pp. S281–S295. doi: 10.3233/JPD-191721.
- Borisova, T. *et al.* (2010) 'Diverse presynaptic mechanisms underlying methyl- $\beta$ -cyclodextrin-mediated changes in glutamate transport', *Cellular and Molecular Neurobiology*, 30(7), pp. 1013–1023. doi: 10.1007/s10571-010-9532-x.
- Bové, J. *et al.* (2005) 'Toxin-induced models of Parkinson's disease', *NeuroRx*, 2, pp. 484–494. doi: 10.1602/neurorx.2.3.484.

Bowen, A. B. *et al.* (2017) 'Golgi-Independent secretory trafficking through recycling endosomes in neuronal dendrites and spines', *eLife*, 6, pp. 1–27. doi: 10.7554/eLife.27362.

Braak, H. *et al.* (2003) 'Staging of brain pathology related to sporadic Parkinson's disease', *Neurobiology of Aging*, 24(2), pp. 197–211. doi: 10.1016/S0197-4580(02)00065-9.

Braschi, E. *et al.* (2010) 'Vps35 mediates vesicle transport between the mitochondria and peroxisomes.', *Current biology : CB*, 20(14), pp. 1310–5. doi: 10.1016/j.cub.2010.05.066.

Breckenridge, C. B. *et al.* (2016) 'Association between Parkinson's disease and cigarette smoking, rural living, well-water consumption, farming and pesticide use: Systematic review and meta-analysis', *PLoS ONE*, 11(4), pp. 1–42. doi: 10.1371/journal.pone.0151841.

Bridi, J. C. and Hirth, F. (2018) 'Mechanisms of  $\alpha$ -Synuclein induced synaptopathy in parkinson's disease', *Frontiers in Neuroscience*. doi: 10.3389/fnins.2018.00080.

Brigidi, G. S. *et al.* (2014) 'Palmitoylation of  $\delta$ -catenin by DHHC5 mediates activity-induced synapse plasticity.', *Nature neuroscience*, 17(4), pp. 522–32. doi: 10.1038/nn.3657.

Brown, T. C. *et al.* (2007) 'Functional compartmentalization of endosomal trafficking for the synaptic delivery of AMPA receptors during long-term potentiation', *Journal of Neuroscience*, 27(48), pp. 13311–13315. doi: 10.1523/JNEUROSCI.4258-07.2007.

Bruno, J. *et al.* (2016) 'SEC16A is a RAB10 effector required for insulin-stimulated GLUT4 trafficking in adipocytes', *Journal of Cell Biology*, 214(1), pp. 61–76. doi: 10.1083/jcb.201509052.

Bu, X. Le *et al.* (2015) 'The association between infectious burden and Parkinson's disease: A case-control study', *Parkinsonism and Related Disorders*, 21(8), pp. 877–881. doi: 10.1016/j.parkreldis.2015.05.015.

Budnik, V. and Salinas, P. C. (2011) 'Wnt signaling during synaptic development and plasticity', *Current Opinion in Neurobiology*. Elsevier Ltd, 21(1), pp. 151–159. doi: 10.1016/j.conb.2010.12.002.



- Bugarcic, A. *et al.* (2011) 'Vps26A and Vps26B Subunits Define Distinct Retromer Complexes', *Traffic*, 12(12), pp. 1759–1773. doi: 10.1111/j.1600-0854.2011.01284.x.
- Bugarcic, A. *et al.* (2015) 'Vps26B-retromer negatively regulates plasma membrane resensitization of PAR-2', *Cell Biology International*, 39(11), pp. 1299–1306. doi: 10.1002/cbin.10508.
- Burd, C. and Cullen, P. J. (2014) 'Retromer: A Master Conductor of Endosome Sorting', *Cold Spring Harbor Perspectives in Biology*, 6(2). doi: 10.1101/cshperspect.a016774.
- Burré, J., Sharma, M. and Südhof, T. C. (2018) 'Cell biology and pathophysiology of  $\alpha$ -synuclein', *Cold Spring Harbor Perspectives in Medicine*, 8(3), pp. 1–28. doi: 10.1101/cshperspect.a024091.
- Cannon, J. R. and Greenamyre, J. T. (2013) 'Gene-environment interactions in Parkinson's disease: Specific evidence in humans and mammalian models', *Neurobiology of Disease*. Elsevier Inc., 57, pp. 38–46. doi: 10.1016/j.nbd.2012.06.025.
- Canuel, M. *et al.* (2008) 'AP-1 and retromer play opposite roles in the trafficking of sortilin between the Golgi apparatus and the lysosomes', *Biochemical and Biophysical Research Communications*, 366(3), pp. 724–730. doi: 10.1016/j.bbrc.2007.12.015.
- Carlton, J. *et al.* (2004) 'Sortin Nexin-1 Mediates Tubular Endosome-to-TGN Transport through Coincidence Sensing of High-Curvature Membranes and 3-Phosphoinositides', *Current Biology*, 14, pp. 1791–1800. doi: 10.1016/j.
- Carrion, M. D. P. *et al.* (2017) 'The LRRK2 G2385R variant is a partial loss-of-function mutation that affects synaptic vesicle trafficking through altered protein interactions', *Scientific Reports*. Springer US, 7(5377), pp. 1–15. doi: 10.1038/s41598-017-05760-9.
- Cataldi, S. *et al.* (2018) 'Altered dopamine release and monoamine transporters in Vps35 p.D620N knock-in mice', *npj Parkinson's Disease*. Springer US, 4(1), pp. 1–11. doi: 10.1038/s41531-018-0063-3.

- Cebrián, C., Loike, J. D. and Sulzer, D. (2014) 'Neuronal mhc-i expression and its implications in synaptic function, Axonal regeneration and parkinson's and other brain diseases', *Frontiers in Neuroanatomy*, 8(OCT), pp. 1–9. doi: 10.3389/fnana.2014.00114.
- Chan, A. S. M. *et al.* (2016) 'Sorting nexin 27 couples PTHR trafficking to retromer for signal regulation in osteoblasts during bone growth', *Molecular Biology of the Cell*, 27(8), pp. 1367–1382. doi: 10.1091/mbc.E15-12-0851.
- Chang, D. *et al.* (2017) 'A meta-analysis of genome-wide association studies identifies 17 new Parkinson's disease risk loci', *Nature Genetics*. Nature Publishing Group, 49(10), pp. 1511–1516. doi: 10.1038/ng.3955.
- Chartier-Harlin, M.-C. *et al.* (2004) 'α-synuclein locus duplication as a cause of familial Parkinson's disease', *Lancet*, 364(9440), pp. 1167–1169. doi: 10.1111/j.1475-1313.2011.00822.x.
- Chaudhuri, K. R., Healy, D. G. and Schapira, A. H. (2006) 'Non-motor symptoms of Parkinson's disease: diagnosis and management.', *Lancet Neurology*, 5, pp. 235–245. doi: 10.4314/njm.v19i2.56496.
- Chen, C. K., Wu, Y. T. and Chang, Y. C. (2017) 'Periodontal inflammatory disease is associated with the risk of Parkinson's disease: A population-based retrospective matched-cohort study', *PeerJ*, 2017(8), pp. 1–14. doi: 10.7717/peerj.3647.
- Chen, H. and Ritz, B. (2018) 'The search for environmental causes of Parkinson's disease: Moving forward', *Journal of Parkinson's Disease*, 8(s1), pp. S9–S17. doi: 10.3233/JPD-181493.
- Chen, X. *et al.* (2019) 'Parkinson's disease-linked D620N VPS35 knock-in mice manifest tau neuropathology and dopaminergic neurodegeneration', *Proceedings of the National Academy of Sciences of the United States of America*, 116(12), pp. 5765–5774. doi: 10.1073/pnas.1814909116.
- Chen, Y. *et al.* (2005) 'Rab10 and myosin-Va mediate insulin-stimulated GLUT4 storage vesicle translocation in adipocytes', 198(4), pp. 545–560. doi: 10.1083/jcb.201111091.

- Chesselet, M.-F. and Richter, F. (2011) 'Modelling of Parkinson's disease in mice', *The Lancet Neurology*. Elsevier Ltd, 10(12), pp. 1108–1118. doi: 10.1016/S1474-4422(11)70227-7.
- Choy, R. W.-Y. *et al.* (2014) 'Retromer mediates a discrete route of local membrane delivery to dendrites.', *Neuron*. Elsevier Inc., 82(1), pp. 55–62. doi: 10.1016/j.neuron.2014.02.018.
- Cirnar, M. D. *et al.* (2014) 'LRRK2 kinase activity regulates synaptic vesicle trafficking and neurotransmitter release through modulation of LRRK2 macro-molecular complex.', *Frontiers in molecular neuroscience*, 7(May), p. 49. doi: 10.3389/fnmol.2014.00049.
- Clairfeuille, T. *et al.* (2016) 'A molecular code for endosomal recycling of phosphorylated cargos by the SNX27-retromer complex', *Nature Structural and Molecular Biology*. Nature Publishing Group, 23(10), pp. 921–932. doi: 10.1038/nsmb.3290.
- Collins, B. M. *et al.* (2005) 'Vps29 has a phosphoesterase fold that acts as a protein interaction scaffold for retromer assembly', *Nature Structural and Molecular Biology*, 12(7), pp. 594–602. doi: 10.1038/nsmb954.
- Cookson, M. R. (2010) 'DJ-1, PINK1, and their effects on mitochondrial pathways.', *Movement disorders : official journal of the Movement Disorder Society*, 25 Suppl 1, pp. 44–48. doi: 10.1002/mds.22713.
- Correia, S. S. *et al.* (2008) 'Motor protein-dependent transport of AMPA receptors into spines during long-term potentiation.', *Nature neuroscience*, 11(4), pp. 457–66. doi: 10.1038/nn2063.
- Cui, Y. *et al.* (2019) 'Retromer has a selective function in cargo sorting via endosome transport carriers', *Journal of Cell Biology*, 218(2), pp. 615–631. doi: 10.1083/jcb.201806153.
- Cullen, P. J. and Korswagen, H. C. (2011) 'Sorting nexins provide diversity for retromer-dependent trafficking events.', *Nature cell biology*. Nature Publishing Group, 14(1), pp. 29–37. doi: 10.1038/ncb2374.
- Dächsel, J. C. *et al.* (2010) 'A comparative study of Lrrk2 function in primary neuronal cultures', *Parkinsonism and Related Disorders*. Elsevier Ltd, 16(10), pp. 650–655. doi:

10.1016/j.parkreldis.2010.08.018.

DeCaprio, J. and Kohl, T. O. (2017) 'Detergent lysis of animal tissues for immunoprecipitation', *Cold Spring Harbor Protocols*, 2017(12), pp. 1009–1011. doi: 10.1101/pdb.prot098566.

Demi, M. (2005) 'On the gray-level central and absolute central moments and the mass center of the gray-level variability in low-level image processing', *Computer Vision and Image Understanding*, 97(2), pp. 180–208. doi: 10.1016/j.cviu.2004.07.003.

Derivery, E. *et al.* (2009) 'The Arp2/3 activator WASH controls the fission of endosomes through a large multiprotein complex.', *Developmental cell*, 17(5), pp. 712–23. doi: 10.1016/j.devcel.2009.09.010.

Derivery, E. *et al.* (2012) 'Actin polymerization controls the organization of WASH domains at the surface of endosomes.', *PloS one*, 7(6), p. e39774. doi: 10.1371/journal.pone.0039774.

Dhungel, N. *et al.* (2015) 'Parkinson's disease genes VPS35 and EIF4G1 interact genetically and converge on  $\alpha$ -synuclein.', *Neuron*. Elsevier, 85(1), pp. 76–87. doi: 10.1016/j.neuron.2014.11.027.

Dickson, D. W., Braak, H., *et al.* (2009) 'Neuropathological assessment of Parkinson's disease: refining the diagnostic criteria', *The Lancet Neurology*. Elsevier Ltd, 8(12), pp. 1150–1157. doi: 10.1016/S1474-4422(09)70238-8.

Dickson, D. W., Fujishiro, H., *et al.* (2009) 'Neuropathology of non-motor features of Parkinson disease', *Parkinsonism & Related Disorders*. Elsevier Ltd, 15, pp. S1–S5. doi: 10.1016/S1353-8020(09)70769-2.

Diering, G. H., Gustina, A. S. and Huganir, R. L. (2014) 'PKA-GluA1 coupling via AKAP5 controls AMPA receptor phosphorylation and cell-surface targeting during bidirectional homeostatic plasticity', *Neuron*. Elsevier Inc., 84(4), pp. 790–805. doi: 10.1016/j.neuron.2014.09.024.

Diering, G. H. and Huganir, R. L. (2018) 'The AMPA Receptor Code of Synaptic Plasticity',

*Neuron*. Elsevier Inc., 100(2), pp. 314–329. doi: 10.1016/j.neuron.2018.10.018.

Dorsey, E. R. *et al.* (2018) ‘Global, regional, and national burden of Parkinson’s disease, 1990–2016: a systematic analysis for the Global Burden of Disease Study 2016’, *The Lancet Neurology*, 17(11), pp. 939–953. doi: 10.1016/S1474-4422(18)30295-3.

Duleh, S. N. and Welch, M. D. (2010) ‘WASH and the Arp2/3 complex regulate endosome shape and trafficking’, *Cytoskeleton*, 67(3), pp. 193–206. doi: 10.1002/cm.20437.

Edgar, A. J. and Polak, J. M. (2000) ‘Human homologues of yeast vacuolar protein sorting 29 and 35’, *Biochemical and Biophysical Research Communications*, 277(3), pp. 622–630. doi: 10.1006/bbrc.2000.3727.

Ehlers, M. D. (2000) ‘Reinsertion or Degradation of AMPA Receptors Determined by Activity-Dependent Endocytic Sorting’, *Neuron*, 28(2), pp. 511–525. doi: 10.1016/S0896-6273(00)00129-X.

Esteves da Silva, M. *et al.* (2015) ‘Positioning of AMPA Receptor-Containing Endosomes Regulates Synapse Architecture’, *Cell Reports*, 13(5), pp. 933–943. doi: 10.1016/j.celrep.2015.09.062.

Fahn, S. (2015) ‘The medical treatment of Parkinson disease from James Parkinson to George Cotzias’, *Movement Disorders*, 30(1), pp. 4–18. doi: 10.1002/mds.26102.

Fan, Y. *et al.* (2018) ‘Interrogating Parkinson’s disease LRRK2 kinase pathway activity by assessing Rab10 phosphorylation in human neutrophils’, *Biochemical Journal*, 475(1), pp. 23–44. doi: 10.1042/BCJ20170803.

Farmer, T. *et al.* (2017) ‘Control of mitochondrial homeostasis by endocytic regulatory proteins’, *Journal of Cell Science*, 130(14), pp. 2359–2370. doi: 10.1242/jcs.204537.

Farmer, T. *et al.* (2019) ‘Retromer facilitates the localization of Bcl-xL to the mitochondrial outer membrane’, *Molecular Biology of the Cell*, 30(10), pp. 1138–1146. doi: 10.1091/mbc.E19-01-0044.

- Fazio, P. *et al.* (2018) 'Nigrostriatal dopamine transporter availability in early Parkinson's disease', *Movement Disorders*, 33(4), pp. 592–599. doi: 10.1002/mds.27316.
- Feinstein, T. N. *et al.* (2011) 'Retromer terminates the generation of cAMP by internalized PTH receptors', *Nature Chemical Biology*. Nature Publishing Group, 7(5), pp. 278–284. doi: 10.1038/nchembio.545.
- Feinstein, T. N. *et al.* (2013) 'Noncanonical control of vasopressin receptor type 2 signaling by retromer and arrestin', *Journal of Biological Chemistry*, 288(39), pp. 27849–27860. doi: 10.1074/jbc.M112.445098.
- Fell, M. J. *et al.* (2015) 'MLi-2, a potent, selective, and centrally active compound for exploring the therapeutic potential and safety of LRRK2 kinase inhibition', *Journal of Pharmacology and Experimental Therapeutics*, 355(3), pp. 397–409. doi: 10.1124/jpet.115.227587.
- Ferrari, E. *et al.* (2020) 'From cell lines to pluripotent stem cells for modelling Parkinson's Disease', *Journal of Neuroscience Methods*. Elsevier, 340(April), p. 108741. doi: 10.1016/j.jneumeth.2020.108741.
- Fitzgerald, E., Murphy, S. and Martinson, H. A. (2019) 'Alpha-synuclein pathology and the role of the microbiota in Parkinson's disease', *Frontiers in Neuroscience*, 13(APR), pp. 1–13. doi: 10.3389/fnins.2019.00369.
- Foffani, G. and Obeso, J. A. (2018) 'A Cortical Pathogenic Theory of Parkinson's Disease', *Neuron*, 99(6), pp. 1116–1128. doi: 10.1016/j.neuron.2018.07.028.
- Follett, J. *et al.* (2013) 'The Vps35 D620N Mutation Linked to Parkinson's Disease Disrupts the Cargo Sorting Function of Retromer.', *Traffic (Copenhagen, Denmark)*, (6). doi: 10.1111/tra.12136.
- Follett, J. *et al.* (2019) 'DNAJC13 p.Asn855Ser, implicated in familial parkinsonism, alters membrane dynamics of sorting nexin 1', *Neuroscience Letters*. Elsevier, 706(April), pp. 114–122. doi: 10.1016/j.neulet.2019.04.043.

- Fortalezas, S., Marques-da-Silva, D. and Gutierrez-Merino, C. (2018) 'Methyl- $\beta$ -cyclodextrin impairs the phosphorylation of the  $\beta$ 2 subunit of L-type calcium channels and cytosolic calcium homeostasis in mature cerebellar granule neurons', *International Journal of Molecular Sciences*, 19(11). doi: 10.3390/ijms19113667.
- Freeman, C. L., Hesketh, G. and Seaman, M. N. J. (2014) 'RME-8 coordinates the WASH complex with the retromer SNX-BAR dimer to control endosomal tubulation', *Journal of Cell Science*, p. jcs.144659. doi: 10.1242/jcs.144659.
- Fujita, Y. *et al.* (2006) 'Fragmentation of Golgi apparatus of nigral neurons with  $\alpha$ -synuclein-positive inclusions in patients with Parkinson's disease', *Acta Neuropathology*, 112, pp. 261–265. doi: 10.1007/s00401-006-0114-4.
- Fuse, A. *et al.* (2015) 'VPS29–VPS35 intermediate of retromer is stable and may be involved in the retromer complex assembly process', *FEBS Letters*. Federation of European Biochemical Societies, 589(13), pp. 1430–1436. doi: 10.1016/j.febslet.2015.04.040.
- Galli, S. *et al.* (2014) 'Deficient Wnt signalling triggers striatal synaptic degeneration and impaired motor behaviour in adult mice.', *Nature communications*. Nature Publishing Group, 5, p. 4992. doi: 10.1038/ncomms5992.
- Gallon, M. *et al.* (2014) 'A unique PDZ domain and arrestin-like fold interaction reveals mechanistic details of endocytic recycling by SNX27-retromer', *Proceedings of the National Academy of Sciences of the United States of America*, 111(35). doi: 10.1073/pnas.1410552111.
- Galter, D. *et al.* (2006) 'LRRK2 expression linked to dopamine-innervated areas', *Annals of Neurology*, 59(4), pp. 714–719. doi: 10.1002/ana.20808.
- Garretti, F. *et al.* (2019) 'Autoimmunity in parkinson's disease: The role of  $\alpha$ -synuclein-specific T cells', *Frontiers in Immunology*, 10(FEB), pp. 1–12. doi: 10.3389/fimmu.2019.00303.
- Gerfen, C. R. and Surmeier, D. J. (2011) 'Modulation of striatal projection systems by dopamine.', *Annual review of neuroscience*, 34, pp. 441–66. doi: 10.1146/annurev-neuro-

061010-113641.

Gerges, N. Z., Backos, D. S. and Esteban, J. A. (2004) 'Local control of AMPA receptor trafficking at the postsynaptic terminal by a small GTPase of the Rab family', *Journal of Biological Chemistry*, 279(42), pp. 43870–43878. doi: 10.1074/jbc.M404982200.

Glodowski, D. R. *et al.* (2007) 'RAB-10 regulates glutamate receptor recycling in a cholesterol-dependent endocytosis pathway', *Molecular Biology of the Cell*, 18(November), pp. 4387–4396. doi: 10.1091/mbc.E07.

Goetz, C. G. (2011) 'The history of Parkinson's disease: Early clinical descriptions and neurological therapies', *Cold Spring Harbor Perspectives in Medicine*, 1(1), pp. 1–15. doi: 10.1101/cshperspect.a008862.

Gokool, S., Tattersall, D. and Seaman, M. N. J. (2007) 'EHD1 interacts with retromer to stabilize SNX1 tubules and facilitate endosome-to-golgi retrieval', *Traffic*, 8(12), pp. 1873–1886. doi: 10.1111/j.1600-0854.2007.00652.x.

Goldman, J. G. and Postuma, R. (2014) 'Premotor and nonmotor features of Parkinson's disease.', *Current opinion in neurology*, 27(4), pp. 434–41. doi: 10.1097/WCO.0000000000000112.

Gómez-Suaga, P., Rivero-Ríos, P., *et al.* (2014) 'LRRK2 delays degradative receptor trafficking by impeding late endosomal budding through decreasing Rab7 activity', *Human Molecular Genetics*, 23(25), pp. 1–18. doi: 10.1093/hmg/ddu395.

Gómez-Suaga, P., Fdez, E., *et al.* (2014) 'Novel insights into the neurobiology underlying LRRK2-linked Parkinson's disease', *Neuropharmacology*, 85, pp. 45–56. doi: 10.1016/j.neuropharm.2014.05.020.

Gomez, T. S. and Billadeau, D. D. (2009) 'A FAM21-containing WASH complex regulates retromer-dependent sorting.', *Developmental cell*. Elsevier Ltd, 17(5), pp. 699–711. doi: 10.1016/j.devcel.2009.09.009.



- Good, P. F. *et al.* (1998) 'Protein Nitration in Parkinson's Disease', *Journal of Neuropathology and Experimental Neurology*, 47(4), pp. 338–342.
- Greggio, E. *et al.* (2008) 'The Parkinson disease-associated leucine-rich repeat kinase 2 (LRRK2) is a dimer that undergoes intramolecular autophosphorylation', *Journal of Biological Chemistry*, 283(24), pp. 16906–16914. doi: 10.1074/jbc.M708718200.
- Greggio, E. and Cookson, M. R. (2009) 'Leucine-rich repeat kinase 2 mutations and Parkinson's disease: Three questions', *ASN Neuro*, 1(1), pp. 13–24. doi: 10.1042/AN20090007.
- Griffin, C. T., Trejo, J. and Magnuson, T. (2005) 'Genetic evidence for a mammalian retromer complex containing sorting nexins 1 and 2.', *Proceedings of the National Academy of Sciences of the United States of America*, 102(42), pp. 15173–15177. doi: 10.1073/pnas.0409558102.
- Gustavsson, E. K. *et al.* (2015) 'Genetic variability of the retromer cargo recognition complex in parkinsonism', *Movement Disorders*, 30(4), pp. 580–584. doi: 10.1002/mds.26104.
- Haft, C. R. *et al.* (2000) 'Human orthologs of yeast vacuolar protein sorting proteins Vps26, 29, and 35: assembly into multimeric complexes.', *Molecular biology of the cell*, 11(12), pp. 4105–16. doi: 10.1091/mbc.11.12.4105.
- Harbour, M. E. *et al.* (2010) 'The cargo-selective retromer complex is a recruiting hub for protein complexes that regulate endosomal tubule dynamics.', *Journal of cell science*, 123(Pt 21), pp. 3703–17. doi: 10.1242/jcs.071472.
- Harbour, M. E., Breusegem, S. Y. and Seaman, M. N. J. (2012) 'Recruitment of the endosomal WASH complex is mediated by the extended "tail" of Fam21 binding to the retromer protein Vps35', *Biochemical Journal*, 442(1), pp. 209–220. doi: 10.1042/BJ20111761.
- Hardingham, G. E. and Bading, H. (2010) 'Synaptic versus extrasynaptic NMDA receptor signalling: Implications for neurodegenerative disorders', *Nature Reviews Neuroscience*. Nature Publishing Group, 11(10), pp. 682–696. doi: 10.1038/nrn2911.
- Harrison, M. S. *et al.* (2014) 'A mechanism for retromer endosomal coat complex assembly with

cargo', *Proceedings of the National Academy of Sciences of the United States of America*, 111(1), pp. 267–272. doi: 10.1073/pnas.1316482111.

Harterink, M. *et al.* (2011) 'A SNX3-dependent retromer pathway mediates retrograde transport of the Wnt sorting receptor Wntless and is required for Wnt secretion', *Nature Cell Biology*. Nature Publishing Group, 13(8), pp. 914–923. doi: 10.1038/ncb2281.

Hartveit, E. and Veruki, M. L. (2007) 'Studying properties of neurotransmitter receptors by non-stationary noise analysis of spontaneous postsynaptic currents and agonist-evoked responses in outside-out patches', *Nature Protocols*, 2(2), pp. 434–448. doi: 10.1038/nprot.2007.47.

Healy, D. G. *et al.* (2008) 'Phenotype, genotype, and worldwide genetic penetrance of LRRK2-associated Parkinson's disease: a case-control study', *The Lancet Neurology*, 7(7), pp. 583–590. doi: 10.1016/S1474-4422(08)70117-0.

Helfer, E. *et al.* (2013) 'Endosomal recruitment of the WASH complex: Active sequences and mutations impairing interaction with the retromer', *Biology of the Cell*, 105(5), pp. 191–207. doi: 10.1111/boc.201200038.

Heo, J. M. *et al.* (2018) 'RAB7A phosphorylation by TBK1 promotes mitophagy via the PINK-PARKIN pathway', *Science Advances*, 4(11), pp. 1–18. doi: 10.1126/sciadv.aav0443.

Hesketh, G. *et al.* (2014) 'VARP is recruited on to endosomes by direct interaction with retromer, where together they function in export to the cell surface', *Developmental Cell*, 29(5), pp. 591–606. doi: 10.1016/j.devcel.2014.04.010.

Hierro, A. *et al.* (2007) 'Functional architecture of the retromer cargo-recognition complex', *Nature*, 449(7165), pp. 1063–1067. doi: 10.1038/nature06216.

Hinkle, K. M. *et al.* (2012) 'LRRK2 knockout mice have an intact dopaminergic system but display alterations in exploratory and motor co-ordination behaviors', *Molecular Neurodegeneration*, 7(1), pp. 1–17. doi: 10.1186/1750-1326-7-25.

Hirayama, T. *et al.* (2019) 'A Golgi-targeting fluorescent probe for labile Fe(ii) to reveal an

abnormal cellular iron distribution induced by dysfunction of VPS35', *Chemical Science*. Royal Society of Chemistry, 10(5), pp. 1514–1521. doi: 10.1039/c8sc04386h.

Hornykiewicz, O. (2002) 'Dopamine miracle: From brain homogenate to dopamine replacement', *Movement Disorders*, 17(3), pp. 501–508. doi: 10.1002/mds.10115.

Hui, W. *et al.* (2011) 'Evaluation of cholesterol depletion as a marker of nephrotoxicity in vitro for novel  $\beta$ -cyclodextrin derivatives', *Food and Chemical Toxicology*. Elsevier Ltd, 49(6), pp. 1387–1393. doi: 10.1016/j.fct.2011.03.026.

Hulihan, M. M. *et al.* (2008) 'LRRK2 Gly2019Ser penetrance in Arab-Berber patients from Tunisia: a case-control genetic study', *The Lancet Neurology*, 7(7), pp. 591–594. doi: 10.1016/S1474-4422(08)70116-9.

Hussain, N. K. *et al.* (2014) 'Sorting Nexin 27 regulates basal and activity-dependent trafficking of AMPARs.', *Proceedings of the National Academy of Sciences of the United States of America*, 111(32), pp. 1–7. doi: 10.1073/pnas.1412415111.

Ibanez, L. *et al.* (2017) 'Parkinson disease polygenic risk score is associated with Parkinson disease status and age at onset but not with alpha-synuclein cerebrospinal fluid levels', *BMC Neurology*. BMC Neurology, 17(1), pp. 1–9. doi: 10.1186/s12883-017-0978-z.

Ibanez, P. *et al.* (2004) 'Causal relation between alpha-synuclein gene duplication and familial Parkinson's disease.', *Lancet*, 364(9440), pp. 1169–1171.

Inestrosa, N. C. and Arenas, E. (2010) 'Emerging roles of Wnts in the adult nervous system', *Nature Reviews Neuroscience*. Nature Publishing Group, 11(2), pp. 77–86. doi: 10.1038/nrn2755.

Inoshita, T. *et al.* (2017) 'Vps35 in cooperation with LRRK2 regulates synaptic vesicle endocytosis through the endosomal pathway in *Drosophila*', *Human molecular genetics*, 26(15), pp. 2933–2948. doi: 10.1093/hmg/ddx179.

Ishizu, N. *et al.* (2016) 'Impaired striatal dopamine release in homozygous Vps35 D620N knock-

in mice.', *Human molecular genetics*, 0(0), p. ddw279. doi: 10.1093/hmg/ddw279.

Islam, M. S. *et al.* (2016) 'Human R1441C LRRK2 regulates the synaptic vesicle proteome and phosphoproteome in a Drosophila model of Parkinson's disease', *Human Molecular Genetics*, 25(24), pp. 5365–5382. doi: 10.1093/hmg/ddw352.

Ito, G. *et al.* (2016) 'Phos-tag analysis of Rab10 phosphorylation by LRRK2: a powerful assay for assessing kinase function and inhibitors.', *The Biochemical journal*, 473, pp. 2671–2685. doi: 10.1042/BCJ20160557.

Jaafari, N., Henley, J. M. and Hanley, J. G. (2012) 'PICK1 Mediates Transient Synaptic Expression of GluA2-Lacking AMPA Receptors during Glycine-Induced AMPA Receptor Trafficking', *Journal of Neuroscience*, 32(34), pp. 11618–11630. doi: 10.1523/JNEUROSCI.5068-11.2012.

Jeong, G. R. *et al.* (2018) 'Dysregulated phosphorylation of Rab GTPases by LRRK2 induces neurodegeneration', *Molecular Neurodegeneration*. Molecular Neurodegeneration, 13(1), pp. 1–17. doi: 10.1186/s13024-018-0240-1.

Jia, D. *et al.* (2012) 'Multiple repeat elements within the FAM21 tail link the WASH actin regulatory complex to the retromer.', *Molecular biology of the cell*, 23(12), pp. 2352–61. doi: 10.1091/mbc.E11-12-1059.

Jia, D. *et al.* (2016) 'Structural and mechanistic insights into regulation of the retromer coat by TBC1d5', *Nature Communications*. Nature Publishing Group, 7, pp. 1–11. doi: 10.1038/ncomms13305.

Jimenez-Orgaz, A. *et al.* (2018) 'Control of RAB 7 activity and localization through the retromer-TBC1D5 complex enables RAB 7-dependent mitophagy', *The EMBO Journal*, 37(2), pp. 235–254. doi: 10.15252/embj.201797128.

Kalia, L. V. and Lang, A. E. (2015) 'Parkinson's disease', *The Lancet*. Elsevier Ltd, 386, pp. 896–912. doi: 10.1016/S0140-6736(14)61393-3.

- Kang, Y. *et al.* (2014) 'A combined transgenic proteomic analysis and regulated trafficking of neuroligin-2', *Journal of Biological Chemistry*, 289(42), pp. 29350–29364. doi: 10.1074/jbc.M114.549279.
- Kashani, A. *et al.* (2007) 'Altered expression of vesicular glutamate transporters VGLUT1 and VGLUT2 in Parkinson disease', *Neurobiology of Aging*, 28, pp. 568–578. doi: 10.1016/j.neurobiolaging.2006.02.010.
- Kaufman, A. M. *et al.* (2012) 'Opposing roles of synaptic and extrasynaptic NMDA receptor signaling in cocultured striatal and cortical neurons.', *The Journal of neuroscience : the official journal of the Society for Neuroscience*, 32(12), pp. 3992–4003. doi: 10.1523/JNEUROSCI.4129-11.2012.
- Kelada, S. N. P. *et al.* (2006) '5' and 3' region variability in the dopamine transporter gene (SLC6A3), pesticide exposure and Parkinson's disease risk: A hypothesis-generating study', *Human Molecular Genetics*, 15(20), pp. 3055–3062. doi: 10.1093/hmg/ddl247.
- Kelly, K. *et al.* (2018) 'The G2019S mutation in LRRK2 imparts resiliency to kinase inhibition', *Experimental Neurology*, 309(July), pp. 1–13. doi: 10.1016/j.expneurol.2018.07.012.
- Kendall, A. K. *et al.* (2020) 'Mammalian Retromer Is an Adaptable Scaffold for Cargo Sorting from Endosomes', *Structure. Elsevier Ltd.*, 28(4), pp. 393-405.e4. doi: 10.1016/j.str.2020.01.009.
- Kiely, A. P. *et al.* (2013) 'A-synucleinopathy associated with G51D SNCA mutation: A link between Parkinson's disease and multiple system atrophy?', *Acta Neuropathologica*, 125(5), pp. 753–769. doi: 10.1007/s00401-013-1096-7.
- Killinger, B. A. and Kordower, J. H. (2019) 'Spreading of alpha-synuclein – relevant or epiphenomenon?', *Journal of Neurochemistry*, 150(5), pp. 605–611. doi: 10.1111/jnc.14779.
- Kin, K. *et al.* (2019) 'Animal models for Parkinson's disease research: Trends in the 2000s', *International Journal of Molecular Sciences*, 20(21). doi: 10.3390/ijms20215402.

- Klöpffer, T. H. *et al.* (2012) 'Untangling the evolution of Rab G proteins: implications of a comprehensive genomic analysis', *BMC Biology*, 10. doi: 10.1186/1741-7007-10-71.
- Kopec, C. D. *et al.* (2006) 'Glutamate receptor exocytosis and spine enlargement during chemically induced long-term potentiation', *Journal of Neuroscience*, 26(7), pp. 2000–2009. doi: 10.1523/JNEUROSCI.3918-05.2006.
- Kordower, J. H. *et al.* (2008) 'Lewy body-like pathology in long-term embryonic nigral transplants in Parkinson's disease', *Nature Medicine*, 14(5), pp. 504–506. doi: 10.1038/nm1747.
- Kordower, J. H. *et al.* (2013) 'Disease duration and the integrity of the nigrostriatal system in Parkinson's disease', *Brain*, 136(8), pp. 2419–2431. doi: 10.1093/brain/awt192.
- Kovtun, O. *et al.* (2018) 'Structure of the membrane-assembled retromer coat determined by cryo-electron tomography', *Nature*. Springer US, 561(7724), pp. 561–564. doi: 10.1038/s41586-018-0526-z.
- Kreitzer, A. C. (2009) 'Physiology and pharmacology of striatal neurons.', *Annual review of neuroscience*, 32, pp. 127–47. doi: 10.1146/annurev.neuro.051508.135422.
- Kreitzer, A. C. and Malenka, R. C. (2008) 'Striatal plasticity and basal ganglia circuit function.', *Neuron*. Elsevier Inc., 60(4), pp. 543–54. doi: 10.1016/j.neuron.2008.11.005.
- Kriegstein, a R. and Dichter, M. a (1983) 'Morphological classification of rat cortical neurons in cell culture.', *The Journal of neuroscience : the official journal of the Society for Neuroscience*, 3(8), pp. 1634–1647.
- Kruger, R. *et al.* (1998) 'Ala30Pro mutation in the gene encoding a-synuclein in Parkinson's disease', *Nature Genetics*, 18(3), pp. 231–236. doi: 10.1038/ng0598-51.
- Kvainickas, A. *et al.* (2017) 'Cargo-selective SNX-BAR proteins mediate retromer trimer independent retrograde transport.', *The Journal of cell biology*, <https://doi.org/10.1083/jcb.201702137>, p. jcb.201702137. doi: 10.1083/jcb.201702137.
- Lai, B. *et al.* (2002) 'Occupational and environmental risk factors for Parkinson's disease',

- Parkinsonism & Related Disorders*, 8, pp. 297–309. doi: 10.1136/oem.2006.027003.
- Langston, J. W. (2006) 'The Parkinson's complex: parkinsonism is just the tip of the iceberg.', *Annals of neurology*, 59(4), pp. 591–6. doi: 10.1002/ana.20834.
- Lee, A. *et al.* (2018) 'Emerging roles of mitochondria in synaptic transmission and neurodegeneration', *Current Opinion in Physiology*, June(3), pp. 139–148. doi: 10.1016/j.physbeh.2017.03.040.
- Lee, S., Chang, J. and Blackstone, C. (2016) 'FAM21 directs SNX27-retromer cargoes to the plasma membrane by preventing transport to the Golgi apparatus.', *Nature communications*. Nature Publishing Group, 7, p. 10939. doi: 10.1038/ncomms10939.
- Lesage, S. *et al.* (2013) 'G51D  $\alpha$ -synuclein mutation causes a novel Parkinsonian-pyramidal syndrome', *Annals of Neurology*, 73(4), pp. 459–471. doi: 10.1002/ana.23894.
- Lesage, S. and Brice, A. (2009) 'Parkinson's disease: From monogenic forms to genetic susceptibility factors', *Human Molecular Genetics*, 18(R1), pp. 48–59. doi: 10.1093/hmg/ddp012.
- Li, Y. C. and Kavalali, E. T. (2017) 'Synaptic vesicle-recycling machinery components as potential therapeutic targets', *Pharmacological Reviews*, 69(2), pp. 141–160. doi: 10.1124/pr.116.013342.
- Lim, J. *et al.* (2018) 'LRRK2 G2019S induces anxiety/depression-like behavior before the onset of motor dysfunction with 5-HT 1A receptor upregulation in mice', *Journal of Neuroscience*, 38(7), pp. 1611–1621. doi: 10.1523/JNEUROSCI.4051-15.2017.
- Lin, G. *et al.* (2018) 'Phospholipase PLA2G6, a Parkinsonism-Associated Gene, Affects Vps26 and Vps35, Retromer Function, and Ceramide Levels, Similar to  $\alpha$ -Synuclein Gain', *Cell Metabolism*. Elsevier Inc., 28(4), pp. 605–618.e6. doi: 10.1016/j.cmet.2018.05.019.
- Linardopoulou, E. V. *et al.* (2007) 'Human Subtelomeric WASH Genes Encode a New Subclass of the WASP Family', *PLoS Genetics*, 3(12), p. e237. doi: 10.1371/journal.pgen.0030237.

- Linhart, R. *et al.* (2014) 'Vacuolar protein sorting 35 (Vps35) rescues locomotor deficits and shortened lifespan in *Drosophila* expressing a Parkinson's disease mutant of Leucine-Rich Repeat Kinase 2 (LRRK2).', *Molecular neurodegeneration*, 9, p. 23. doi: 10.1186/1750-1326-9-23.
- Lis, P. *et al.* (2018) 'Development of phospho-specific Rab protein antibodies to monitor in vivo activity of the LRRK2 Parkinson's disease kinase', *Biochemical Journal*, 475(1), pp. 1–22. doi: 10.1042/BCJ20170802.
- Liu, Z. *et al.* (2018) 'LRRK2 phosphorylates membrane-bound Rabs and is activated by GTP-bound Rab7L1 to promote recruitment to the trans-Golgi network', *Human Molecular Genetics*, 27(2), pp. 385–395. doi: 10.1093/hmg/ddx410.
- Logan, T. *et al.* (2017) 'α-Synuclein promotes dilation of the exocytotic fusion pore', *Nature Neuroscience*, 20(5). doi: 10.1038/nn.4529.
- Lucas, M. *et al.* (2016) 'Structural Mechanism for Cargo Recognition by the Retromer Complex', *Cell*, 167(6), pp. 1623-1635.e14. doi: 10.1016/j.cell.2016.10.056.
- Luke, D. R. *et al.* (2012) 'Review of the Basic and Clinical Pharmacology of Sulfobutylether-B-Cyclodextrin (SBECD)', *Journal of pharmaceutical sciences*, 101(7), pp. 2271–2280. doi: 10.1002/jps.
- Ma, Q. *et al.* (2017) 'SorCS2-mediated NR2A trafficking regulates motor deficits in Huntington's disease', *JCI insight*, 2(9), pp. 1–16. doi: 10.1172/jci.insight.88995.
- MacDonald, V. and Halliday, G. M. (2002) 'Selective loss of pyramidal neurons in the pre-supplementary motor cortex in Parkinson's disease', *Movement Disorders*, 17(6), pp. 1166–1173. doi: 10.1002/mds.10258.
- MacIsaac, S. *et al.* (2020) 'Neuron-autonomous susceptibility to induced synuclein aggregation is exacerbated by endogenous *Lrrk2* mutations and ameliorated by *Lrrk2* genetic knock-out', *Brain Communications*, 2(1). doi: 10.1093/braincomms/fcz052.



MacLeod, D. A. *et al.* (2013) 'RAB7L1 interacts with LRRK2 to modify intraneuronal protein sorting and Parkinson's disease risk', *Neuron*, 77(3), pp. 425–439. doi: 10.1016/j.neuron.2012.11.033.RAB7L1.

Di Maio, R. *et al.* (2018) 'LRRK2 activation in idiopathic Parkinson's disease', *Science Translational Medicine*, 10(451), p. eaar5429. doi: 10.1126/scitranslmed.aar5429.

Malik, B. R., Godena, V. K. and Whitworth, A. J. (2015) 'VPS35 pathogenic mutations confer no dominant toxicity but partial loss of function in *Drosophila* and genetically interact with parkin', *Human Molecular Genetics*, 24(21), pp. 6106–6117. doi: 10.1093/hmg/ddv322.

Manyam, B. V. (1990) 'Paralysis agitans and levodopa in "Ayurveda": Ancient Indian medical treatise', *Movement Disorders*, 5(1), pp. 47–48. doi: 10.1002/mds.870050112.

Martinez, A. *et al.* (2017) 'Quantitative proteomic analysis of Parkin substrates in *Drosophila* neurons', *Molecular Neurodegeneration*. *Molecular Neurodegeneration*, 12(1), pp. 1–19. doi: 10.1186/s13024-017-0170-3.

Martinez, T. N. and Greenamyre, J. T. (2012) 'Toxin models of mitochondrial dysfunction in Parkinson's disease', *Antioxidants and Redox Signaling*, 16(9), pp. 920–934. doi: 10.1089/ars.2011.4033.

Matikainen-Ankney, B. A. *et al.* (2016) 'Altered Development of Synapse Structure and Function in Striatum Caused by Parkinson's Disease-Linked LRRK2-G2019S Mutation.', *The Journal of neuroscience : the official journal of the Society for Neuroscience*, 36(27), pp. 7128–41. doi: 10.1523/JNEUROSCI.3314-15.2016.

Matikainen-Ankney, B. A. *et al.* (2018) 'Parkinson's disease-linked *lrrk2*-g2019s mutation alters synaptic plasticity and promotes resilience to chronic social stress in young adulthood', *Journal of Neuroscience*, 38(45), pp. 9700–9711. doi: 10.1523/JNEUROSCI.1457-18.2018.

Matta, S. *et al.* (2012) 'LRRK2 controls an EndoA phosphorylation cycle in synaptic endocytosis.', *Neuron*, 75(6), pp. 1008–21. doi: 10.1016/j.neuron.2012.08.022.

McGarvey, J. C. *et al.* (2016) 'Actin-sorting nexin 27 (SNX27)-retromer complex mediates rapid parathyroid hormone receptor recycling', *Journal of Biological Chemistry*, 291(21), pp. 10986–11002. doi: 10.1074/jbc.M115.697045.

McGough, Ian J. *et al.* (2014) 'Identification of molecular heterogeneity in SNX27-retromer-mediated endosome-to-plasma-membrane recycling', *Journal of Cell Science*, 127(22), pp. 4940–4953. doi: 10.1242/jcs.156299.

McGough, Ian J. *et al.* (2014) 'Retromer Binding to FAM21 and the WASH Complex Is Perturbed by the Parkinson Disease-Linked VPS35(D620N) Mutation', *Current Biology*. The Authors, 24(14), pp. 1670–1676. doi: 10.1016/j.cub.2014.06.024.

McGough, I. J. *et al.* (2018) 'SNX3-retromer requires an evolutionary conserved MON2:DOPEY2:ATP9A complex to mediate Wntless sorting and Wnt secretion', *Nature Communications*, 9(1), pp. 1–13. doi: 10.1038/s41467-018-06114-3.

McNally, K. E. *et al.* (2017) 'Retriever is a multiprotein complex for retromer-independent endosomal cargo recycling', *Nature Cell Biology*, 19(10), pp. 1214–1225. doi: 10.1038/ncb3610.

McNeill, T. H. *et al.* (1988) 'Atrophy of medium spiny I striatal dendrites in advanced Parkinson's disease.', *Brain research*, 455(1), pp. 148–152. doi: 10.1016/0006-8993(88)90124-2.

Mecozzi, V. J. *et al.* (2014) 'Pharmacological chaperones stabilize retromer to limit APP processing.', *Nature chemical biology*. Nature Publishing Group, 10(6), pp. 443–449. doi: 10.1038/nchembio.1508.

Melrose, H. L. *et al.* (2006) 'Parkinson's disease: A rethink of rodent models', *Experimental Brain Research*, 173(2), pp. 196–204. doi: 10.1007/s00221-006-0461-3.

Melrose, H. L. *et al.* (2007) 'A comparative analysis of leucine-rich repeat kinase 2 (Lrrk2) expression in mouse brain and Lewy body disease', *Neuroscience*. IBRO, 147(4), pp. 1047–1058. doi: 10.1016/j.neuroscience.2007.05.027.

- Melrose, H. L. *et al.* (2010) 'Impaired dopaminergic neurotransmission and microtubule-associated protein tau alterations in human LRRK2 transgenic mice', *Neurobiology of Disease*, 40(3), pp. 503–517. doi: 10.1016/j.nbd.2010.07.010.
- Migheli, R. *et al.* (2013) 'LRRK2 Affects Vesicle Trafficking, Neurotransmitter Extracellular Level and Membrane Receptor Localization', *PLoS ONE*, 8(10), p. e77198. doi: 10.1371/journal.pone.0077198.
- Mikhaylova, M. *et al.* (2016) 'A Dendritic Golgi Satellite between ERGIC and Retromer', *Cell Reports*. The Authors, 14(2), pp. 189–199. doi: 10.1016/j.celrep.2015.12.024.
- Milnerwood, A. J. *et al.* (2010) 'Early Increase in Extrasynaptic NMDA Receptor Signaling and Expression Contributes to Phenotype Onset in Huntington's Disease Mice', *Neuron*. Elsevier Ltd, 65(2), pp. 178–190. doi: 10.1016/j.neuron.2010.01.008.
- Milnerwood, A. J. *et al.* (2012) 'Mitigation of augmented extrasynaptic NMDAR signaling and apoptosis in cortico-striatal co-cultures from Huntington's disease mice.', *Neurobiology of disease*. Elsevier Inc., 48(1), pp. 40–51. doi: 10.1016/j.nbd.2012.05.013.
- Milnerwood, A. J. and Raymond, L. A. (2010) 'Early synaptic pathophysiology in neurodegeneration: Insights from Huntington's disease', *Trends in Neurosciences*. Elsevier Ltd, 33(11), pp. 513–523. doi: 10.1016/j.tins.2010.08.002.
- Mir, R. *et al.* (2018) 'The Parkinson's disease VPS35[D620N] mutation enhances LRRK2-mediated Rab protein phosphorylation in mouse and human', *Biochemical Journal*, 475(11), pp. 1861–1883. doi: 10.1042/BCJ20180248.
- Miura, E. *et al.* (2014) 'VPS35 dysfunction impairs lysosomal degradation of  $\alpha$ -synuclein and exacerbates neurotoxicity in a Drosophila model of Parkinson's disease', *Neurobiology of Disease*. Elsevier Inc., 71, pp. 1–13. doi: 10.1016/j.nbd.2014.07.014.
- Morales, I. *et al.* (2015) 'The degeneration of dopaminergic synapses in Parkinson's disease: A selective animal model', *Behavioural Brain Research*. Elsevier B.V., 289, pp. 19–28. doi:

10.1016/j.bbr.2015.04.019.

Muhammad, A. *et al.* (2008) 'Retromer deficiency observed in Alzheimer's disease causes hippocampal dysfunction, neurodegeneration, and Abeta accumulation.', *Proceedings of the National Academy of Sciences of the United States of America*, 105(20), pp. 7327–32. doi: 10.1073/pnas.0802545105.

Munsie, L. *et al.* (2015) 'Retromer-dependent neurotransmitter receptor trafficking to synapses is altered by the Parkinson's disease VPS35 mutation p.D620N', *Human Molecular Genetics*, 24(6), pp. 1691–1703. doi: 10.1093/hmg/ddu582.

Murphy, K. E. and Halliday, G. M. (2014) 'Glucocerebrosidase deficits in sporadic Parkinson disease', *Autophagy*, 10(7), pp. 1350–1351. doi: 10.4161/auto.29074.

Nalls, M. A. *et al.* (2014) 'Large-scale meta-analysis of genome-wide association data identifies six new risk loci for Parkinson's disease', *Nature Genetics*. Nature Publishing Group, 46(9), pp. 989–993. doi: 10.1038/ng.3043.

Nalls, M. A. *et al.* (2019) 'Identification of novel risk loci, causal insights, and heritable risk for Parkinson's disease: a meta-analysis of genome-wide association studies', *The Lancet Neurology*, 18(12), pp. 1091–1102. doi: 10.1016/S1474-4422(19)30320-5.

Nguyen, M. *et al.* (2019) 'Synaptic, Mitochondrial, and Lysosomal Dysfunction in Parkinson's Disease', *Trends in Neurosciences*. Elsevier Ltd, 42(2), pp. 140–149. doi: 10.1016/j.tins.2018.11.001.

Nguyen, M. and Krainc, D. (2018) 'LRRK2 phosphorylation of auxilin mediates synaptic defects in dopaminergic neurons from patients with Parkinson's disease', *Proceedings of the National Academy of Sciences of the United States of America*, 115(21), pp. 5576–5581. doi: 10.1073/pnas.1717590115.

Olanow, C. W. and Mcnaught, K. (2011) 'Parkinson's disease, proteins, and prions: Milestones', *Movement Disorders*, 26(6), pp. 1056–1071. doi: 10.1002/mds.23767.

Opazo, P. and Choquet, D. (2011) 'A three-step model for the synaptic recruitment of AMPA receptors', *Molecular and Cellular Neuroscience*. Elsevier Inc., 46(1), pp. 1–8. doi: 10.1016/j.mcn.2010.08.014.

Ozelius, L. J. *et al.* (2006) 'LRRK2 G2019S as a cause of Parkinson's disease in Ashkenazi Jews [14]', *New England Journal of Medicine*, 354(4), pp. 424–425. doi: 10.1056/NEJMc055509.

Paisan-Ruiz, C. *et al.* (2004) 'Cloning of the gene containing mutations that cause PARK8-linked Parkinson's disease', *Neuron*. 2004/11/16, 44(4), pp. 595–600. doi: 10.1016/j.neuron.2004.10.023.

Pan-Montojo, F. *et al.* (2012) 'Environmental toxins trigger PD-like progression via increased alpha-synuclein release from enteric neurons in mice', *Scientific Reports*, 2, pp. 1–12. doi: 10.1038/srep00898.

Pan, P. Y. *et al.* (2017) 'Parkinson's disease-associated LRRK2 hyperactive kinase mutant disrupts synaptic vesicle trafficking in ventral midbrain neurons', *Journal of Neuroscience*, 37(47), pp. 11366–11376. doi: 10.1523/JNEUROSCI.0964-17.2017.

Pan, X. *et al.* (2017) 'Sortilin and retromer mediate retrograde transport of Glut4 in 3T3-L1 adipocytes', *Molecular Biology of the Cell*, 28(12), pp. 1667–1675. doi: 10.1091/mbc.E16-11-0777.

Parashar, A. and Udayabanu, M. (2017) 'Gut microbiota: Implications in Parkinson's disease', *Parkinsonism and Related Disorders*. Elsevier Ltd, 38, pp. 1–7. doi: 10.1016/j.parkreldis.2017.02.002.

Parisiadou, L. *et al.* (2009) 'Phosphorylation of ezrin/radixin/moesin proteins by LRRK2 promotes the rearrangement of actin cytoskeleton in neuronal morphogenesis', *Journal of Neuroscience*, 29(44), pp. 13971–13980. doi: 10.1523/JNEUROSCI.3799-09.2009.

Parisiadou, L. *et al.* (2014) 'LRRK2 regulates synaptogenesis and dopamine receptor activation through modulation of PKA activity', *Nature Neuroscience*, 17(3), pp. 367–376. doi:

10.1038/nm.3636.

Park, L. *et al.* (2013) 'Cyclical action of the WASH complex: FAM21 and capping protein drive WASH recycling, not initial recruitment.', *Developmental cell*. Elsevier Inc., 24(2), pp. 169–81. doi: 10.1016/j.devcel.2012.12.014.

Park, P. *et al.* (2018) 'The Role of Calcium-Permeable AMPARs in Long-Term Potentiation at Principal Neurons in the Rodent Hippocampus', *Frontiers in Synaptic Neuroscience*, 10(November), pp. 1–11. doi: 10.3389/fnsyn.2018.00042.

Parkinson, J. (2002) 'An essay on the shaking palsy. 1817.', *The Journal of neuropsychiatry and clinical neurosciences*, 14(2), pp. 223–36; discussion 222. Available at: <http://www.ncbi.nlm.nih.gov/pubmed/11983801>.

Pasanen, P. *et al.* (2014) 'A novel  $\alpha$ -synuclein mutation A53E associated with atypical multiple system atrophy and Parkinson's disease-type pathology', *Neurobiology of Aging*. Elsevier Ltd, 35(9), pp. 2180.e1-2180.e5. doi: 10.1016/j.neurobiolaging.2014.03.024.

Pavlos, N. J. and Jahn, R. (2011) 'Distinct Yet Overlapping Roles of Rab GTPsases on Synaptic Vesicles', *Small GTPases*, 2(2), pp. 77–81. doi: 10.4161/sgtp.2.2.15201.

Pellegrini-Giampietro, D. E., Bennett, M. V. L. and Zukin, R. S. (1992) 'Are  $\text{Ca}^{2+}$ -permeable kainate/AMPA receptors more abundant in immature brain?', *Neuroscience Letters*, 144(1–2), pp. 65–69. doi: 10.1016/0304-3940(92)90717-L.

Pellegrini, L. *et al.* (2017) 'Back to the tubule: microtubule dynamics in Parkinson's disease', *Cellular and Molecular Life Sciences*, 74(3), pp. 409–434. doi: 10.1007/s00018-016-2351-6.

Pérez-Victoria, F. J. and Bonifacino, J. S. (2009) 'Dual Roles of the Mammalian GARP Complex in Tethering and SNARE Complex Assembly at the trans-Golgi Network', *Molecular and Cellular Biology*, 29(19), pp. 5251–5263. doi: 10.1128/mcb.00495-09.

Pérez-Victoria, F. J., Mardones, G. A. and Bonifacino, J. S. (2007) 'Requirement of the Human GARP Complex for Mannose 6-phosphate-receptor-dependent Sorting of Cathepsin D to

Lysosomes', *Molecular Biology of the Cell*, 18(June), pp. 3250–3263. doi: 10.1091/mbc.E07.

Perfeito, R., Cunha-Oliveira, T. and Rego, A. C. (2013) 'Reprint of: revisiting oxidative stress and mitochondrial dysfunction in the pathogenesis of Parkinson disease-resemblance to the effect of amphetamine drugs of abuse.', *Free radical biology & medicine*. Elsevier, 62, pp. 186–201. doi: 10.1016/j.freeradbiomed.2013.05.042.

Phan, J. A. *et al.* (2017) 'Early synaptic dysfunction induced by  $\alpha$ -synuclein in a rat model of Parkinson's disease', *Scientific Reports*. Springer US, 7(1), pp. 1–17. doi: 10.1038/s41598-017-06724-9.

Piccoli, G. *et al.* (2011) 'LRRK2 controls synaptic vesicle storage and mobilization within the recycling pool.', *The Journal of neuroscience : the official journal of the Society for Neuroscience*, 31(6), pp. 2225–37. doi: 10.1523/JNEUROSCI.3730-10.2011.

Piccoli, G. *et al.* (2014) 'Leucine-Rich Repeat Kinase 2 Binds to Neuronal Vesicles through Protein Interactions Mediated by Its C-Terminal WD40 Domain', *Molecular and Cellular Biology*, 34(12), pp. 2147–2161. doi: 10.1128/mcb.00914-13.

Picconi, B., Piccoli, G. and Calabresi, P. (2012) 'Synaptic Dysfunction in Parkinson's Disease', in Kreutz, M. R. and Sala, C. (eds). Vienna: Springer Vienna (Advances in Experimental Medicine and Biology), pp. 553–572. doi: 10.1007/978-3-7091-0932-8.

del Pino, I. *et al.* (2011) 'The trafficking proteins Vacuolar Protein Sorting 35 and Neurobeachin interact with the glycine receptor  $\beta$ -subunit', *Biochemical and Biophysical Research Communications*. Elsevier Inc., 412(3), pp. 435–440. doi: 10.1016/j.bbrc.2011.07.110.

Polymeropoulos, M. H. *et al.* (1997) 'Mutation in the  $\alpha$ -synuclein gene identified in families with Parkinson's disease', *Science*, 276(5321), pp. 2045–2047. doi: 10.1126/science.276.5321.2045.

Purkey, A. M. and Dell'Acqua, M. L. (2020) 'Phosphorylation-Dependent Regulation of  $\text{Ca}^{2+}$ -Permeable AMPA Receptors During Hippocampal Synaptic Plasticity', *Frontiers in Synaptic Neuroscience*, 12(March). doi: 10.3389/fnsyn.2020.00008.

Purlyte, E. *et al.* (2018) 'Rab29 activation of the Parkinson's disease-associated LRRK2 kinase', *The EMBO Journal*, 37(1), pp. 1–18. doi: 10.15252/embj.201798099.

Puthenveedu, M. A. *et al.* (2010) 'Sequence-Dependent Sorting of Recycling Proteins by Actin-Stabilized Endosomal Microdomains', *Cell*. Elsevier Ltd, 143(5), pp. 761–773. doi: 10.1016/j.cell.2010.10.003.

Rajput, A. *et al.* (2015) 'VPS35 and DNAJC13 disease-causing variants in essential tremor', *European Journal of Human Genetics*, 23(6), pp. 887–888. doi: 10.1038/ejhg.2014.164.

Requejo-Aguilar, R. *et al.* (2015) 'DJ1 represses glycolysis and cell proliferation by transcriptionally up-regulating Pink1', *Biochemical Journal*, 467(2), pp. 303–310. doi: 10.1042/BJ20141025.

Riboldi, G. and Di Fonzo, A. B. (2019) 'GBA, Gaucher Disease, and Parkinson's Disease: From Genetic to Clinic to New Therapeutic Approaches', *Cells*, 8(364).

Ritz, B., Paul, K. and Bronstein, J. (2016) 'Of Pesticides and Men: A California Story of Genes and Environment in Parkinson's Disease', *Curr Environ Health Rep*, 3(1), pp. 40–52.

Rivero-Ríos, P. *et al.* (2019) 'The G2019S variant of leucine-rich repeat kinase 2 (LRRK2) alters endolysosomal trafficking by impairing the function of the GTPase RAB8A', *Journal of Biological Chemistry*, 294(13), pp. 4738–4758. doi: 10.1074/jbc.RA118.005008.

Rivero-Ríos, P. *et al.* (2020) 'Distinct Roles for RAB10 and RAB29 in Pathogenic LRRK2-Mediated Endolysosomal Trafficking Alterations', *Cells*, 9(7), p. 1719. doi: 10.3390/cells9071719.

Rojas, R. *et al.* (2007) 'Interchangeable but Essential Functions of SNX1 and SNX2 in the Association of Retromer with Endosomes and the Trafficking of Mannose 6-Phosphate Receptors', *Molecular and Cellular Biology*, 27(3), pp. 1112–1124. doi: 10.1128/MCB.00156-06.

Rojas, R. *et al.* (2008) 'Regulation of retromer recruitment to endosomes by sequential action of Rab5 and Rab7', *Journal of Cell Biology*, 183(3), pp. 513–526. doi: 10.1083/jcb.200804048.

Salinas, P. C. (2012) 'Wnt signaling in the vertebrate central nervous system: From axon



guidance to synaptic function', *Cold Spring Harbor Perspectives in Biology*, 4(2). doi: 10.1101/cshperspect.a008003.

Samii, A., Nutt, J. G. and Ransom, B. R. (2004) 'Parkinson's disease', *Lancet*, 363, pp. 1783–1793. doi: 10.1016/S0140-6736(04)16305-8.

Satake, W. *et al.* (2009) 'Genome-wide association study identifies common variants at four loci as genetic risk factors for Parkinson's disease', *Nature Genetics*. Nature Publishing Group, 41(12), pp. 1303–1307. doi: 10.1038/ng.485.

Schreij, A. M. *et al.* (2015) 'LRRK2 localizes to endosomes and interacts with clathrin-light chains to limit Rac1 activation.', *EMBO reports*, 16(1), pp. 79–86. doi: 10.15252/embr.201438714.

Seaman, M. N. J. *et al.* (1997) 'Endosome to Golgi retrieval of the vacuolar protein sorting receptor, Vps10p, requires the function of the VPS29, VPS30, and VPS35 gene products', *Journal of Cell Biology*, 137(1), pp. 79–92. doi: 10.1083/jcb.137.1.79.

Seaman, M. N. J. (2004) 'Cargo-selective endosomal sorting for retrieval to the Golgi requires retromer', *Journal of Cell Biology*, 165(1), pp. 111–122. doi: 10.1083/jcb.200312034.

Seaman, M. N. J. *et al.* (2009) 'Membrane recruitment of the cargo-selective retromer subcomplex is catalysed by the small GTPase Rab7 and inhibited by the Rab-GAP TBC1D5', *Journal of Cell Science*, 122(14), pp. 2371–2382. doi: 10.1242/jcs.048686.

Seaman, M. N. J. (2018) 'Retromer and the cation-independent mannose 6-phosphate receptor—Time for a trial separation?', *Traffic*, 19(2), pp. 150–152. doi: 10.1111/tra.12542.

Seaman, M. N. J., Gautreau, A. and Billadeau, D. D. (2013) 'Retromer-mediated endosomal protein sorting: all WASHed up!', *Trends in cell biology*. Elsevier Ltd, 23(11), pp. 522–8. doi: 10.1016/j.tcb.2013.04.010.

Seaman, M. N. J., Mukadam, A. S. and Breusegem, S. Y. (2018) 'Inhibition of TBC1D5 activates Rab7a and can enhance the function of the retromer cargo-selective complex', *Journal of Cell*

- Science*, 131(12), p. jcs217398. doi: 10.1242/jcs.217398.
- Seaman, M. N., McCaffery, J. M. and Emr, S. D. (1998) 'A membrane coat complex essential for endosome-to-Golgi retrograde transport in yeast.', *The Journal of cell biology*, 142(3), pp. 665–81. doi: 10.1083/jcb.142.3.665.
- Seeböhm, G. *et al.* (2012) 'Identification of a novel signaling pathway and its relevance for GluA1 recycling', *PLoS ONE*, 7(3). doi: 10.1371/journal.pone.0033889.
- Selkoe, D. J. (2002) 'Alzheimer's disease is a synaptic failure', *Science*, 298(5594), pp. 789–791. doi: 10.1126/science.1074069.
- Sepulveda, B. *et al.* (2013) 'Short- and Long-Term Effects of LRRK2 on Axon and Dendrite Growth', *PLoS ONE*, 8(4), pp. 1–9. doi: 10.1371/journal.pone.0061986.
- Sharpe, N. A. and Tepper, J. M. (1998) 'Postnatal development of excitatory synaptic input to the rat neostriatum: An electron microscopic study', *Neuroscience*, 84(4), pp. 1163–1175. doi: 10.1016/S0306-4522(97)00583-6.
- Shen, W. *et al.* (2008) 'Dichotomous dopaminergic control of striatal synaptic plasticity.', *Science (New York, N.Y.)*, 321(5890), pp. 848–51. doi: 10.1126/science.1160575.
- Sheng, Z. *et al.* (2012) 'Ser1292 autophosphorylation is an indicator of LRRK2 kinase activity and contributes to the cellular effects of PD mutations.', *Science translational medicine*, 4(164). doi: 10.1126/scitranslmed.3004485.
- Shi, H. *et al.* (2006) 'The retromer subunit Vps26 has an arrestin fold and binds Vps35 through its C-terminal domain', *Nature Structural and Molecular Biology*, 13(6), pp. 540–548. doi: 10.1038/nsmb1103.
- Shimizu, K. *et al.* (2003) 'Paraquat induces long-lasting dopamine overflow through the excitotoxic pathway in the striatum of freely moving rats', *Brain Research*, 976(2), pp. 243–252. doi: 10.1016/S0006-8993(03)02750-1.
- Shin, N. *et al.* (2008) 'LRRK2 regulates synaptic vesicle endocytosis', *Experimental Cell*

*Research*, 314(10), pp. 2055–2065. doi: 10.1016/j.yexcr.2008.02.015.

Sibarov, D. A., Poguzhelskaya, E. E. and Antonov, S. M. (2018) 'Downregulation of calcium-dependent NMDA receptor desensitization by sodium-calcium exchangers: A role of membrane cholesterol', *BMC Neuroscience*. BioMed Central, 19(1), pp. 1–9. doi: 10.1186/s12868-018-0475-3.

Simón-Sánchez, J. *et al.* (2006) 'LRRK2 is expressed in areas affected by Parkinson's disease in the adult mouse brain', *European Journal of Neuroscience*, 23(3), pp. 659–666. doi: 10.1111/j.1460-9568.2006.04616.x.

Simón-Sánchez, J. *et al.* (2009) 'Genome-wide association study reveals genetic risk underlying Parkinson's disease', *Nature Genetics*. Nature Publishing Group, 41(12), pp. 1308–1312. doi: 10.1038/ng.487.

Simonetti, B. *et al.* (2017) 'Sequence-dependent cargo recognition by SNX-BARs mediates retromer-independent transport of CI-MPR', *The Journal of Cell Biology*, <https://doi.org/10.1083/jcb.201703015>, pp. 1–18. doi: 10.1083/jcb.201703015.

Singleton, A. B. *et al.* (2003) 'α-Synuclein Locus Triplication Causes Parkinson's Disease', *Science*, 302(5646), p. 841. doi: 10.1126/science.1090278.

Small, S. A. *et al.* (2005) 'Model-guided microarray implicates the retromer complex in Alzheimer's disease', *Annals of Neurology*, 58(6), pp. 909–919. doi: 10.1002/ana.20667.

Small, S. A. and Petsko, G. A. (2017) 'Retromer in Alzheimer disease, Parkinson disease and other neurological disorders', *Occupational and Environmental Health*, pp. 531–542. doi: 10.1093/oso/9780190662677.003.0026.

Smith-Dijak, A. I. *et al.* (2019) 'Impairment and Restoration of Homeostatic Plasticity in Cultured Cortical Neurons From a Mouse Model of Huntington Disease', *Frontiers in Cellular Neuroscience*, 13. doi: 10.3389/fncel.2019.00209.

Smith, Y., Villalba, R. M. and Raju, D. V (2009) 'Striatal spine plasticity in Parkinson's disease:

pathological or not?', *Parkinsonism & related disorders*. Elsevier Ltd, 15 Suppl 3, pp. S156-61.

doi: 10.1016/S1353-8020(09)70805-3.

Sohur, U. S. *et al.* (2014) 'Feature article: Anatomic and molecular development of corticostriatal projection neurons in mice', *Cerebral Cortex*, 24(2), pp. 293–303. doi: 10.1093/cercor/bhs342.

Song, P. *et al.* (2016) 'Parkin modulates endosomal organization and function of the endo-lysosomal pathway', *Journal of Neuroscience*, 36(8), pp. 2425–2437. doi: 10.1523/JNEUROSCI.2569-15.2016.

Spang, A. (2011) 'Signalling gets sorted by retromer.', *The EMBO journal*. Nature Publishing Group, 30(15), pp. 2988–9. doi: 10.1038/emboj.2011.232.

Steger, M. *et al.* (2016) 'Phosphoproteomics reveals that Parkinson's disease kinase LRRK2 regulates a subset of Rab GTPases', *eLife*, 5. doi: 10.7554/eLife.12813.

Steger, M. *et al.* (2017) 'Systematic proteomic analysis of LRRK2-mediated rab GTPase phosphorylation establishes a connection to ciliogenesis', *eLife*, 6(i), pp. 1–22. doi: 10.7554/eLife.31012.

Steinberg, F. *et al.* (2013) 'A global analysis of SNX27-retromer assembly and cargo specificity reveals a function in glucose and metal ion transport.', *Nature cell biology*. Nature Publishing Group, 15(5), pp. 461–71. doi: 10.1038/ncb2721.

Stella, V. J. and He, Q. (2008) 'Cyclodextrins', *Toxicologic Pathology*, 36, pp. 30–42. doi: 10.1177/0192623307310945.

Stephens, B. *et al.* (2005) 'Evidence of a breakdown of corticostriatal connections in Parkinson's disease', *Neuroscience*, 132(3), pp. 741–754. doi: 10.1016/j.neuroscience.2005.01.007.

Stoessl, A. J. and Rivest, J. (1999) 'Differential diagnosis of parkinsonism', *Can J Neurol Sci*, 26, p. Suppl. 2-S1-S4. doi: 10.1017/s0317167100000020.

Stoker, T. B. and Greenland, J. C. (eds) (2018) *Parkinson's Disease: Pathogenesis and Clinical*

*Aspects*. Brisbane, Australia: Codon Publications. Available at: <https://codonpublications.com>.

Struhal, W. *et al.* (2014) 'VPS35 Parkinson's disease phenotype resembles the sporadic disease.', *Journal of neural transmission (Vienna, Austria : 1996)*, 121(7), pp. 755–9. doi: 10.1007/s00702-014-1179-1.

Sulzer, D. (2007) 'Multiple hit hypotheses for dopamine neuron loss in Parkinson's disease', *Trends in Neurosciences*, 30(5), pp. 244–250. doi: 10.1016/j.tins.2007.03.009.

Sulzer, D. and Edwards, R. H. (2019) 'The physiological role of  $\alpha$ -synuclein and its relationship to Parkinson's Disease', *Journal of Neurochemistry*, 150(5), pp. 475–486. doi: 10.1111/jnc.14810.

Sweet, E. S. *et al.* (2015) 'The Parkinson's disease-associated mutation LRRK2-G2019S impairs synaptic plasticity in mouse hippocampus', *Journal of Neuroscience*, 35(32), pp. 11190–11195. doi: 10.1523/JNEUROSCI.0040-15.2015.

Tang, F.-L. *et al.* (2015) 'VPS35 in Dopamine Neurons Is Required for Endosome-to-Golgi Retrieval of Lamp2a, a Receptor of Chaperone-Mediated Autophagy That Is Critical for - Synuclein Degradation and Prevention of Pathogenesis of Parkinson's Disease', *Journal of Neuroscience*, 35(29), pp. 10613–10628. doi: 10.1523/JNEUROSCI.0042-15.2015.

Tang, F. L. *et al.* (2015) 'VPS35 Deficiency or Mutation Causes Dopaminergic Neuronal Loss by Impairing Mitochondrial Fusion and Function', *Cell Reports*. The Authors, 12(10), pp. 1631–1643. doi: 10.1016/j.celrep.2015.08.001.

Tang, F. L. *et al.* (2020) 'Coupling of terminal differentiation deficit with neurodegenerative pathology in Vps35-deficient pyramidal neurons', *Cell Death and Differentiation*, 1. doi: 10.1038/s41418-019-0487-2.

Tarasenko, A. S. *et al.* (2010) 'Cholesterol depletion from the plasma membrane impairs proton and glutamate storage in synaptic vesicles of nerve terminals', *Journal of Molecular Neuroscience*, 41(3), pp. 358–367. doi: 10.1007/s12031-010-9351-z.

- Taylor, M. and Alessi, D. R. (2020) 'Advances in elucidating the function of leucine-rich repeat protein kinase-2 in normal cells and Parkinson's disease', *Current Opinion in Cell Biology*. Elsevier Ltd, 63, pp. 102–113. doi: 10.1016/j.ceb.2020.01.001.
- Temkin, P. *et al.* (2011) 'SNX27 mediates retromer tubule entry and endosome-to-plasma membrane trafficking of signalling receptors.', *Nature cell biology*. Nature Publishing Group, 13(6), pp. 715–21. doi: 10.1038/ncb2252.
- Temkin, P. *et al.* (2017) 'The Retromer Supports AMPA Receptor Trafficking During LTP', *Neuron*. Elsevier Inc., 94(1), pp. 74-82.e5. doi: 10.1016/j.neuron.2017.03.020.
- Tepper, J. M. *et al.* (1998) 'Postnatal development of the rat neostriatum: Electrophysiological, light- and electron-microscopic studies', *Developmental Neuroscience*, 20(2–3), pp. 125–145. doi: 10.1159/000017308.
- Thirstrup, K. *et al.* (2017) 'Selective LRRK2 kinase inhibition reduces phosphorylation of endogenous Rab10 and Rab12 in human peripheral mononuclear blood cells', *Scientific Reports*, 7(1), pp. 1–18. doi: 10.1038/s41598-017-10501-z.
- Tian, Y. *et al.* (2015) 'VPS35-deficiency results in an impaired AMPA receptor trafficking and decreased dendritic spine maturation', *Molecular Brain*. Molecular Brain, 8(1), p. 70. doi: 10.1186/s13041-015-0156-4.
- Traynelis, S. F., Silver, R. A. and Cull-candy, S. C. (1993) 'Estimated Conductance of G lutamate Receptor Channels Activated during EPSCs at the Cerebellar Mossy Fiber-Granule Cell Synapse', *Neuron*, 11, pp. 279–289.
- Trinh, J. and Farrer, M. (2013) 'Advances in the genetics of Parkinson disease.', *Nature reviews. Neurology*. Nature Publishing Group, 9(8), pp. 445–54. doi: 10.1038/nrneurol.2013.132.
- Tritsch, N. X. and Sabatini, B. L. (2012) 'Dopaminergic modulation of synaptic transmission in cortex and striatum.', *Neuron*. Elsevier Inc., 76(1), pp. 33–50. doi: 10.1016/j.neuron.2012.09.023.

- Trotta, L. *et al.* (2012) 'SNCA and MAPT genes: Independent and joint effects in Parkinson disease in the Italian population', *Parkinsonism and Related Disorders*. Elsevier Ltd, 18(3), pp. 257–262. doi: 10.1016/j.parkreldis.2011.10.014.
- Truckenbrodt, S. *et al.* (2018) 'Newly produced synaptic vesicle proteins are preferentially used in synaptic transmission', *The EMBO Journal*, 37(15), pp. 1–24. doi: 10.15252/emboj.201798044.
- Tsai, W.-H. (1985) 'Moment-preserving thresholding: A new approach', *Computer Vision, Graphics, and Image Processing*, 29(3), pp. 377–393. doi: 10.1016/0734-189X(85)90133-1.
- Tsika, E. *et al.* (2014) 'Parkinson's Disease-Linked Mutations in VPS35 Induce Dopaminergic Neurodegeneration.', *Human molecular genetics*, 23(17), pp. 4621–38. doi: 10.1093/hmg/ddu178.
- Vargas, K. J. *et al.* (2014) 'Synucleins regulate the kinetics of synaptic vesicle endocytosis.', *The Journal of neuroscience : the official journal of the Society for Neuroscience*, 34(28), pp. 9364–76. doi: 10.1523/JNEUROSCI.4787-13.2014.
- Vazquez-Sanchez, S. *et al.* (2018) 'VPS35 depletion does not impair presynaptic structure and function', *Scientific Reports*. Springer US, 8(1), pp. 1–12. doi: 10.1038/s41598-018-20448-4.
- Venda, L. L. *et al.* (2010) 'α-Synuclein and dopamine at the crossroads of Parkinson's disease', *Trends in Neurosciences*, 33(12), pp. 559–568. doi: 10.1016/j.tins.2010.09.004.
- Vergés, M. *et al.* (2004) 'The mammalian retromer regulates transcytosis of the polymeric immunoglobulin receptor.', *Nature cell biology*, 6(8), pp. 763–769. doi: 10.1038/ncb1153.
- Vilariño-Güell, C. *et al.* (2011) 'VPS35 mutations in Parkinson disease.', *American journal of human genetics*, 89(1), pp. 162–7. doi: 10.1016/j.ajhg.2011.06.001.
- Vilariño-Güell, C. *et al.* (2013) 'DNAJC13 mutations in Parkinson disease.', *Human molecular genetics*, pp. 1–8. doi: 10.1093/hmg/ddt570.
- Vingill, S., Connor-Robson, N. and Wade-Martins, R. (2018) 'Are rodent models of Parkinson's disease behaving as they should?', *Behavioural Brain Research*. Elsevier, 352(July 2017), pp.

133–141. doi: 10.1016/j.bbr.2017.10.021.

Volpicelli-Daley, L. A. *et al.* (2016) 'G2019s-LRRK2 expression augments  $\alpha$ -synuclein sequestration into inclusions in neurons', *Journal of Neuroscience*, 36(28), pp. 7415–7427. doi: 10.1523/JNEUROSCI.3642-15.2016.

Volpicelli-Daley, L. and Brundin, P. (2018) *Prion-like propagation of pathology in Parkinson disease*. 1st edn, *Handbook of Clinical Neurology*. 1st edn. Elsevier B.V. doi: 10.1016/B978-0-444-63945-5.00017-9.

Volta, M. *et al.* (2015) 'Chronic and acute LRRK2 silencing has no long-term behavioral effects, whereas wild-type and mutant LRRK2 overexpression induce motor and cognitive deficits and altered regulation of dopamine release', *Parkinsonism & Related Disorders*. Elsevier Ltd, 21(10), pp. 1156–1163. doi: 10.1016/j.parkreldis.2015.07.025.

Volta, M. *et al.* (2017) 'Initial elevations in glutamate and dopamine neurotransmission decline with age, as does exploratory behavior, in LRRK2 G2019S knock-in mice', *eLife*, 6. doi: 10.7554/eLife.28377.

Volta, M., Milnerwood, A. J. and Farrer, M. J. (2015) 'Insights from late-onset familial parkinsonism on the pathogenesis of idiopathic Parkinson's disease', *The Lancet Neurology*. Elsevier Ltd, 14(10), pp. 1054–1064. doi: 10.1016/S1474-4422(15)00186-6.

Wandinger-Ness, A. and Zerial, M. (2014) 'Rab Proteins and the Compartmentalization of the Endosomal System', *Cold Spring Harbor Perspectives in Biology*, 6(11), p. a022616. doi: 10.1101/cshperspect.a022616.

Wang, C.-L. *et al.* (2012) 'VPS35 regulates developing mouse hippocampal neuronal morphogenesis by promoting retrograde trafficking of BACE1.', *Biology open*, 1(12), pp. 1248–57. doi: 10.1242/bio.20122451.

Wang, C. *et al.* (2016) 'VPS35 regulates cell surface recycling and signaling of dopamine receptor D1', *Neurobiology of Aging*. Elsevier Inc, 46, pp. 22–31. doi:



10.1016/j.neurobiolaging.2016.05.016.

Wang, D. *et al.* (2005) 'Crystal structure of human vacuolar protein sorting protein 29 reveals a phosphodiesterase/nuclease-like fold and two protein-protein interaction sites', *Journal of Biological Chemistry*, 280(24), pp. 22962–22967. doi: 10.1074/jbc.M500464200.

Wang, H. *et al.* (2014) 'In vivo evidence of pathogenicity of VPS35 mutations in the *Drosophila*', *Molecular Brain*, 7(73), pp. 1–6.

Wang, P. *et al.* (2016) 'RAB-10 Promotes EHBP-1 Bridging of Filamentous Actin and Tubular Recycling Endosomes', *PLoS Genetics*, 12(6), pp. 1–28. doi: 10.1371/journal.pgen.1006093.

Wang, W. *et al.* (2016) 'Parkinson's disease-associated mutant VPS35 causes mitochondrial dysfunction by recycling DLP1 complexes', *Nature Medicine*, 22(1), pp. 54–63. doi: 10.1038/nm.3983.

Wang, W. *et al.* (2017) 'A conserved retromer sorting motif is essential for mitochondrial DLP1 recycling by vps35 in parkinson's disease model', *Human Molecular Genetics*, 26(4), pp. 781–789. doi: 10.1093/hmg/ddw430.

Wasser, C. R. *et al.* (2007) 'Cholesterol-dependent balance between evoked and spontaneous synaptic vesicle recycling', *Journal of Physiology*, 579(2), pp. 413–429. doi: 10.1113/jphysiol.2006.123133.

Wassmer, T. *et al.* (2007) 'A loss-of-function screen reveals SNX5 and SNX6 as potential components of the mammalian retromer.', *Journal of cell science*, 120(1), pp. 45–54. doi: 10.1242/jcs.03302.

Webber, P. J. *et al.* (2011) 'Autophosphorylation in the Leucine-Rich Repeat Kinase 2 (LRRK2) GTPase Domain Modifies Kinase and GTP-Binding Activities', *J Mol Biol*, 412(1), pp. 94–110. doi: 10.1038/jid.2014.371.

van Weering, J. R. T., Verkade, P. and Cullen, P. J. (2012) 'SNX-BAR-mediated endosome tubulation is co-ordinated with endosome maturation', *Traffic*, 13(1), pp. 94–107. doi:

10.1111/j.1600-0854.2011.01297.x.

Wen, L. *et al.* (2011) 'VPS35 haploinsufficiency increases Alzheimer's disease neuropathology', *Journal of Cell Biology*, 195(5), pp. 765–779. doi: 10.1083/jcb.201105109.

West, A. B. *et al.* (2005) 'Parkinson's disease-associated mutations in leucine-rich repeat kinase 2 augment kinase activity', *Proceedings of the National Academy of Sciences of the United States of America*, 102(46), pp. 16842–16847. doi: 10.1073/pnas.0507360102.

Westphal, C. H. and Chandra, S. S. (2013) 'Monomeric synucleins generate membrane curvature.', *The Journal of biological chemistry*, 288(3), pp. 1829–40. doi: 10.1074/jbc.M112.418871.

Williams, E. T. *et al.* (2018) 'Parkin mediates the ubiquitination of VPS35 and modulates retromer-dependent endosomal sorting', *Human Molecular Genetics*, 27(18), pp. 3189–3205. doi: 10.1093/hmg/ddy224.

Wishart, T. M., Parson, S. H. and Gillingwater, T. H. (2006) 'Synaptic vulnerability in neurodegenerative disease', *Journal of Neuropathology and Experimental Neurology*, 65(8), pp. 733–739. doi: 10.1097/01.jnen.0000228202.35163.c4.

Wu, Q. *et al.* (2016) 'Retrograde trafficking of VMAT2 and its role in protein stability in non-neuronal cells', *Journal of Biomedical Research*, 30(6), pp. 502–509. doi: 10.7555/JBR.30.20160061.

Wu, S. *et al.* (2017) 'The dopamine transporter recycles via a retromer-dependent postendocytic mechanism: Tracking studies using a novel fluorophore-coupling approach', *Journal of Neuroscience*, 37(39), pp. 9438–9452. doi: 10.1523/JNEUROSCI.3885-16.2017.

Yahalom, G. *et al.* (2020) 'Age at Onset of Parkinson's Disease Among Ashkenazi Jewish Patients: Contribution of Environmental Factors, LRRK2 p.G2019S and GBA p.N370S Mutations', *Journal of Parkinson's Disease*, pp. 1–10. doi: 10.3233/jpd-191829.

Yap, C. C. *et al.* (2017) 'The endosomal neuronal proteins Nsg1/NEEP21 and Nsg2/P19 are

itinerant, not resident proteins of dendritic endosomes', *Nature Scientific Reports*. Springer US, 7(1), pp. 1–17. doi: 10.1038/s41598-017-07667-x.

Yin, X. *et al.* (2013) 'Retromer maintains basolateral distribution of the type II TGF- $\beta$  receptor via the recycling endosome.', *Molecular biology of the cell*, 24(14), pp. 2285–98. doi: 10.1091/mbc.E13-02-0093.

Yue, M. *et al.* (2015) 'Progressive dopaminergic alterations and mitochondrial abnormalities in LRRK2 G2019S knock in mice', *Neurobiology of Disease*. Elsevier Inc., 78, pp. 172–195. doi: 10.1016/j.nbd.2015.02.031.

Yun, H. J. *et al.* (2013) 'LRRK2 phosphorylates Snapin and inhibits interaction of Snapin with SNAP-25.', *Experimental & molecular medicine*. Nature Publishing Group, 45(8), p. e36. doi: 10.1038/emmm.2013.68.

Zaja-Milatovic, S. *et al.* (2005) 'Dendritic degeneration in neostriatal medium spiny neurons in Parkinson disease.', *Neurology*, 64(3), pp. 545–7. doi: 10.1212/01.WNL.0000150591.33787.A4.

Zarranz, J. J. *et al.* (2004) 'The New Mutation, E46K, of  $\alpha$ -Synuclein Causes Parkinson and Lewy Body Dementia', *Annals of Neurology*, 55(2), pp. 164–173. doi: 10.1002/ana.10795.

Zavodszky, E. *et al.* (2014) 'Mutation in VPS35 associated with Parkinson's disease impairs WASH complex association and inhibits autophagy', *Nature Communications*. Nature Publishing Group, 5(May), p. 3828. doi: 10.1038/ncomms4828.

Zhang, D. *et al.* (2012) 'RAB-6.2 and the retromer regulate glutamate receptor recycling through a retrograde pathway.', *The Journal of cell biology*, 196(1), pp. 85–101. doi: 10.1083/jcb.201104141.

Zhang, P. *et al.* (2000) 'Cloning and characterization of human VPS35 and mouse Vps35 and mapping of VPS35 to human chromosome 16q13-q21', *Genomics*, 70(2), pp. 253–257. doi: 10.1006/geno.2000.6380.

Zhang, Q. *et al.* (2018) 'The Mitochondrial Unfolded Protein Response Is Mediated Cell-Non-

autonomously by Retromer-Dependent Wnt Signaling', *Cell*. Elsevier Inc., 174(4), pp. 870-883.e17. doi: 10.1016/j.cell.2018.06.029.

Zhao, Y. *et al.* (2018) 'Reduced LRRK2 in association with retromer dysfunction in post-mortem brain tissue from LRRK2 mutation carriers', *Brain*, 141(2), pp. 486–495. doi: 10.1093/brain/awx344.

Zhao, Y. and Dzamko, N. (2019) 'Recent Developments in LRRK2-Targeted Therapy for Parkinson's Disease', *Drugs*. Springer International Publishing, 79(10), pp. 1037–1051. doi: 10.1007/s40265-019-01139-4.

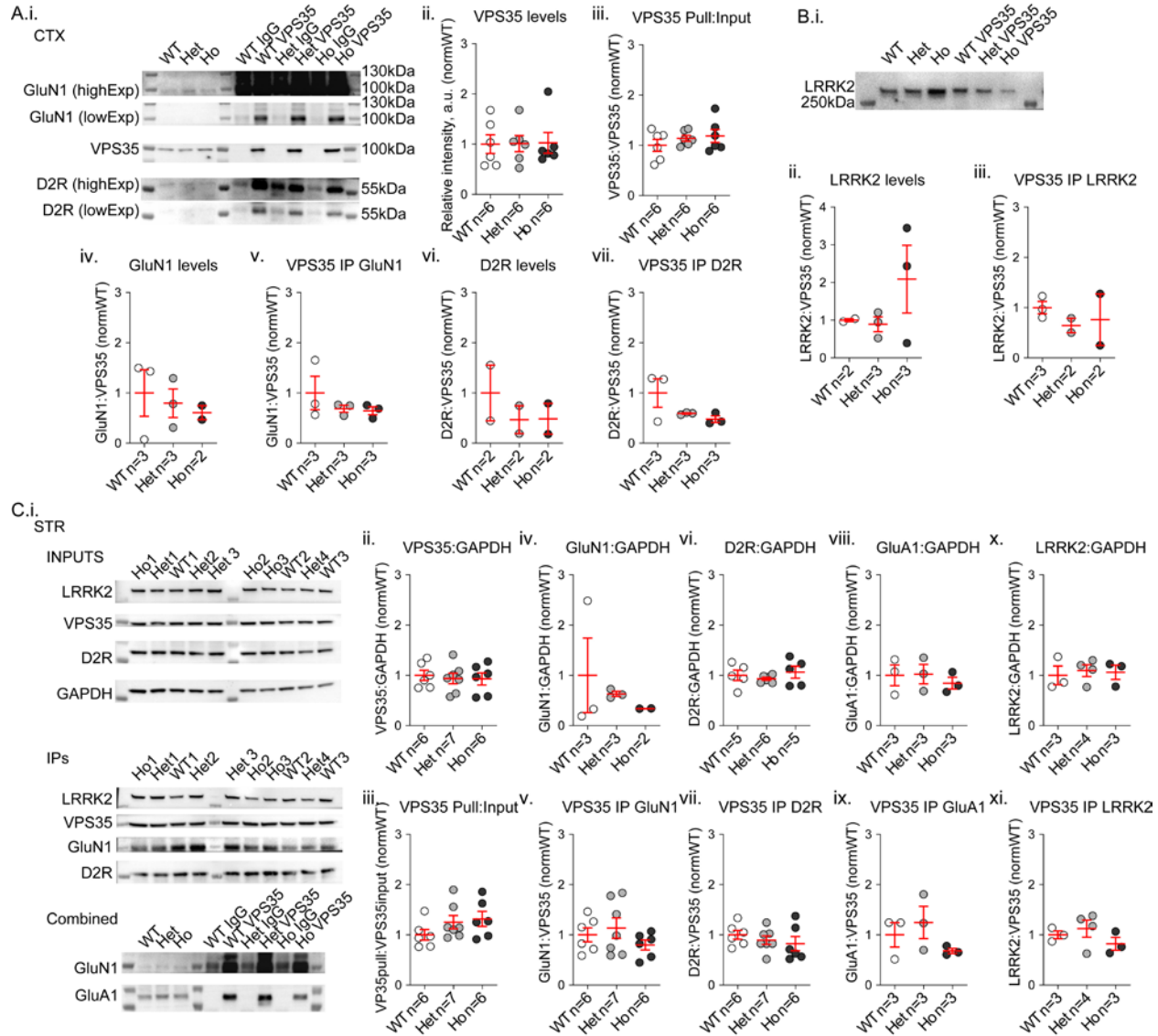
Zhou, L. *et al.* (2017) 'Parkinson's disease-associated pathogenic VPS35 mutation causes complex I deficits', *BBA Molecular Basis of Disease*, 1863(11), pp. 2791–2795.

Zimprich, A. *et al.* (2004) 'Mutations in LRRK2 cause autosomal-dominant parkinsonism with pleomorphic pathology', *Neuron*, 44(4), pp. 601–607. doi: 10.1016/j.neuron.2004.11.005.

Zimprich, A. *et al.* (2011) 'A mutation in VPS35, encoding a subunit of the retromer complex, causes late-onset Parkinson disease.', *American journal of human genetics*, 89(1), pp. 168–75. doi: 10.1016/j.ajhg.2011.06.008.

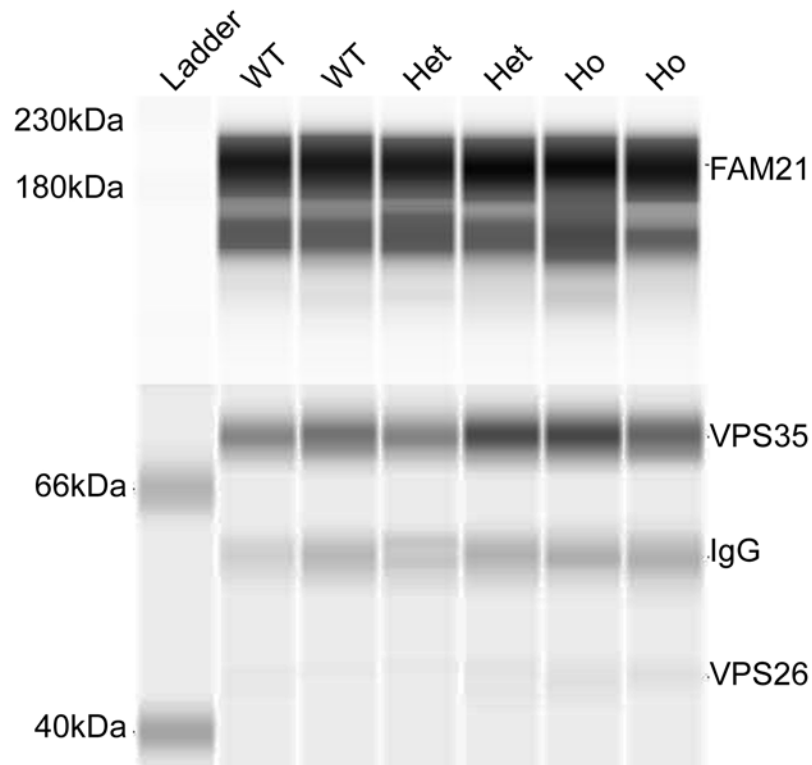
# Appendices

## Appendix A - Supplements to Chapter 2



**Appendix A-1 Co-immunoprecipitation in cortical and striatal lysates from 3-month-old mice reveals novel neuronal VPS35 cargoes and no mutant effects on neurotransmitter cargo binding. A.i)** Co-immunoprecipitation and lysates were quantified by chemi-luminescent western blotting by running samples on an electrophoresis gel and probing for VPS35, D2R, GluA1, GluN1, GluA1, LRRK2, and GAPDH (loading control), and normalized to WT. There were no significant differences in VPS35 levels or pull by the antibody (ii-iii, 1-way ANOVA  $p > 0.99$ ; Kruskal-Wallis  $p = 0.62$ , respectively). NMDA-receptor subunit GluN1 association with retromer has not previously been published; the mutation did not affect GluN1 levels nor coIP with VPS35 (iv-v, Kruskal-Wallis

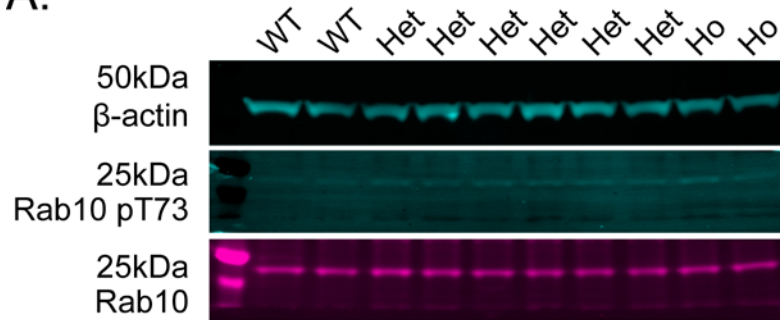
**(Appendix A-1 cont.)**  $p=0.76$ ;  $p=0.44$ , respectively). D2-type dopamine receptors are a novel retromer cargo; there was no significant mutation effect on D2R levels or coIP with VPS35 (vi-vii, Kruskal-Wallis  $p=0.80$ ;  $p=0.44$ , respectively). **B.i)** Co-immunoprecipitation of cortical lysates were quantified as in A. There were no significant genotype effects on LRRK2 levels or association of LRRK2 with VPS35 by coIP (ii-iii Kruskal-Wallis  $p=0.76$ ;  $p=0.52$ , respectively). **C.i)** Striatal lysates were co-immunoprecipitated and quantified as in A & B. There were no genotype effects on VPS35 levels or pull by the antibody (ii-iii, Kruskal-Wallis  $p=0.97$ ;  $p=0.13$ , respectively); GluN1 levels or coIP (iv-v, Kruskal-Wallis  $p=0.51$ ;  $p=0.42$ , respectively); D2R levels or coIP (vi-vii Kruskal-Wallis  $p=0.70$ ;  $p=0.45$ , respectively); GluA1 levels or coIP (viii-ix, Kruskal-Wallis  $p=0.83$ ;  $p=0.44$ , respectively); or LRRK2 levels or coIP (x-xi, Kruskal-Wallis  $p>0.99$ ;  $p=0.40$ , respectively). For all panels, n= number of experimental animals.



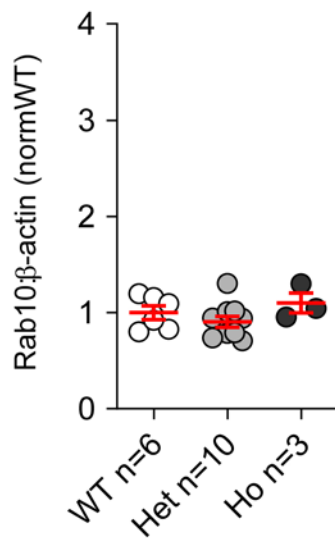
**Appendix A-2 Co-immunoprecipitation of whole brain lysate from 3-month-old mice shows that immunoprecipitation of FAM21 can pull down VPS35.** Co-immunoprecipitation and lysates were visualized by running samples on a WES capillary-based western blotting system and probing for VPS35, FAM21 and VPS26. A pull with FAM21 antibody shows VPS35 association in brain tissue.

## Appendix B - Supplements to Chapter 3

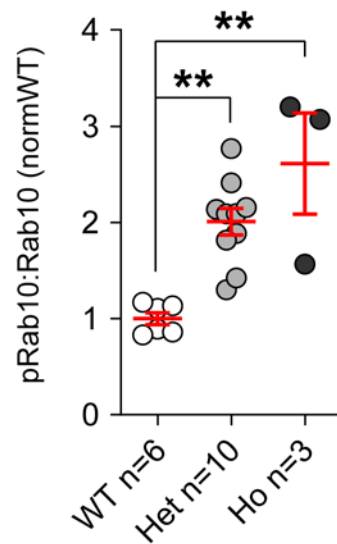
A.



B. Rab10:β-actin

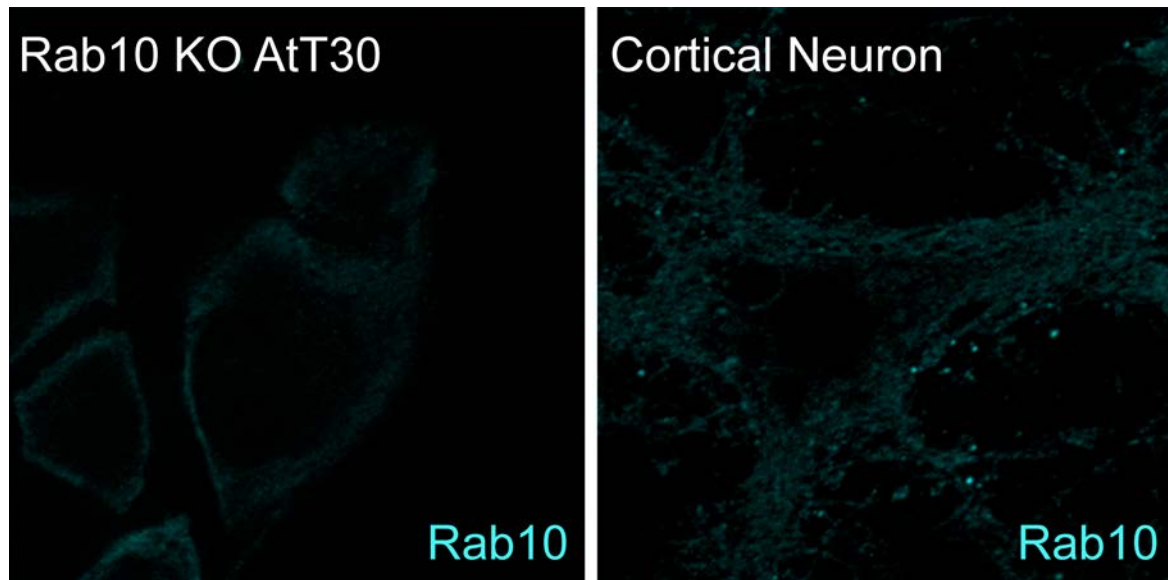


C. pRab10:Rab10

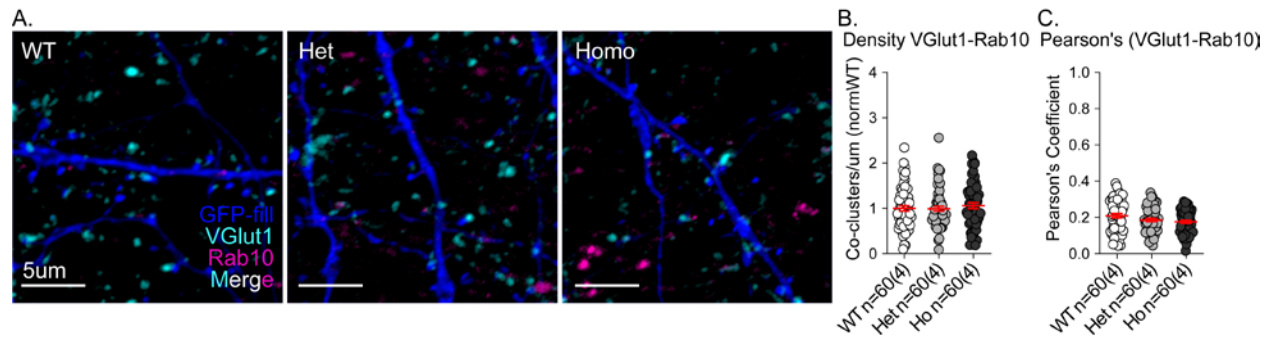


**Appendix B-1 Western blot of whole brain lysate from 3-month-old mice reveals a statistically significant genotype effect on Rab10 phosphorylation.** A) Whole brain lysates were quantified by separation in an electrophoresis gel followed by probing for Rab10, Rab10 pT73, and β-actin. There were no significant genotype effects on levels of total Rab10 (B Kruskal-Wallis  $p=0.16$ ); however there was a significant genotype effect on the phosphorylation of Rab10 at T73 (C Kruskal-Wallis  $p=0.0001$ ; Het  $**p<0.003$ , Ho  $**p<0.003$ ).





**Appendix B-2 Knock-out testing of specificity of Rab10 antibody for immunocytochemistry. A)** Cultured cortical neurons and Rab10 knock-out AtT30 cells were stained by immunocytochemistry for Rab10, demonstrating punctate staining in the cortical neuron that is absent from the knock-out cells.



**Appendix B-3 Visualization of VGlut1 and Rab10 in cultured cortical neuron dendrites reveals that mutant-specific increases in Rab10 cluster density are not associated with VGlut1-positive terminals.**

**A)** GFP-filled cultured cortical neurons were fixed at DIV21 and stained for GFP (blue), VGlut1 (cyan), and Rab10 (magenta). Co-cluster density and Pearson's coefficient were not significantly altered by genotype (B-C Kruskal-Wallis  $p=0.63$ ,  $p=0.07$ , respectively).